Development and utilization of Luminex biomarker assays for diagnosis and monitoring of neurodegenerative disease

Ph.D. Thesis

Kurimun Ismail

Lancaster University

2016

I, Kurimun Ismail, confirm that the work presented in this thesis is my own and has not been submitted in substantially the same form for the award of a higher degree elsewhere. Where information has been derived from other sources, I confirm this has been indicated in the thesis.

Submitted in part fulfilment of the requirements for the degree of Doctor of Philosophy

Abstract

A common pathological feature of various neurodegenerative disorders is the accumulation of misfolded proteins in the brain. Neurodegenerative disorders associated with protein misfolding include Alzheimer's disease (AD), Parkinson's disease (PD), dementia with Lewy bodies (DLB), fronto-temporal lobar degeneration (FTLD), motor neuron disease (MND), Huntington's disease and the prion diseases. The incidence and prevalence of most of these diseases is rising, especially those that cause dementia, due to an increase in the average human life span.

The diagnosis of neurodegenerative disorders is heavily reliant on physical examinations and assessment of clinical symptoms. The clinical symptoms of many of these neurodegenerative diseases overlap, which poses a huge difficulty for accurate diagnosis, especially in the early stages. This has led to an interest in identifying reliable and robust discriminatory molecular biomarkers. A successful biomarker test will not only provide a more accurate means of diagnosis, but will allow efficient tracking of disease progression, benefitting the process of developing therapeutic strategies.

In this project, the development and validation of a bead based assay system that has multiplexing capabilities (simultaneously measure multiple analytes in a single sample via a single assay) has been described. This assay system uses the Luminex technology and has been developed to quantitatively measure phosphorylated α-synuclein, total α-synuclein, total DJ-1 and LRRK2 in human CSF and plasma. These proteins are predominantly implicated in diseases collectively termed α-synucleinopathies. The initial aim of the project was to develop assays for proteins that span a range of neurodegenerative disorders, however, for reasons discussed in the final chapter of this thesis, this was not possible.

This project provides evidence on how the use of plasma as a possible matrix for potential markers associated with brain diseases can be justified, since levels of phosphorylated α-synuclein in matched plasma and CSF samples positively correlated with each other. Plasma would be an ideal sample source for biomarker studies, since it is less invasive than obtaining CSF, thus allowing longitudinal studies to be performed.

It was also shown how the DJ-1 protein in plasma may carry diagnostic potential by allowing differentiation between PD patients and healthy controls ($p=0.004$) as well as between PD and MSA patients ($p=0.005$). The discrimination between PD and MSA is vital since the two diseases are symptomatically very similar, thus posing a greater issue with accurate diagnosis.

There has been minimal research discussing the presence of LRRK2 in human biological fluids such as plasma and CSF. This thesis presents the use of western blotting, high performance liquid chromatography (HPLC) and the Luminex technology as a means of detecting this protein in human CSF and plasma. The data related to LRRK2 in this thesis, opens up avenues for further research into this protein; to definitively show whether it can be detected in such biological fluids and whether it has any value as a biomarker.

Acknowledgements

First and foremost, I would like to thank Professor David Allsop for his time, valuable input and for giving me the opportunity to embark on a PhD project. I would also like to thank Dr Fiona Benson for being my secondary Supervisor and stepping in when required. Sincere thanks goes to Dr Penny Foulds, Professor David Mann and Dr Mark Taylor for their efforts and willingness to share their science related experiences and knowledge.

I would also like to thank Dr Abdul Hye, Dr Joanna Riddoch and Professor Simon Lovestone from Kings College in London, for allowing me to spend time in their laboratory to learn key skills in developing Luminex bead based assays, and helping me with troubleshooting the total α-synuclein Luminex assay.

This project would not have been possible without the biological fluid samples i.e. plasma and CSF. A massive thank you, to those who donated samples to research and fellow scientists who were not hesitant to share these samples with us; especially Professor David Mann and Dr Nadia Magdalinou from UCL.

The PhD experience would not have been enjoyable without the presence of fellow PhD students within the Allsop group and other disciplines within the Lancaster University Biological Sciences Department. Thus I would like to take this opportunity to thank them for their support too.

Table of Contents

Chapter 2a: Materials

Chapter 2b: Methods

Chapter 3: Phosphorylated α-synuclein: Luminex assay development and validation

Chapter 4: Phosphorylated α-synuclein: sample analysis results

Chapter 5: Total α-synuclein and total DJ-1: Luminex assay development

Chapter 6: Total α-synuclein and total DJ-1: sample analysis results

List of Tables

List of Figures

Abbreviations

αsyn	alpha-synuclein
µg	Microgram
µL	Microlitre
4PL	4-Parameter Logistic
5PL	5-Parameter Logistic
Ab	Antibody
AD	Alzheimer's disease
ALS	Amyotrophic Lateral Sclerosis
ATP	Adenosine Triphosphate
BSA	Bovine serum albumin
bvFTLD	Behavioural Variant FTLD
CBS	Corticobasal Syndrome
CMA	Chaperone-mediated autophagy
CNS	Central Nervous System
COMT	Catechol-O-methyl transferase
CSF	Cerebrospinal Fluid
CV	Coefficient of variation
dAb	Detection antibody
DDC	Dopa-carboxylase
DLB	Dementia with Lewy Body
DNA	Deoxyribonucleic acid

DNs	Dystrophic Neurites
DTT	Dithiothreitol
EDC	1-Ethyl-3-[3-dimethylaminopropyl] carbodiimide hydrochloride
EDTA	Ethylenediaminetetraacetic acid
ELISA	Enzyme-Linked Immuno-Sorbent Assay
EMG	Electromyography
FBS	Fetal bovine serum
FDA	Food and drug administration
FTLD	Fronto-temporal Lobar Dementia
FUS	Fused in sarcoma protein
GMNC	Greater Manchester Neurosciences Centre
h	hour(s)
HC	Healthy controls
HD	Huntington's disease
HPLC	High performance liquid chromatography
HQ	High QC
HRP	Horseradish peroxidase
HSPs	Heat Shock Proteins
HVS	High validation samples
iPD	Idiopathic Parkinson’s disease
kDa	Kilo Dalton
LB	Lewy Body

L-Dopa	Levadopa
LLOQ	Lower Limit of Quantification
LLOQ	Lower limit of quantification
LN	Lewy Neurite
LOD	Limit of Detection
LQ	Low QC
LRRK2	Leucine - rich repeat kinase 2
LVS	Low validation sample
mAb	Monoclonal antibody
MAO-B	Monoamine Oxidase B
MFI	Median Fluorescence Intensity
min	Minute(s)
mL	Millilitre
MND	Motor Neurone Disease
MQ	Middle QC
MRD	Minimum Required Dilution
MRI	Magnetic resonance imaging
mRNA	Messenger ribonucleic acid
MSA	Multiple System Atrophy
MVS	Middle validation sample
n	number
NCIs	Neuronal Cytoplasmic Inclusions
ng	Nanogram

Nrf2	Nuclear factor erythroid-2 related factor 2
pAb	Polyclonal antibody
PBS	Phosphate buffered saline
PBST	PBS/Tween
PD	Parkinson's disease
PPA	Primary Progressive Aphasia
PSF	Polypyrimidine tract binding protein associated splicing factor
Pαsyn	Phosphorylated α-synuclein
QC	Quality control sample
RBD	Rapid eye movement disorder behaviour
RE	recovery
RNA	Ribonucleic acid
ROC	Ras of complex proteins
ROS	Reactive oxygen species
rpm	Revolutions per minute
RT	Room temperature
SD	Standard Deviation
SDS	Sodium dodecyl sulphate
SDS-PAGE	Sodium dodecyl sulphate polyacrylamide gel electrophoresis
sMND	Sporadic Motor Neurone Disease
SN	Substantia Nigra

SNARE	Soluble NSF Attachment Protein
Streptavidin-EU	Streptavidin-europium
Streptavidin-RPE	Streptavidin R-Phycoerythrin
Sulfo-NHS	N-hydroxysulfosuccinimide
TARDBP	Transactive Response DNA Binding Protein
tau-ir	Tau – immunoreactive
TDP-43	TAR-DNA binding protein 43 kDa
TFA	Trifluoroacetic acid
TH	Tyrosine hydroxylase
TMB	3,3′,5,5′-Tetramethylbenzidine
Ub	Ubiquitin
ub-ir	Ubiquitin – immunoreactive
UCL	University College Hospital, London
ULOQ	Upper Limit of Quantification
UPDRS	United Parkinson's disease Rating Scale
UPS	Ubiquitin Proteasome Pathway System
V	Volt
VS	Validation Sample

Formulae used

% difference and % RE	((observed – expected)/expected *100)
% CV or CV%	(SD/mean)*100

Chapter 1: Introduction

1.1 Project Overview

The general goal of this project was to develop and validate a biomarker multiplex assay system utilising the bead based Luminex technology (refer to Chapter 2b for details on this method). The multiplex system was used to analyse a range of plasma/CSF samples associated with various neurodegenerative diseases.

α-Synuclein and DJ-1 are amongst the most sought after biomarkers related to α-synucleinopathies and interest in LRRK2 has risen dramatically too.

It was initially thought that α-synuclein exists solely as an intracellular protein due to the lack of a "signal sequence" directing the protein to the endoplasmic reticulum (ER) for secretion into the extracellular space. However, revelations showing the presence of α-synuclein in CSF and blood plasma have now led to the theory that neurones secrete α-synuclein into the circulatory system (El-Agnaf *et al*, 2003; Lee *et al*, 2006a). Although the mechanisms involved in the secretory pathway of α-synuclein are not yet fully understood, the possibility and interest for using α-synuclein as a biomarker for various neurodegenerative diseases has since intensified.

Research into DJ-1 levels in CSF has been performed on cross sectional samples taken from Parkinson's disease (PD) and healthy control samples (Waragai *et al*, 2006; Hong *et al*, 2010, Herbert *et al*, 2014). Fewer studies investigating DJ-1 levels in plasma have been reported (Waragai *et al*, 2007; Shi *et al*, 2010). In this project, plasma and CSF samples from individuals with a range of neurodegenerative disorders, including PD, multiple system atrophy (MSA), dementia with Lewy bodies (DLB) and Alzheimer's disease (AD), have been analysed in order to ascertain if DJ-

1 has the potential to differentiate the various disease groups from healthy individuals, as well as to differentiate between clinically similar diseases.

LRRK2 is a relatively novel protein – its use as a biomarker has not been determined so far. Its physiological role is not fully understood but a lot of interest into the protein has been generated from findings that multiple mutations in *LRRK2* are associated with the onset of PD. The initial aim of this project regarding this protein is to see if LRRK2 is detectable and thus measurable in human biological fluids such as CSF and plasma.

By developing a multiplex assay in which biomarkers such as α-synuclein, DJ-1 and LRRK2 are included, the aim is to ascertain whether there is a trend in certain biomarker levels that will allow differentiation between clinically similar neurodegenerative disorders. Furthermore, by analysing these protein levels in both CSF and plasma, this project will show whether there is a correlation between peripheral levels of particular proteins and the diseased brain pathology.

1.2 Chapter Overview

The formation and accumulation of insoluble protein aggregates has been implicated in the pathogenesis of many diseases, including, sickle cell disease (Horwich, 2002), α-1-antitrypsin deficiency (Gregersen *et al*, 2005) and neurodegenerative diseases (Aguzzi *et al*, 2010). These disorders are collectively termed “amyloidoses”, due to protein aggregates presenting themselves as highly ordered cross-β-spine structures named amyloid fibrils (Aguzzi *et al*, 2010).

In order to design and implement therapeutic strategies for the management of protein aggregation diseases, it is important to understand why protein aggregates occur, the mechanisms leading to their formation and what pathological changes they exert. This chapter commences with an overview on the current theories related to how protein aggregates occur, including a discussion on the role of Molecular Chaperones and the Ubiquitin Proteasome System (UPS).

The chapter continues with particular focus on protein aggregation in neurodegenerative disease. Neurodegenerative diseases include AD, PD, DLB, fronto-temporal lobar dementia (FTLD), motor neurone disease (MND) and prion disease (Kokalj *et al*, 2005). PD, DLB, and MSA will be the main disorders discussed in this report, with a description on the role of some of the major proteins implicated in their pathogenesis; α-synuclein (PD, DLB, MSA), DJ-1 (PD) and LRRK2 (PD).

The report concludes by highlighting the potential use of these proteins as biomarkers which sets the scene for the subsequent research project.

1.3 Protein Aggregation and Disease

The human body contains approximately 100,000 different types of proteins which all have a vital role to play in virtually every chemical process upon which our lives depend (Dobson, 2004).

Post translation, each polypeptide chain adopts a unique folded tertiary structure. The biological activity and flawless functionality of each protein is dependent on the act of protein folding. The importance of protein folding has encouraged a great interest into this phenomenon. Dobson (2004) has summarised very effectively the proposed ideas on how proteins fold and what factors influence the final protein structure. Protein folding does not involve a simple cascade of events that take place in a step by step fashion; instead, evidence has indicated that protein folding involves a "stochastic/random" search of the many conformations available to a newly synthesised polypeptide chain. Amongst these various structures, the fold that achieves the most stability under physiological conditions is the fold that is most favoured. This stochastic approach is also referred to as the "new view" and employs the concept of "energy landscapes", where the final structure of a protein is the conformation that requires the least free energy (Dobson, 2005).

The number of different conformations available to a newly synthesised polypeptide chain is vast and complex, thus the prospect and occurrence of misfolding is inevitable. The cause of many diseases, including some important neurodegenerative diseases, has been attributed to the occurrence of misfolded proteins (Wolozin, 2012). In various diseases misfolding of the protein can diminish or alter its normal functionality, leading to some of the symptomatic effects associated with the disease.

Furthermore, the misfolded proteins can also form aggregates within cells in the form of intracellular inclusions or in the extracellular space as amyloid fibrils (Dobson, 2005).

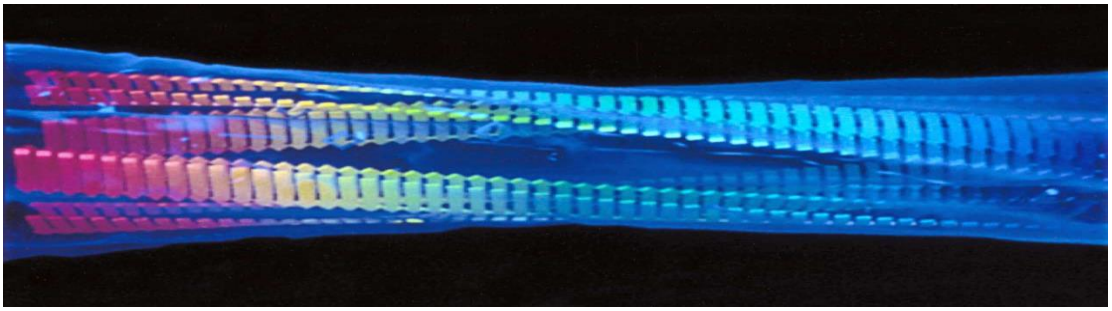

Figure 1.1: Image of an amyloid fibril: *A molecular model of an amyloid fibril derived from cryo-EM analysis. The fibril consists of four protofilaments twisted around one another, forming a hollow tube with a diameter of 6 nm (Dobson, 2004).*

Each amyloid disease (amyloidosis) involves the aggregation of one or more specific proteins, protein fragments or peptides. Studies have revealed important features of protein aggregates that have allowed scientists to theoretically piece together the steps leading up to protein aggregation. The core structure of amyloid fibrils is found to be stabilised by hydrogen bonds, primarily involving the protein "main chain/backbone" that is common amongst all proteins – this explains why protein fibrils with very different amino acid sequences can form fibrils that are ultra-structurally very similar. The protein aggregation process can be split into three major stages:

- Stage 1: Formation of oligomers – involves monomeric proteins binding to one another. They are often described as being disorganised structures that expose hydrophobic areas of the protein that would normally be hidden. In some cases, oligomers have been reported to exhibit a distinct structure in the form of a "doughnut" shape.

- Stage 2: Formation of protofibrils or protofilaments – the oligomeric structures enjoin to form short, thin, sometimes curly fibril like species.

- Stage 3: Formation of mature fibril – the protofilaments associate laterally and twist around each other to form a mature fibril that constitutes the main component of the aggregate (Dobson, 2004).

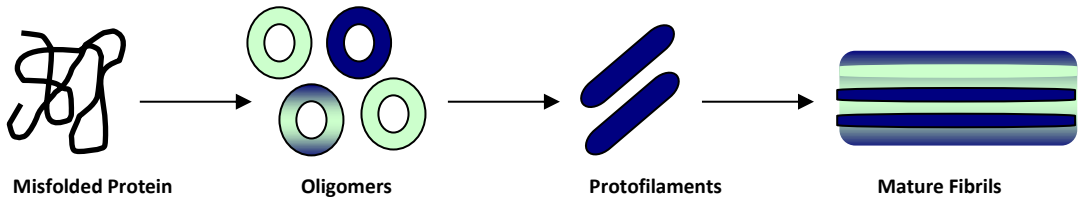

Figure 1.2: Protein Aggregation Process: *Diagram illustrating the stages leading to amyloid fibrilisation.*

It is yet debatable at which stage the aggregate elicits its toxic effect, i.e. is it the final fibril or the prior structures?

In the overall scheme of things, the process of protein synthesis is highly complex. Its efficiency is a testament to evolutionary biology, where the physiologically favoured protein structures have been passed through generations via natural selection. Furthermore, the human body is equipped with quality control mechanisms in order to minimise the risk and occurrence of misfolded proteins and their undesired effects. Unfortunately, the existence of misfolded protein diseases makes it clear that misfolding still occurs, and it has been proposed that in diseased states, such quality control mechanisms may be faulty or inadequate. The combinatory actions of molecular chaperones, the ubiquitin proteasome system (UPS) and the autophagy lysosomal pathway (ALP) form the major quality control mechanisms, and are described in subsequent sections.

1.4 The Ubiquitin Proteasome System

Molecular chaperones act to prevent the actual misfolding of proteins and are defined as proteins that aid other proteins in reaching their native stable conformational state. They are also known as “heat shock proteins” (HSPs). The name originates from the fact that their levels are abundantly increased in response to stressed conditions such as increase in temperature, and more relevantly, during an increase in the concentration of protein intermediates prone to aggregation (Frydman, 2001).

In brief, chaperones/HSPs perform their role by binding to the protein being synthesised on a temporary basis until the protein folding is complete. It has already been established that proteins undergo a search for the conformation that suits them in terms of their physiological stability. During this search, the protein passes through a stage where it exists in a partially folded state. These partially folded proteins expose hydrophobic amino acid residues which can encourage misfolding and aggregate formation. Chaperones/HSPs bind to these hydrophobic amino acid residues to prevent this misfolding. If however, misfolding has already occurred, Chaperone/HSPs have the ability to direct the offending protein to either be refolded or undergo protein degradation (Hartl *et al*, 2011). The latter activity, involving protein degradation, is when the UPS comes into play.

Muchowski *et al* (2005) and Lecker *et al*, (2006) have very elegantly and simply highlighted the role of the UPS in proteolytic degradation. The UPS involves a series of ATP-dependent enzymatic reactions. These enzymatic activities link chains of a polypeptide co-factor, ubiquitin (Ub), onto proteins that are destined to be degraded.
It has been mentioned previously, that protein aggregates associated with different diseases share many morphological features (Dobson, 2004). Another similar trait is that the aggregated proteins are often ubiquitinated and associated with

chaperones/HSPs (Huang *et al*, 2010). This suggests that the functionality of these two systems may be defective to some extent.

Many amyloid diseases including those involved in neurodegeneration are diseases of old age. Soti *et al* (2002) define ageing as "a multicausal process leading to a gradual decay in self defensive mechanisms" (Soti *et al*, 2002). The slow breakdown of self-defensive mechanisms that normal cells rely on for homeostasis results in an accumulation of damage at a molecular level. In relation to protein misfolding, such damage reflects stressful conditions in which the demand for chaperone/HSPs and UPS activity is greatly increased. It is proposed by Soti *et al* (2002), that chaperones/HSPs and UPS struggle with this sudden high demand, as ageing progresses, the need for these protective systems increases even more. In addition, Huang *et al* (2010), state that proteasome function declines with age. Studies with *Drosophila Melanogaster* have revealed reduced ATP levels in old flies when compared to levels in young flies. The 26S proteasome degradation unit is ATP driven, thus supporting the theory that ageing decreases the quality control mechanisms associated with maintaining cell homeostasis and preventing diseased states (Soti *et al*, 2002). This could be one of the reasons why protein misfolding diseases often occur in old age.

1.5 Autophagy Lysosomal Pathway

The UPS and ALP are two independent but complementary degradation systems - when one system fails the other compensates. The term "autophagy" is greek for "self-eating" and involves degrading and decomposing target components using the lysosomal compartment. The pathway can be divided into three types:

I. *Chaperone mediated autophagy (CMA):* as the name suggests, the actions of a chaperone; specifically cytosolic hsc70, is pivotal to this system (Chiang *et al*, 1989). The CMA pathway is unique since it only degrades proteins that have a specific amino acid sequence – KFERQ, this motif is found in approximately 30% cytoplasmic proteins (Dice, 1990). Hsc70 binds to proteins with this particular amino acid sequence which is then directed to the lysosomal membrane where it interacts with LAMP-2A to initiate a series of downstream events leading to the degradation of the protein (Cuervo *et al*, 1996; Agarraberes *et al*, 1997; Eskelinen *et al*, 2005).

II. *Macroautophagy:* this system is defined by the formation of *de novo* double membrane bound vesicles, called autophagosomes, as a way of isolating and taking components to be degraded to the lysosomes (Noda *et al*, 2002; Kraft *et al*, 2012). The outer membrane of the autophagosomes then fuses with the lysosome to receive its constituents, including, lysosomal hydrolase. Lysosomal hydrolase degrades the autophagosomal membrane and its contents.

III. *Microautophagy:* first proposed by de Duve and Wattiaux around 50 years ago (de Duve and Wattiaux, 1966). In contrast to macroautophagy, the components to be degraded are directly engulfed by the lysosomes as opposed to being isolated and delivered to lysosomes via autophagosomes.

Amongst the many proteins destined to be degraded by the ALP is α-synuclein. The importance and relevance of this protein to disease is discussed in subsequent sections, but in summary, the aggregates of this protein are the pathological hallmarks of a range of diseases that fall under the “synucleinopathies” group. Monomeric α-synuclein can be degraded by both the UPS and ALP (Liu *et al*, 2003; Cuervo *et al*, 2004), but oligomeric and aggregated forms of the protein are

predominantly degraded by the ALP (Lee *et al*, 2004). Studies by Cuervo *et al* (2000) have shown that LAMP-2A down regulation, decreasing CMA activity is observed in ageing. In addition, certain genetic mutations, namely A53T, in the α-synuclein gene *SNCA* associated with the onset of PD have been shown to block the CMA pathway (Xilouri *et al*, 2009). There is not much evidence linking α-synuclein to microautophagy but overexpression of α-synuclein has been shown to interfere with macroautophagy (Winslow *et al*, 2010) and its aggregates have been shown to inhibit it (Tanik *et al*, 2013).

1.6 Protein Aggregation and Neurodegenerative Diseases

Neurodegenerative diseases involve the degeneration of a specific subpopulation of nerve cells in the CNS, which lead to the disease related clinical symptoms. Many neurodegenerative diseases are associated with an accumulation of abnormally folded proteins. Table 1.1 lists the neurodegenerative disease and the corresponding misfolded protein:

Neurodegenerative disease	Protein(s) implicated
AD*	β-amyloid (Aβ), tau
PD**	α-synuclein
FTLD*	TDP-43, FUS, tau
MND*	TDP-43, FUS, SOD-1
DLB**	α-synuclein
Huntington's disease (HD)*	Huntingtin
Prion diseases***	Prion protein (PrP)

Table 1.1: Misfolded proteins associated with neurodegenerative diseases:
** summarised from Dunning et al, 2010. ** Spillantini et al, 1998. ***Prusiner et al, 1982*

1.7 α-Synucleinopathies

The neurodegenerative diseases studied for the purpose of this project are referred to as the "synucleinopathies". As the name suggests and as briefly mentioned in section 1.5, this disease group is comprised of disorders that share a common pathological feature – protein aggregates formed of α-synuclein. PD, DLB and MSA are amongst the disorders included in this group. α-Synuclein was first described in 1988 by Maroteaux *et al*, but the defining studies strongly implicating the protein in neurodegenerative disease came from genetic findings showing that genetic mutations in the *SNCA* coding for α-synuclein lead to disease (Polymeropoulos *et al*, 1996; Polymeropoulos *et al*, 1997; Kruger *et al*, 1998; Zarranz *et al*, 2004) and that this protein is found in the inclusions that have become the pathological hallmarks for these disorders (Spillantini *et al*, 1997; Iwatsubo *et al*, 1996; Spillantini *et al*, 1998; Wakabayashi *et al*, 1998a; Wakabayashi *et al*, 1998b). The role of α-synuclein in PD, DLB and MSA are discussed in the following sections.

1.8 Overview of Parkinson's Disease

Neurodegenerative diseases can be broadly categorised into three groups; movement disorders, neuromuscular disorders and dementing disorders. Parkinson's disease (PD) falls primarily under the movement disorder category.

The classical features of PD include tremors, rigidity, bradykinesia (slow, reduced movement) and postural instability. Although, PD is often classified as a movement disorder, during the advanced stages, affected individuals can exhibit episodes of depression or anxiety and develop dementia (Aarsland *et al*, 2003; Hely, 2008).

PD is the second most common neurodegenerative disease following AD. Statistics estimate that PD carries a 2% lifetime risk of development (Dunning *et al*, 2012).

Age has been shown to be a major risk factor for the disease, with the percentage of affected individuals within a population rising from 1% at 65 years old to 5% at 85 years old. Most cases are idiopathic, but some cases show a clear genetic correlation. Many gene mutations have been revealed to be strongly linked to the onset of PD (Wood-Kaczmar *et al*, 2006) and some of them are associated with protein misfolding and aggregation, key examples of which are *PARKIN* (Kitada *et al*, 1998), which encodes a ubiquitin protein ligase.

1.8.1 History and Aetiology of Parkinson's Disease

References to this disease date back to AD175, where it is referred to as the "shaking palsy syndrome", by a Physician known as Galen. Post this citation; there is no mention of the disease in any western literature until 1817, when a London physician called James Parkinson authored a detailed medical essay, adeptly titled "An essay on the shaking palsy". The publication revolves around individuals from the doctor's neighbourhood who presented with the disease. The intention of the essay was and is fairly transparent - to encourage and highlight the need for research in to the disease and have it recognised as a specific medical condition. It wasn't until approximately 60 years later that these intentions proved fruitful. A French neurologist, Jean Martin Charcot, built upon Parkinson's case studies and promoted recognition of the condition to an international level. Charcot renamed the "shaking palsy syndrome" as Parkinson's disease in reverence to the immense work that Dr. James Parkinson performed in order to bring medical attention to this debilitating condition (www.parkinsons.org).

For many decades, it was believed that the sole pathological feature and cause of PD was the progressive loss of dopaminergic neurones in the substantia nigra (SN)

of the brain, which decreased the level of neurotransmission into the basal ganglia, causing the movement disorders typical of PD.

Advances in the PD research field have now revealed that as well as the loss of dopaminergic neurones in the SN, surviving neurones within the SN and other brain regions contain insoluble protein inclusions. These protein inclusions are found in the neuronal cell body and/or neuronal processes. Inclusions in the cell body are referred to as Lewy bodies (LBs) and those enclosed in the neuronal processes are called Lewy neurites (LNs). The terminology originates from the first founder of this pathological feature, Friedrich Lewy (Lewy, 1912). LBs appear as spherical globules, consisting of a dense core surrounded by a pale stained halo of radiating filaments. LNs appear as a thread-like structure (Forno, 1996). Both LBs and LNs have been found to be enriched with filaments of a protein called α-synuclein, as well as other proteins and they are often highly ubiquitinated (Shimura *et al*, 2001; Hasegawa *et al*, 2002).

1.8.2 Diagnosis and Treatment of Parkinson's Disease

The diagnosis of PD is heavily reliant on patient history and examination of visible symptoms (Savitt *et al*, 2006). A scoring device named The United Parkinson's Disease Rating Scale (UPDRS) has been generated in order to provide a standardized assessment tool and a means of tracking and documenting disease and treatment progression. The scale is subdivided into four categories - mental effects, limitations in activities of daily living, motor impairment and treatment complications. A diagnosis of PD is attained if the following cardinal signs are visible upon physical examinations:

- Distal or resting tremor of 3 to 6 Hz
- Rigidity
- Bradykinesia
- Asymmetrical onset

The clinical manifestations of PD are very similar to some other neurological disorders. For instance, resting tremor is the most common feature amongst PD patients, yet, 20% of patients with autopsy confirmed PD fail to display this clinical feature (Suchowersky *et al*, 2006). Furthermore, even after careful examinations, the level of PD misdiagnosis is stated to be at approximately 25% (Hughes *et al*, 2001; Savitt *et al*, 2006). Thus, the clinical heterogeneity of PD compromises accurate diagnosis. There are certain factors that aid in ruling out PD, such as lack of response to PD treatments and presence of dementia. Advances in brain imaging techniques have not provided much advantage since a specific pattern that can be assigned to PD has not been established, but can aid in ruling out or confirming other ailments such as brain tumours (Rao *et al*, 2006).

The discovery that PD is due to a loss of dopaminergic neurones has led to treatment strategies aimed at replacing the lost dopamine levels. Unfortunately, dopamine does not cross the blood brain barrier and therefore cannot be administered directly as a form of therapy. However, the dopamine precursor Levadopa (L-Dopa) does cross the blood brain barrier and has become the gold standard mode of treating PD. During the early years of using Levadopa, extremely high doses were required to have significant effects. These high doses led to undesired side effects such as nausea and vomiting. It was made apparent that these adverse effects were due to the rapid breakdown of L-Dopa by the enzyme dopa-decarboxylase (DDC), in the periphery of the body before it enters the brain. Administering Levadopa in conjunction with a peripherally acting DDC inhibitor, reduced the required dosage of

L-Dopa by 70%. Unfortunately, by inhibiting DDC, another enzyme was found to breakdown dopamine, called Catechol-O-methyl transferase (COMT). Thus, currently, L-Dopa is administered together with both a peripheral DDC inhibitor and peripheral COMT inhibitor. This drug cocktail increases the levels of L-Dopa reaching the brain where it can be metabolised into dopamine and utilised as a neurotransmitter (www.epda.eu.com).

There is no cure for PD but treatment methods are aimed at relieving symptoms in order to make lives more comfortable for patients. Treatment strategies are flexible and are designed for various stages of the disease (Savitt *et al*, 2006; www.parkinsons.org).

Early stage treatment involves using L-Dopa with DCC and COMT inhibitors. Dopamine agonists that stimulate dopamine receptors and mimic its actions are also used. The enzyme Monoamine Oxidase B (MAO-B) degrades dopamine at the nerve terminals, thus (MAO-B) inhibitors have also been used to alleviate mild symptoms seen in the very early stages of PD and reduce motor disabilities without the need for L-Dopa treatment. Patients are categorised into the early stage group if they have been diagnosed with the disease for less than five years (Rao *et al*, 2006).

Patients already receiving the L-Dopa treatment are grouped into the “late stage phase” of the disease. Approximately 40% of patients receiving L-Dopa treatment develop a “wearing off” effect, where the benefits of therapy dwindle and PD symptoms, such as motor complications reappear. Some patients also experience an “on and off” effect from L-Dopa therapy, where unpredictable fluctuations in the symptoms occur. Such late stage phase patients are given dopamine agonists or higher doses of the DDC and COMT inhibitors as an attempt to relieve the “wearing off” and “on and off” effect.

Patients within the advanced stages of the disease do not only contend with motor complications but may suffer from depression, anxiety and psychosis. Depression is treated with selective serotonin reuptake inhibitors. Psychosis is a side effect from the use of dopamine agonists and high doses of L-Dopa, therefore decreasing the dose of administration is a common way of managing these non-motor related symptoms. Surgical procedures have also become an option. Deep Brain Stimulation of the subthalamic nucleus has been shown to improve motor related symptoms associated with PD (Rao *et al*, 2006).

There are only a few options available for the treatment, and as explained these do not offer a consistent improvement in the quality of life for the patients. They also do not treat the on-going loss of dopaminergic neurones. This highlights the importance of continuing research into the underlying pathology behind PD. Further research may lead to more effective, reliable strategies as well as potential preventative measures.

1.9 Overview of Multiple System Atrophy

MSA is a progressive neurodegenerative disorder with patients experiencing symptoms that affect the autonomic nervous system and/or movement (Rehman, 2001). The disease is believed to affect 3 in 100000 persons worldwide and is considered as being rare, but this figure may not be accurate, since the symptoms of MSA in the early stages are very similar to PD and thus prone to misdiagnosis (www.patient.co.uk/doctor/multiple-system-atrophy). MSA is often categorised into two groups based on the symptoms that are most prominent during clinical examinations:

- MSA-P : also known as the Parkinsonian type. As the subtype name suggests, the dominating symptoms within this group are very similar to PD i.e. rigidity, tremors, gait and speech issues.

- MSA-C : referred to as the cerebellar type. The main symptoms are due to the degeneration of an area of the brain called the cerebellum and include the progressive loss of coordination and balance (Gilman *et al*, 2008 and www.multiplesystematrophy.org/about-msa/types-symptoms).

1.9.1 History and Aetiology of Multiple System Atrophy

The varying nature of the symptoms associated with MSA, originally resulted in the invention of three distinct diseases – Shy Drager syndrome, striatonigral degeneration and sporadic olivopontocerebellar atrophy - these terms are no longer used and all three diseases are now defined as MSA. Bearing this in mind, the first case of MSA may have been described in 1925 by Bradbury and Eggleston. The current terminology of MSA was not invented until 1969 (www.parkinsons.ie/Atypical-MSA).

The key pathological feature of MSA is the presence of α-synuclein aggregates in the form of cytoplasmic inclusions in the glial cells of the basal ganglia, primary motor cortices and the protocellebellar, giving rise to the aforementioned symptoms (Gilman *et al*, 2008 and www.msatrust.org.uk/wp-content/uploads/2011/07/MSA-Trust-Research-Strategy.pdf).

1.9.2 Diagnosis and Treatment of Multiple System Atrophy

Diagnosis of MSA is challenging since symptoms are very similar to PD and there are no tests that are specific to MSA. Thus, diagnosis is heavily reliant on the physical examination of visible symptoms, medical history and ruling out other possible causes of symptoms. MRI scans are often performed to dismiss other brain lesions as the source of symptoms. Tests designed to investigate the blood pressure control system and autonomic nervous system can aid with diagnosis too (Gilman *et al*, 2008 and www.mayoclinic.org/diseases-conditions/multiple-system-atrophy/basics/tests-diagnosis/con-20027096).

There is no cure for MSA, but treatments directed at alleviating symptoms are available.

Table 1.2 lists a few medications for some symptoms. The diverse range in symptoms involved in MSA means that a multidisciplinary team approach is required to ensure MSA patients are treated effectively whilst improving their quality of life (Gilman *et al*, 2008 and msatrust.org.uk/living-with-msa/newly-diagnosed/treatment-management-of-msa).

Clinical symptom	Medication	Comments
Movement problems	L-Dopa Amantadine	Used for treating PD symptoms. Response to L-Dopa has been found to be disappointing with MSA.

Clinical symptom	Medication	Comments
Bladder control	Antimuscarinic drugs Desmospray/Desmotabs (DDAVP)	Antimuscarinic drugs can reduce the urgency and frequency. DDAVP have the ability to reduce the amount of urine produced overnight – thus, may help with sleep patterns.
Erectile dysfunction	Sildenofil Todalofil Vordenafil	Caution must be taken with these drugs as they may cause high blood pressure.
Dizziness	Fludrocortisone Ephedrine	These drugs work to increase blood pressure, since dizziness is often attributed to low blood pressure.

Table 1.2: **MSA symptoms and medications:** c*ommon clinical symptoms associated with MSA and the medications given to alleviate such symptoms. Taken from* (msatrust.org.uk/living-with-msa/newly-diagnosed/treatment-management-of-msa).

1.10 Overview of Dementia with Lewy Bodies

DLB accounts for approximately 25% of dementia cases and is usually found in people aged 60 – 90 years. It presents itself with a mixture of AD and PD like symptoms (Breitve *et al*, 2014). In addition to dementia and movement disorders, DLB patients exhibit symptoms such as hallucinations, delusions, sleeping problems i.e. Rapid eye movement Behaviour Disorder (RBD) and anxiety (McKeith *et al*, 2005a).

1.10.1 History and Aetiology of Dementia with Lewy Bodies

As the name suggests, the pathological feature for DLB is the presence of Lewy bodies (LB) and Lewy neurites (LN) similar to those found in PD, in the cortical and limbal regions of the brain. The distribution of these abnormal α-synuclein aggregates differ slightly between PD and DLB. In DLB affected brains, the LBs and LNs are more concentrated in the cortical area, as opposed to the substantia nigra where they are prominent in PD affected individuals (Armstrong, 2014).

DLB is sporadic, with a very low genetic association. A study investigating risk factors for DLB revealed that depression and low caffeine intake increases the risk for developing DLB (Boot, 2013), however there is no one definitive cause for DLB.

1.10.2 Diagnosis and Treatment of Dementia with Lewy Bodies

A single test to conclusively diagnose an individual with DLB is non-existent. As discussed for other neurodegenerative disorders, diagnosis is reliant on physical assessments of visible symptoms and careful judgement by the specialists involved. The heavy overlap of DLB symptoms with AD and PD has led to criteria designed to help differentiate between the clinically similar conditions.

To distinguish between DLB and PD the following rules are used (McKeith *et al*, 2005a and www.alz.org/dementia/dementia-with-lewy-bodies-symptoms.asp):

- Diagnosis is PD if movement issues present themselves at least 1 year before the onset of dementia.
- Diagnosis is DLB if dementia develops at least 1 year before or simultaneously with movement problems.

The following guidelines are adopted to help differentiate between DLB and AD (www.emedicine.medscape.com/article.com/article/1135041-overview):

- Memory loss is a dominating symptom in the early stages of AD compared to DLB
- Visual hallucinations are more frequent in the early stages of DLB compared to AD
- RBD is more common in early DLB patients compared to AD. Ferman *et al* (2011) followed 234 neurodegenerative patients until autopsy and suggested that RBD could be used as a core clinical feature to improve diagnostic accuracy for DLB.

There is no cure for DLB, but treatments designed to manage symptoms do exist. Medications used for alleviating AD and PD symptoms are obviously ideal for treating DLB. Medicines include acetylcholinesterase inhibitors to help with hallucinations, Memantine to improve cognitive functions, L-Dopa to ease movement and coordination issues and anti-depressants to relieve depressive symptoms (www.emedicine.medscape.com/article/1135041-treatment).

1.11 α-Synuclein

α-Synuclein belongs to a family of proteins known as “the synucleins”. Other members of the family include β- and γ-synuclein. The genes coding for α-, β- and γ-synuclein proteins are located on chromosome 4q.21.3 - q22 and are referred to as the *SNCA, SNCB and SNCG* genes, respectively (Goedert, 2001; George, 2002).

α-Synuclein is a much conserved, acidic, 140 amino-acid residue long protein, with an approximate molecular weight of 14 kDa. It is abundantly found residing in neuronal presynaptic terminals and in close proximity to synaptic vesicles. In some diseased states, it has been hypothesised that the synuclein inclusions appear early in the disease process and follow a sequence of ascension, commencing from the lower brainstem and then spreading up towards to the central and wider cortical areas (Braak *et al,* 2003; Mckeith *et al* 2005a; Kovacs *et al*, 2014; Vekrellis *et al*, 2011).

The fact that an aggregated form of α-synuclein is a key feature of the aforementioned neurodegenerative disorders has encouraged research into the physiological role of this protein. Since the functionality of a particular protein is closely related to its structure, many studies have been conducted in order to deduce the structure of α-synuclein. The primary structure of α-synuclein has been shown to consist of seven, 11-residue repeat sequences that form five amphiphatic α-helices within the amino terminal region of the protein. Helices 1 to 4 are predicted to be involved with binding to lipid vesicles and helix 5 appears to be responsible for protein-protein interactions. The acidic carboxyl terminal region is believed to remain unstructured and may have a role in hindering fibril formation (Eliezer *et al,* 2001; Bisaglia *et al*, 2009). Between the two terminals, residues 61 to 95 make up the

most hydrophobic region that is hypothesised to be the aggregate-prone area (Beyer, 2006).

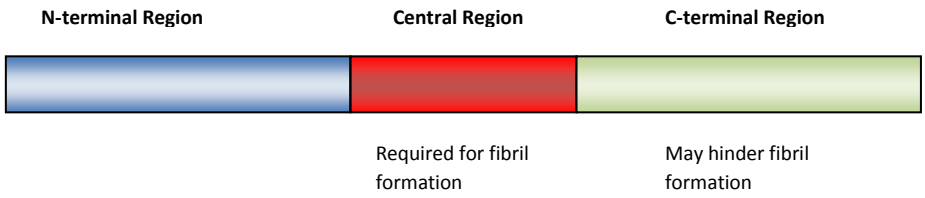

Figure 1.3: α-Synuclein structure: *Diagram showing the three sections of α-synuclein; N-terminal, Central and C-terminal regions* (Bisaglia *et al*, 2009)

There are different opinions with regard to the structural state of α-synuclein intrinsically under physiological conditions. α-Synuclein is described to be an intrinsically unstructured protein lacking a well-defined secondary or tertiary structure (Bisaglia *et al*, 2009). It is widely accepted that α-synuclein resides in an unfolded state until it binds to or comes into contact with the acidic phospholipids on membranes and synaptic vesicles (Yates, 2011). However, findings by Bartels *et al* (2011) challenge this opinion. They have proposed that α-synuclein actually exists as a tetramer made up of four α-helical structures bound together. In normal conditions these tetramers do not aggregate, but in pathological cases these tetramers are somehow destabilised and then become prone to aggregation. Bartels *et al* (2011) state that the protein may have been unfolded in other scientific studies due to the harsh conditions used during the experiments or due to the proteins being expressed in *E. coli* bacterium. Bartels *et al* (2011) claim to have studied α-synuclein protein purified from human cells using gentler methods. The native structure of α-synuclein is therefore debatable, but the link between α-synuclein aggregation and neurodegenerative disorders is indisputable (Bartels *et al*, 2011).

1.11.1 Normal Physiological role of α-synuclein

α-Synuclein is heterogeneously expressed in the human brain, with highest levels found in the SN and is normally a presynaptic protein. It is synthesised in the cell body and transported to the nerve terminals via axonal transport (Lykkebo, 2002). The normal physiological role for α-synuclein is poorly understood, but structural studies in conjunction with transgenic mouse models have resulted in a few suggestions, which will be discussed (Vekrellis *et al*, 2011; Beyer, 2006; Bisaglia *et al*, 2009).

Proteins with a disordered structure possess key features such as the ability to bind to distinct partners with high potential binding strength and increased speed of interaction. Such features are found in many chaperones. The disordered structure of α-synuclein suggests that this protein may also serve as a chaperone. It has been found that α-synuclein shares homology with the phospho-dependent signalling chaperone protein 14-3-3 (Ostrerova, 1999). 14-3-3 is known to bind to tyrosine hydroxylase – an enzyme involved in the rate limiting synthesis of dopamine. Similarly, α-synuclein has been shown to bind to tyrosine hydroxylase and regulate the concentration of cytoplasmic dopamine (Bisaglia *et al*, 2009; Recchia *et al*, 2004).

α-synuclein knockout mice demonstrate a lacklustre neurological phenotype. In particular, the mice show a reduction in the number of vesicles in the presynaptic pool. Thus, α-synuclein may play a role in the trafficking of synaptic vesicles (Lashuel *et al*, 2013; Bellani *et al*, 2010). Synaptic vesicles are mainly composed of lipids and store various neurotransmitters. From structural studies, the N-terminal region of α-synuclein has been shown to bind to lipid membranes, strengthening the possibility of this role for α-synuclein. Burre *et al* (2010) have provided further evidence in support of this theory. The phenomenon of neurotransmission requires a

series of tightly co-ordinated reactions that involves generating a membrane fusion complex. The core component of this membrane fusion complex is Soluble NSF Attachment Protein (SNARE). During each neurotransmitter release, the protein fusion complex undergoes assembly followed by disassembly. It is suggested that α-synuclein plays a vital role in promoting the assembly of the membrane fusion complex by interacting with SNARE. More specifically, the N-terminal region of α-synuclein may bind to the phospholipid membrane and the C-terminal region to the SNARE protein synaptobrevin-2 (Burre *et al*, 2010). Furthermore, a genome wide screening in yeast reveal that approximately one third of the genes that enhance the toxicity of α-synuclein are involved in vesicle trafficking (Bisaglia *et al*, 2009).

A novel physiological role for α-synuclein has emerged recently, implicating α-synuclein in the sustenance of nerve terminals and protecting them from cell death. It has already been mentioned that the protein 14-3-3 is a chaperone that binds to tyrosine hydroxylase. 14-3-3 has additional jobs as a participant in neuronal development, cell growth control and regulating apoptosis. Xu *et al* (2002) have claimed that α-synuclein binds to 14-3-3, forming a 54 to 83kDa protein complex. It is suggested that α-synuclein binds to 14-3-3 as an attempt to prevent apoptosis and give the cell a chance to recuperate from the damage it has undergone or deal with the stress it is under.

In summary, while the exact physiological function of α-synuclein is still work in progress, its conformational flexibility and disordered structure has shed light onto the possible roles it may play. It is not entirely necessary for synaptic formation and cell survival but plays a vital role in neuronal sustenance.

1.11.2 The α-synuclein aggregation model

Under certain conditions, α-synuclein misfolds into a β-sheet conformation and gradually assembles into fibrils with a typical amyloid like morphology. This conformational change is referred to as the "aggregation" process and is believed to be the causal factor behind the neuronal toxicity typical of PD and other α-synucleinopathies. (Vekrellis *et al* 2011). Amyloid fibrils are structurally classed into two groups:

I. *Fibrils generated from already folded proteins via the refolding mechanism or the gain of interaction model*. The refolding mechanism is adopted by proteins that natively exist as folded proteins. These proteins unfold and then refold into a β-sheet enriched secondary structure that resembles the amyloid fibril configuration. Fibrils generated from the gain of interaction method are rather more complicated. This model involves proteins with regions that are natively disordered, exposing a previously inaccessible region of its structure and binding to the surfaces of other proteins to gradually build an amyloid fibril (Breydo *et al*, 2011).

II. *Fibrils generated from intrinsically unfolded/disordered proteins*. Fibrils composed of α-synuclein belong to this structural class. α-synuclein exposes a hydrophobic region that interacts with other α-synuclein proteins to form a well-defined β-sheet containing secondary structure (Serpell, 2000).

The review by Breydo *et al* (2012) summarises a collection of structural studies performed to elucidate a more detailed structural picture of the α-synuclein amyloid fibril. These studies have used x-ray crystallography and x-ray diffraction methods to reveal that α-synuclein amyloid fibrils are formed from several β-strands running in

parallel to one another. Furthermore, the side chains protruding from any two β-sheets within the fibril, interlock with one another to form “steric zippers”. These steric zippers prevent water from reaching the interface between the two strands, which explains the insoluble property of amyloid fibrils (Breydo *et al,* 2012).

The aggregation process of α-synuclein is nucleation dependent, requiring the formation of “fibril nuclei” in order to generate the finalised fibrillar aggregate (Wood, 1999). The fibril nuclei are the oligomeric intermediates that are randomly formed from partial folding and interactions between individual monomers. Following the formation of fibril nuclei, a fibril literally grows by adopting a “dock and lock” mechanism, in which free α-synuclein monomers bind to (dock onto) previously buried and now exposed regions of the oligomer in an irreversible manner (lock) (Esler *et al,* 2000).

The aggregation of α-synuclein is a multistep process, thus in order to direct therapeutic strategies onto a successful pathway it is important to identify which part of the process is actually eliciting the neurotoxic effects and how. Three mechanism of how aggregation may lead to neurotoxicity have been proposed:

The first proposed mechanism is “toxic gain of function”, where in simple terms, α-synuclein adopts a neurotoxic property. α-synuclein has been shown to undergo cytotoxic modifications when exposed to metals such as iron and copper as well dopamine metabolites. The significance of copper interactions is yet to be identified, but the environment in which α-synuclein is largely present, i.e. presynaptic terminals of the SN, is high in iron and dopamine metabolite content (Dickson, 2001).

The second proposed mechanism is “toxic loss of function”. The possible loss of the quality control systems UPS and chaperones have already been discussed in

previous sections. In addition to these systems being dysfunctional, it is proposed that in pathological conditions where α-synuclein is sequestered in an aggregated form, it is no longer available to perform its normal duties. One of the roles of α-synuclein is to control dopamine levels by acting as a negative regulator for tyrosine hydroxylase. A failure to suspend the activities of tyrosine hydroxylase results in an increase in dopamine levels. Cell death due to high levels of dopamine is believed to be caused by the formation of highly reactive oxygen species that create an environment of oxidative stress leading to neuronal cell death (Dickson, 2001).

The final suggested mode of neurotoxicity is “mechanical disruption”. Oligomers also known as fibril nuclei, have been shown to have the ability to penetrate through cellular membranes and create pore-like channels. The formation of these pores abnormally increases the membranes ionic permeability and cause cell death (Bennett, 2005; Breydo *et al*, 2011).

1.11.3 The α-synuclein “prion-like” hypothesis

The possibility that proteins implicated in the pathogenesis of various neurodegenerative disorders behave in a “prion-like” manner has been proposed. A prion is a type of misfolded protein that can recruit and trigger normal proteins to fold abnormally via a self-templating model. Prion proteins also have the ability to transfer from cell to cell and thus act as an infectious agent that confers disease onset and its progression (Griffith 1967; Prusiner, 1982). Prion diseases include scrapies, bovine spongiform encephalopathy (BSE) and Creutzfeldt-Jakob disease (CJD) (Cullie *et al*, 1939; Chandler, 1961; Gibbs *et al*, 1968; Bradley, 1991).

The protein α-synuclein has been proposed to behave in a prion-like manner. This prion-like behaviour originated from findings that embryonic dopaminergic neurones transplanted into the putamen of PD patients developed α-synuclein positive inclusions; 11-16 years post transplantation. It was suggested that this time period was not enough for such inclusions to be generated naturally, and thus the possibility of α-synuclein spreading from diseased areas to non-diseased areas was proposed (Kordower *et al*, 2008; Brundin *et al*, 2008). The possible mechanism for α-synuclein self-templating and transmitting from cell to cell is as follows:

- Misfolded α-synuclein can access the extracellular space via exocytosis or nanotubes (Emmanouilidou *et al*, 2010). This is consistent with detectable levels of α-synuclein in extracellular fluids such as plasma and CSF (discussed in chapters 5 and 6). Alternatively, misfolded α-synuclein may also be transmitted via direct synaptic contact
- Neighbouring cells internalize the α-synuclein via passive diffusion, endocytosis and/or nanotubes (Hansen *et al*, 2011).
- Within the cells, α-synuclein acts as a seed and induces normal α-synuclein to undergo a conformational change and conjoin with the misfolded protein to generate amyloid like fibrils.

Evidence for α-synuclein being a prion is still in its infancy. The most compelling evidence includes the research reported by Luk *et al* (2012), where non-transgenic mice, inoculated with preformed α-synuclein fibrils, generated a clear time and connectivity spread of α-synuclein inclusions with abundant pathology in the dopaminergic neurones of the substantia nigra. This pathology was not observed in mice lacking α-synuclein – suggesting that host α-synuclein is necessary for α-synuclein pathology. Current studies reported by Prusiner (2015) supports the idea

of α-synuclein being a prion, but, it is important to stress that this prion-like behaviour for α-synuclein is still in its infancy. It is still not clear whether, the results observed in transgenic mice is translatable into humans and furthermore, there is no evidence of α-synuclein being contagious which is a feature that prion proteins responsible for BSE, CJD and scrapies, possess (Irwin *et al*, 2013).

1.12 DJ-1

The *DJ-1* gene was initially identified as a novel oncogene by Nagakubo *et al* (1997). Later, in 2003, research by Bonifati *et al* (2003) revealed data that linked the *DJ-1* gene with the onset of PD. Bonifati *et al* (2003) showed a 4 kD homozygous chromosomal deletion and a homozygous L166P missense mutation (Baulac *et al*, 2004), in Italian and Dutch PD patients, attributing *DJ-1* as a causative gene for familial PD with recessive inheritance. The link between *DJ-1* and PD has directed research into the physiological and pathological role of the DJ-1 protein.

DJ-1 is a 189 amino acid long protein that exists as a dimer (Cookson, 2003). The protein is comprised of seven β-strands and nine α-helices in total and is expressed in most cells and tissues, including neurones and glial cells of the brain (Ariga *et al*, 2013). Oxidative stress is amongst the various hypothesis associated with the cause of PD. It has been proposed that DJ-1 plays a neuroprotective role against oxidative stress and its loss of function may lead to PD pathogenesis (Baulac *et al*, 2004). Ariga *et al* (2013) have reviewed the physiological and pathological roles of DJ-1 which will be summarised and discussed in subsequent sections.

1.12.1 DJ-1: Physiological and Pathological role in disease

DJ-1 is a multifunctional protein involved in reducing the level of damage caused by oxidative stress. Its activity is highly dependent on the reduction of cysteine residue 106 (C106). During oxidative stress, the level of C106 reduction is proportional to the intensity and exposure time of oxidative stress, where C106 is first oxidised to SOH, then SO_2H, followed by SO_3H. DJ-1 is rendered inactive when C106 is oxidised to SO_3H, and it is this form of DJ-1 that is found in PD and AD patients (Bandopadhyay *et al*, 2004). This suggests that DJ-1 protects cells against oxidative stress by oxidising itself. Other protective measures against oxidative stress include transcriptional regulation, mitochondrial regulation as well as exercising chaperone activity (Lin *et al*, 2012).

DJ-1 has been shown to regulate the transcription of nuclear factor erythroid-2-related factor 2 (Nrf2), p53 and polypyrimidine tract binding protein associated splicing factor (PSF). The regulation of all three factors is important during anti-oxidative stress response (Ariga *et al*, 2013). Nrf2 normally resides in the cytoplasm as a protein complex with Keap1, which is then degraded by the UPS. However, under oxidative stress conditions, DJ-1 sequesters Keap1, resulting in the translocation of Nrf2 to the nucleus where it activates anti-oxidative stress genes with the aim to reduce ROS levels (Clements *et al*, 2006). p53 is a tumour suppressor gene and has the role of inducing apoptotic events in response to oxidative stress. DJ-1 binds to p53 in order to prevent apoptosis and give the affected cells time to repair themselves against damage (Kato *et al*, 2013). The PSF protein is involved in reducing transcription of the *tyrosine hydroxylase (TH)* gene. This gene encodes for the enzyme tyrosine hydroxylase which plays a vital role in dopamine synthesis. Tyrosine hydroxylase converts tyrosine to L-DOPA, which is then converted to dopamine by another enzyme called L-DOPA decarboxylase (DDC). DJ-1 positively

regulates TH transcription during oxidative stress by sequestering PSF (Zhong *et al*, 2006). Researchers have shown that when SOH and SO_2H forms of DJ-1 exceed 50%, *TH* transcription is increased (Shendelman *et al*, 2004).

An interesting example of DJ-1 chaperone activity involves inhibiting α-synuclein aggregation during oxidative stress. Zhou *et al* (2006) showed that native DJ-1 does not affect α-synuclein aggregation. However upon oxidation of C106 to SO_2H, significant anti-aggregation of α-synuclein was detected. Thus, DJ-1 is an oxidative stress induced chaperone that prevents α-synuclein aggregation.

Dysfunctional mitochondria are a feature observed in PD patients as well as in DJ-1 knockout mice. DJ-1 has been found to be translocated into the mitochondria during oxidative stress when C106 is oxidised to SO_2H. The detailed mechanism of how DJ-1 performs its anti-oxidative stress response within mitochondria is not yet clearly understood, but the role of mitophagy has been proposed, where DJ-1 clears damaged mitochondria (Thomas *et al*, 2011).

The identified physiological roles of DJ-1 makes it easier to comprehend how a loss of DJ-1 activity can lead to oxidative stress induced diseases such as PD. The loss of DJ-1 functionality in familial PD is attributable to the mutations associated with *DJ-1*. Continuous exposure to oxidative stress that renders DJ-1 inactive provides a plausible explanation of how DJ-1 may contribute to the cause of sporadic PD.

1.13 LRRK2

Mutations identified in certain genes implicated in the onset of familial neurodegenerative diseases, have paved the way in understanding the role of the encoded protein in disease pathogenesis.

Missense mutations in *LRRK2* have been linked to autosomal dominant and sporadic PD (Li *et al*, 2014, Mata *et al*, 2006). This section summarises the current knowledge on the normal physiological functions of LRRK2 as well as its pathological implications in PD.

LRRK2 is a large protein; 286 kDa, made up of 2527 amino acids (Mata *et al*, 2006b, Li *et al*, 2014). Figure 1.4, illustrates the structure of LRRK2, showing a few mutations known to cause PD. As depicted in the diagram, LRRK2 is a multidomain protein; these domains give a good indication on the normal physiological role of the protein, and, the mutations promote understanding on the possible role of LRRK2 in disease pathogenesis.

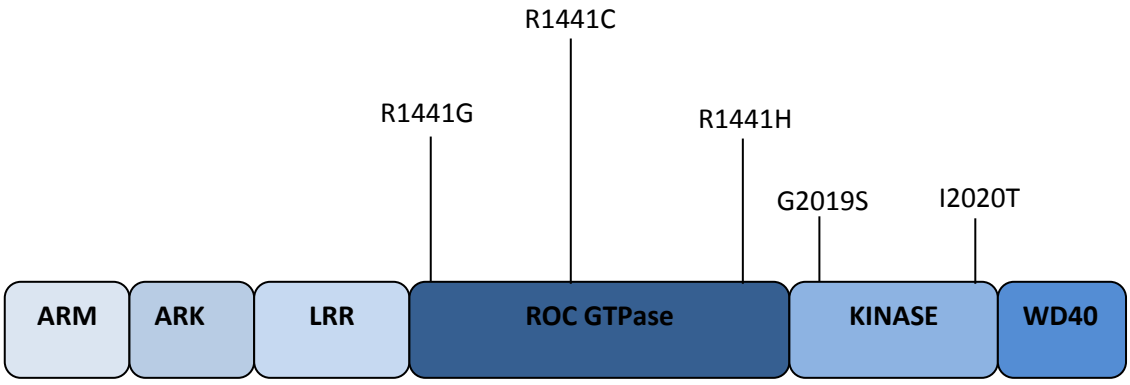

Figure 1.4: LRRK2 structure: *diagram depicting the multidomains making up the LRRK2 protein structure. ARM = armadillo repeats, ARK = ankyrin repeats, LRR = leucine rich repeat sequence. A few known LRRK2 mutations are also highlighted. The G2019S affecting the kinase domain is the most common (Mata et al, 2006b).*

1.13.1 LRRK2: Physiological and Pathological role in disease

The absolute physiological role for LRRK2 is still research ongoing. However, revelations into the structural components of this large protein indicate the potential roles it may undertake.

LRRK2 has two enzymatic domains – a kinase domain and a ROC GTPase domain (Cookson, 2010 and Kawakami, 2015). The kinase domain suggests a role for LRRK2 in catalysing phosphorylation reactions. Amongst the substrates found for this kinase domain, include the microtubule associating protein tau – which is interesting since tau has been linked to many neurodegenerative disorders including PD and AD. The physiological relevance of the ROC-GTPase domain is largely unknown. However, it structurally resembles the Rab GTPase family that has been shown to play a role in vesicular trafficking. The presence of repetitive sequences within the LRRK2 protein structure confers a protein-protein interaction functionality, where it may play a role in bringing together a multiprotein signalling pathway (Mata *et al*, 2006b).

Amongst the many mutations found in LRRK2, pG2019S has been studied the most. This particular mutation is situated in the kinase domain, resulting in hyperactive kinase activity. It has been hypothesised that hyperphosphorylation of LRRK2 substrates initiates pathways that are ultimately toxic to cells. Experimental evidence from *C.elegans* and *Drosophilia* has shown that the pG2019S mutation leads to loss of dopaminergic neurones and locomotor activity in an age-dependent manner (Kawakami, 2015 and Li *et al*, 2014).

The role of α-synuclein in the pathogenesis of certain neurodegenerative disorders has already been discussed in Section 1.9.2. The finding that mutations in both *LRRK2* and *SNCA* are associated with the onset of autosomal dominant PD and sporadic PD, has initiated an interest into whether the roles of these two proteins in disease are related.

α-synuclein inclusions, which are characteristic features for PD, DLB and MSA, are predominantly phosphorylated at S129 (Fujiwara *et al*, 2002; Anderson *et al*, 2006; Wakabayashi *et al*, 1998). The most common LRRK2 mutation involves a hyperactive kinase domain. Thus, the question arises as to whether α-synuclein is a substrate for LRRK2. Guerreiro *et al* (2013) set out to investigate this possibility. Their research showed that the two proteins do interact with one another but this interaction was not affected by the presence/lack of LRRK2 G2019S mutation; suggesting that the kinase domain is not an essential requirement for the interaction. However, co-localization experiments showed that LRRK2 levels positively correlated with the level of α-synuclein phosphorylation and aggregation in PD affected brain regions. This finding leads to the conclusion that the presence of LRRK2 rather than LRRK2 kinase activity may play a role in disease pathogenesis involving α-synuclein phosphorylation, accumulation and aggregation (Guerreiro *et al*, 2013).

Another possible relationship between LRRK2 and α-synuclein has been elegantly described by Orenstein *et al* (2013). Orenstein *et al* (2013) have published a role for LRRK2 in the lysosomal degradation pathway. As previously described, the lysosomal pathway, is chaperone mediated and is classified into various forms. The specific form of lysosomal degradation which highlights a possible relationship between LRRK2 and α-synuclein is called the CMA form mediated by the chaperone hsc70.

CMA is a pathway that is responsible for delivering up to 30% of cytosolic proteins to the lysosome for degradation. LRRK2 is amongst this 30%, possessing structural motifs that are specific for binding with hsc70. This LRRK2-hsc70 complex is then recognised by the LAMP-2A protein present on the outer membranes of lysosomes. This binding activates a series of events leading to the importation of LRRK2 into the lysosomes for degradation.

Orenstein *et al* (2013) showed that wild type LRRK2 utilises the UPS and CMA degradation pathways. However, the mutant forms rely on the UPS pathway; furthermore – these mutant forms are poorly degraded by the CMA system. This finding has led the researchers to hypothesise that mutant LRRK2 may be blocking the CMA pathway i.e. upon binding to the LAMP-2A; the subsequent series of events are not initiated. This blockage means that other cytosolic proteins destined to be degraded cannot be degraded either. Interestingly, α-synuclein also uses the CMA system for degradation, therefore, blockage of the CMA by mutant LRRK2 means poor degradation of α-synuclein that should be removed – resulting in its accumulation and aggregation which is a hallmark characteristic of various neurodegenerative disorders including PD (Yue, 2013).

1.14 Biomarkers

Biomarkers are defined as characteristics that can be used as an indicator of normal biological processes as well as pathological processes. Additionally, biomarkers can directly show the nature of a pharmacological response upon therapeutic interventions (Michell *et al*, 2004). Biomarkers can be in various forms, such as, genetic and biochemical markers as well as data obtained from imaging techniques. This section discusses the potential use of biomarkers in the field of neurodegenerative diseases.

As echoed in previous sections of this report, diagnosis of neurodegenerative disease is difficult and heavily reliant on physical examinations with little or no laboratory/clinical data to support or aid the diagnosis. Furthermore, symptoms of neurodegenerative conditions present themselves once neuronal cell death and damage has already occurred. Nerve cells do not have the ability to regenerate, therefore, once cell death has occurred there is no going back. Biomarkers may serve to allow diagnosis of neurodegenerative diseases in their earlier stages. They may also allow us to predict the probability of an individual developing the disease in the future. Furthermore, symptoms experienced by patients with neurodegenerative diseases are very similar amongst the various conditions, thus the ability to differentiate between the different diseases, and their subtypes, is a feat that might be achieved via the measurement of specific biomarkers.

Post diagnosis, the potential role for biomarkers extends into the field of pharmaceutical clinical trials. Surrogate biomarkers are often adopted during longitudinal clinical trials. Surrogate biomarkers aim to substitute the use of clinical end points. In neurodegenerative trials, a successful surrogate biomarker must be reliably detectable despite the fluctuating physical symptoms.

To summarise, biomarkers carry the potential to aid and improve diagnosis, Furthermore, they open up avenues for monitoring disease progression and therapeutic effects, more accurately. In order to be classed as a "good" biomarker, its measurements need to be precise and reliable. The data obtained from the measurement must be distinguishable between normal and diseased cases and allow differentiation between the subtypes of the same disease (Rachakonda *et al*, 2004).

1.15 Project Aims

The specific aims of this project are as follows:

1. To develop and validate a singleplex Luminex assay for measuring phosphorylated α-synuclein in human plasma and CSF.

2. To develop and validate a multiplex assay to measure total α-synuclein, total DJ-1 and LRRK2 in human plasma and CSF.

3. To analyse cross sectional plasma and CSF samples from individuals with various neurodegenerative disorders and age matched healthy controls, using the developed and validated Luminex assays.

4. To measure total α-synuclein, total DJ-1 in longitudinal plasma samples taken from PD patients for up to 4 years, using the developed and validated multiplex assay.

5. To screen human plasma and CSF samples for the presence of LRRK2, using the Luminex assay, HPLC and western botting.

By meeting the above aims it will be deduced whether α-synuclein, DJ-1 and LRRK2 carry the potential to be biomarkers for differentiating between various neurodegenerative disorders and healthy individuals. The subsequent chapters of this thesis describe the development and validation of Luminex assays in detail followed by our findings from the aforementioned sample analysis.

Chapter 2a: Materials

2a.1 Antibodies and recombinant proteins

2a.1.1 Phosphorylated α-synuclein

Product Name	Product Code	Manufacturer/Distributor
P-syn/81A mouse anti-α-synuclein phospho-specific (Ser129) mAb	MMS-5091	Manufactured by Covance Inc., US Distributed by Cambridge Biosciences, Cambridge, UK
N-19 goat anti-α/β-synuclein pAb	sc-7012	Santa Cruz Biotechnology Inc.
EP1536Y rabbit anti-α-synuclein (phospho S129) mAb	EP1536Y or ab51253	Epitomics now supplied by Abcam
Biotinylated goat anti-α-synuclein pAb	BAF1338	R&D Systems, Abingdon, UK
Syn211 mouse anti-α-synuclein mAb	32-8100	Life Technologies-Invitrogen, Paisley, UK
Human recombinant phosphorylated α-synuclein	NA	Produced in house by Dr Penny Foulds Lancaster University, UK

2a.1.2 Total α-synuclein

Product Name	Product Code	Manufacturer/Distributor
C211 mouse anti-α-synuclein mAb	sc-12767	Santa Cruz Biotech. Inc., Santa Cruz, CA

Product Name	Product Code	Manufacturer/Distributor
FL140 rabbit anti-α/β/γ-synuclein pAb	sc-10717	Santa Cruz Biotech. Inc., Santa Cruz, CA
Syn211 mouse anti-α-synuclein mAb	32-8100	Life Technologies-Invitrogen, Paisley, UK
Biotinylated goat anti-α-synuclein pAb	BAF1338	R&D Systems, Abingdon, UK
Human α-synuclein recombinant protein	na	Produced in house by Dr Penny Foulds Lancaster University, UK

2a.1.3 Total DJ-1

Product Name	Product Code	Manufacturer/Distributor
Rabbit anti-DJ-1 mAb	NB-100-483	Novus Biologicals, Ltd,. Cambridge, UK
Mouse anti-DJ-1 mAb	SIG-39830	Manufactured by Covance Inc., US Distributed by Cambridge Biosciences, Cambridge, UK
Biotinylated goat anti-DJ-1 pAb	BAF3995	R&D Systems, Abingdon, UK
Human DJ-1 recombinant protein	SIG-39900	Manufactured by Covance Inc., US Distributed by Cambridge Biosciences, Cambridge, UK

2a.1.4 LRRK2

Product Name	Product Code	Manufacturer/Distributor
LRRK2 monoclonal antibody; Covance (1 mg/mL)	SIG39840	Covance
LRRK2 rabbit monoclonal antibody; Abcam (0.01 mg/mL)	ab133474	Abcam
LRRK2 full length protein	A15197	ThermoFisher Scientific

2a.2 Buffers and additional reagents

2a.2.1 Luminex assay buffers

Buffer Name	Buffer Composition
Triton activation buffer	0.1 M sodium phosphate pH 6.1 + 0.025% (v/v) triton x-100
Activation buffer	0.1 M sodium phosphate pH 6.1
Triton coupling buffer	50mM MES pH 5.0 + 0.025% (v/v) triton x-100
Coupling buffer	50mM MES pH 5.0
Wash buffer	PBS + 0.025% (v/v) triton x-100
Blocking/Storage buffer	PBS + 0.1% BSA (w/v) + 0.02% (v/v) Tween 20 + 0.02 % (w/v) NaN_3
Surmodics® assay buffer	Proprietary buffer from Surmodics® 9924 West 74th Street Eden Prairie, MN 55344 USA

Buffer Name	Buffer Composition
PBS/0.05% (v/v) Tween (PBST)	5 tablets of PBS (Sigma, P4417) in 1L deionised water plus 0.5mL Tween 20 (Sigma, P1379)

2a.2.2 Luminex assay additional reagents

Product Name	Product Code	Manufacturer/Distributor
Luminex Microplex-Microspheres	LC10001-04	Luminex, TX, US
N-hydroxysulfosuccinimide (Sulfo-NHS)	24510	Thermo Scientific Pierce, IL, US
1-Ethyl-3-[3-dimethylaminopropyl] carbodiimide hydrochloride (EDC)	77149	Thermo Scientific Pierce, IL, US
Coupling tubes	FB56075	Thermo Scientific Fisher Brand, IL, US
NAb Protein A/G Spin Columns, 0.2 ml	89954	Thermo Scientific Pierce, IL, US
Ultracentrifugal Filter Tubes 30K	UFC803024	Merck Millipore, MA, US

2a.2.3 Western blot buffers

Buffer Name	Buffer Composition
10 x Resolving gel stock	30.3 g TRIS + 144 g glycine dissolved in 950 mL dH_20 + 50 mL 20% (v/v) SDS
4 x Stacking gel stock	6g TRIS dissolved in 40 mL dH_20. Solution titrated to pH 6.8 with 1M HCL. Solution then made up to a final volume of 100 mL with dH_20
10% (w/v) Ammonium persulfate	1 g ammonium persulphate dissolved in 1 mL dH_20
SuperSignal West Pico Chemiluminescent Substrate	Supplied by Thermo Scientific; product code 34080. Prepared in house by mixing 50:50 Substrate A and Substrate B.

2a.2.4 Immunoprecipitation (IP)

Product/Buffer name	Product code/Buffer composition
Dynabeads® Protein A Immunoprecipitation Kit	10006D, from Life Technologies-Invitrogen, Paisley, UK
SDS sample buffer	0.125 M TrisHCl, pH 6.8, 2% (v/v) SDS, 10% (w/v) glycerol, 0.01% (v/v) bromophenol blue, 0.1 M dithiothreitol

2a.2.5 High Performance Liquid Chromatography (HPLC)

Buffer name	Buffer composition
1% (v/v) TFA in water	100 mL TFA + 900 mL dH_20
1% (v/v) TFA in acetonitrile	100 mL TFA + 900 mL acetonitrile

2a.3 Equipment and Instruments

Equipment/Instrument Name	Seriel Number	Manufacturer/Distributor
Luminex 200	LX10011048401	Manufactured by Luminex, TX, US
Ultracentrifuge	5425 22843	Eppendorf, Stevenage, UK
Sonicator	048103	Ultrawaves, Wirral, UK
Vortex	2-69268	Scientific Industries Inc., NY, US
Plate shaker	010102-1108-0452	Grant Instrument Ltd., Cambridge, UK
Vacuum Filtration Instrument	09511151	Charles Austen Pumps Ltd., Surrey, UK
Nanodrop 2000c	8356	Manufactured by: Thermo Fisher Scientific Inc., DE, US
ChemiDoc™ MP Imaging System	1708280	BioRad, Hertfordshire, UK

2a.4 CSF samples

The CSF samples analysed in this project were collected at the Department of Neurology, University College Hospital, London (UCL), courtesy of Dr Nadia Magdalinou. CSF samples were collected via lumbar puncture into sterile polypropylene tubes and immediately centrifuged at 4000 rpm for 10 minutes at 4^{o}C. The samples were then aliquoted and stored at ≤70 ^{o}C. The CSF samples used in this project are shown:

Disease category	Total number of samples	Number of males	Number of females	Mean age ± SD (years)
HC	26	14	12	61 ± 9
MSA	28	15	13	64 ± 6
PD	22	15	7	68 ± 8
PSP	31	19	12	69 ± 6
CBS	13	4	9	68 ± 7

The age of the patients' enrolled in the UCL study was significantly lower for the HC and MSA groups in comparison to the PD, PSP and CBS categories (p value ≤0.05 as per Mann-Whitney test). Gender distribution within each disease group was even except for the PD and CBS groups, where more males were recruited in the PD category and more females within the CBS group. The gender distribution was statistically insignificant between all disease groups (p value ≥0.05 as per Mann Whitney test).

2a.5 Plasma samples

The plasma samples used in this project were obtained from two individual sites - Out-patient clinics at Greater Manchester Neurosciences Centre (GMNC) at Salford Royal Hospital and Department of Neurology, University College Hospital, London (UCL), courtesy of Dr Nadia Magdalinou.

The blood was collected in EDTA tubes and stored at 4°C prior to centrifugation (within 20 hours of collection). The samples were then centrifuged at 2000 rpm (1000 x g) for 10 minutes at 4°C. The resultant plasma was pipetted off into sterile cryogenic vials prior to storage at ≤ -70°C. The table below show the demographics of the plasma samples from GMNC only followed by GMNC and UCL combined. The plasma samples from UCL were obtained from the same subjects as the CSF samples:

GMNC samples				
Disease category	**Total number of samples**	**Number of males**	**Number of females**	**Mean age ± SD (years)**
HC	72	30	42	68 ± 9
MSA	18	9	9	64 ± 8
PD	61	37	24	69 ± 12
PSP	36	21	15	66 ± 11
CBS	16	8	8	65 ± 10
AD	79	49	30	64 ± 10
DLB	59	44	15	68 ± 11

GMNC + UCL samples combined				
Disease category	**Total number of samples**	**Number of males**	**Number of females**	**Mean age ± SD (years)**
HC	98	44	54	65 ± 11
MSA	46	24	22	65 ± 7
PD	83	52	31	66 ± 10
PSP	67	40	27	70 ± 7
CBS	29	12	17	68 ± 8
AD	79	49	30	64 ± 10
DLB	59	44	15	68 ± 11

The age (GMNC + UCL samples combined) of the patients sampled did not significantly differ between the HC, MSA, PD, CBS, AD and DLB disease groups (p value ≥ 0.05 as per Mann Whitney test). The age was significantly higher for the

PSP and DLB groups in comparison to the remaining disease groups. The gender of patients sampled was evenly distributed within individual disease groups except for in DLB. The difference in gender distribution between the disease groups was not significant except for between HC vs PD, HC vs DLB, CBS vs DLB and MSA vs DLB, where the p value was ≤ 0.05 as per Mann Whitney tests.

Only 8 samples from the UCL site have been pathologically and longitudinally followed up post 2 years. None of the samples from the GMNC site have undergone pathological confirmation; these samples are from an ongoing study thus longitudinal visits have been planned. Information regarding disease duration upon sampling was recorded for all samples from UCL, but only a selected few samples from the GMNC site had this information readily available. The samples for which disease duration data was available ranged from 1.5 – 20 years for the PD samples (n = 20), 2 – 12 years for PSP patients (n = 33), 1.5 – 10 years for MSA (n = 28) and 1 – 11 years for CBS/CBD patients (n = 13).

All samples from GMNC were obtained with informed consent and ethical approval was received from the Oldham Local Research Ethics Committee. Samples from UCL were also obtained with informed consent and ethical approval from London, Queen Square Ethical Committee. Diagnoses of the patients from whom samples were collected were based on internationally established operational criteria (Hughes *et al*, 1992; Litvan *et al*, 1996; Bak *et al*, 2008; McKhann *et al*, 1984; Gilman *et al*, 2008). Patients with PSP, PD and CBS had additional assessments including UPDRS, Mini Mental State Examination (MMSE), PSP rating scale (PSPRS) and Mattis Dementia Rating Scale (Schmidt *et al*, 2005). Healthy control samples were usually spouses and friends of the diseased patients and underwent clinical and neurological examinations to ensure their fit for use as healthy controls.

Chapter 2b: Methods

2b.1 Luminex Technology

The Luminex analyser utilises a combination of scientific technologies involving flow cytometry, microspheres and lasers to offer a versatile platform for developing and performing immunoassays.

The Luminex system is based on the availability of unique Luminex microsphere bead sets. At present, there are 100 bead sets available with each set being colour coded with varying intensities of red and infra-red fluorophores. This internal dye mixture generates the unique characteristic of each bead set and is referred to as the 'spectral signature'. The Luminex analyser has an inbuilt laser component that identifies the varying nature of the spectral signature and thus the individuality of each bead set.

The availability of 100 unique bead sets allows the ability to multiplex assays, where several analytes can be quantified from a single sample well simultaneously.

2b.1.1 Luminex sandwich immunoassay protocol summary

The Luminex is an open platform, meaning that a range of assay formats can be performed using the technology, e.g. competitive immunoassays, sandwich immunoassays and nucleic acid bioassays. For the purpose of this project we developed, validated and used sandwich immunoassays. A summary of the Luminex sandwich immunoassay protocol is described as follows:

Step 1: The analyte of interest was captured using a specific antibody conjugated to the chosen bead set. The surface chemistry of each bead is designed to allow bead coupling – where the desired capture component is covalently attached to the bead.

Step 2: The captured analyte was detected using analyte specific detection antibodies. The detection antibodies were biotinylated.

Step 3: Streptavidin-R-phycoerythrin (Streptavidin-RPE) was added. Streptavidin binds with high affinity to the biotin counterpart of the detection antibody mixture.

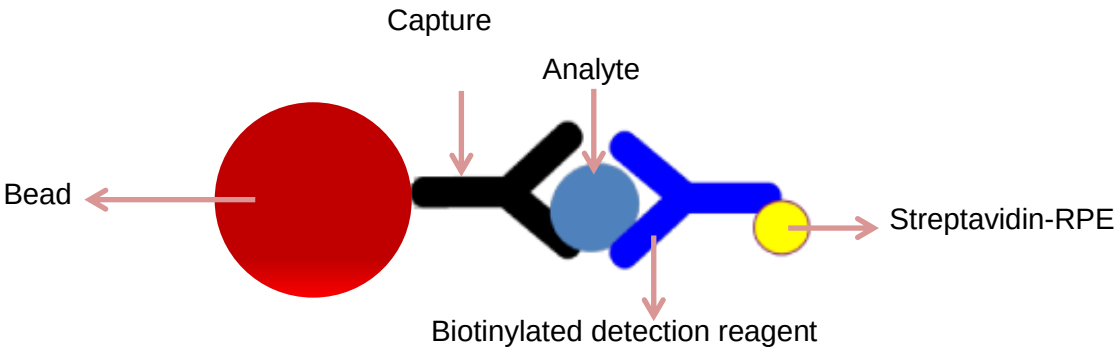

Figure 2b.1: Luminex sandwich assay format: *sandwich immunoassay format utilised for the assays in this project. The capture and detection reagents are specific to the analyte of interest. Streptavidin-RPE acts as a reporter molecule.*

The actual immunoreaction was carried out in a 96 well filter microtitre plate.

Step 4: The Luminex analyser was used to quantify the reaction and yield results. Upon transfer of the microtitre plate into the instrument, the fluidics system of the application aligns the microspheres into a single file and moves them into a flow cell. Within the flow cell each microsphere is exposed to two types of lasers:

Laser 1: 635nm laser – red “classifier” laser, this excites the infra-red and red fluorophore internal dye mixture to identify and classify the bead set.

Laser 2: 532nm laser – green “assay” laser, which excites the R-phycoerythrin linked to the streptavidin to determine the level of analyte captured onto the microsphere and generate a quantifiable result.

During the multiplexing step of this project, various bead sets were used. Each bead set was conjugated to a different analyte specific capture antibody.

A cocktail of analyte specific biotinylated detection antibodies were then utilised to complete the reaction with Streptavidin-RPE.

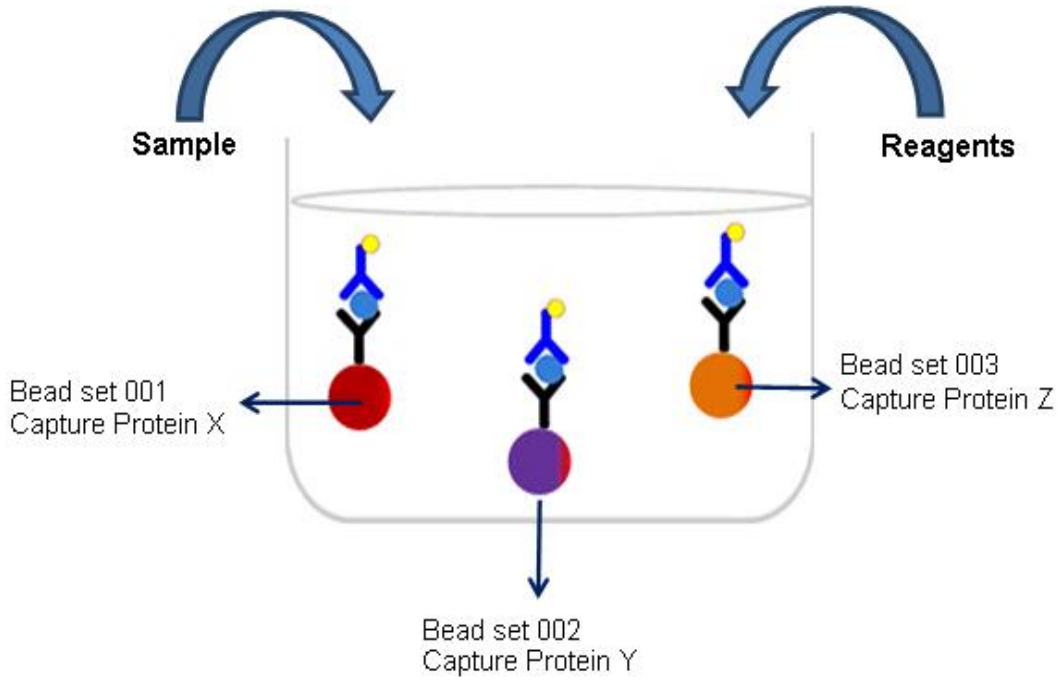

Figure 2b.2: Luminex beads in a multiplex format: *Each bead set attached to a different capture antibody, reacted with a mixture of biotinylated antibodies specific to the analyte of interest.*

2b.1.2 Surmodics® buffer for all assays to reduce matrix effects

The Luminex assays developed for use in this project involved the use of a special buffer from Surmodics®. This buffer was chosen to eliminate any non-specific binding from heterophilic antibodies. Figure 2b.3 summarise how heterophilic antibodies can create false negative and false positive results. The buffer is protein free to avoid any protein cross-reactivity problems within the assays, such as with BSA.

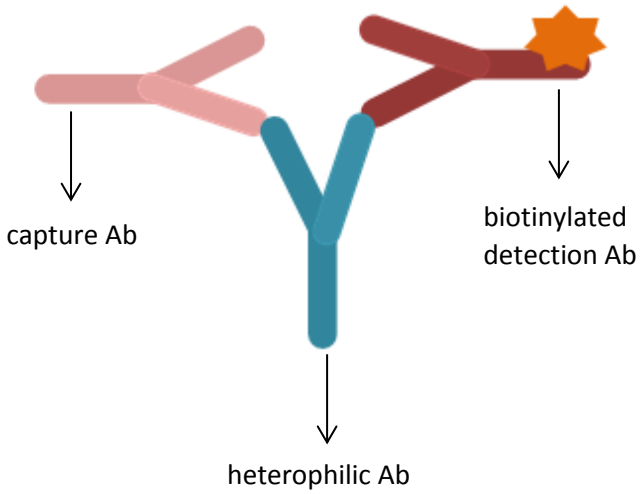

False Positive

The heterophilic antibody acts as a bridge between the capture Ab and detection Ab, resulting in a false positive result.

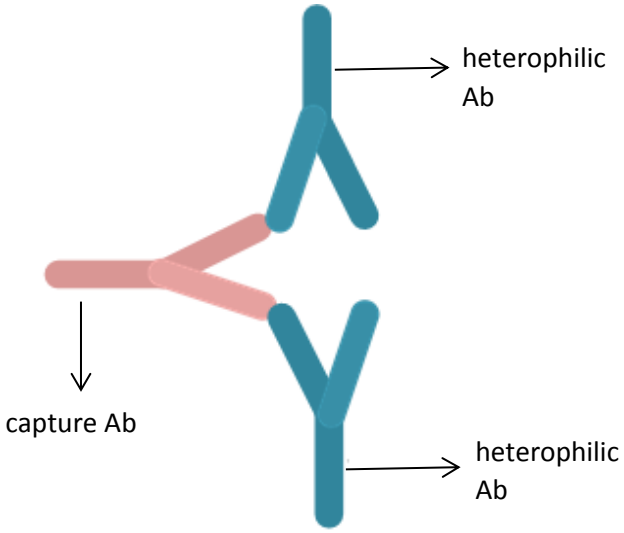

False Negative

The heterophilic antibody prevents any analyte present in the sample from binding to the capture antibody, thus yielding a false negative result.

Figure 2b.3: Heterophilic Ab interference: *heterophilic Abs have been reported to be present in complex matrices such as plasma. Heterophilic Abs can interfere with the assay components and yield either false negative or false positive results.*

2b.1.3 Luminex bead antibody coupling

The Luminex technology requires the capture antibody to be coupled to Luminex microspheres/beads. The coupling process involved a two-step carbodiimide reaction, where the primary amine group of the capture antibody was covalently bonded to free carboxyl groups on the surface of Luminex microspheres. Briefly, 500,000 beads were washed three times with triton/activation buffer via centrifugation at 9,300 x g for 1 min and removal of the supernatant. The washed beads were then activated using 10 µL of 50 mg/mL EDC and 10 µL of 50 mg/mL Sulfo-NHS in 80 µl of activation buffer. After a 30 min incubation and three washes with triton/coupling buffer, the antibody to be coupled was added. Coupling buffer was added to make the volume up to 500 µl. This mixture was incubated for 2 h at room temperature (RT) with end-over-end mixing. Post incubation, the beads were washed three times with wash buffer, and blocked with 150 µL PBS/1% BSA. The coupled beads were stored at 2 – 8^{o}C.

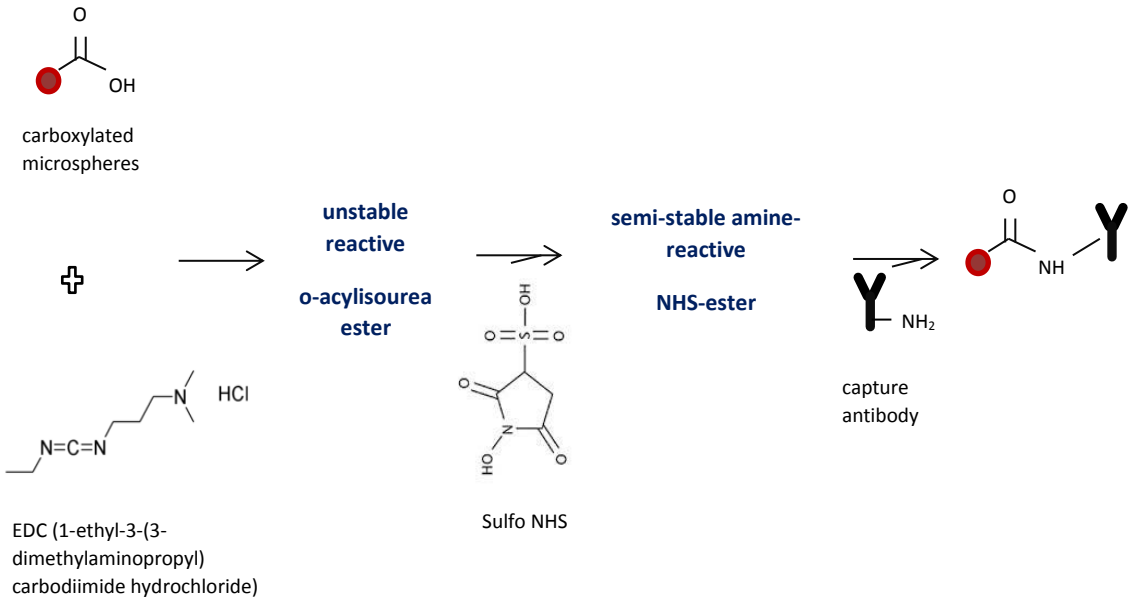

Figure 2b.4: Antibody coupling to Luminex microspheres: *the figure does not represent the order in which the reagents are added. Sulfo NHS was added before the EDC. EDC is unstable once dissolved therefore adding it post the Sulfo NHS allows efficient coupling. The two step carbodimide reaction only takes place once the EDC is added.*

2b.1.4 Antibody biotinylation

The detection antibody to be used in the Luminex technology needs to be biotinylated. The biotinylation was performed using EZ-Link™ NHS-LC-LC-Biotin (Thermo Scientific Pierce). The procedure involved following the manufacturer's recommended protocol. Briefly, 20 – 100 µL of 1 mg/mL of antibody was reacted with 50 mM biotin solution at a 50:1 ratio and sodium bicarbonate at 10:1 ratio. The reaction was allowed to take place at RT for 30 mins with continuous end-over-end mixing. Post incubation, unbound biotin was removed using Zeba desalting columns (Thermo Scientific Pierce) with PBS as the exchange buffer. The biotinylated antibodies were stored at -20^{o}C after the addition of 0.08% (w/v) NaN_3.

2b.1.5 Antibody concentrating

In order to maximise bead coupling and biotinylation efficiency, the antibodies destined for such purposes were used at 1mg/mL concentration. Many of the antibodies used in this project were readily available at this concentration. Antibodies that were only available at < 1mg/mL were concentrated up using one of the following devices:

- Pierce protein concentrators, PES, 3K MWCO, 0.5mL.
- Amicon® Ultra 4mL centrifugal filters.

Both devices work using similar principles; the Pierce 0.5 mL concentrator was used for small volumes of antibodies and the Amicon® filter tubes were used for concentrating up larger volumes of antibody.

2b.1.6 Antibody purification

Prior to undergoing bead coupling and biotinylation, all antibodies had to be free from azide and amine containing substances. The purification step involved using Protein A/G columns (Thermo Scientific Pierce) and ultracentrifugal filter tubes (Merck Millipore).

The manufacturer's protocol was followed for the Protein A/G purification, utilising the immobilised protein columns (Thermo Scientific Pierce). All centrifugation steps were performed at 5,000 x g at RT. 400 µL of binding buffer (Thermo Scientific Pierce) was added to the resin packed column, followed by 500 µL of antibody. After two washes with binding buffer, the bound antibody was eluted using 400 µL elution buffer (Thermo Scientific Pierce) in tubes containing neutralising buffer (Thermo Scientific Pierce).

The eluted antibody solution was purified using the ultra-centrifugal filter tubes, with PBS as the exchange buffer. This involved adding the eluted antibody solution with PBS and centrifuged three times at 4,000 x g for 8 min. The final centrifugation yielded approximately 150 µL of purified antibody solution. The final concentration of this antibody was determined using the Nanodrop (Thermo Fisher Scientific) at 280 nm absorbance.

2b.2 Sodium dodecyl sulphate polyacrylamide gel electrophoresis (SDS-PAGE)

A tris-based gel was used which involved preparing a resolving gel for protein resolution and a stacking gel for sample addition. SDS-PAGE can be performed with varying percentage gels, governed by the concentration of acrylamide used during

gel preparation. Table 2b.1 shows the buffer recipe used for the generation of 2 x 12.5% gel and the stacking gel.

Component	**12.5% gel**	**Stacking Gel**
Acrylamide/Bis mix 30% (v/v)	8.3 mL	1.7 mL
Stacking Gel Buffer	na	2.5 mL
Resolving Gel Buffer	5.0 mL	na
Water	6.3 mL	5.6 mL
10% (v/v) SDS	200 µL	100 µL
10% (w/v) Ammonium persulfate	200 µL	100 µL
TEMED	20 µL	10 µL

Table 2b.1: SDS-PAGE buffer recipe: *12.5% resolving gel and stacking gel buffer recipe.*

The resolving gel was prepared and allowed to set before pouring the stacking gel on top. Once the stacking gel had been set, sample wells were generated using a specialised comb insert.

Samples were prepared by adding SDS sample buffer (0.125 M TrisHCl, pH 6.8, 2% (v/v) SDS, 10% (w/v) glycerol, 0.01% (v/v) bromophenol blue, 0.1 M dithiothreitol (DTT)) and heating at 98^{o}C for 3 mins. Prepared samples plus a molecular weight marker (Kaleidoscope) were then loaded into the sample wells created within the stacking gel and electrophoresed at 125V for 45 mins with TRIS-glycine running buffer, using BioRad equipment.

2b.3 Western blotting

A wet transfer method was used to transfer the proteins resolved via the SDS-PAGE on to a nitrocellulose membrane as shown in Figure 2b.5.

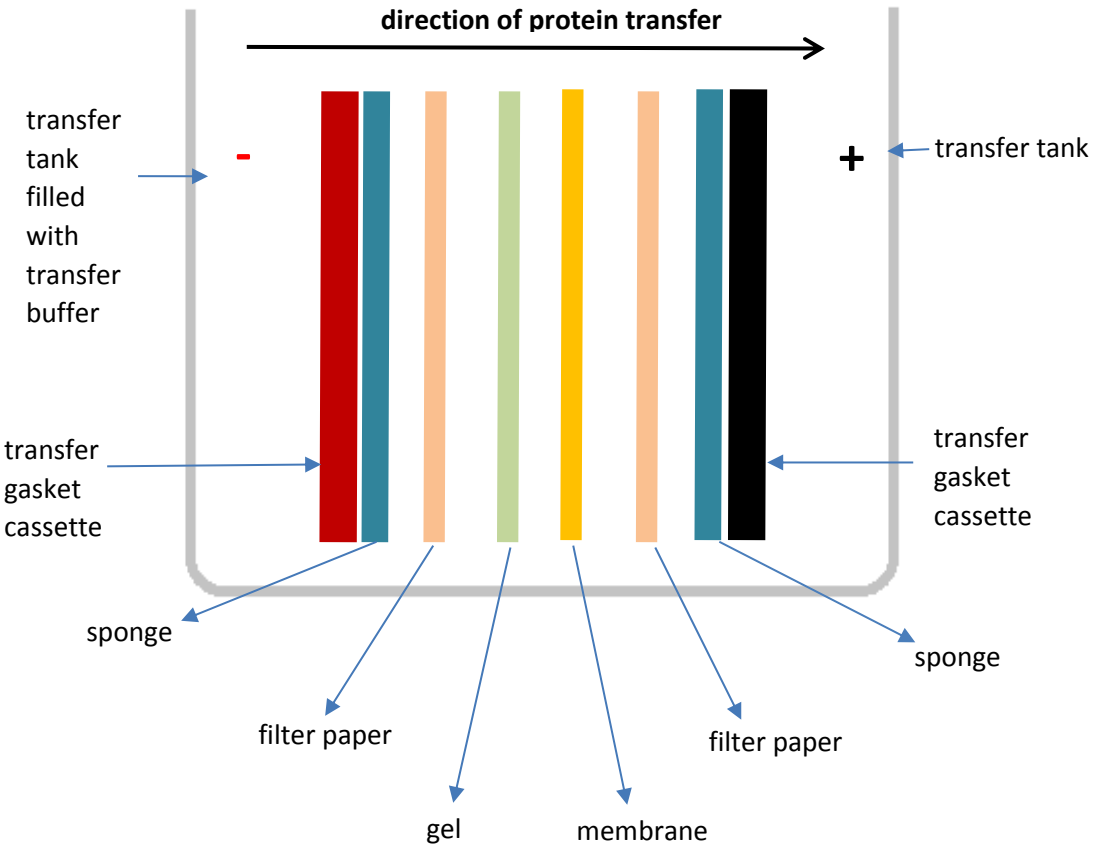

Figure 2b.5: Transfer step for western blot: *the gel and membrane were sandwiched between filter papers and sponges within a transfer cassette and placed into the X Cell Blot module (Invitrogen Inc. and electrophoresed at 25V for 1.5 h. The resolved negatively charged proteins from the gel were therefore migrated towards the positive electrode and thus transferred onto the nitrocellulose membrane.*

Once the transfer step was complete, the membrane was blocked (2% (w/v) milk powder in PBST) for 1 hr at room temperature (RT) whilst shaking. The membrane was then washed 3 x with PBST, then incubated with primary antibody (1:5000 of protein specific antibody), overnight at 4^{o}C whilst shaking. After another series of washes with PBST, the membrane was then incubated with a secondary antibody conjugated to HRP (1:5000, antibody dependant on the primary antibody type used), for 1 hr at RT, again with shaking. The membrane was developed using an ultra-sensitive chemiluminescent substrate after washing with PBST and imaged using the Chemidoc system.

2b.4 Immunoprecipitation

Dynabeads® Protein A Immunoprecipitation Kit was used to purify and obtained a concentrate of the protein of interest from plasma samples. Manufacturer's protocol was used; in summary an analyte specific antibody (5 µg) was conjugated to Dynabeads® (supermagnetic beads) coated with Protein A. The sample to be immunoprecipitated was then added (100 µL – 500 µL) to this Dynabeads®-Ab complex – at this stage any analyte of interest present in the sample would be captured onto the beads. After a series of washes with the washing buffer provided in the kit, any captured analyte was eluted using the kit elution buffer and denatured for use with the SDS-PAGE and western blot by adding SDS sample buffer.

2b.5 HPLC

Reversed phase HPLC was used using the Dionex HPLC system. 100 µL of sample was injected into a C18 or C4 hydrophobic columns; 250 x 4.6 mm with 5 microns particles (supplied by Phenomenex). The mobile phase used in this methodology was 1% (v/v) TFA made up in water and 1% (v/v) TFA made up in acetonitrile. The

eluent gradient was started at 0% then to 60% after 30 minutes, with all samples analysed at 25 ^{o}C.

2b.6 Luminex Assay Validation

There are no government based guidelines such as FDA documentation dictating how biomarker ligand binding assays are to be validated. However, there are publications that discuss how to conduct a "fit for purpose" validation. We have used the papers listed below as guidance when validating the Luminex assays described in this project:

- Lee *et al*. (2006b) Fit-for-Purpose Method Development and Validation for Successful Biomarker Measurement, *Pharmaceutical Research, 23 (2)*

- Lee, (2009) Method validation and application of protein biomarkers: basic similarities and differences from biotherapeutics, *Bioanalysis*, *1(8),* 1461-1474.

This section describes the parameters tested and how:

2b.6.1 Parallelism

This parameter was tested to determine whether sample matrix interference affected the assay system. It was also used to determine the minimum required dilution (MRD) for the samples, i.e. the dilution at which the recovery of analyte of interest is acceptable. This was assessed in two ways:

(i) analysing samples containing high amounts of the protein of interest and conducting a series of dilutions and assessing whether the dilution is linear.

(ii) spiking in the protein of interest into the sample matrix, conducting a series of dilutions and assessing whether the recovery at the different dilution levels is acceptable.

The dilution level at which the % difference of protein recovery was ≤ 20% was used as the proposed MRD.

2b.6.2 Spike Recovery

To ensure that matrix interference was not having an effect on the assay and that the chosen MRD was suitable for use in our assay systems, the spike recovery test was performed.

Six matrix samples were spiked with low and high levels of the protein of interest, diluted at the proposed MRD and analysed using the Luminex test system. The % recovery (RE) was calculated for each test samples. The acceptance criteria were for the % RE and % CV to be ≤ 20%.

2b.6.3 Limit of Detection (LOD)

LOD is the concentration at which the signal can be significantly distinguished from the background signal i.e. signal obtained from the zero calibrator. In order to determine this, the zero calibrator for each assay developed was analysed 20 times. The concentration obtained from the mean of these 20 signals +3 SD was then calculated and defined as the LOD.

2b.6.4 Dilutional Linearity

This test was used to show that samples with protein levels above the ULOQ can be diluted within the quantifiable range. This test was done by spiking protein of interest above the ULOQ into matrix then diluted at various levels. The protein recovery was then calculated. Acceptance criteria were for % difference and % CV to be ≤ 20%.

2b.6.5 Hook effect

The hook effect is also known as the “prozone effect”. False negative results can be obtained when samples contain very large concentrations of the analyte of interest. The phenomenon occurs due to the large concentration of analyte saturating the amount of capture antibody present in the immunoassay system. For the developed assays, this was assessed by spiking in a very large amount of the protein of interest in the sample matrix and analysed. If the signal obtained reduced then hook effect was taking place. The spiked concentrations varied for each assay developed and are mentioned in their respective results chapters.

2b.6.6 Accuracy and Precision

Accuracy refers to the “trueness/bias” of an assay, i.e. how close the results obtained are to the actual true concentration of the analyte being quantified. To assess this, we performed at least five analytical runs, on separate days. Each analytical run consisted of quantifying five “validation samples (VS)”. Each VS comprised of matrix (plasma or CSF) being spiked with the protein of interest to yield five different concentrations:

- VS1 – spiked to proposed lower limit of quantification (LLOQ)
- VS2 – spiked to represent the lower end of the calibration curve, generally 3 x the proposed LLOQ.
- VS3 – spiked to represent the middle part of the calibration curve
- VS4 – spiked to represent the high end of the calibration curve
- VS5 – spiked to the proposed upper limit of quantification (ULOQ)

The inter and intra assay % difference was calculated for each VS sample throughout the five analytical runs as a means of assessing the accuracy of the assay. Acceptable accuracy was defined by % difference ≤ 20% for VS2, VS3, VS4 samples and ≤ 25% for VS1, VS5.

Precision/consistency was also assessed using the data collected from the five analytical runs with the five VS % CV were calculated as used to determine inter and intra assay precision. The acceptance criteria for assay precision were ≤ 20% at VS2, VS3, VS4 and ≤ 25% for VS1 and VS5.

2b.7 Sample analysis run acceptance criteria

Each assay performed for this project involved analysing a calibration curve per assay plate and three levels of Quality controls (LQ, MQ and HQ), straight after the calibration curve and at the end of the plate. These QCs were either spiked samples or actual samples that had been pre-screened and found to contain a suitable amount of protein that can be used as QC. For each assay it was ensured that the QCs span the whole calibration curve. LQ = at least 3 x LLOQ level, MQ = middle of the calibration curve and HQ = towards the top end of the curve.

Each assay was accepted as long as 4 out 6 QCs passed. The acceptance range for each QC was determined from the validation runs; mean ± 3 SD.

Each test sample was diluted three times to its MRD level and analysed in three separate wells. The test result was accepted if the % CV was ≤ 20%.

The statistical analysis on the sample test data performed has been described in the respective results chapters.

Chapter 3:
Phosphorylated α-synuclein: Luminex assay development and validation

3.1 Introduction

An assay for the quantification of phosphorylated α-synuclein in human plasma and CSF has been established previously in ELISA format, utilising N-19 goat anti-α/β-synuclein pAb (Santa Cruz Biotechnology Inc.) as the capture reagent and a phospho-dependent EP1536Y rabbit anti-α-synuclein (phospho S129) mAb (Epitomics) as the detection component. A goat anti-rabbit secondary antibody conjugated to horseradish peroxidase (HRP) plus TMB substrate complex was used as the detection system (Foulds *et al*, 2011). An attempt was made to transfer this assay on to the Luminex system, with the view of developing a more sensitive and specific assay, that could then be multiplexed with other neurodegenerative disease related molecular biomarkers.

This chapter presents the developmental and validation data obtained for the new phosphorylated α-synuclein Luminex assay.

3.2 Luminex assay development

In order to develop a phosphorylated α-synuclein assay on the Luminex bead based system, it was rational to start with the antibody pairings that worked in the ELISA system, where the N-19 pAb was coupled to beads and the EP1536Y mAb was biotinylated in order to function as the detection component. Unfortunately, the N-19 pAb + EP1536Y mAb combination was not successful on the Luminex system and so alternative antibody combinations were tested in order to find a working antibody pair. The successful antibody pairings underwent concentration titration experiments in order to optimise the assay. Once optimal concentrations of antibodies were deduced, the assay was validated fit for purpose.

3.2.1 Antibody combinations

The antibody combinations tested are presented in Table 3.1.

Capture Ab	Supplier	Detection Ab	Supplier
P-syn/81A mouse anti-α-synuclein phospho-specific (Ser129) mAb	Covance	Biotinylated goat anti-α-synuclein pAb	R&D Systems
N-19 goat anti-α/β-synuclein pAb	Santa Cruz Biotechnology Inc.	Biotinylated P-syn/81A mouse anti-α-synuclein phospho-specific (Ser129) mAb	Covance
EP1536Y rabbit anti-α-synuclein (phospho S129) mAb	Epitomics	Biotinylated goat anti-α-synuclein pAb	R&D Systems
Syn211 mouse anti-α-synuclein mAb	Invitrogen Life Technologies	Biotinylated P-syn/81A mouse anti-α-synuclein phospho-specific (Ser129) mAb	Covance

Table 3.1: Phosphorylated α-synuclein antibodies: *Antibodies tested for phosphorylated α-synuclein assay development and validation for use on the Luminex platform.*

Each capture antibody (2 µg/mL = 1 µg in 500 µL coupling buffer) was coupled to 33 µL beads. The biotinylated goat anti-α-synuclein pAb was supplied already biotinylated, but the biotinylated P-syn/81A mouse anti-α-synuclein phospho-specific (Ser129) mAb was biotinylated in house.

The data obtained from these combinations are displayed in Figure 3.1:

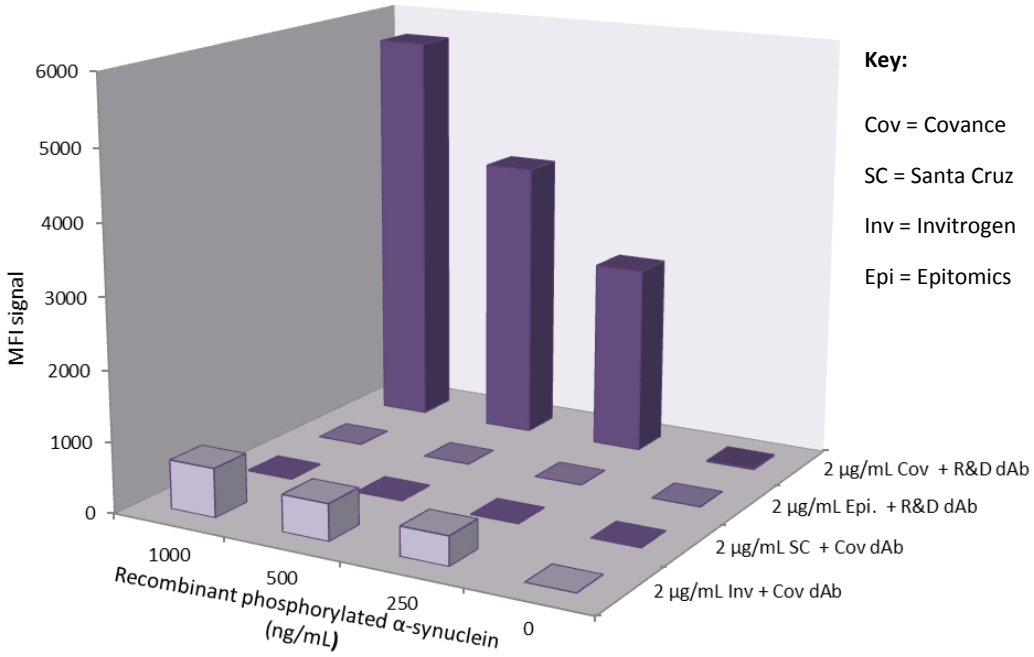

Figure 3.1: Testing different antibody combinations: *Luminex beads coupled with 2 µg/mL of each capture Ab were used to capture 1000, 500, 250, and 0 ng/mL of recombinant phosphorylated α-synuclein. 2 µg/mL of biotinylated detection Ab and 4 µg/mL of streptavidin-RPE were used as the detection system for the assay. The figure shows the raw MFI signals (n=2), achieved with the various antibody combinations.*

Beads coupled with the P-syn/81A mouse anti-α-synuclein phospho-specific (Ser129) mAb from Covance, with biotinylated goat anti-α-synuclein pAb from R&D Systems for detection, generated the best MFI signals. This antibody combination was, therefore, taken into the assay optimisation stage.

3.2.2 Assay optimisation

Capture Ab and detection Ab titration experiments were performed in order to determine the concentrations of these antibodies required, for optimal assay performance.

The capture antibody titration experiment involved coupling beads to varying concentrations of the P-syn/81A mouse anti-α-synuclein phospho-specific (Ser129) mAb. The concentrations tested were; 1, 2 and 3 µg/mL of antibody in coupling buffer. The raw MFI obtained are displayed in Figure 3.2 and the signal to noise ratio is displayed in Figure 3.3.

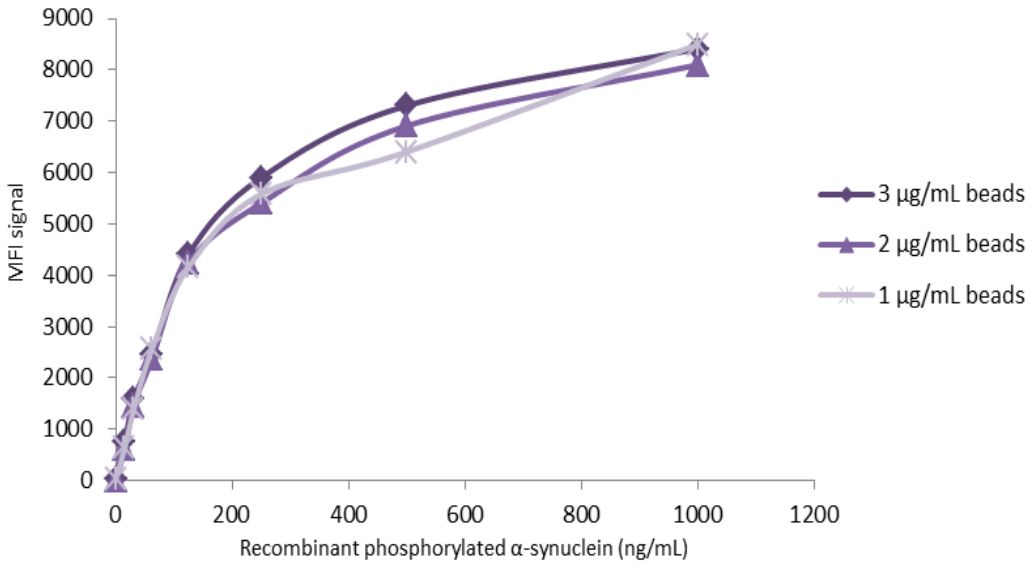

Figure 3.2: Capture antibody titration: *Luminex beads coupled with 1, 2 and 3 µg/mL of P-syn/81A mouse anti-α-synuclein phospho-specific (Ser129) mAb were reacted with recombinant phosphorylated α-synuclein at 1000, 500, 250, 125, 62.5, 31.3, 15.6 and 0 ng/mL. 2 µg/mL of biotinylated detection Ab and 4 µg/mL streptavidin-RPE were used as the detection system for the assay. The figure shows the mean (n=2) MFI signals achieved with the various capture antibody concentrations.*

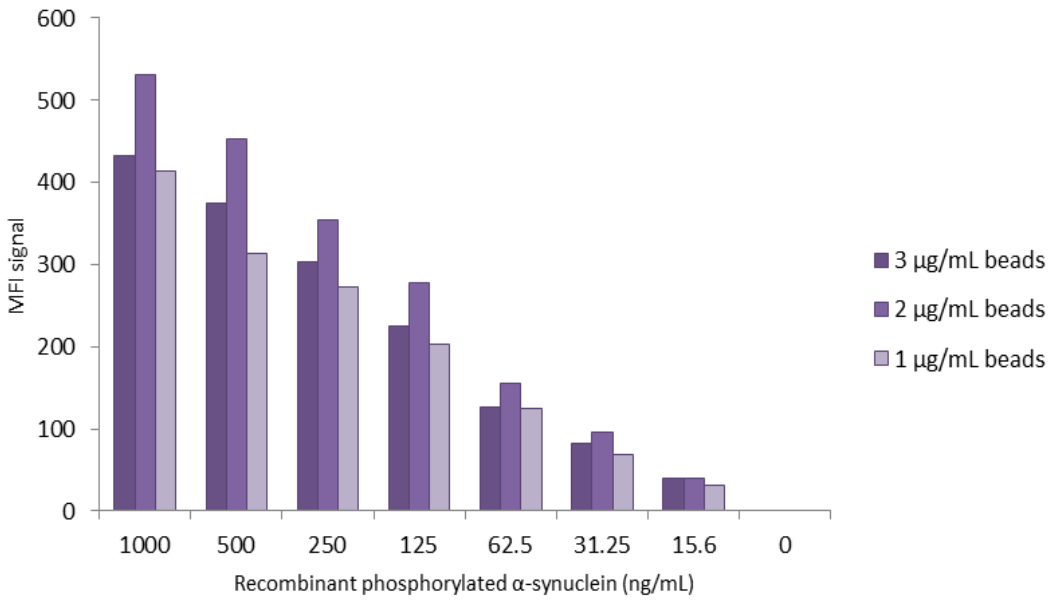

Figure 3.3: Capture antibody titration – signal to noise ratio: *Luminex beads coupled with 1, 2 and 3 µg/mL of P-syn/81A mouse anti-α-synuclein phospho-specific (Ser129) mAb were reacted with recombinant phosphorylated α-synuclein at 1000, 500, 250, 125, 62.5, 31.3, 15.6 and 0 ng/mL. 2 µg/mL of biotinylated detection Ab and 4 µg/mL streptavidin-RPE were used as the detection system for the assay. The figure shows the mean (n=2) MFI signal achieved with the various capture antibody concentrations.*

The data indicated that the best signal to noise ratio was achieved using beads coupled with 2 µg/mL of P-syn/81A mouse anti-α-synuclein phospho-specific (Ser129) capture mAb.

The detection antibody titration experiments involved performing an assay using 2 µg/mL of P-syn/81A mouse anti-α-synuclein phospho-specific (Ser129) capture mAb beads, and the biotinylated goat anti-α-synuclein pAb at varying concentrations.

The signal to noise data obtained are shown in Figure 3.4.

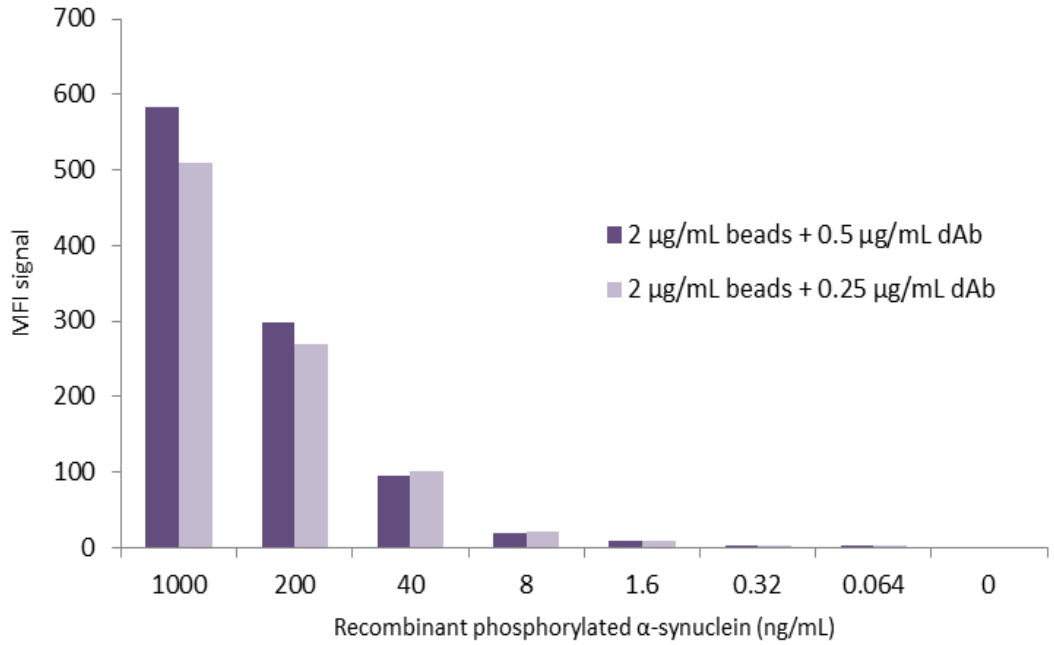

Figure 3.4: Detection antibody titration – signal to noise ratio: *Luminex beads coupled with 0.5 µg/mL of P-syn/81A mouse anti-α-synuclein phospho-specific (Ser129) mAb were reacted with recombinant phosphorylated α-synuclein at 1000, 200, 40, 8, 1.6, 0.32, 0.064 and 0 ng/mL. 1 or 0.5 µg/mL of biotinylated detection Ab with 4 µg/mL streptavidin-RPE was used as the detection system for the assay. The figure shows the mean (n=2) MFI signal achieved with the two different detection antibody concentrations.*

Using capture antibody beads coated with 0.5 µg/mL P-syn/81A mouse anti-α-synuclein phospho-specific (Ser129) mAb and the biotinylated goat anti-α-synuclein pAb at 0.5 µg/mL, generated the best data with recombinant phosphorylated α-synuclein protein. Therefore, this system was taken into the assay validation stage.

Prior to validating the assay, two additional assessments were performed. Firstly, an isoform specificity test was performed to ensure that the assay was specific for phosphorylated α-synuclein and did not detect monomeric and/or oligomeric non-phosphorylated α-synuclein. The data from this investigation are displayed in Figure 3.5.

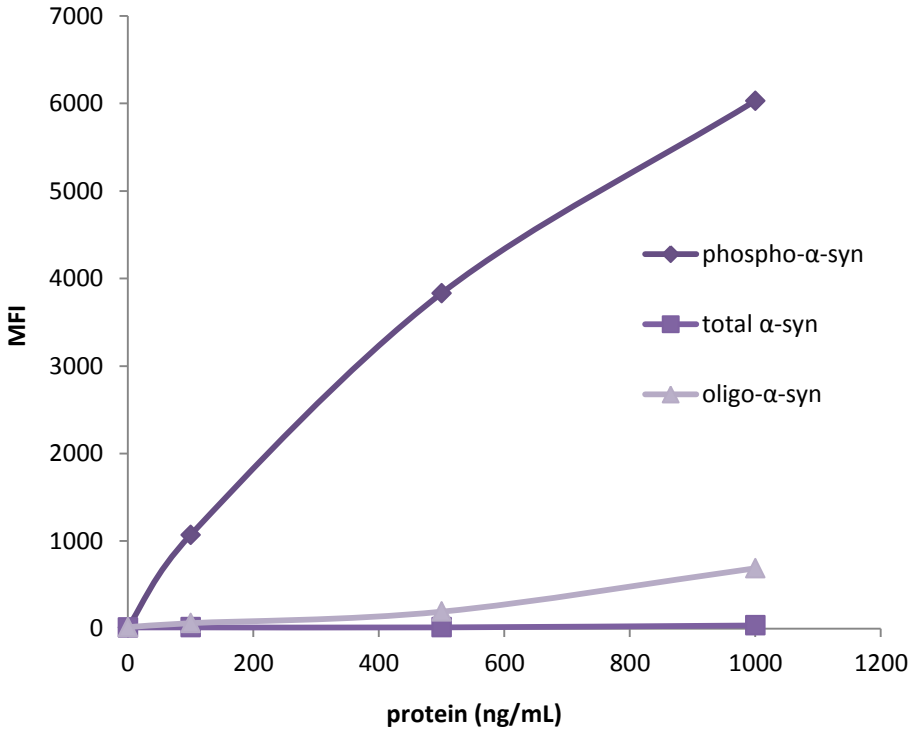

Figure 3.5: Isoform specificity: *Luminex beads coupled with 2 µg/mL of P-syn/81A mouse anti-α-synuclein phospho-specific (Ser129) mAb were reacted with recombinant phosphorylated, monomeric non-phosphorylated or oligomeric non-phosphorylated α-synuclein at 1000, 500, 100 and 0 ng/mL. 0.5 µg/mL of biotinylated detection Ab with 4 µg/mL streptavidin-RPE was used as the detection system for the assay. The figure shows the mean (n=2) of the raw MFI achieved with the different forms of the protein isoforms.*

The assay was found to be predominantly specific for phosphorylated α-synuclein.

Secondly, all assay development experiments displayed so far were performed in assay buffer (SM01:PBS). The final stage in assay development was to deduce what buffer would be suitable for use as an assay diluent for preparing calibration curves and diluting samples, when analysing human plasma and CSF. To deter matrix effects and obtain the best spike recoveries during assay validation, it is advised to prepare assay calibration curves in matrix that closely matches, or is identical, to the matrix of the samples to be analysed (http://www.perkinelmer.com/pdfs/downloads/GDE_ELISAtoAlphaLISA.pdf).

Published literature shows that some researchers use FBS as a surrogate matrix for human plasma for preparing calibrators and diluting samples – we therefore tried FBS at 5% (w/v) and 10% (w/v). In addition to FBS we tested BSA and analyte free human serum and compared assay performance with analyte free human plasma. The data obtained are shown in Figure 3.6.

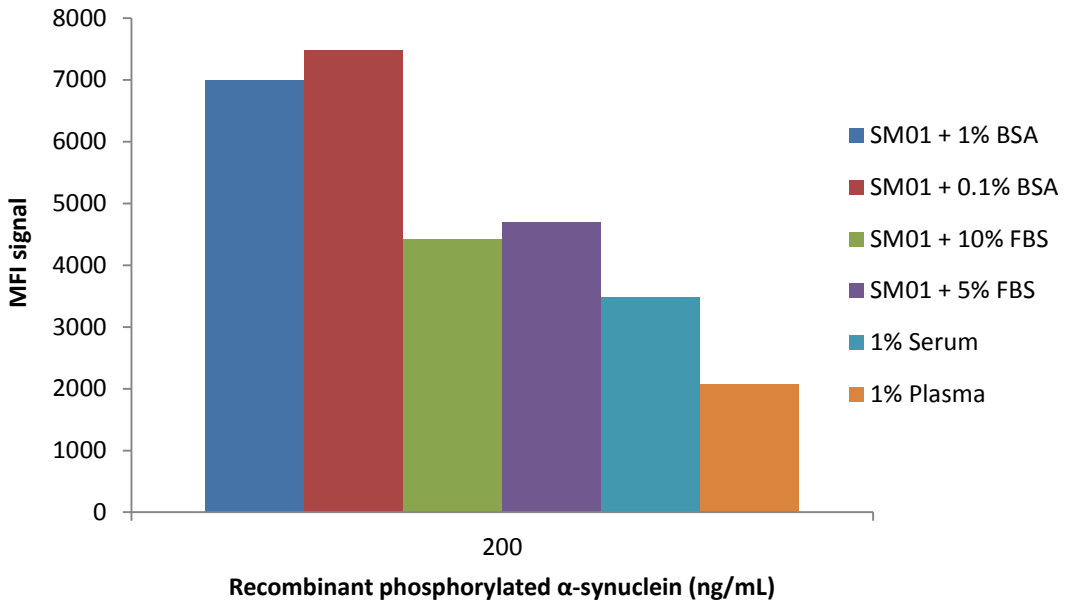

Figure 3.6: Diluent choice: *Luminex beads coupled with 2 µg/mL of P-syn/81A mouse anti-α-synuclein phospho-specific (Ser129) mAb were reacted with recombinant phosphorylated α-synuclein at 1000, 200, 1.6 and 0 ng/mL prepared in various buffers. 0.5 µg/mL of biotinylated detection Ab with 4 µg/mL streptavidin-RPE was used as the detection system for the assay. The figure shows the raw MFI achieved with the different buffers (n=2).*

It was apparent from the data obtained that FBS, BSA and human serum do not behave in the same manner as human plasma in the assay. Thus using analyte-free human plasma for the calibration curve and sample dilutions was chosen. We opted to use plasma diluted in SM01:PBS, to generate 1% (v/v) plasma for use as sample diluent and 1% (v/v) plasma spiked with recombinant phosphorylated α-synuclein for use as calibrator diluent.

In order to continue the theme of using assay diluents that are identical to the sample type; for the CSF assay we decided to use 20% (v/v) analyte free human CSF as sample diluent and 20% (v/v) CSF spiked with recombinant phosphorylated α-synuclein as the calibrator diluent.

The decision on using these diluents were initially based on obtaining good assay signal:noise ratio, since the addition of matrix to the assay reduced MFI signals vastly. The final decision for using these diluents was based on the subsequent validation data. If the validation data achieved was unacceptable, the choice of diluents would have been re-assessed.

3.3 Assay Validation: assay for analysing plasma samples

Currently, there are no official Government-based guidelines dictating how to validate biomarker assays. However, scientific white-papers have been published providing in-depth guidance on qualifying biomarker assays fit for their purpose. For the purpose of this project, the following papers have been used for validating our assays:

- Lee *et al*. (2006b) Fit-for-Purpose Method Development and Validation for Successful Biomarker Measurement, *Pharmaceutical Research, 23 (2)*

- Lee, (2009) Method validation and application of protein biomarkers: basic similarities and differences from biotherapeutics, *Bioanalysis*, *1(8),* 1461-1474.

This section details the validation experiments performed and the data obtained.

3.3.1 Parallelism: plasma assay

Three plasma samples from patients with suspected neurodegenerative disorders were assayed at multiple dilutions; 1/20, 1/40, 1/50, 1/75 and 1/100. The samples were diluted using assay diluent (1% (v/v) plasma in SM01:PBS). The data are shown in Table 3.2 and Figure 3.7:

Dilution Factor	1/Dilution	Mean conc. (ng/mL)	SD	CV%	Dil. Corr. conc. (ng/mL)	Mean Dil. Corr. Conc. (ng/mL)	% Difference
Plasma from Individual 1							
1/20	0.050	12.3	0.40	3.2	246	256	-3.9
1/40	0.025	5.96	0.22	3.6	239		-6.6
1/50	0.020	5.66	0.22	3.8	283		10.8
1/75	0.013	3.43	0.04	1.2	257		0.7
1/100	0.010	2.53	0.09	3.4	253		-1.0
Plasma from Individual 2							
1/20	0.050	39.5	5.54	14.0	789	844	-6.5
1/40	0.025	22.0	0.98	4.4	880		4.3
1/50	0.020	17.3	0.60	3.5	864		2.4
1/75	0.013	10.9	0.52	4.7	820		-2.8
1/100	0.010	8.66	0.40	4.6	866		2.6
Plasma from Individual 3							
1/20	0.050	12.8	0.22	1.7	256	224	14.0
1/40	0.025	5.46	0.11	2.0	218		-2.6
1/50	0.020	4.52	0.29	6.5	226		0.7
1/75	0.013	2.74	0.04	1.6	206		-8.3
1/100	0.010	2.16	0.02	1.0	216		-3.8

Table 3.2: Plasma Parallelism: *Precision (%CV) and % Difference for three plasma samples at 1/20, 1/40, 1/50, 1/75 and 1/100 dilutions with 1% (v/v) plasma assay buffer. % difference calculated from the mean (n=3) result of all dilutions. Each sample analysed in triplicate.*

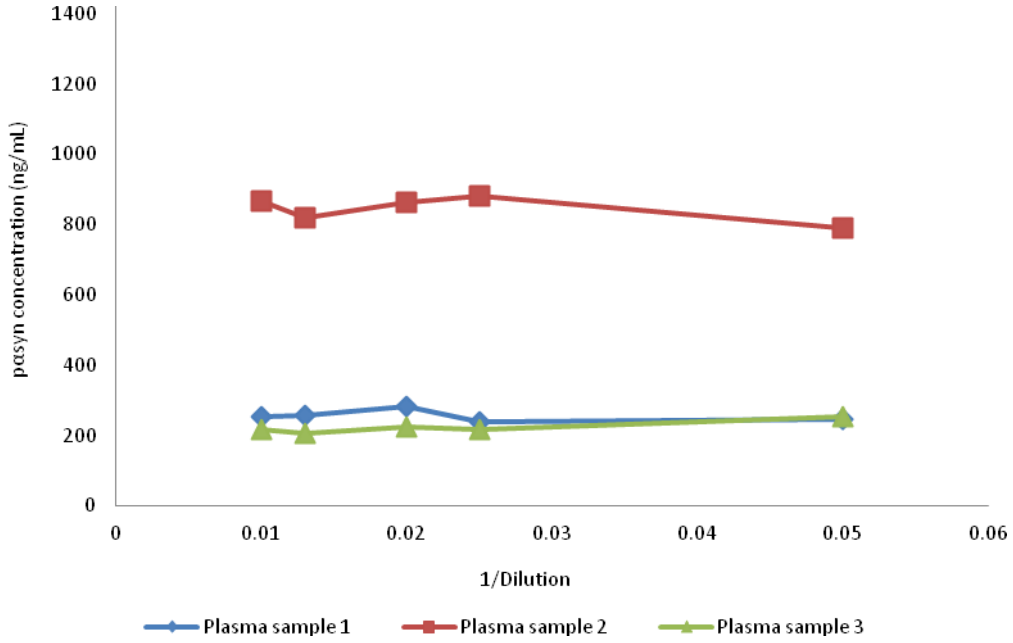

Figure 3.7: Plasma Parallelism: *three plasma samples reacted with Luminex beads coupled with 2 µg/mL of P-syn/81A mouse anti-α-synuclein phospho-specific (Ser129) mAb at various dilutions. 0.5 µg/mL of biotinylated detection Ab with 4 µg/mL streptavidin-RPE was used as the detection system for the assay.*

The % difference was shown to be between -8.3% and 14.0%, with precision (% CV) between 0.97% and 14.0%.

Remaining validation experiments were performed using a calibration curve generated by spiking recombinant phosphorylated α-synuclein into 1% (v/v) plasma diluent at 0, 0.469, 0.938, 1.876, 3.752, 7.50, 15.0, 30.0, and 60.0 and 120 ng/mL (120 ng/mL was used as an anchor calibrator). All plasma samples were diluted x50 with 1% (v/v) plasma diluent. The range of quantitation for the assay was therefore between 25 and 3000 ng/mL.

3.3.2 Spike Recovery: plasma assay

Six patient samples were analysed with 1000 ng/mL of recombinant protein spiked into it. An additional six patient samples were spiked with 90 ng/mL of recombinant phosphorylated α-synuclein and analysed. Each sample was also analysed alone without any spike material. All samples were analysed in triplicate (Table 3.3)

Mean blank (ng/mL)	**CV%**	**Mean spike + 1000 ng/mL**	**CV%**	**Expected (Blank + spike) (ng/mL)**	**% Recovery**
Plasma 1					
295	2.0	1212	1.8	1295	93.6
Plasma 2					
986	0.9	1846	6.1	1986	93.0
Plasma 3					
599	2.2	1447	2.8	1599	90.5
Plasma 4					
1885	6.1	3042	1.3	2885	105.4
Plasma 5					
213	2.9	1000	3.5	1213	82.5
Plasma 6					
0.00	0.00	902	4.8	1000	90.2
Mean blank (ng/mL)	**CV%**	**Mean spike + 90 ng/mL**	**CV%**	**Expected (Blank + spike) (ng/mL)**	**% Recovery**
Plasma 1					
0.00	na	85.0	8.5	90	94.8
Plasma 2					
0.00	na	90.0	3.9	90	99.4
Plasma 3					
0.00	na	93.0	11.6	90	103.3
Plasma 4					
0.00	na	97.0	1.3	90	108.0
Plasma 5					
0.00	na	84.0	9.5	90	93.7
Plasma 6					
0.00	na	85.0	10.3	90	93.9

Table 3.3: Plasma Spike Recovery: *% recovery and precision (%CV) for six plasma samples spiked with 1000 ng/mL and 90 ng/mL of recombinant phosphorylated α-synuclein.*

The % recovery for the spiked samples ranged between 82.5% and 105.4% at the high level spikes with a precision between 1.3% and 6.1%. The low spike recoveries ranged between 93.7% and 108.0% with a precision of 1.3% to 11.6%.

3.3.3 Dilutional linearity and Hook Effect: plasma assay

A pooled plasma sample (made up of several healthy donors from Blood Transfusion Unit, Manchester, UK) was spiked with 20000 ng/mL of recombinant phosphorylated α-synuclein. This spiked sample was diluted 1/50, 1/100, 1/200, 1/400, 1/800, 1/1600 and 1/3200. Each diluted sample was analysed in triplicate on the Luminex and the data obtained are shown in Table 3.4

Dilution	1/Dilution	Result (ng/mL)			Mean Result (ng/mL)	Expected Result (ng/mL)	% Difference
1/50	0.02	> ULOQ	> ULOQ	> ULOQ	> ULOQ	na	na
1/100	0.01	> ULOQ	> ULOQ	> ULOQ	> ULOQ	na	na
1/200	0.005	> ULOQ	> ULOQ	> ULOQ	> ULOQ	na	na
1/400	0.0025	16404	16892	16692	16663	20000	-16.7
1/800	0.00125	17496	17792	18704	17997	20000	-10.0
1/1600	0.000625	18000	18416	16800	17739	20000	-11.3
1/3200	0.0003125	16736	17440	17984	17387	20000	-13.1

Table 3.4: Plasma Dilutional Linearity: *% difference for a pooled plasma sample diluted at 1/50, 1/100, 1/200, 1/400, 1/800, 1/1600 and 1/3200 with 1% (v/v) plasma assay buffer.*

The difference between the expected result and the obtained result was ≤ -16.7 %, showing that samples can be diluted up to 3200 times without compromising the achieved result. To further show the linearity of the dilutions, a regression plot was performed using Microsoft Excel and is displayed as Figure 3.8

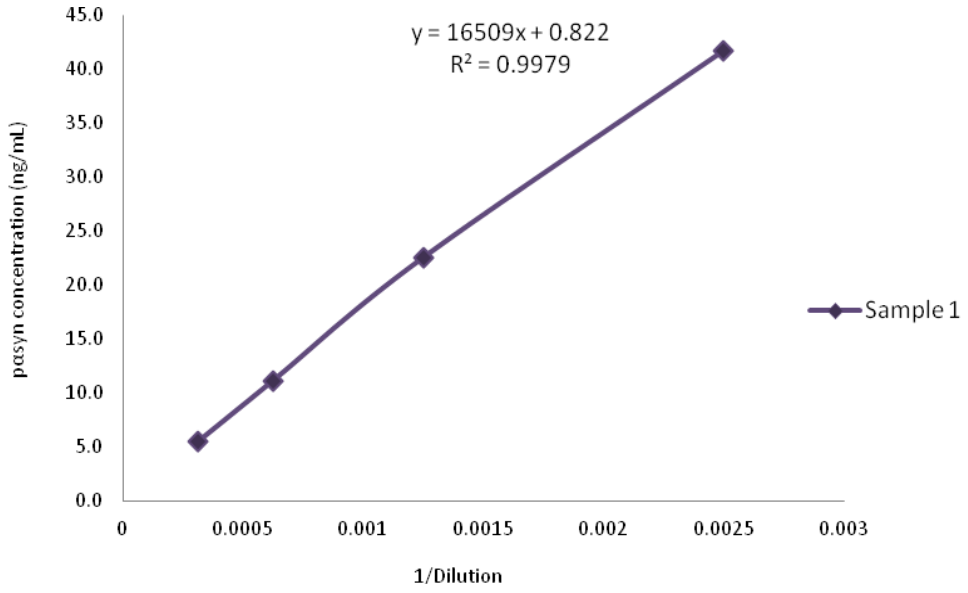

Figure 3.8: Plasma Dilutional Linearity: *pooled plasma sample underwent a series of dilutions. Each diluted sample was reacted with Luminex beads coupled with 2 µg/mL of P-syn/81A mouse anti-α-synuclein phospho-specific (Ser129) mAb. 0.5 µg/mL of biotinylated detection Ab with 4 µg/mL streptavidin-RPE was used as the detection system for the assay.*

The R^2 value was 0.9979, showing that the sample diluted in a linear fashion.

This experiment was also used to assess hook effect for the assay (refer to Chapter 2b for the definition of hook effect). The results (Table 3.5 and Figure 3.9) showed that the MFI signal at 20000 ng/mL of recombinant phosphorylated α-synuclein does not reduce. A reduction in the signal would have indicated a hook effect.

Dilution	1/Dilution	Raw MFI Result			Mean MFI Result
1/50	0.02	5017	4802	4847	4889
1/100	0.01	4156	4132	4059	4116
1/200	0.005	2711	2969	3053	2911
1/400	0.0025	1688	1731	1713	1711
1/800	0.00125	968	983	1029	993
1/1600	0.000625	524.5	536	492	518
1/3200	0.0003125	256.5	266.5	274.5	266

Table 3.5: Plasma Hook Effect: *Raw Luminex MFI data for pooled plasma sample spiked with 20000 ng/mL and analysed post a series of dilutions starting with 1/50.*

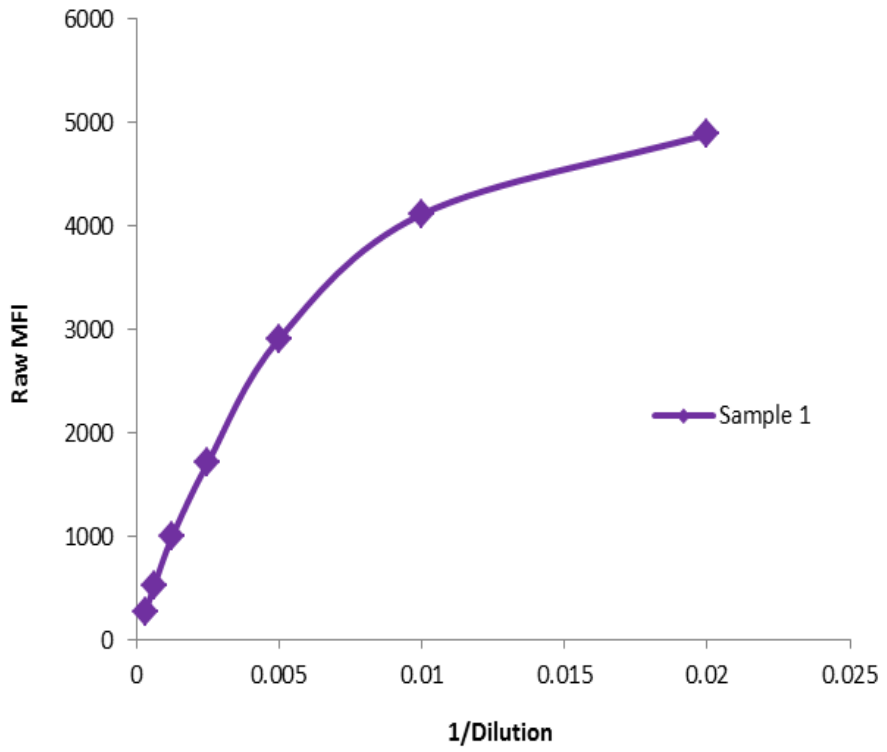

Figure 3.9: Plasma Hook Effect: *pooled plasma sample underwent a series of dilutions. Each diluted sample was reacted with Luminex beads coupled with 2 µg/mL of P-syn/81A mouse anti-α-synuclein phospho-specific (Ser129) mAb. 0.5 µg/mL of biotinylated detection Ab with 4 µg/mL streptavidin-RPE was used as the detection system for the assay. Raw MFI data are plotted to deduce if the signal was reduced in the presence of high levels of recombinant phosphorylated α-synuclein.*

3.3.4 Accuracy and Precision: plasma assay

A total of six assays were performed on different dates to assess the accuracy and precision of the assay. Five samples; ULOQ, HVS, MVS, LVS and LLOQ, were generated and used for this assessment.

The ULOQ sample was generated by spiking 3000 ng/mL of recombinant phosphorylated α-synuclein into neat blank plasma to yield a MFI assay reading in the region of 60 ng/mL after the x 50 assay dilution.

A number of plasma samples from patients with various neurodegenerative disorders were screened in order to select samples that would serve as the HVS, MVS and LVS. Three samples were identified and used for assessing the precision of the assay at different regions of the calibration curve. The approximate concentrations of these samples were 2000 – 2500 ng/mL, 750 – 1000 ng/mL and 50 – 75 ng/mL, respectively. These equated to 40 – 50 ng/mL, 15 – 25 ng/mL and 1 – 1.5 ng/mL post the x 50 assay dilution.

The LLOQ sample was generated by spiking 25 ng/mL of recombinant phosphorylated α-synuclein into neat blank plasma to yield a MFI assay reading in the region of 0.5 ng/mL after the x50 assay dilution.

Each sample was assayed in three wells on each assay plate. Both Inter-assay and Intra-assay precision and accuracy was determined. Table 3.6 shows the inter-assay data and Table 3.7 shows the intra-assay data:

Assay Date	ULOQ	HQ	MQ	LQ	LLOQ
27-Mar-14	63.0	40.8	18.7	1.12	0.42
	61.5	37.9	19.0	0.99	0.45
	59.4	40.2	17.7	1.11	0.40
28-Mar-14	60.6	38.7	18.1	1.12	0.50
	61.4	37.7	18.6	1.13	0.53
	54.3	37.6	19.7	0.95	0.41
01-Apr-14	57.0	39.0	16.4	1.19	0.51
	59.7	41.2	18.5	1.16	0.54
	62.5	43.9	16.7	1.09	0.46
03-Apr-14	57.3	41.7	18.8	1.29	0.43
	53.5	30.4	17.9	1.20	0.38
	55.9	42.0	18.1	1.12	0.56
05-Apr-14	66.4	34.3	16.9	1.16	0.45
	60.1	34.7	17.4	1.23	0.46
	65.6	39.9	15.5	1.17	0.57
11-Apr-14	52.3	37.8	16.6	1.07	0.34
	64.0	43.5	18.8	1.10	0.42
	65.1	46.1	19.0	1.04	0.43
Inter-assay data					
Mean	60.0	39.3	17.9	1.12	0.459
SD	4.218	3.770	1.129	0.082	0.064
CV%	7.0	9.6	6.3	7.3	13.9
% Difference/Bias	0.0	na	na	na	-8.2

Table 3.6: Plasma Inter-assay Accuracy and Precision: *ULOQ, HVS, MVS, LVS and LLOQ samples were analysed on the Luminex for the quantification of phosphorylated α-synuclein. The precision was calculated using %CV (SD/mean %) and the bias for ULOQ and LLOQ was calculated using %difference ((observed-expected)/expected * 100)*

Assay Date	Intra-assay data	ULOQ	HQ	MQ	LQ	LLOQ
27-Mar-14	Mean	61.3	39.6	18.5	1.07	0.42
	SD	1.79	1.57	0.71	0.07	0.03
	CV%	2.9	4.0	3.9	6.7	5.9
	%Difference/Bias	2.2	na	na	na	-15.3
28-Mar-14	Mean	58.7	38.0	18.8	1.07	0.48
	SD	3.90	0.60	0.81	0.10	0.06
	CV%	6.6	1.6	4.3	9.5	13.0
	%Difference/Bias	-2.1	na	na	na	-4.0
01-Apr-14	Mean	59.7	41.4	17.2	1.15	0.50
	SD	2.80	2.48	1.14	0.05	0.04
	CV%	4.7	6.0	6.6	4.5	8.0
	%Difference/Bias	-0.5	na	na	na	0.7
03-Apr-14	Mean	55.6	38.0	18.2	1.20	0.46
	SD	1.91	6.64	0.46	0.09	0.09
	CV%	3.4	17.5	2.5	7.1	20.3
	%Difference/Bias	-7.4	na	na	na	-8.7
05-Apr-14	Mean	64.0	36.3	16.6	1.19	0.49
	SD	3.45	3.12	1.00	0.04	0.07
	CV%	5.4	8.6	6.0	3.2	13.5
	%Difference/Bias	6.7	na	na	na	-1.3
11-Apr-14	Mean	60.5	42.5	18.1	1.07	0.40
	SD	7.08	4.20	1.37	0.03	0.05
	CV%	11.7	9.9	7.6	2.8	12.4
	%Difference/Bias	0.8	na	na	na	-20.7
Intra-assay data	Intra-CV%	5.8	7.9	5.1	5.6	12.2

Table 3.7: Plasma Intra-assay Accuracy and Precision: *ULOQ, HVS, MVS, LVS and LLOQ samples were analysed on the Luminex for the quantification of phosphorylated α-synuclein. The precision was calculated using CV% (SD/mean %) and the bias for ULOQ and LLOQ was calculated using %difference ((observed-expected)/expected * 100). Intra assay precision was calculated from the average CV% from each individual assay.*

The average inter assay precision was shown to be ≤ 13.9% and the bias based on the spiked known concentrations was ≤ -8.2%.

The assay intra assay precision averaged at ≤ 12.2%, and the bias of the spiked known concentrations ranged from -20.7 to 6.7%.

3.3.5 Limit of detection: plasma assay

As defined by Armbruster *et al* (2008), the limit of detection (LOD) is the lowest analyte concentration that may be reliably distinguished from a blank sample. The method used to ascertain this limit entailed analysing a blank sample 20 times, determining the mean value and then using the mean + 3SD as the LOD.

The mean MFI reading from 20 replicates of the blank sample for this assay was measured at 7.5 with a standard deviation of 0.6. Therefore, the mean MFI + 3*SD was calculated to be 9.39.

The Luminex software cannot be manipulated in order to generate a value for the mean blank + 3SD MFI signal, therefore, a readily available software program called "Elisa analysis" (available at http://elisaanalysis.com/app) was used for this task. According to this program, a MFI signal of 9.39 correlates to a concentration of 0.02 ng/mL of phosphorylated α-synuclein. Correcting this value for the proposed minimum dilution of x 50 for the assay, the LOD was calculated to be 1 ng/mL (0.02 * 50).

3.4 Assay Validation: assay for analysing human CSF samples

The Luminex assay for the quantification of phosphorylated α-synuclein was also used to measure phosphorylated α-synuclein levels in CSF. The assay underwent slight modifications and a similar validation procedure as described in previous sections, in order to qualify the assay fit for use with human CSF samples.

The assay modifications included determining the minimum required dilution of samples. This was determined by performing spike recovery experiments at a series of sample dilutions. The minimum required dilution was x5 and the spike recovery data obtained at this dilution are shown in section 3.4.2.

The calibration curve was performed using 20% (v/v) blank human CSF spiked with recombinant phosphorylated α-synuclein at 200, 80, 32, 12.8, 5.12, 2.05, 0.819, 0.327, 0 ng/mL. The complete validation data obtained are displayed in this section.

3.4.1 Parallelism: CSF assay

One sample was used to assess this parameter due to very low detectable levels of phosphorylated α-synuclein present in CSF. The data from this one sample are show in Table 3.8 and Figure 3.10:

Dilution Factor	1/Dilution	Mean conc. (ng/mL)	SD	CV%	Dil. Corr. conc. (ng/mL)	Overall Mean Dil. Corr. Conc. (ng/mL)	% Difference
CSF from Individual 1							
1/5	0.000	197	4.64	2.4	197	213	-7.3
1/10	0.500	114	5.15	4.5	228		7.0
1/20	0.250	53.4	1.80	3.4	214		0.4
1/40	0.125	27.3	0.49	1.8	218		2.6
1/80	0.063	12.9	0.79	6.1	207		-2.7

Table 3.8: CSF Parallelism: *Precision (%CV) and % Difference for one CSF sample Analysed at various dilutions with 20% (v/v) CSF assay buffer. % difference calculated form the overall mean result of all dilutions. Each sample analysed in triplicate.*

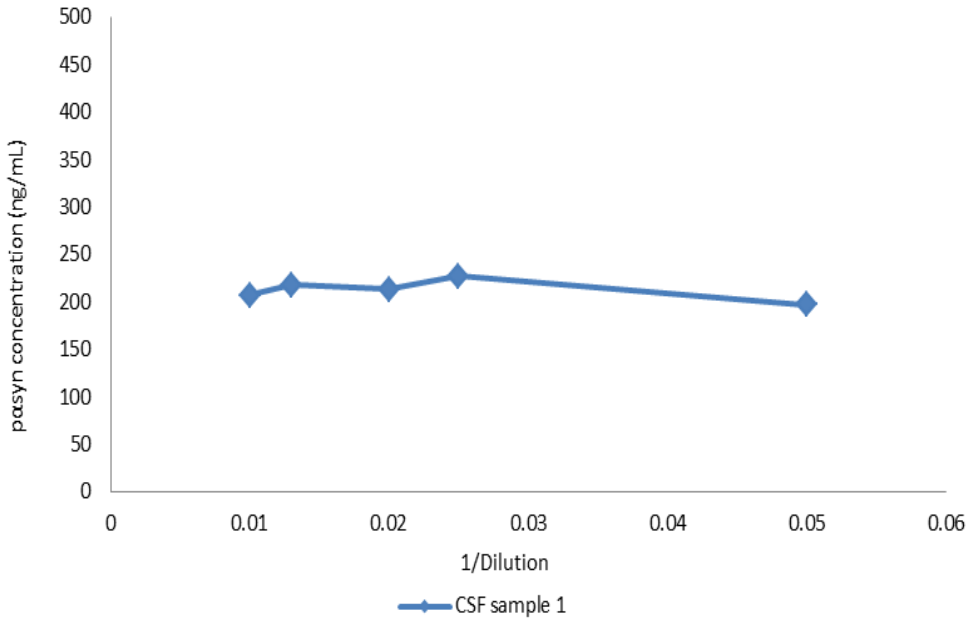

Figure 3.10: CSF Parallelism: *a CSF sample analysed at various dilutions; 1/5, 1/10, 1/20, 1/40 and 1/80.*

The % difference was shown to be between -7.3% and 7.0%, with precision between 1.8% and 6.1%.

3.4.2 Spike Recovery: CSF assay

Patient CSF samples were spiked with various concentrations of phosphorylated α-synuclein; 150, 100, 2 or 15 ng/mL. The results obtained are displayed in Table 3.9.

Mean blank (ng/mL)	CV%	Spike (+100 ng/mL)			Mean spike (ng/mL)	CV%	Expected (Blank + spike) (ng/mL)	% Recovery
CSF sample 1								
1.11	16.1	106	98.4	104	103	3.7	101	101.6
CSF sample 2								
0.3	0.0	109	115	112	112	2.7	100	111.9
CSF sample 3								
0.7	13.4	97.4	98.7	98.2	98.1	0.7	101	97.4
Mean blank (ng/mL)	**CV%**	**Spike (+150 ng/mL)**			**Mean spike (ng/mL)**	**CV%**	**Expected (Blank + spike) (ng/mL)**	**% Recovery**
CSF sample 4								
0.0	0.0	144	183	174	167	12.2	150	111.4
CSF sample 5								
0.18	50.4	144	152	135	144	5.7	150	95.6
CSF sample 6								
0.48	0.0	169	168	181	173	4.2	150	114.7
Mean blank (ng/mL)	**CV%**	**Spike (+2 ng/mL)**			**Mean spike (ng/mL)**	**CV%**	**Expected (Blank + spike) (ng/mL)**	**% Recovery**
CSF sample 7								
1.11	16.1	2.23	2.68	2.68	2.53	10.3	2.61	96.8
CSF sample 8								
0.3	0.00	1.28	1.90	1.59	1.59	19.5	1.76	90.3
CSF sample 9								
0.7	13.4	2.13	2.64	2.05	2.27	14.1	2.23	101.8
Mean blank (ng/mL)	**CV%**	**Spike (+15 ng/mL)**			**Mean spike (ng/mL)**	**CV%**	**Expected (Blank + spike) (ng/mL)**	**% Recovery**
CSF sample 10								
1.1	16.1	14.2	13.0	13.6	13.6	4.5	16.1	84.4
CSF sample 11								
0.18	50.4	12.8	14.4	16.5	14.6	12.5	15.2	95.9
CSF sample 12								
0.48	0.0	14.0	13.1	11.5	12.9	9.9	15.5	83.0

Table 3.9: CSF spike recovery: *% recovery and precision (%CV) for a total of 12 CSF samples spiked with 100, 150, 2 or 15 ng/mL of recombinant phosphorylated α-synuclein*

The % recovery for the spiked samples ranged between 95.6% and 114.7% at the high level spikes (100 and 150 ng/mL) with a precision between 0.7% and 12.2%. The low spike recoveries (2 and 15 ng/mL) ranged between 83.0% and 101.8% with a precision of 4.5% to 19.5%.

3.4.3 Dilutional linearity and Hook Effect: CSF assay

Three CSF samples taken from individuals with various neurodegenerative disorders were spiked with 2000 ng/mL of recombinant phosphorylated α-synuclein.

The spiked samples were then diluted 1 in 5, 1 in 25, 1 in 125, 1 in 625, and 1 in 3125 with 20% (v/v) CSF assay diluent. Each diluted sample was analysed on the Luminex and the data obtained are shown in Table 3.10.

Dilutional linearity sample 1				
Dilution	1/Dilution	Mean Result	Expected Result	% Difference
1/5	0.02	na	<ULOQ	na
1/25	0.04	76.2	81.3	-6.4
1/125	0.008	16.0	16.3	-1.6
1/625	0.0016	3.3	3.3	2.4
1/3125	0.00032	0.9	<LLOQ	na
Blank	0	1.3	Na	na
Dilutional linearity sample 2				
Dilution	1/Dilution	Mean Result	Expected Result	% Difference
1/5	0.02	na	<ULOQ	na
1/25	0.04	76.9	80.8	-4.8
1/125	0.008	15.8	16.2	-2.3
1/625	0.0016	3.6	3.2	11.7
1/3125	0.00032	0.8	<LLOQ	na
Blank	0	0.8	Na	na
Dilutional linearity sample 3				
Dilution	1/Dilution	Mean Result	Expected Result	% Difference
1/5	0.02	na	<ULOQ	na
1/25	0.04	79.4	80.5	-1.4
1/125	0.008	16.4	16.1	1.6
1/625	0.0016	3.6	3.2	11.5
1/3125	0.00032	0.8	<LLOQ	na
Blank	0	0.5	0	na

Table 3.10: CSF Dilutional Linearity: *% Difference for three CSF samples diluted at 1/5, 1/25, 1/125, 1/625, and 1/3125 with 20% (v/v) CSF assay buffer. Each sample analysed in triplicate.*

The % difference between the expected result and actual result was ≤ 11.7%, showing that samples can be diluted up to 3125 times without compromising the result. To further show the linearity of sample dilution, a regression plot for each of the three samples was performed as displayed in Figure 3.11.

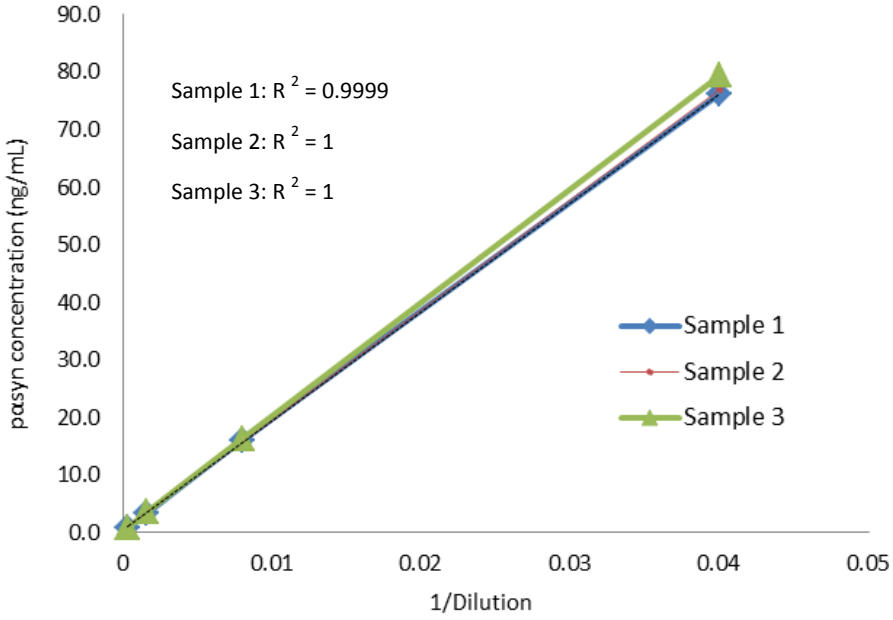

Figure 3.11: CSF Dilutional Linearity: *three CSF samples underwent a series of dilutions. Each diluted sample was reacted with Luminex beads coupled with 2 µg/mL of P-syn/81A mouse anti-α-synuclein phospho-specific (Ser129) mAb. 0.5 µg/mL of biotinylated detection Ab with 4 µg/mL streptavidin-RPE was used as the detection system for the assay.*

This experiment was also used to assess hook effect for the assay. The results in Table 3.11 and Figure 3.12 show that the MFI signal at 2000 ng/mL of recombinant phosphorylated α-synuclein does not reduce. A reduction in the signal would have indicated hook effect. Only data for sample 1 have been displayed, the other two samples generated similar results:

Dilution	1/Dilution	Raw MFI Result			Mean MFI Result
1/5	0.2	3052	3055	3196	3101
1/25	0.04	692	688	697	693
1/125	0.008	124	130	133	129
1/625	0.0016	28	25	28	27
1/3125	0.00032	11	10	10	10

Table 3.11: CSF Hook Effect: *Raw Luminex MFI data CSF sample 1 spiked with 2000 ng/mL and analysed post a series of dilutions starting with 1/5.*

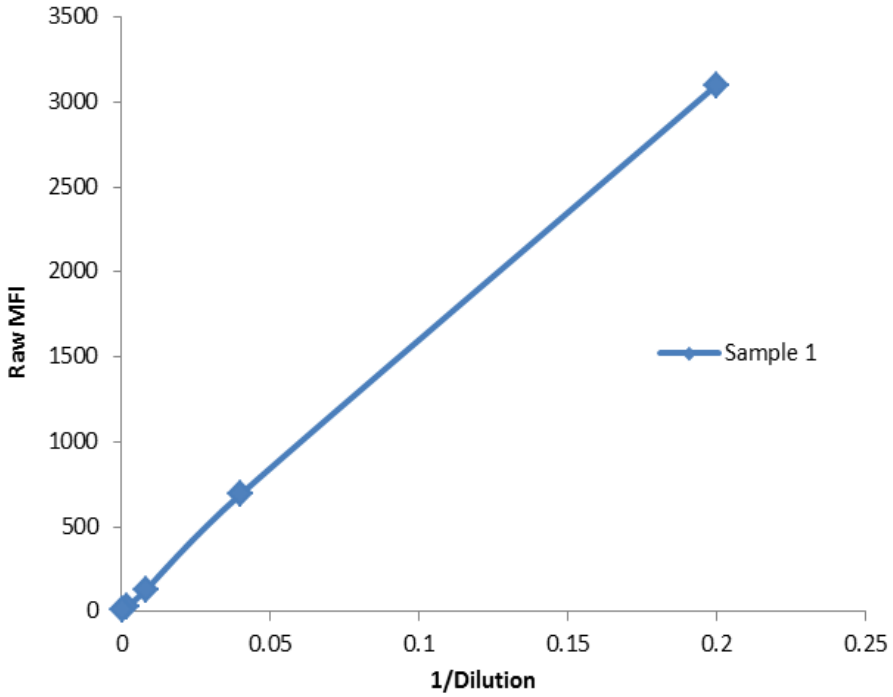

Figure 3.12: CSF Hook Effect: *three CSF were spiked with 2000 ng/mL of recombinant phosphorylated α-synuclein and then underwent a series of dilutions. The spiked sample and the each diluted sample was analysed. Raw MFI data are plotted to deduce if the signal was reduced in the presence of high levels of recombinant phosphorylated α-synuclein. Data for CSF sample 1 only are displayed.*

3.4.4 Accuracy and Precision: CSF assay

Assays were performed on different dates to assess the accuracy and precision of the assay using five prepared samples; ULOQ, HVS, MVS, LVS and LLOQ.

CSF samples, both from individuals with suspected neurodegenerative disorders and healthy individuals were screened in order to find and select samples that could serve as the ULOQ, HVS, MVS, LVS and LLOQ samples. Unfortunately, no samples were suitable for this purpose; therefore, all samples were generated by spiking recombinant phosphorylated α-synuclein into blank CSF.

The ULOQ sample was generated by spiking 200 ng/mL of recombinant phosphorylated α-synuclein into neat blank CSF and then diluted x 5. The HVS, MVS, LVS and LLOQ samples were generated in a similar fashion by spiking 150, 50, 12.5 and 1.2 ng/mL of recombinant phosphorylated α-synuclein into the blank CSF.

Each sample was assayed in three wells on each assay plate. Both Inter-assay and Intra-assay precision and accuracy has been determined from ≥ 7 different assay runs. Table 3.12 shows the inter-assay data and Table 3.13 shows the intra-assay data:

Assay Date	ULOQ	HQ	MQ	LQ	LLOQ
12-Sep-14	192	138	49.9	na	na
	169	136	52.5	na	na
	193	142	50.0	na	na
13-Sep-14	179	145	47.0	13.4	0.97
	x	133	49.6	13.0	0.97
	192	144	51.0	12.8	0.97
18-Sep-14	188	136	55.1	13.7	1.23
	185	157	45.2	14.2	1.07
	209	146	45.7	12.9	1.18
06-07 Oct 2014	210	167	64.0	14.8	1.45
	220	154	62.9	13.4	1.58
	163	160	56.0	10.4	1.13
07-08 Oct 2014	184	155	51.2	12.5	1.41
	na	170	52.9	11.1	1.64
	na	171	57.1	11.3	1.04
10-11 Oct 2014	200	176	48.9	12.2	na
	196	151	54.2	12.2	na
	196	148	46.6	11.3	na
15-16 Oct 2014	215	159	52.8	11.9	1.72
	201	169	55.8	11.0	na
	216	162	58.2	11.8	na
15-16 Oct 2014 b	na	181	56.6	11.5	1.24
	na	186	55.7	12.3	1.27
	na	171	46.1	12.2	1.35
18-19 Oct 2014	na	175	55.1	13.7	1.52
	na	173	66.7	12.2	1.36
	na	173	58.3	13.8	1.36
21-22 Oct 2014 b	na	170	64.7	13.3	1.28
	na	197	52.2	15.3	1.02
	na	173	57.8	11.7	1.15
Inter-assay data					
Mean	195	161	54.0	12.6	1.27
SD	15.667	16.360	5.723	1.197	0.223
CV%	8.0	10.2	10.6	9.5	17.6
% Difference/Bias	-2.6	7.0	8.0	0.6	5.7

Table 3.12: CSF Inter-assay Accuracy and Precision: *ULOQ, HVS, MVS, LVS and LLOQ samples were analysed on the Luminex for the quantification of phosphorylated α-synuclein. The precision was calculated using %CV (SD/mean %) and the accuracy was calculated using %difference ((observed-expected)/expected * 100)*

Assay Date	Intra-assay data	ULOQ	HQ	MQ	LQ	LLOQ
12-Sep-14	Mean	185	139	50.8	na	na
	SD	13.29	3.41	1.48	na	na
	CV%	7.2	2.5	2.9	na	na
	%Difference/Bias	-7.6	-7.6	1.6	na	na
13-Sep-14	Mean	185	140	49.2	13.0	0.97
	SD	9.29	6.87	1.99	0.30	0.00
	CV%	5.0	4.9	4.1	2.3	0.0
	%Difference/Bias	-7.4	-6.4	-1.6	4.2	-19.2
18-Sep-14	Mean	194	146	48.7	13.6	1.16
	SD	12.69	10.36	5.56	0.62	0.08
	CV%	6.54	7.09	11.42	4.56	7.06
	%Difference/Bias	-3.0	-2.6	-2.6	8.8	-3.3
06-07 Oct 2014	Mean	198	161	61.0	12.86	1.39
	SD	30.27	6.37	4.32	2.27	0.23
	CV%	15.3	4.0	7.1	17.6	16.7
	%Difference/Bias	-1.2	7.1	na*	2.9	15.6
07-08 Oct 2014	Mean	184	166	53.7	11.6	1.4
	SD	na	9.17	3.04	0.74	0.30
	CV%	na	5.54	5.66	6.41	22.2
	%Difference/Bias	-8.2	10.3	7.5	-7.2	13.6
10-11 Oct 2014	Mean	197	158	49.9	11.9	na
	SD	2.68	15.42	3.87	0.51	na
	CV%	1.4	9.8	7.7	4.3	na
	%Difference/Bias	-1.4	5.4	-0.2	-4.8	na
15-16 Oct 2014	Mean	211	163	55.6	11.5	1.7
	SD	8.33	5.24	2.72	0.51	0.70
	CV%	3.9	3.2	4.9	4.5	40.7
	%Difference/Bias	5.4	8.9	11.2	-7.7	43.3
15-16 Oct 2014 b	Mean	na	179	52.8	12.0	1.3
	SD	na	7.82	5.80	0.42	0.06
	CV%	na	4.36	10.98	3.50	4.42
	%Difference/Bias	na	na*	5.6	-3.8	7.2
18-19 Oct 2014 b	Mean	na	173	60.0	13.2	1.4
	SD	na	1.01	6.01	0.86	0.09
	CV%	na	0.6	10.0	6.5	6.5
	%Difference/Bias	na	15.6	na*	5.7	17.8
21-22 Oct 2014 b	Mean	na	180	58.3	13.4	1.2
	SD	na	14.88	6.25	1.77	0.13
	CV%	na	8.3	10.7	13.2	11.3
	%Difference/Bias	na	na*	16.5	7.4	-4.2

Intra-assay data	Intra-CV%	6.6	5.0	7.6	7.0	13.6

Table 3.13: CSF Intra-assay Accuracy and Precision: *ULOQ, HVS, MVS, LVS and LLOQ samples were analysed on the Luminex for the quantification of phosphorylated α-synuclein. The precision was calculated using CV% (SD/mean %) and the accuracy was calculated using %difference ((observed-expected)/expected * 100). Intra assay precision was calculated from the average CV% from each individual assay. na* represents data exclusion due to known error during assay.*

The average inter assay precision ranged between 8.0% and 17.6% and the bias, based on the spiked known concentrations, was between -2.6% and 8.0%.

The assay mean intra assay precision was between 5.0% and 13.6%, and the bias of the spiked known concentrations (ULOQ to LLOQ levels) ranged from -19.2% and 17.8% (43.3% bias was achieved in one assay at LLOQ).

3.4.5 Limit of detection: CSF assay

The method used to ascertain the LOD entailed analysing a blank sample (20% (v/v) CSF) 20 times, determining the mean value and then using the mean + 3SD as the LOD. The mean MFI for the 20 blank sample replicates was 5.63 with a standard deviation of 0.78. The mean MFI + 3*SD was therefore calculated to be 7.95.

The “Elisa anlaysis” program (available at http://elisaanalysis.com/app) was used for converting the Luminex MFI signal into a concentration value of CSF phosphorylated α-synuclein in the blank CSF sample. According to this program, a MFI signal of 7.95 correlates to a concentration of 0.32 ng/mL of phosphorylated α-synuclein.

3.5 Discussion

This chapter presented the development and validation of a Luminex assay for the quantification of phosphorylated α-synuclein levels in human plasma and CSF. An ELISA assay for this purpose was already developed in house, but the purpose of this project was to transfer this assay onto a more sensitive platform and then use this for subsequent sample analysis. Unfortunately the antibodies used in the original ELISA assay; N-19 (capture antibody) and EP1536Y (detection antibody), did not work well with the Luminex technology and as a result alternative antibodies were selected and used.

Two possible reasons can be offered as to why the original ELISA antibodies did not work on the Luminex platform. It should be noted that these possible reasons were not proven experimentally but may serve to explain the possible causes for the assay transfer failure:

1. Inefficient coupling of the capture antibody to the beads: the N-19 pAb was supplied at 200 µg/mL with 0.1 % gelatin and sodium azide. For optimal bead coupling, it is recommended that the antibody is free from BSA, glycine, sodium azide and other TRIS or amine containing additives. The antibody did undergo a buffer exchange step and was concentrated to 1 mg/mL prior to the coupling reaction, but it is possible that some of the interfering components remained and thus compromised the bead coupling reaction. Also, procedures such as buffer exchange can lead to loss of antibody and this may have contributed to the fact that the assay failed to work with N-19 as the capture antibody (http://www.bio-rad.com/webroot/web/pdf/lsr/literature/4110012B.pdf).

2. Poor biotinylation of the detection antibody: the EP1536Y antibody was supplied in 50% glycerol. The biotinylation technique adopted in this project involved biotinylating the antibody via the formation of a NHS ester. The presence of high levels of glycerol interferes with this reaction. Again, as with the N-19 antibody, a buffer exchange step was performed prior to biotinylation, but this may not have been effective at removing such large concentrations of glycerol, thus leading to poor biotinylation (https://www.lifetechnologies.com/order/catalog/product/20217). The original ELISA assay that utilised the EP1536Y antibody for detection did not require being biotinylated, thus the buffer constituents and interference with biotinylation would not have posed an issue.

The guidelines (Lee *et al*, 2006b and 2009) used for validating the phosphorylated α-synuclein Luminex assay provide detailed descriptions of the parameters to validate and how, but do not provide acceptance criteria for the various assessments. Cummings *et al* (2010) have published a set of guidelines with acceptance criteria to support biomarker assessments for anti-cancer drug clinical trials. These acceptance criteria are summarised (Table 3.14):

Validation Parameter	Acceptance criteria
Inter assay bias	≤ 20% recovery at HQ, MQ and LQ level ≤ 25% recovery at LLOQ and ULOQ
Intra assay bias	≤ 20% recovery at HQ, MQ and LQ level ≤ 25% recovery at LLOQ and ULOQ
Inter assay precision	≤ 20% CV at HQ, MQ and LQ level ≤ 25% CV at LLOQ and ULOQ
Intra assay precision	≤ 20% CV at HQ, MQ and LQ level ≤ 25% CV at LLOQ and ULOQ
Parallelism	≤ 20% bias ≤ 30% precision
Dilutional linearity	≤ 20% bias ≤ 30% precision
Spike Recovery	Not specified, but we have adopted the same criteria as Parallelism and Dilutional linearity

Table 3.14: Assay validation acceptance criteria: *parameters assessed for the Luminex assay and the acceptance criteria used.*

The validation data obtained for the quantification of phosphorylated α-synuclein in human plasma and CSF met all the criteria outlined by Cummings *et al* (2010). A "Draft – not to be implemented Guidance for Industry" document was released in September 2013 by the FDA in the US and includes acceptance criteria that closely relate to those summarised in table 3.14 (US Department of Health and Human Services, 2013). Therefore, if this draft document becomes an official document, the data shown in this chapter will meet the Government based requirements.

One of the aims for developing a Luminex assay was to improve the sensitivity at which levels of phosphorylated α-synuclein can be detected and measured in human plasma and CSF. The LOD for the ELISA assay was calculated prior to the commencement of this project, by Dr Penny Foulds. The ELISA for quantifying phosphorylated α-synuclein in human plasma had a LOD of 40 ng/mL and 3 ng/mL in CSF. The Luminex assay for quantifying phosphorylated α-synuclein was found to have a LOD of 1 ng/mL for human plasma and 0.3 ng/mL for CSF. Thus the Luminex assay provided a much more sensitive assay than the original ELISA.

Chapter 4:

Phosphorylated α-synuclein: sample analysis results

4.1 Introduction

Chapter 3 described the development and validation of a Luminex assay for quantifying phosphorylated α-synuclein in human plasma and CSF. This assay was used to analyse a series of plasma and CSF samples taken from individuals affected by various neurodegenerative disorders such as AD, PD, MSA, PSP and CBD.

Samples obtained from two independent sites were analysed. One set of samples was obtained from patients attending out-patient clinics at Greater Manchester Neurosciences Centre (GMNC) at Salford Royal Hospital; a total of 269 plasma samples, taken from patients with AD, PD, MSA, PSP and CBD were received. Additionally, 94 matched plasma and CSF samples were obtained from the Department of Neurology, University College Hospital, London (UCL), courtesy of Dr Nadia Magdalinou. These matched plasma and CSF samples were collected from patients with MSA, PD, PSP and CBS. Both sites also provided a set of samples taken from healthy controls; 72 from GMNC and 26 from UCL.

All samples were analysed in triplicate (3 wells) against a standard curve and minimum three levels of quality controls at the beginning and end of each assay plate as described in the Methods section (Chapter 2b) and Appendix 1. Data from samples were only used if they met the acceptance criteria outlined in Chapter 2b.

The aim was to see if levels of phosphorylated α-synuclein show significant differences between the different disease groups. The availability of matched plasma and CSF samples also provided the opportunity to assess whether levels of phosphorylated α-synuclein correlate in plasma and CSF.

This chapter displays the data obtained from the sample analysis and the outcomes from this investigation.

4.2 Phosphorylated α-synuclein levels in plasma samples from GMNC

The data for phosphorylated α-synuclein levels collected from the plasma samples from GMNC were analysed statistically using IBM SPSS Statistics 21 package. Data obtained from the Luminex software were sorted into the different disease groups and then checked for normality using Kolgomorov-Smirnov test. The data was not normally distributed; therefore the non-parametric Kruskal-Wallis (K-W) test (with post-hoc Mann-Whitney test when K-W was significant) was used in order to determine whether phosphorylated α-synuclein levels were significantly different between the different disease groups. A summary of the data obtained is tabulated in Table 4.1.

Disease group	n	pαsyn mean (ng/mL)	pαsyn median (ng/mL)	SD
AD	66	335	15	1344
PD	58	456	13	2378
DLB	63	518	12	1362
MSA	18	60	4	206
PSP	32	702	21	2173
CBD	15	83	13	248
Healthy Controls	69	236	24	461

Table 4.1: Plasma samples from GMNC data summary: *mean, median and SD calculated using Microsoft Excel 2010. Each sample was analysed in triplicate.*

By K-W test, the levels of phosphorylated α-synuclein between AD, PD, DLB, MSA, PSP, CBD and healthy controls were not significantly different (p=0.289).

4.3 Relationship between *APOE* genotype and phosphorylated α-synuclein levels in plasma samples from GMNC

An independent t-test was performed in order to investigate whether phosphorylated α-synuclein levels in plasma were influenced by the *APOE* genotype. This involved stratifying the phosphorylated α-synuclein levels according to the presence of at least one *APOE* ε4 allele, i.e. individuals who were heterozygous or homozygous for *APOE* ε4 allele, versus individuals without *APOE* ε4 allele. The test was done for each of the individual disease groups to see if the presence of *APOE* ε4 allele influenced phosphorylated α-synuclein levels in individuals with a particular disorder, or in healthy controls. Table 4.2 summarises the P-values obtained from this test:

Disease group	n with APOE E4	n without APOE E4	P value
AD	54	12	0.947
PD	42	16	0.422
DLB	30	33	0.207
MSA	12	6	0.546
PSP	25	7	0.547
CBD	6	8	0.273
Healthy Controls	56	12	0.525

Table 4.2: Independent t-test data summary: *phosphorylated α-synuclein levels stratified against the presence of APOE ε4 allele for individuals within each disease group.*

The P-value for each group was > 0.05, therefore it can be concluded that the presence of *APOE* ε4 allele has no influence on the levels of phosphorylated α-synuclein in plasma.

4.4 Phosphorylated α-synuclein levels in plasma samples from UCL

Data obtained from the UCL plasma samples were also analysed using the IBM SPSS Statistics 21 package. Again, the data were grouped according to disease type and checked for normality using the Kolgomorov-Smirnov test. The data was not normally distributed; therefore the K-W test was used to determine whether the levels of phosphorylated α-synuclein in plasma differed between disease groups. Table 4.3 summarises the data.

Disease group	n	pαsyn mean (ng/mL)	pαsyn median (ng/mL)	SD
PD/DLB	22	297	43	728
MSA	28	211	25	392
PSP	31	320	39	616
CBS	13	92	15	140
Healthy controls	26	229	23	355

Table 4.3: Plasma samples from UCL data summary: *mean, median and SD calculated using Microsoft Excel 2010. Each sample was analysed in triplicate.*

There was no significant difference in phosphorylated α-synuclein levels between PD/DLB, MSA, PSP, CBS and healthy controls (p=0.843 by K-W test).

4.5 Phosphorylated α-synuclein levels in samples from GMNC and UCL combined

The data obtained from GMNC and UCL were combined and then analysed as described previously.

Table 4.4 summarises the combined data:

Disease group	n	pαsyn mean (ng/mL)	pαsyn median (ng/mL)	SD
AD	66	335	15	1344
PD/DLB	143	294	43	728
MSA	46	211	25	391
PSP	63	322	29	636
Healthy controls	95	238	23	359

Table 4.4: Plasma samples from GMNC and UCL combined, data summary: *mean, median and SD calculated using Microsoft Excel 2010.*

There was no significant difference in the levels of plasma phosphorylated α-synuclein between the various neurodegenerative disorders (p=0.508 by K-W test).

4.6 Phosphorylated α-synuclein levels in CSF samples from UCL

The UCL plasma samples had matched CSF samples, and these were also analysed for levels of phosphorylated α-synuclein within the different disease groups (Table 4.5).

Disease group	n	pαsyn mean (ng/mL)	pαsyn median (ng/mL)	SD
PD/DLB	21	0.48	0.38	0.46
MSA	28	0.61	0.44	0.61
PSP	31	1.32	0.38	2.77
CBS	13	0.54	0.26	0.93
Healthy controls	26	0.62	0.30	0.95

Table 4.5: CSF samples from UCL data summary: *mean, median and SD calculated using Microsoft Excel 2010. Each sample was analysed in triplicate.*

There was no significant difference in the levels of phosphorylated α-synuclein in CSF between the different disease groups and healthy controls (p=0.245 by K-W test).

4.7 Correlation between phosphorylated α-synuclein levels in plasma and matched CSF samples from UCL

The availability of matched plasma and CSF samples allowed us to investigate whether levels of phosphorylated α-synuclein measured in plasma of a particular individual, correlated with levels quantified in the CSF sample collected from that same individual. This was initially determined by combining the phosphorylated α-synuclein plasma and CSF data from all patient groups.

The data set was checked for normality using the Kolgomorov-Smirnov test and was found to be non-normally distributed. Therefore, the Spearman rank correlation test was adopted to test for any correlation between plasma and CSF measures of phosphorylated α-synuclein (Table 4.6; Figure 4.1).

		Plasma pαsyn	CSF pαsyn
Plasma pαsyn	Correlation coefficient	1.000	0.651
	Sig (2 tailed)	na	0.000
	n	119	119
CSF pαsyn	Correlation coefficient	0.651	1.000
	Sig (2 tailed)	0.000	na
	n	119	119

Table 4.6: Matched plasma vs CSF samples from UCL correlation: *spearman rank statistical data obtained from IBM SPSS Statistics 21 package.*

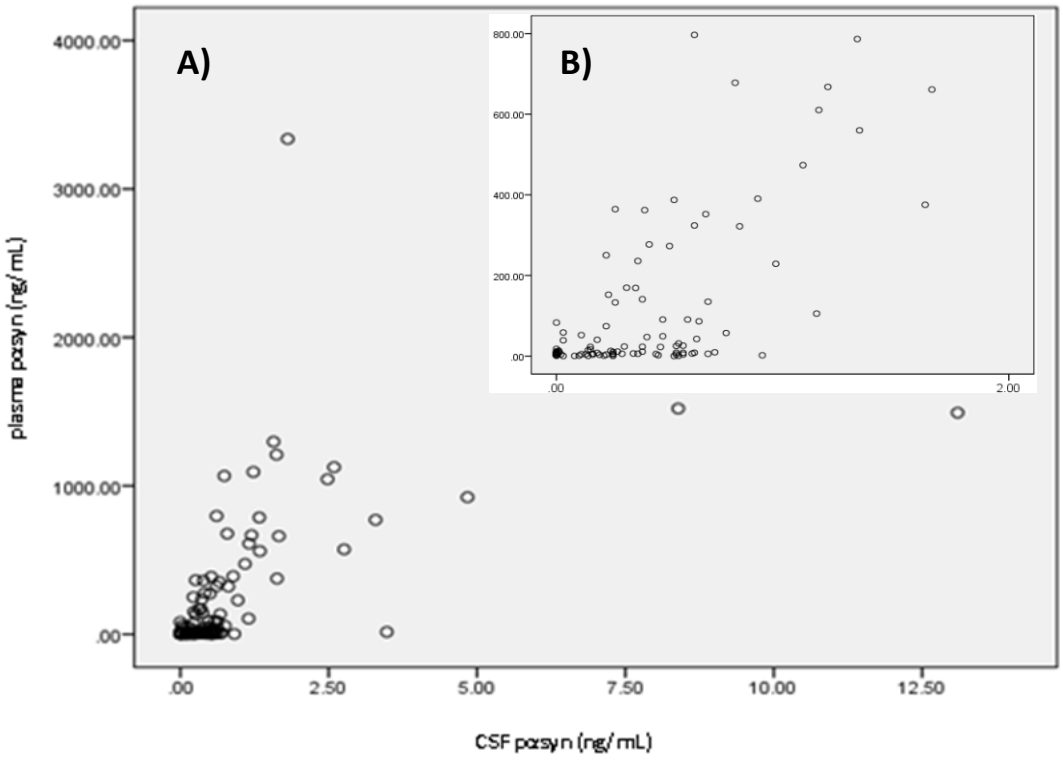

Figure 4.1: Scatter plot for matched plasma vs CSF samples: *all disease groups. A) full scatter plot, B) data concentrated in the lower end of full plot*

Overall, the levels of phosphorylated α-synuclein in plasma correlated with the levels in CSF ($p<0.05$ by Spearman rank correlation test). In order to determine whether the overall positive correlation was driven by any particular patient group, correlation test was performed on data according to the individual disease type.

Table 4.7 and Figure 4.2 represent the results from PD/DLB samples:

		Plasma pαsyn	CSF pαsyn
Plasma pαsyn	Correlation coefficient	1.000	0.707
	Sig (2 tailed)	na	0.000
	n	21	21
CSF pαsyn	Correlation coefficient	0.707	1.000
	Sig (2 tailed)	0.000	na
	n	21	21

Table 4.7: PD/DLB matched plasma vs CSF samples from UCL correlation: *spearman rank statistical data obtained from IBM SPSS Statistics 21 package.*

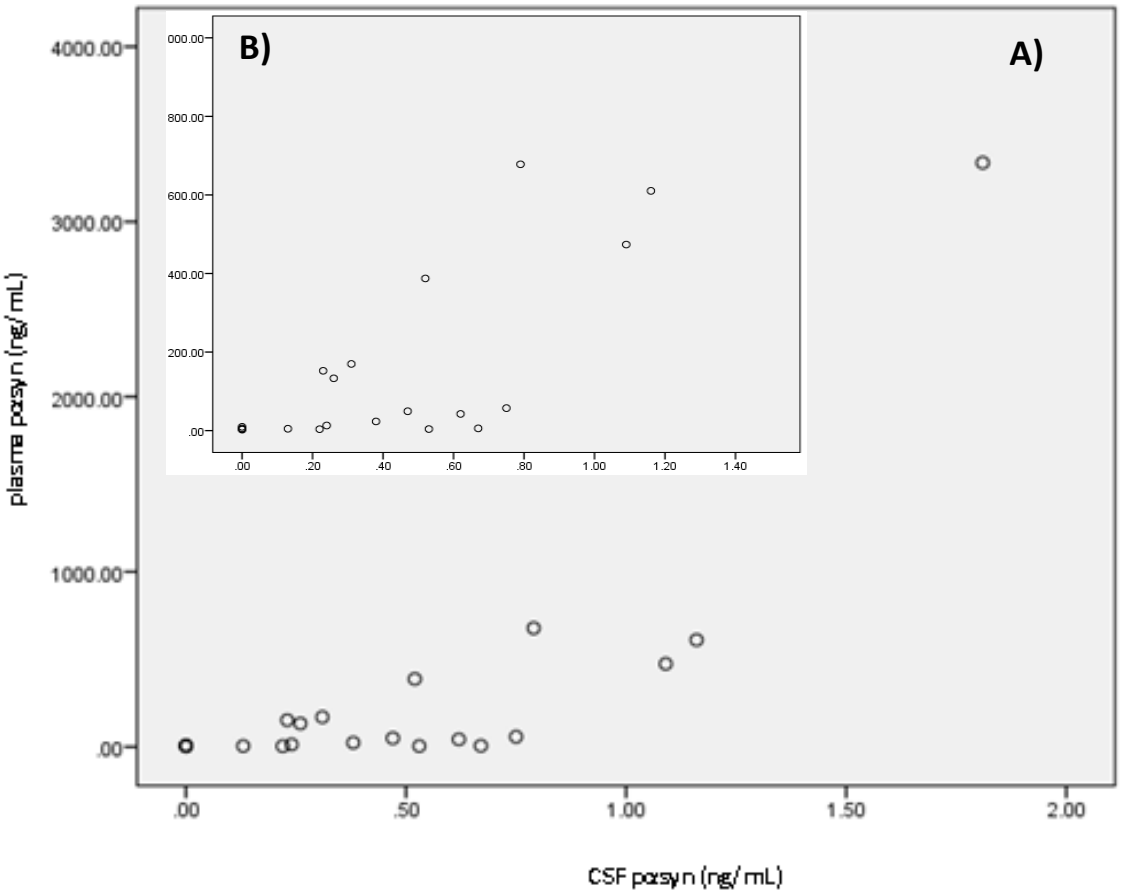

Figure 4.2: PD/DLB matched plasma vs CSF samples from UCL correlation: *scatter plot depicting the spearman rank correlation. A) full scatter plot, B) data concentrated in the lower end of full plot.*

Table 4.8 and Figure 4.3 represent the results from MSA samples.

		Plasma pαsyn	CSF pαsyn
Plasma pαsyn	Correlation coefficient	1.000	0.626
	Sig (2 tailed)	na	0.000
	n	28	28
CSF pαsyn	Correlation coefficient	0.626	1.000
	Sig (2 tailed)	0.000	na
	n	28	28

Table 4.8: MSA matched plasma vs CSF samples from UCL correlation: *spearman rank statistical data obtained from IBM SPSS Statistics 21 package.*

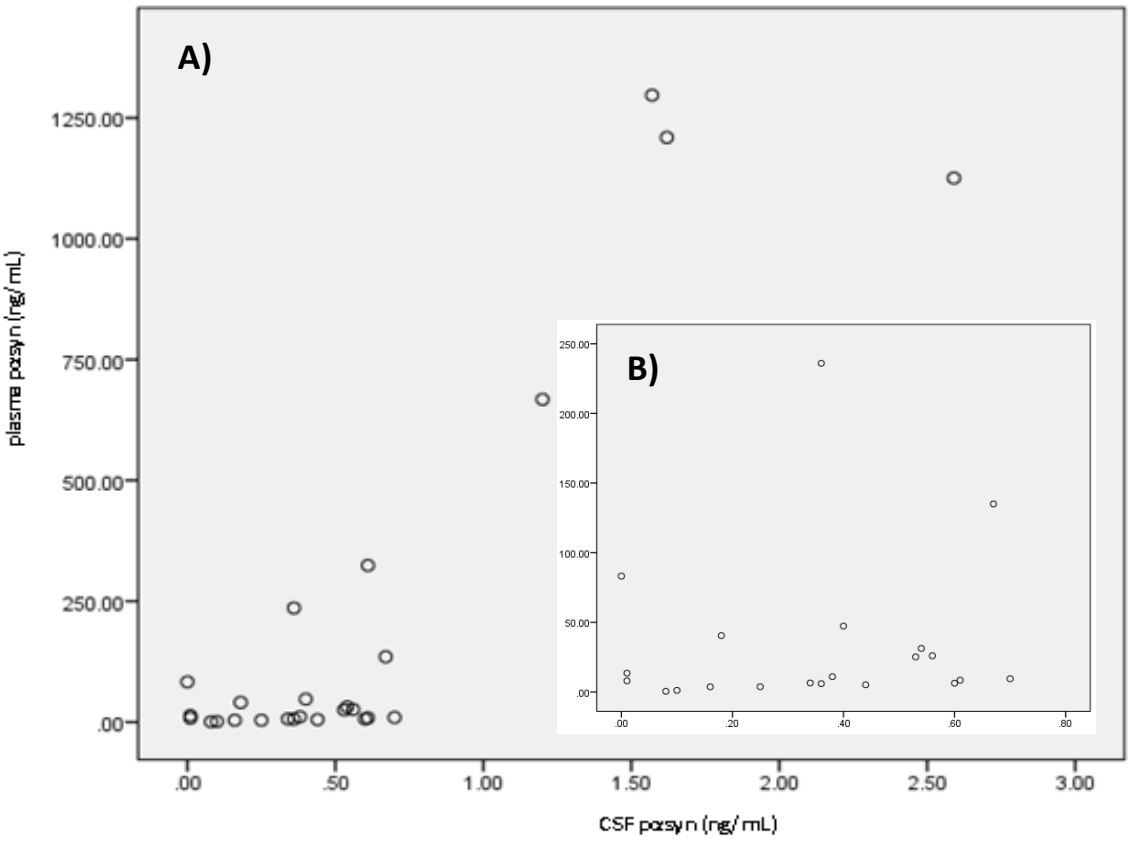

Figure 4.3: MSA matched plasma vs CSF samples from UCL correlation: *scatter plot depicting the spearman rank correlation. A) full scatter plot, B) data concentrated in the lower end of full plot.*

Table 4.9 and Figure 4.4 represent the results from PSP samples.

		Plasma pαsyn	CSF pαsyn
Plasma pαsyn	Correlation coefficient	1.000	0.770
	Sig (2 tailed)	na	0.000
	n	31	31
CSF pαsyn	Correlation coefficient	0.770	1.000
	Sig (2 tailed)	0.000	na
	n	31	31

Table 4.9: PSP matched plasma vs CSF samples from UCL correlation*: spearman rank statistical data obtained from IBM SPSS Statistics 21 package.*

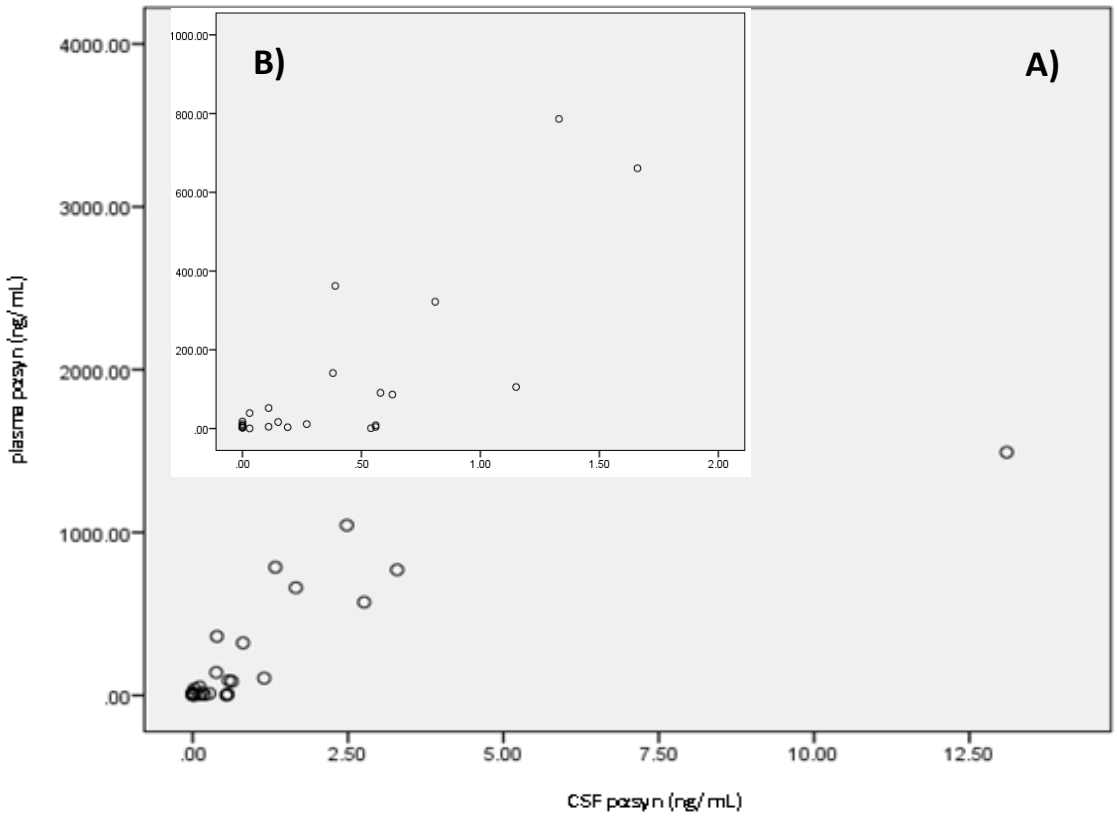

Figure 4.4: PSP matched plasma vs CSF samples from UCL correlation*: scatter plot depicting the spearman rank correlation. A) full scatter plot, B) data concentrated in the lower end of full plot.*

Table 4.10 and Figure 4.5 represent the results from CBS samples.

		Plasma pαsyn	CSF pαsyn
Plasma pαsyn	Correlation coefficient	1.000	0.289
	Sig (2 tailed)	na	0.338
	n	13	13
CSF pαsyn	Correlation coefficient	0.289	1.000
	Sig (2 tailed)	0.338	na
	n	13	13

Table 4.10: CBS matched plasma vs CSF samples from UCL correlation: *spearman rank statistical data obtained from IBM SPSS Statistics 21 package.*

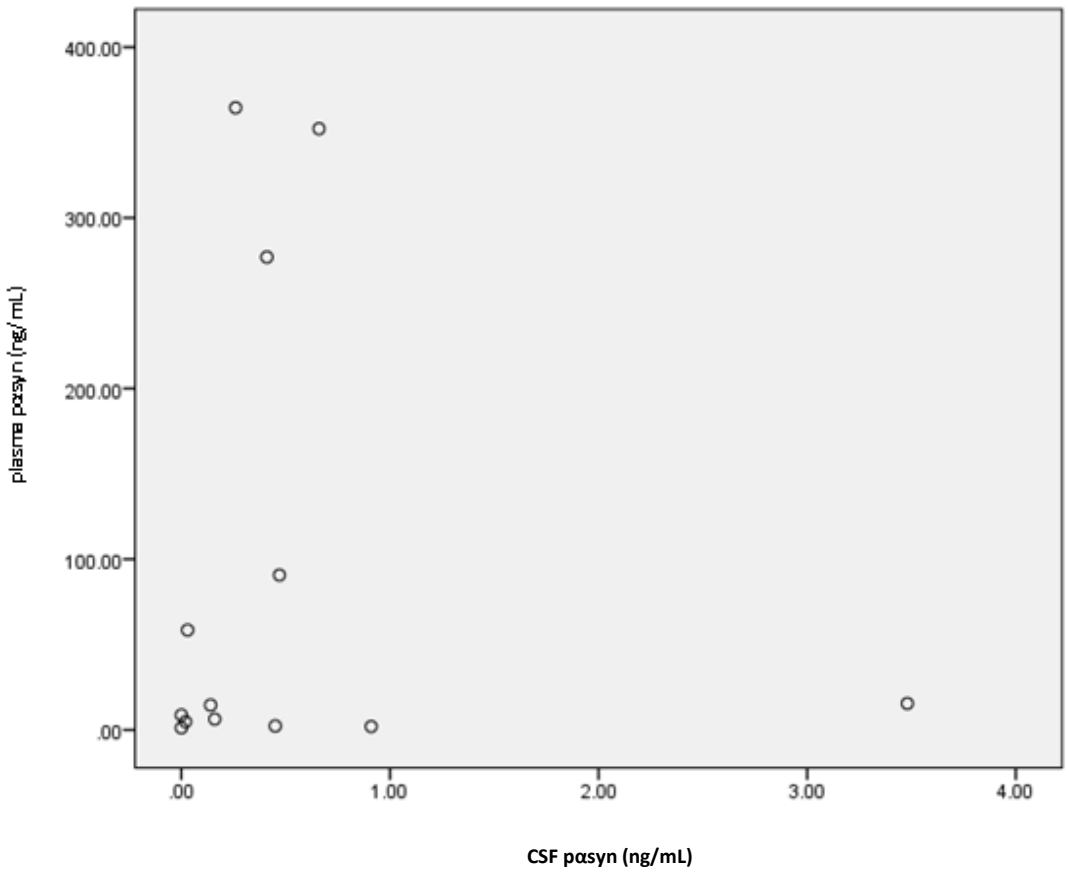

Figure 4.5: CBS matched plasma vs CSF samples from UCL correlation*: scatter plot depicting the spearman rank correlation.*

Table 4.11 and Figure 4.6 represent the results from healthy control samples.

		Plasma pαsyn	CSF pαsyn
Plasma pαsyn	Correlation coefficient	1.000	0.658
	Sig (2 tailed)	na	0.000
	n	26	26
CSF pαsyn	Correlation coefficient	0.658	1.000
	Sig (2 tailed)	0.000	na
	n	26	26

Table 4.11: Healthy controls matched plasma vs CSF samples from UCL correlation: *spearman rank statistical data obtained from IBM SPSS Statistics 21 package.*

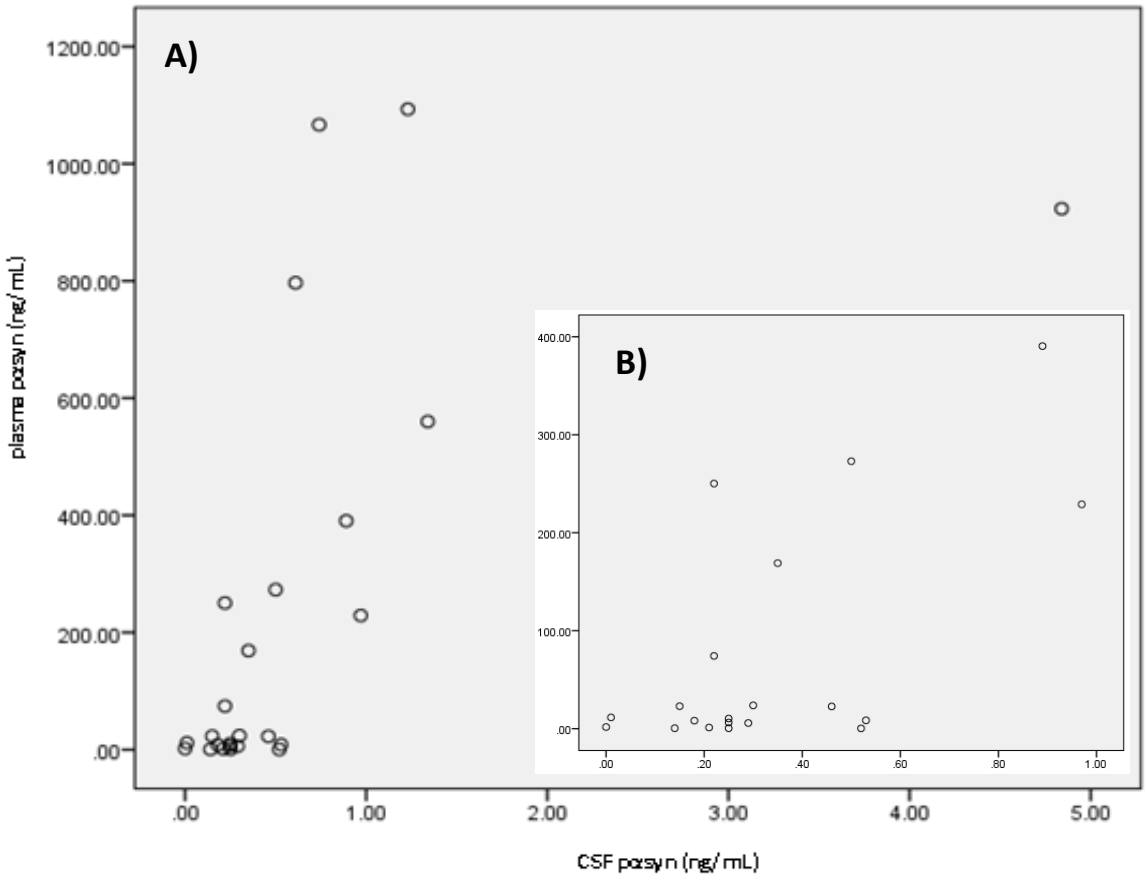

Figure 4.6: Healthy controls matched plasma vs CSF samples from UCL correlation*: scatter plot depicting the spearman rank correlation. A) full scatter plot, B) data concentrated in the lower end of full plot.*

A significant correlation ($p<0.05$) between plasma and CSF levels of phosphorylated α-synuclein was found for individuals with PD/DLB, MSA and PSP, as well as in the healthy controls. Individuals with CBS category did not show a significant correlation ($p>0.05$).

4.8 Discussion

The strong pathological relationship between α-synuclein and various neurodegenerative disorders, such as PD, MSA and DLB, has initiated a great deal of interest in the biological implications of this protein. The discovery that α-synuclein can be detected in biological fluids, such as CSF and plasma, has led to many investigations as to whether α-synuclein has the potential to act as a biomarker.

Studies comparing levels of CSF α-synuclein in the α-synucleinopathies versus other neurological disorders and healthy controls have been reported, with differing results (Table 4.12).

Research group	**No. of samples studied**	**Methodology for quantification**	**Summary of findings**
Hong *et al* (2010)	PD = 117 AD = 50 HC = 132	Luminex	Decreased levels in PD vs AD and HC
Reesink *et al* (2010)	DLB = 35 AD = 63 PD = 18 HC = 35	ELISA	No significant difference
Park *et al* (2011)	PD = 23 HC = 18	ELISA	No significant difference
Shi *et al* (2011)	PD = 126 MSA = 32 AD = 50 HC = 137	Luminex	Decreased levels in PD vs HC and AD

Research group	No. of samples studied	Methodology for quantification	Summary of findings
Aerts *et al* (2012)	PD = 58 MSA = 47 DLB = 3 PSP = 10 CBD = 2	ELISA	No significant difference
Tateno *et al* (2012)	AD = 9 DLB = 6 PD = 11 MSA = 11 HC = 11	ELISA	Increased levels in AD vs HC Decreased levels in PD, DLB AND MSA vs AD
Kang *et al* (2013)	PD = 39 HC = 63	ELISA	Decreased levels PD vs HC
Van Dijk *et al* (2013)	PD = 53 HC = 50	TR-FRET	Decreased levels PD vs HC
Wennstrom *et al* (2013)	PD = 38 DLB = 33 AD = 46 HC = 52	ELISA	Decreased levels in PD and AD vs AD and HC
Parnetti *et al* (2014)	PD = 44 HC = 25	ELISA	Ratio of oligo:total synuclein decreased in PD vs HC

Table 4.12: Summary of studies investigating the use of CSF total α-synuclein as a biomarker for neurodegenerative disorders: *adopted and modified from Magdalinou et al, 2014.*

Some studies reported no significant differences in the diseased groups investigated versus healthy controls (Aerts *et al*, 2012; Park *et al,* 2011; Reesink *et al*, 2010), whereas, most groups found decreased levels of CSF α-synuclein in PD compared to AD and healthy controls (Hong *et al*, 2010; Kang *et al*, 2013; Shi *et al*, 2011; Wennstrom *et al*, 2013). Tateno *et al* (2012) appears to be the only group to find

increased levels of α-synuclein in CSF from AD patients compared to healthy individuals.

Similarly, results from measuring α-synuclein in plasma have also differed (Table 4.13).

Research group	No. of samples studied	Methodology for quantification	Summary of findings
Lee *et al* (2006c)	PD = 105 MSA = 38 HC = 51	ELISA	Increased levels in PD and MSA vs HC
Li *et al* (2007)	PD = 27 HC = 11	IP-WB	Decreased levels in PD vs HC
Duran *et al* (2010)	PD = 95 HC = 60	ELISA	Increased levels in PD vs HC
Park *et al* (2011)	PD = 23 HC = 29	ELISA	No significant difference
Shi *et al* (2010)	HC = 95 AD = 33 PD = 117	Luminex	No significant difference

Table 4.13: Summary of studies investigating the use of plasma total α-synuclein as a biomarker for neurodegenerative disorders: *adopted and modified from Kasuga et al, 2012.*

Lee *et al* (2006c) and Duran *et al* (2010) showed that levels of plasma α-synuclein are higher in PD and MSA patients compared to controls, whereas Li *et al* (2007) reported that levels are lower in PD. Shi *et al* (2010) and Park *et al* (2011) found no significant difference between the α-synucleinopathies and healthy controls.

The aforementioned studies all involved measuring levels of total α-synuclein, whereas, in this chapter, investigations have focussed specifically on the phosphorylated form of α-synuclein. This particular interest in phosphorylated α-synuclein stems from the finding that the protein aggregates found in PD, DLB or MSA brains are hyperphosphorylated at Ser129 (Fujiwara *et al*, 2002; Anderson *et al*, 2006; Wakabayashi *et al*, 1998). Thus, Ser129 phosphorylated α-synuclein represents a 'pathological' form of the protein that might be particularly suitable as a biomarker. Publications investigating the use of phosphorylated α-synuclein as a biomarker are relatively few (Foulds *et al*, 2011; Foulds *et al* 2013). Foulds *et al* (2011) showed that phosphorylated α-synuclein levels in plasma from PD patients were significantly higher than those in healthy controls. Present data disagree with these previous findings, in that no significant difference in levels of plasma phosphorylated α-synuclein between diseased groups and healthy controls was found. This discrepancy may be due to differences in the assay methodology. Foulds *et al* (2011 and 2013) used an ELISA for the quantification, utilising two different polyclonal antibodies. Present assay was developed specifically for use with the Luminex analyser, with a monoclonal phosphospecific antibody for capture and a polyclonal detection antibody. The different antibodies may be one possible reason for the difference in our results compared to those of Foulds *et al* (2011 and 2013). Another plausible reason may lie in differences in number of samples analysed. Foulds *et al* (2013) analysed a total of 189 samples from PD patients and 91 healthy controls, whereas only 79 plasma samples from PD patients and 94 healthy control samples were analysed in the present study.

Wang *et al* (2012) investigated the use of CSF phosphorylated α-synuclein in PD, MSA, PSP patients and healthy controls. The quantification method used was the same as described here – the Luminex – but they used different antibodies that are

not commercially available. They noted that phosphorylated α-synuclein levels in CSF do not appear to be a suitable biomarker, agreeing with present results. As well as phosphorylated α-synuclein, Wang *et al* (2012) measured total α-synuclein in CSF and found that the ratio between total α-synuclein : phosphorylated α-synuclein levels may serve as a better biomarker. In chapter 6, it is investigated whether this can be achievable with plasma as opposed to CSF, since plasma would be a more easily accessible biological fluid for use as a biomarker.

In addition to investigating whether phosphorylated α-synuclein in plasma and CSF has the potential to be a diagnostic marker, we were able to show that levels of phosphorylated α-synuclein in CSF correlated with levels in plasma. A previous study in PD with longitudinally obtained samples showed that levels of α-synuclein in plasma are highly variable between individuals, i.e. some individuals are naturally high expressors and others are low expressors – this variability has been shown to be consistent over time in repeat samples taken from the same individual (Foulds *et al*, 2013). From our study, we can conclude that this variability in α-synuclein levels amongst individuals also appears to be consistent between the CNS (CSF) and periphery (blood) and not confined to just one body fluid. From a biomarker point of view, this suggests that plasma is a suitable matrix for determining overall levels of α-synuclein expression, and for highlighting differences in expression between individuals.

Additionally, the positive correlation between plasma and CSF phosphorylated α-synuclein levels suggests that levels in plasma could reflect pathological conditions/events taking place within the CNS. This would be helpful because plasma is much more accessible as a biological fluid for biomarker investigations than CSF, and more amenable to longitudinal investigations. This correlation could be due to an

exchange of phosphorylated α-synuclein between CSF (brain) and blood. Shi *et al* (2014) and Sui *et al* (2014) used radiolabelled α-synuclein to show that this protein crosses the blood brain barrier (BBB), allowing its transportation in a bidirectional manner, i.e. blood to brain and brain to blood. The specific mechanisms involved in this transportation across the BBB are still unclear, but it may resemble the process implicated in the transportation of β-amyloid peptides. Amongst the main components involved in the transportation of β-amyloid across the BBB is lipoprotein receptor related protein-1 (LRP-1) (Deane *et al*, 2009). Interestingly enough, the study by Sui *et al* (2014) has shown a potential role for LRP-1 in the transportation of α-synuclein across the BBB also. In general, this supports the concept that plasma protein levels can potentially evidence changes occurring in the brain – but this would need further investigation.

Chapter 5:

Total α-synuclein and total DJ-1:

Luminex assay development

5.1 Introduction

The ability to multiplex different biomarkers is the main attractive feature offered by the Luminex technology. One of the aims of this project was to develop a multiplex assay to quantify total α-synuclein, total DJ-1 and LRRK2 levels in human CSF and plasma samples from individuals with various neurodegenerative diseases and healthy controls. These three markers have been predominantly linked to PD and other synucleinopathies, for which, well established commercial assays are not readily available for. Thus, multiplexing these markers was deemed to be a good starting point. Unfortunately, initial assay development experiments revealed that the LRRK2 assay components cross reacted with both the total α-synuclein and total DJ-1 assay components. Thus, a duplex assay quantifying total α-synuclein and total DJ-1 was developed and validated for use with human plasma and CSF. The LRRK2 assay was developed separately as a singleplex assay and is discussed in Chapter 7.

To develop the duplex assay, a singleplex assay for the two analytes (total α-synuclein and total DJ-1) was first developed and then combined to form the duplex assay.

This chapter describes the development of each individual singleplex and the series of experiments leading to the formation of the duplex assay.

5.2 Total α-synuclein

An ELISA for the quantification of total α-synuclein in human plasma and CSF has been established previously, utilising C211 mouse anti-α-synuclein mAb (Santa Cruz Biotech. Inc.) as the capture reagent and FL140 rabbit anti-α/β/γ-synuclein pAb

(Santa Cruz Biotech. Inc.) as the detection component (Foulds *et al*, 2011). In order to develop a total α-synuclein assay on the Luminex bead system, it was rational to start with the antibody pairings that worked in the ELISA system, where the C211 mAb was coupled to beads and the FL140 pAb was biotinylated. The ELISA assay did not require the FL140 pAb detection antibody to be biotinylated. Instead, it utilised a goat anti-rabbit secondary antibody conjugated to horseradish peroxidase (HRP) plus TMB substrate complex as the detection system (Foulds *et al*, 2011). Unfortunately, the C211 mAb + FL140 pAb combination was not successful on the Luminex system. This section reports the investigative steps taken which eventually led to the identification of the problem and allowed the development of a functional assay.

5.3 Total α-synuclein Luminex assay troubleshooting

C211 mouse anti-α-synuclein mAb (Santa Cruz Biotech. Inc.) was coupled to microspheres and FL140 rabbit anti-α/β/γ-synuclein pAb (Santa Cruz Biotech. Inc.) was biotinylated as per the procedures described in the Methods section. The two components were then used to perform a Luminex assay using the in house recombinant α-synuclein protein at 600, 200, 66.7, 22.2, 7.4, 2.5, 0.82, 0 ng/ml, prepared in assay buffer (PBS/SM01). This assay generated zero MFI signals. The assay was repeated again to exclude the possibility of experimental error, but the same result was obtained. In order to identify why the assay was not working, four questions were addressed:

Q1: Had the C211 mAb coupled to the beads successfully?

Q2: If the C211 mAb has coupled to the beads then does it still bind to α-synuclein?

Q3: Had the FL140 pAb conjugated to biotin successfully?

Q4: If the FL140 pAb has biotinylated then does it still bind to α-synuclein?

In order to answer these questions the antibody coupling confirmation, antibody functionality, biotinylation confirmation and biotinylation functionality tests were conducted, respectively.

The antibody coupling confirmation test used goat anti-mouse IgG conjugated to R-phycoerythrin. The C211 anti-α-synuclein capture antibody was a mouse mAb, thus the anti-mouse IgG-PE would only bind and generate a signal in the presence of the C211 mouse anti-α-synuclein mAb. Varying mass of antibody was coupled to beads; 0.5, 2, 4, 8 and 10 µg. The results from this test are displayed in Figure 5.1:

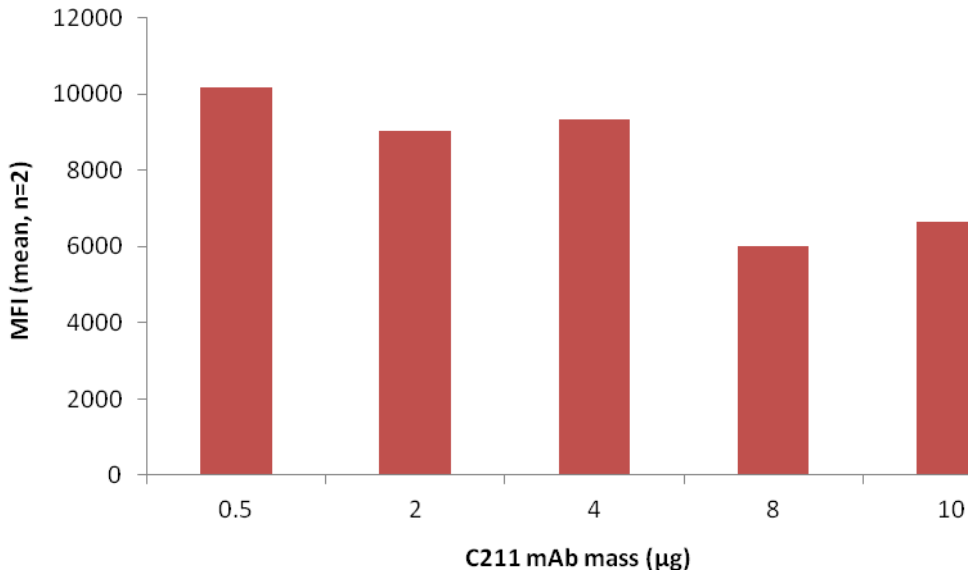

Figure 5.1: C211 anti-α-synuclein mAb bead coupling confirmation: *C211 mouse anti-α-synuclein mAb (Santa Cruz Biotech. Inc.) were coupled at varying mass (µg) to Luminex beads. Each bead set coupled with varying antibody mass (µg) was reacted with 4 µg/mL anti-mouse IgG-PE to show whether the C211 mouse mAb was present on the beads.*

These results suggested that C211 mouse anti-α-synuclein mAb was present on the beads. 0.5 µg of the antibody coupled to beads generated the best MFI signal, suggesting that this amount of antibody, would be best suited for use in the Luminex

assay. However, it was possible that the coupling process may have modified the antibody in a manner that destroyed its ability to bind to its target protein.

In order to determine whether the coupled C211 mAb had retained its binding properties, the antibody coupling functionality test was performed, where biotinylated α-synuclein recombinant protein was reacted with each bead set coupled to varying mass of antibody. The results are displayed in Figure 5.2:

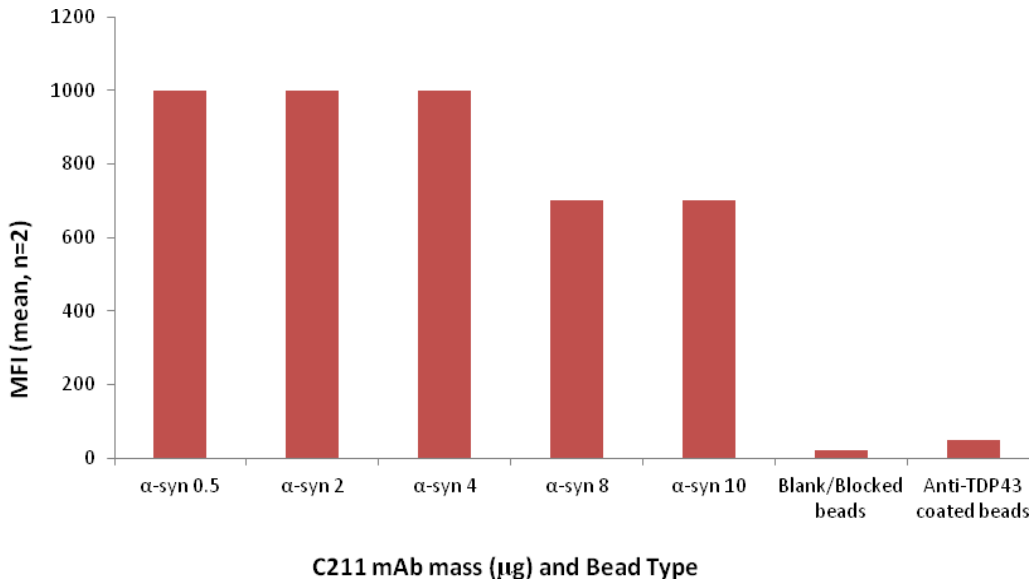

Figure 5.2: C211 mAb coupled to beads functionality test: *Beads coupled to 0.5, 2, 4, 8 and 10 µg of C211 mAb were reacted with biotinylated α-synuclein. Beads coated with 1% (w/v) BSA only and beads coated with anti-TDP43 mAb were used as controls for the assay. The level of α-synuclein binding by each bead set was quantified using the Luminex analyser.*

The beads coupled with C211 mAb were able to capture α-synuclein and thus were not the non-functional component. Therefore, the biotinylation of FL140 was assessed next.

Two tests were performed simultaneously; biotin confirmation and biotin functionality. Figure 5.3 summarises the results obtained.

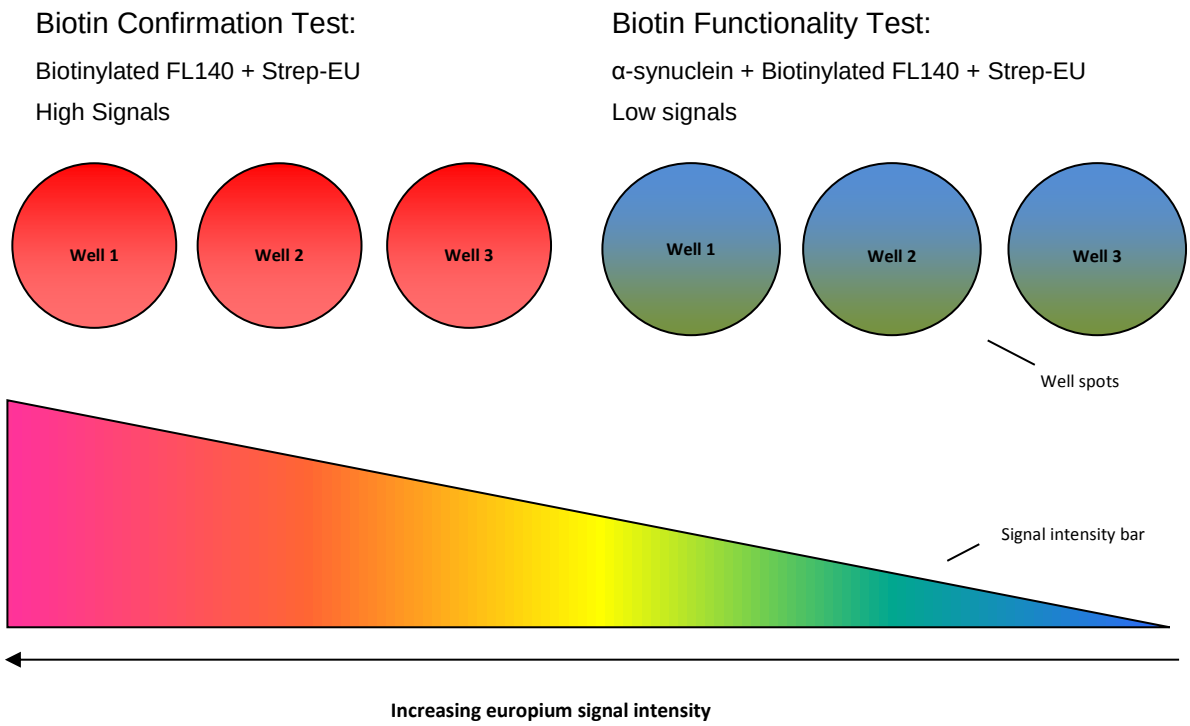

Figure 5.3: FL140 Biotin Confirmation and Functionality Test: *The biotinylation of FL140 pAb was confirmed by reacting the biotinylated FL140 pAb with Streptavidin-EU. The functionality of biotinylated FL140 was assessed by reacting the pAb with recombinant α-synuclein, followed by quantification of bound biotinylated FL140-protein complex via streptavidin-EU. The figure displays the signals achieved for the confirmation and functionality tests. The numbers in each "well spot" in the figure represent the signal. The colours of each well spot also indicate the intensity of the signal. The "signal intensity bar" below the well spots shows that blue indicates low signal and red indicates a high signal.*

The high signal obtained in the biotin functionality test showed that FL140 pAb was conjugated to biotin. The low signal generated from the biotin functionality test suggested that although biotin was present on the FL140 pAb, its ability to bind α-synuclein was compromised.

The in house recombinant α-synuclein was used for all assays. In order to ensure that the in house α-synuclein protein was not dysfunctional and to verify that the C211 mAb recognised the protein, a western blot was performed. As a comparator, a western blot was also performed in parallel on α-synuclein protein obtained from a

commercial company (Zapaloid). The results from this test showed that the in house protein was viable and that the C211 mAb binds to α-synuclein. The data obtained are shown in Figure 5.4.

In house α-synuclein recombinant protein:

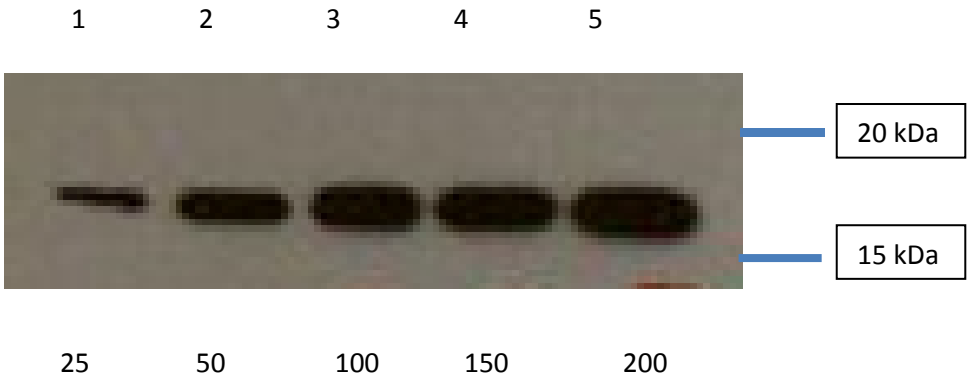

Zapaloid α-synuclein recombinant protein:

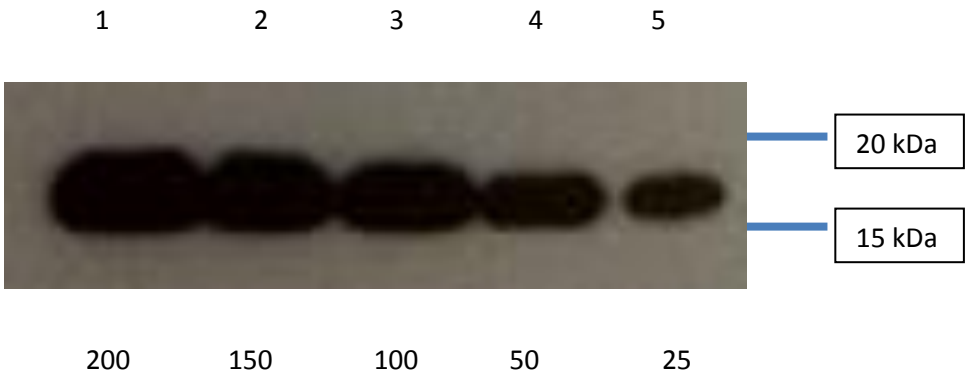

Figure 5.4: Western blot of α-synuclein protein: *C211 mAb was used as the primary antibody for detecting the presence of α-synuclein recombinant protein from our in house preparation and the protein provided from Zapaloid. Lanes 1 to 5 are shown. Each lane represents an increasing amount of protein; 25, 50, 100, 150 and 200 ng, respectively. α-synuclein runs at approximately 16 kDa on a western blot gel – the bands shown in this figure are at 16 kDa, thus representing the protein of interest - α-synuclein.*

These troubleshooting exercises suggested that biotinylation of FL140 rendered the antibody inactive in terms of its ability to bind to α-synuclein. Alternative antibodies supplied by Santa Cruz Biotechnology Inc. were biotinylated and tried in combination with C211 mAb coupled beads, but these generated the same negative results as the pairing with FL140 pAb.

Potential detection antibodies from alternative manufacturers/vendors were sought. At the same time, alternative capture antibody and recombinant protein were purchased in order to assess various antibody pairing combinations. The additional reagents tested were:

- Syn211 mouse anti-α-synuclein mAb (Life Technologies-Invitrogen)
- Biotinylated goat anti-α-synuclein pAb (R&D Systems)
- Human α-synuclein recombinant protein (rPeptide)
- Human α-synuclein recombinant protein (Merck Millipore)

0.5 µg of the Syn211 mouse anti-α-synuclein mAb was coupled to Luminex beads. These antibody coupled beads and the previously 0.5 µg C211 mAb coupled beads were assayed with 1 µg/mL human α-synuclein recombinant proteins from rPeptide, Merck Millipore and our in house preparation, using the biotinylated goat anti-α-synuclein pAb as the detection component. The antibody and protein combinations investigated are shown in Figure 5.5, together with the results obtained:

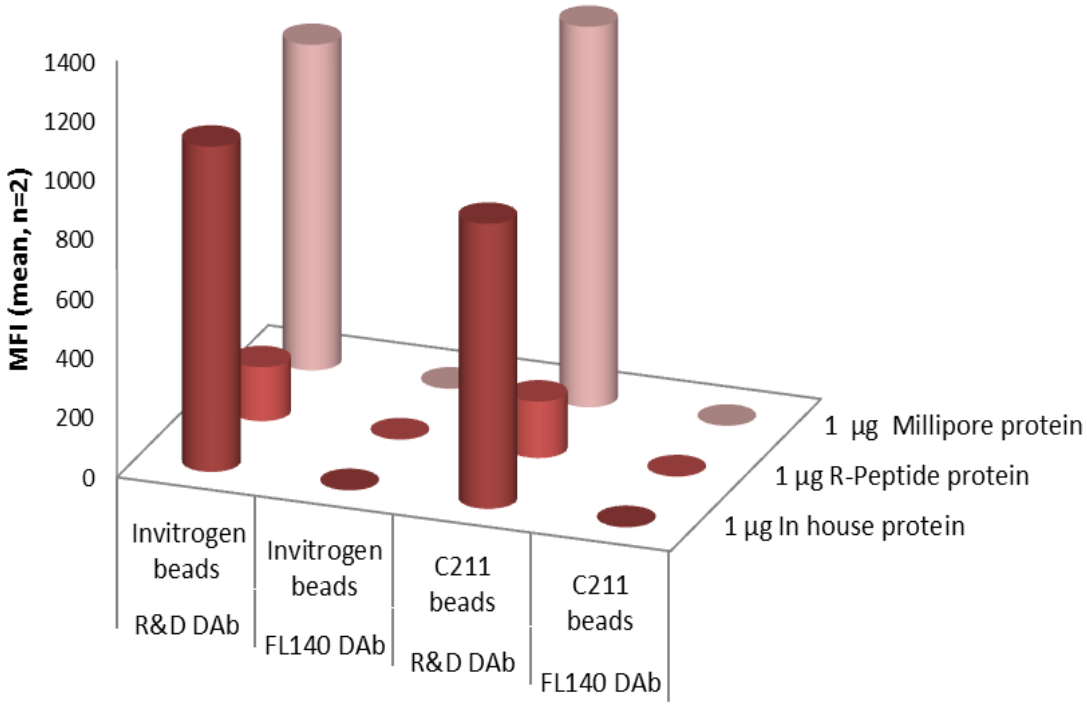

Figure 5.5: Testing different antibody combinations: *Luminex beads coupled with 0.5 µg of Syn211 mouse anti-α-synuclein mAb (Life Technologies-Invitrogen) and 0.5 µg of C211 mouse anti-α-synuclein mAb (Santa Cruz Biotech. Inc.) were used to detect α-synuclein levels in human α-synuclein recombinant proteins from rPeptide, Merck Millipore and our in house preparation. 1 µg/mL of each recombinant protein was used in the assay with 2 µg/mL biotinylated goat anti-α-synuclein pAb (R&D Systems) and 4 µg/mL streptavidin-RPE as the detection system for the assay. The figure shows the mean (n=2) MFI signals achieved with the various antibody and protein combinations.*

It was found that the biotinylated detection pAb from R&D systems generated signals with both 0.5 µg of the Syn211 mouse anti-α-synuclein mAb and the 0.5 µg C211 mAb coupled beads.

In order to distinguish whether a higher MFI signal could be achieved, the Syn211 mouse anti-α-synuclein mAb and C211 mAb were coupled to beads with an increasing amount of capture antibody, i.e. 1 µg rather than 0.5 µg.

This data revealed that 1 µg Syn 211 mAb generated MFI signals of approximately 8500 when assayed with 1 µg/ml of in house α-synuclein protein and 2 µg/mL of biotinylated goat anti-α-synuclein pAb. The 1 µg C211 mAb coupled beads failed to generate signals as high as the 1 µg Syn211 mAb coupled beads.

Therefore, the antibody combination of Syn211 mouse anti-α-synuclein mAb coupled beads with biotinylated detection pAb from R&D systems was chosen and taken into the assay optimisation step. The in house α-synuclein recombinant protein preparation was used in all subsequent assays.

5.4 Total α-synuclein Luminex assay optimisation

The optimisation step involved assessing assay performance upon modification of various steps within the whole assay set up. The aim of the assessment was to find the assay conditions that achieved optimal performance in terms of sensitivity, and reproducibility. Altering two assay conditions were considered; capture phase and detection phase – this section details the findings from this investigation.

5.4.1 Capture phase optimisation

The mass of antibody used to couple beads was evaluated by a titration assay where data obtained from coupling 0.5 µg of Syn 211 mAb to beads was compared to 1, 1.5 and 2 µg of antibody coupled to beads. The data obtained are shown in Figure 5.6:

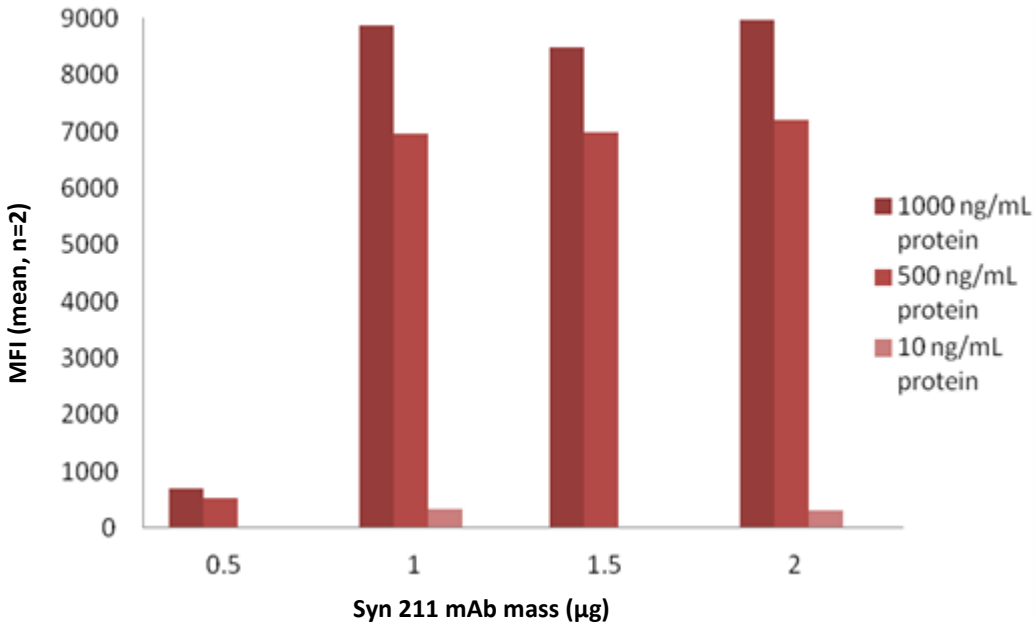

Figure 5.6: Syn211 mAb mass titration for bead coupling: *Luminex beads coupled with 0.5, 1, 1.5 and 2 µg were assayed with 0, 10, 500 and 1000 ng/mL of in house α-synuclein recombinant protein prepared in assay buffer and 2 µg/mL biotinylated detection pAb (R&D systems) with 4 µg/ml streptavidin-RPE. The figure shows the MFI signals obtained with each bead set at the varying α-synuclein recombinant protein concentrations*.

The data obtained indicated that increasing the amount (µg) of antibody during the coupling reaction does not make a significant difference to MFI signals when detecting α-synuclein. Due to this reason, beads coupled with 1 µg of Syn211 mAb were used for the remaining optimisation experiments.

Beads coupled with 1 µg of Syn 211 mAb were subjected to an experiment that tested the effect of increasing the capture step incubation from 2 h to an overnight incubation. The data obtained are displayed in Figure 5.7:

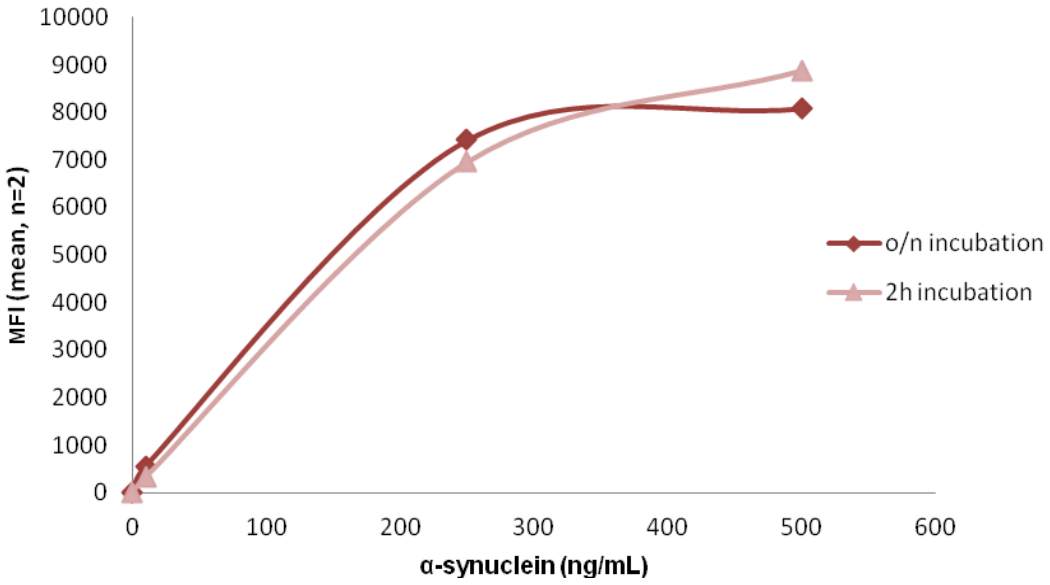

Figure 5.7: Increasing capture incubation step: *Luminex beads coupled with 1 µg of Syn 211 mAb were assayed with 0, 10, 250 and 500 ng/mL of in house α-synuclein recombinant protein prepared in assay buffer. 2 µg/mL biotinylated detection pAb (R&D systems) and 4 µg/mL of streptavidin-RPE was used. The capture step incubation was increased from 2 h to an overnight incubation at 4^0C, shaking. The figure displays the MFI signals from the overnight experiment and the data obtained when performing the assay with the capture step incubation at 2 h.*

The difference in signal between 2 h and overnight capture step incubation was very small, however, an overnight incubation was preferred over the 2 h incubation and subsequent optimisation tests were performed with an overnight capture step.

5.4.2 Detection phase optimisation

The detection phase optimisation involved evaluating the effect of varying the biotinylated detection pAb (R&D systems) concentration and incubation as well as the streptavidin-RPE concentration and incubation. The prospect of using less antibody and reagent was more desirable, in order to develop assays that are cost effective.

The detection pAb titration step involved testing 2, 1 and 0.5 µg/mL concentrations of the biotinylated pAb. The signal to noise ratio was calculated for the data obtained by dividing the MFI signal obtained at 500, 250 and 10 ng/mL of α-synuclein protein by the MFI signal obtained at 0 ng/mL of protein. The results from this test are depicted in Figure 5.8.

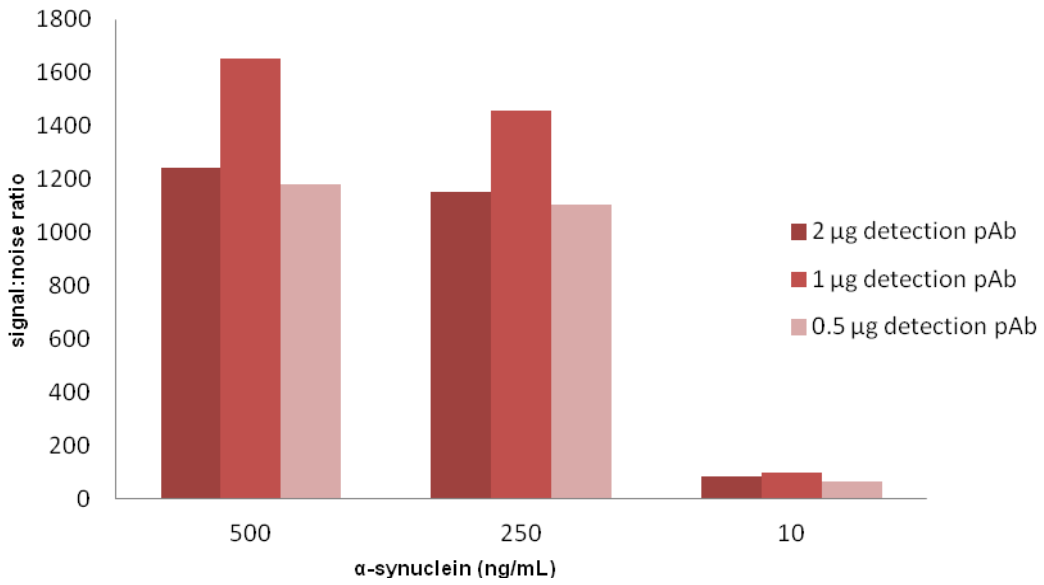

Figure 5.8: Detection antibody titration test: *Luminex beads coupled with 1 µg Syn 211 mAb was assayed with 500, 250, 10 and 0 ng/mL of in house α-synuclein recombinant protein and incubated overnight at 4°C whilst shaking. Biotinylated detection pAb was added at 2, 1 and 0.5 µg/mL respectively and incubated for 1 h before reading on the Luminex analyser. The figure shows the signal to noise ratio at each protein concentration when 2, 1 and 0.5 µg/mL of biotinylated detection pAb was reacted with the captured protein complex.*

The largest signal to noise ratio was obtained with the addition of 1 µg/mL of biotinylated detection antibody. The effect of increasing the detection incubation step from 1 h to 4 h had no effect on the MFI signal achieved (data not shown). For subsequent optimisation steps, the biotinylated detection pAb concentration used was 1 µg/mL and the incubation time was retained at 1 h.

The streptavidin-RPE reagent was tested at 6 and 2 µg/mL and the data compared to the 4 µg/mL concentration. The streptavidin incubation was extended to 1 h as opposed to 30 mins. The data obtained from the reagent titration are displayed in Figure 5.9. The increased incubation had no effect (data not shown).

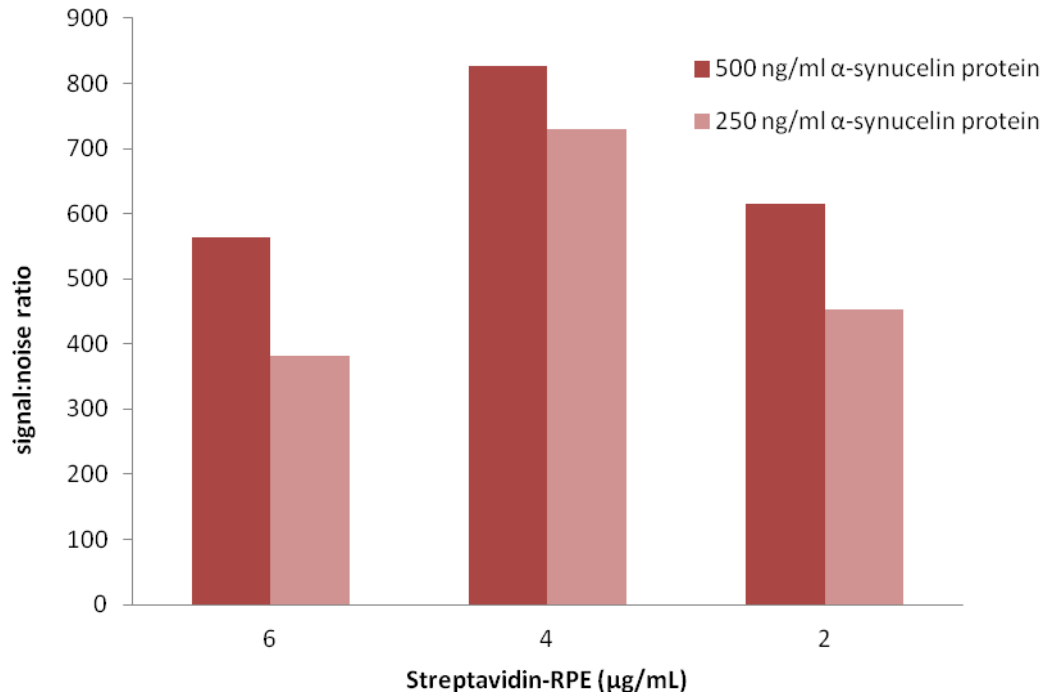

Figure 5.9: Streptavidin-RPE titration: *Luminex beads coupled with 1 µg of Syn 211 mAb were assayed with 0, 10, 250 and 500 ng/mL of in house α-synuclein recombinant protein prepared in assay buffer. 1 µg/mL biotinylated detection pAb (R&D systems) with varying concentrations of streptavidin-RPE was assessed. The figure displays the signal to noise ratio calculated for each streptavidin-RPE concentration. The signal to noise ratio was calculated from dividing the MFI signal achieved at 500 and 250 ng/mL α-synuclein protein by the MFI signal achieved from the 0 ng/mL protein concentration, respectively.*

Using 4 µg/mL of streptavidin-RPE with 1 µg/mL of biotinylated detection pAb generated the optimal signal to noise ratio.

Findings from the assay optimisation steps showed that using 1 µg Syn 211 antibody coupled beads reacted with in house α-synuclein protein overnight at 4^{o}C whilst

shaking generated the best conditions for capturing the protein. Reaction with 1 µg/mL of biotinylated detection pAb for 1 h followed by incubation with 4 µg/mL of streptavidin-RPE for 30 mins was sufficient for detecting the captured protein. These conditions were thus utilised for subsequent total α-synuclein assays.

5.5 Total DJ-1

The assay published by Hong *et al* (2010) involved coating Luminex beads with rabbit anti-DJ-1 mAb from Novus Biologicals Ltd. and biotinylated goat anti-DJ-1 pAb from R&D Systems as the detection component. The same antibody pair was tested in our laboratory. Unfortunately the assay performance was not comparable to the published method. These results and the steps taken to improve the assay are displayed and discussed in this section.

5.6 Total DJ-1 Luminex assay development

0.5, 1 and 1.5 µg of rabbit anti-DJ-1 mAb (Novus Biologicals Ltd.) was coupled to Luminex beads. Each coupled bead set was assayed with 2 µg/mL of biotinylated goat anti-DJ-1 pAb (R&D Systems) to measure MFI signals achieved in the presence of 1000, 500, 250 and 0 ng/mL of DJ-1 recombinant protein (Covance Inc.). The MFI signals obtained with each bead set for the different DJ-1 protein concentrations are displayed in Figure 5.10:

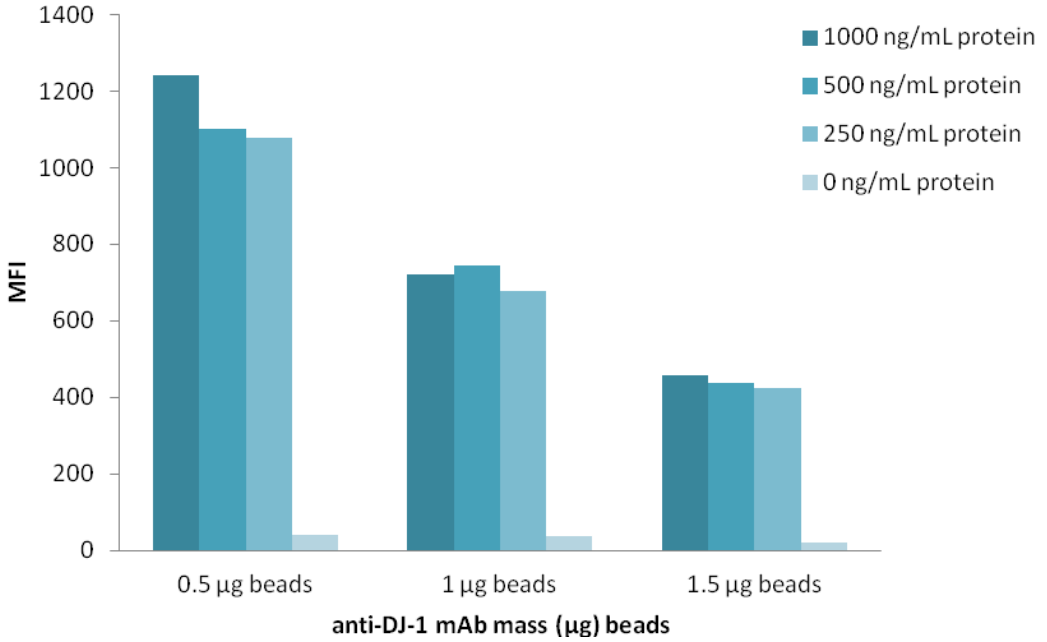

Figure 5.10: Total DJ-1 Luminex assay using anti-DJ-1 mAb (Novus Biologicals Ltd.)*:* *Luminex beads coupled with 0.5, 1 and 1.5 µg of ant-DJ-1 mAb (Novus Biologicals Ltd.) were assayed with 0, 10, 500, 1000 ng/mL of DJ-1 recombinant protein (Covance Inc.) prepared in assay buffer. 2 µg/mL biotinylated anti-DJ-1 detection pAb (R&D systems) with 4 µg/ml streptavidin-RPE was used. Figure shows MFI signals obtained with each bead set at varying DJ-1 protein concentrations.*

These data showed that signals with 0.5 µg of anti-DJ-1 mAb (Novus Biologicals Ltd.) coupled to Luminex beads generated the best MFI. Hong *et al* (2010) state that their assay yielded a signal to noise ratio of 66 – the assay dynamic range is not provided but from the calibration graphs it appears that 175 ng/mL was their top calibrator. This was not achieved with our assay - the background signal was relatively high and the highest signal was fairly low, yielding a signal to noise ratio of approximately 30 - 40. The first approach to improve assay performance was to decrease the mass (µg) of anti-DJ-1 mAb used to couple Luminex beads to 0.25 µg. The logic behind reducing the bead coating was based on the initial data (Figure 5.10) showing that as more anti-DJ-1 mAb is added the MFI is reduced. The data from this experiment are shown in Figures 5.11 and 5.12:

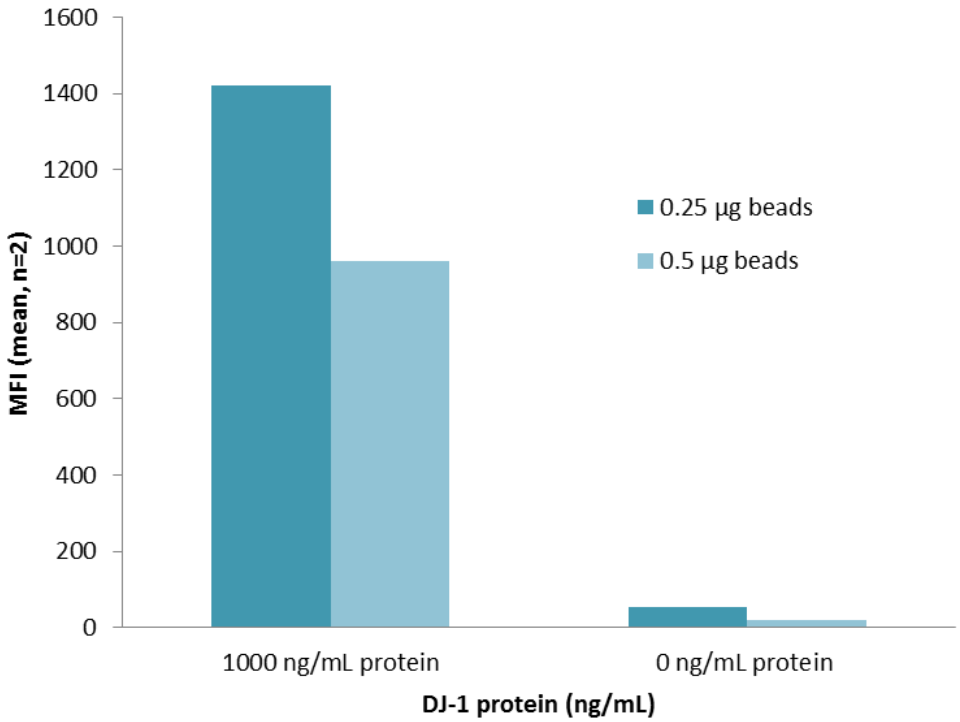

Figure 5.11: Lowering anti-DJ-1 mAb (Novus Biologicals Ltd.) bead coupling:
Luminex beads coupled with 0.25 and 0.5 µg of ant-DJ-1 mAb (Novus Biologicals Ltd.) were assayed with 0 and 1000 ng/mL of DJ-1 recombinant protein (Covance Inc.) prepared in assay buffer. 2 µg/mL biotinylated anti-DJ-1 detection pAb (R&D systems) with 4 µg/ml streptavidin-RPE was used. The figure shows the MFI signals obtained with each bead set at the varying DJ-1 recombinant protein concentrations.

Figure 5.11 shows that the MFI at 1000 ng/mL increases when decreasing the mass (µg) of anti-DJ-1 mAb (Novus Biologicals Ltd.) coupled to beads. However, the background increases too, reducing the signal:noise ratio even further in comparison to data achieved with 0.5 µg coated beads. The signal:noise ratio comparison is depicted in Figure 5.12.

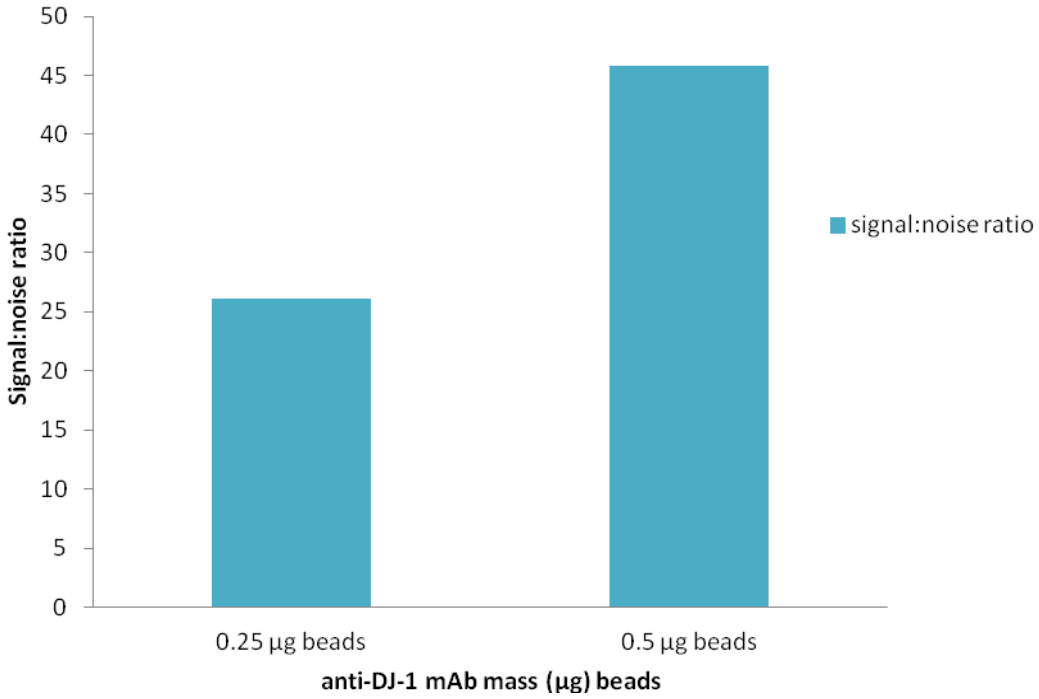

Figure 5.12: Lowering anti-DJ-1 mAb (Novus Biologicals Ltd.) bead coupling:
Luminex beads coupled with 0.25 and 0.5 µg were assayed with 0 and 1000 ng/mL of DJ-1 recombinant protein (Covance Inc.) prepared in assay buffer. 2 µg/mL biotinylated anti-DJ-1 detection pAb (R&D systems) with 4 µg/ml streptavidin-RPE was used. The figure shows the signal:noise ratio obtained with each bead set at the varying DJ-1 recombinant protein concentrations. Signal:noise ratio was calculated by dividing the mean MFI signal at 1000 ng/mL DJ-1 protein concentration by the MFI at 0 ng/mL.

The signal:noise ratio with 0.5 µg beads was better in comparison to the 0.25 µg beads. Thus, for subsequent assays, the 0.5 µg beads were used.

The next approach to improve assay performance was to investigate the effect of decreasing biotinylated anti-DJ-1 goat pAb (R&D Systems) from 2 µg/mL to 0.5 µg/mL – it was hypothesised that decreasing the detection antibody may reduce the background signals whilst maintaining the high MFI signal at the top DJ-1 concentration and thus increase the signal:noise ratio. Figure 5.13 show the data obtained from this test.

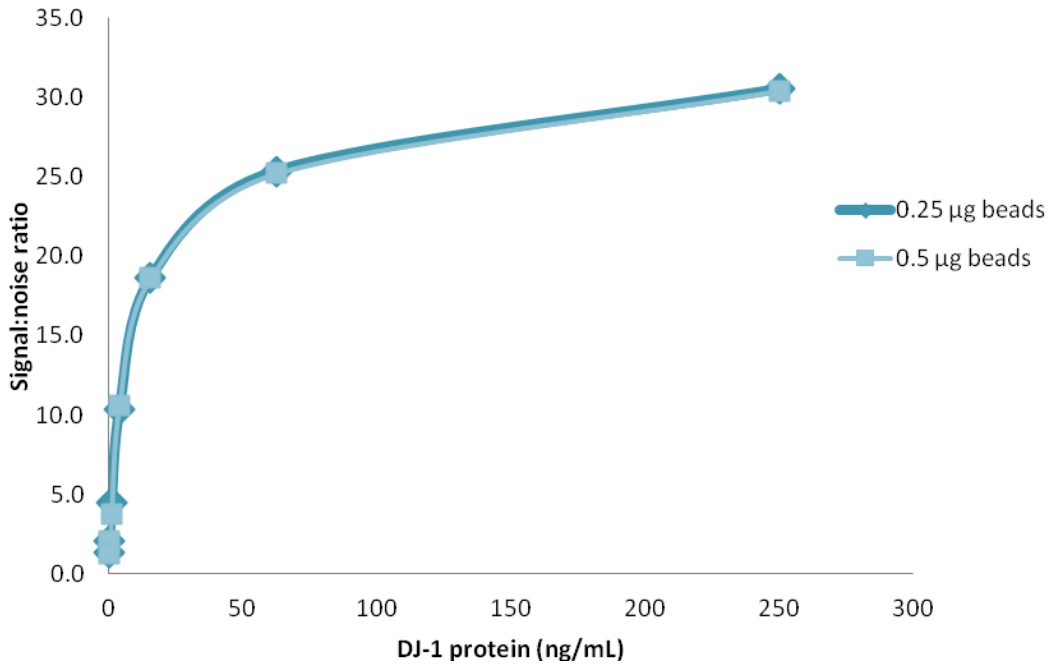

Figure 5.13: Lowering biotinylated anti-DJ-1 pAb (R&D Systems) concentration: *Luminex beads coupled with 0.25 and 0.5 µg were assayed with 250, 62.5, 15.6, 3.9, 0.98, 0.24, 0.06 and 0 ng/mL of DJ-1 recombinant protein (Covance Inc.) prepared in assay buffer. 0.5 µg/mL of biotinylated anti-DJ-1 detection pAb (R&D systems) with 4 µg/ml streptavidin-RPE were used. The figure shows the signal:noise ratio obtained with each bead set at the varying DJ-1 recombinant protein concentrations. Signal:noise ratio was calculated by dividing the mean MFI signal at each DJ-1 protein concentration by the MFI at 0 ng/mL.*

These data showed that the signal:noise ratio was identical for both bead sets. As shown in Figure 5.13, the signal:noise ratio achieved was approximately 30 – 35; no match to the 66 fold published in Hong *et al* (2010) paper.

Alternative antibody pairings were explored; commencing the investigation with changing the capture antibody bound to the Luminex beads. The antibody chosen was mouse anti-DJ-1 mAb (Covance Inc.). 0.25, 0.5, 1 and 1.5 µg of the antibody was coated to Luminex beads. A Luminex sandwich assay was performed with each bead set using the biotinylated anti-DJ-1 pAb (R&D Systems) as the detection component of the assay. The data obtained are displayed in Figure 5.14.

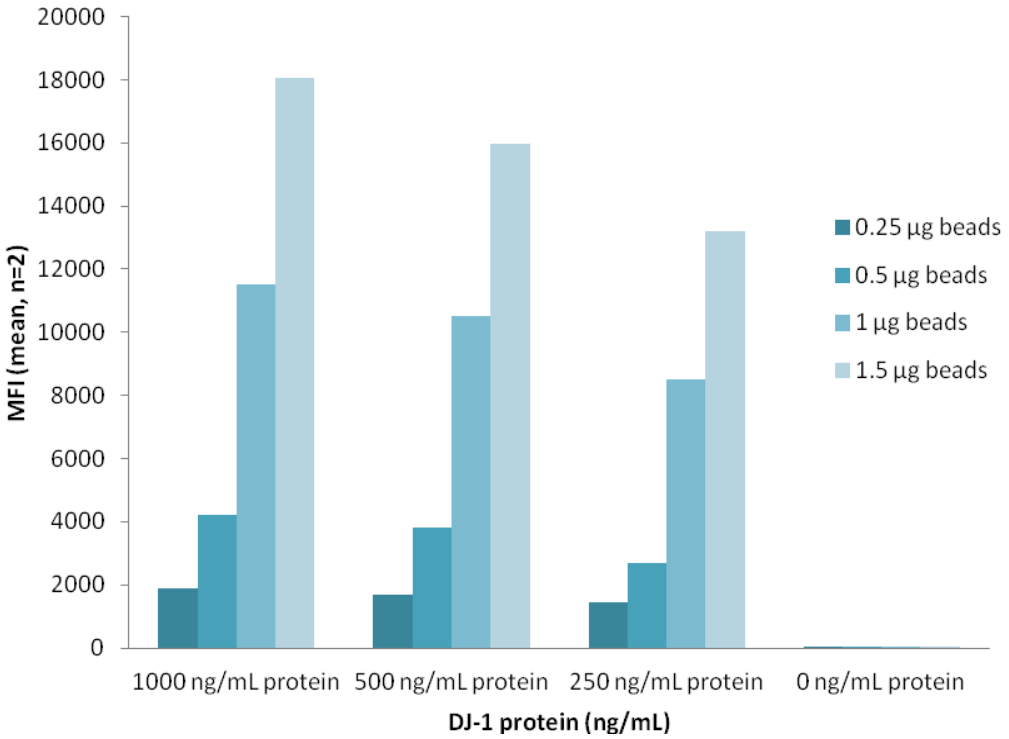

Figure 5.14: Total DJ-1 Luminex assay using anti-DJ-1 mAb (Covance Inc.): *Luminex beads coupled with 0.25, 0.5, 1 and 1.5 µg of anti-DJ-1 mAb (Covance Inc.) were assayed with 0, 10, 500, 1000 ng/mL of DJ-1 recombinant protein (Covance Inc.) prepared in assay buffer. 2 µg/mL biotinylated anti-DJ-1 detection pAb (R&D systems) with 4 µg/ml streptavidin-RPE was used. This figure shows MFI signals obtained with each bead set at varying DJ-1 protein concentrations.*

The MFI with anti-DJ-1 mAb from Covance Inc. in comparison to the anti-DJ-1 mAb from Novus Biological Ltd. as the capture reagent was shown to be markedly higher. The greatest MFI was achieved with beads coated with 1.5 µg of the Covance Inc. anti-DJ-1 mAb. In light of this result, the anti-DJ-1 mAb from Covance Inc. and biotinylated anti-DJ-1 goat pAb from R&D Systems was chosen to take further into the assay optimisation stage.

5.7 Total DJ-1 Luminex assay optimisation

The Luminex assay for quantifying DJ-1 involved ensuring that the optimum mass of anti-DJ-1 mAb (Covance Inc.) was coupled to beads. This was based on previous data (Figure 4.5) showing that as the anti-DJ-1 mAb mass (µg) increased, the MFI signals increased too. Furthermore, the assays during the development phase used 2 µg/mL of the biotinylated anti-DJ-1 goat pAb (R&D Systems) – it was interesting to see if we could use less detection antibody in order to generate an assay that was cost effective without compromising its performance.

5.7.1 Increasing anti-DJ-1 mAb (Covance Inc.) bead coupling

Increasing the mass (µg) of anti-DJ-1 mAb (Covance Inc.) from 1.5 µg to 2 and 3 µg was assessed. The data obtained are shown in Figure 5.15:

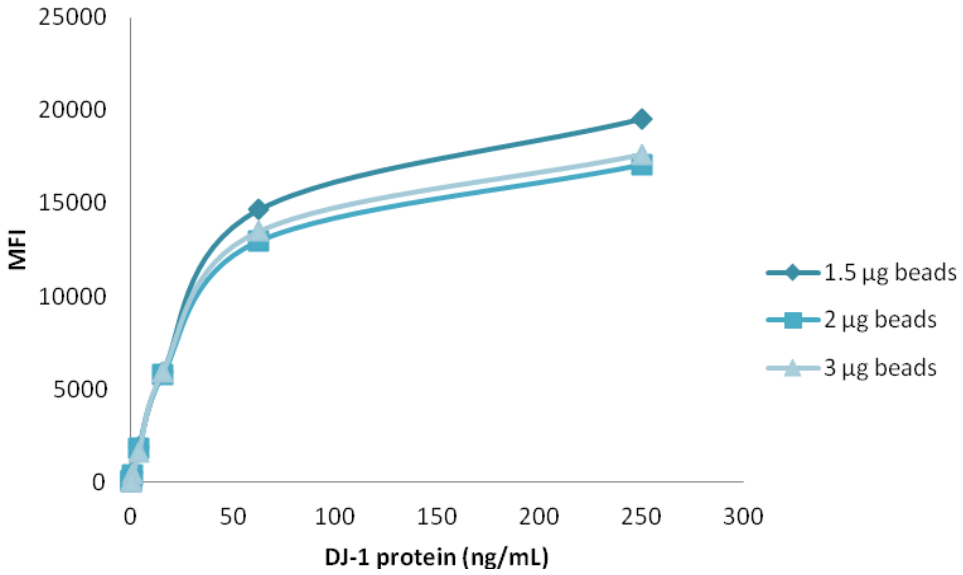

Figure 5.15: Increasing anti-DJ-1 mAb (Covance Inc.) bead coupling: *Luminex beads coupled with 1.5, 2 and 3 µg of ant-DJ-1 mAb (Covance Inc.) were assayed with 250, 62.5, 15.6, 3.9, 0.98, 0.24, 0.06 and 0 ng/mL of DJ-1 recombinant protein (Covance Inc.) prepared in assay buffer. 2 µg/mL biotinylated anti-DJ-1 detection pAb (R&D systems) with 4 µg/ml streptavidin-RPE was used. The figure shows the MFI signals obtained with each bead set at the varying DJ-1 recombinant protein concentrations.*

Increasing the mass of anti-DJ-1 mAb to couple Luminex beads did not increase the MFI, rather it decreased the signal, suggesting that beads coupled with 1.5 µg of capture anti-DJ-1 mAb was optimal. For the remaining optimisation tests, 2 µg beads were tested alongside 1.5 µg beads, to see if changes in the detection phase of the assay affected assay performance in the form of higher signal:noise ratio.

5.7.2 Detection antibody titration

Luminex sandwich assay was performed with beads coated with 1.5 and 2 µg of the anti-DJ-1 mAb with decreasing concentrations of the biotinylated anti-DJ-1 goat pAb (R&D Systems). 1 and 0.5 µg/mL of biotinylated anti-DJ-1 pAb was tested and the data are shown in Figure 5.16:

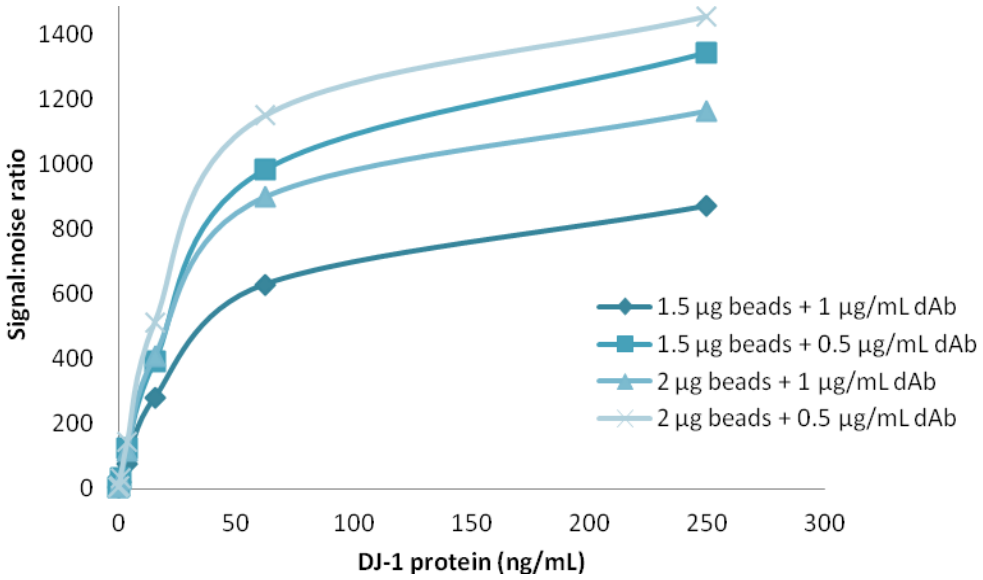

Figure 5.16: Detection antibody titration effect on signal:noise ratio: *Luminex beads coupled with 1.5 and 2 µg of ant-DJ-1 mAb (Covance Inc.) were assayed with 250, 62.5, 15.6, 3.9, 0.98, 0.24, 0.06 and 0 ng/mL of DJ-1 recombinant protein (Covance Inc.) prepared in assay buffer. 1 and 0.5 µg/mL biotinylated anti-DJ-1 detection pAb (R&D systems) with 4 µg/ml streptavidin-RPE was used. This figure shows the signal:noise ratio with each bead set at the varying DJ-1 recombinant protein concentrations. Signal:noise ratio was calculated by dividing the mean MFI at each protein concentration by the mean MFI at 0 ng/mL of protein*

The MFI signals achieved at all bead and detection antibody combinations were >11,000 at 250 ng/ml. There was a difference in the background signal and this produced the marked difference in the signal:noise ratio for each bead/detection antibody combination.

The optimisation data suggested that 2 µg beads with 0.5 µg/mL biotinylated anti-DJ-1 detection antibody yield the best signal:noise ratio. The effect of reducing the concentration of Streptavidin-RPE was not investigated since the plan was to include this assay with the α-synuclein assay as a multiplex panel. Since 4 µg/mL was found to yield the best data for α-synuclein – this will have to be used for the DJ-1 assay.

5.8 Duplex assay development: total α-synuclein and total DJ-1

Three experiments were performed in order to test for cross reactivity between the total α-synuclein and total DJ-1 assays. Details of these tests and the results are shown in this section. Optimisation and validation of the duplex assay is also described in this section.

5.8.1 Cross reactivity tests

Out of the three cross reactivity tests, the first experiment involved checking for cross reactivity between the two sets of antibody coupled beads. The second experiment tested whether there would be cross reactivity if the beads and detection antibody components were multiplexed. The final test involved multiplexing all three assay components; the beads, protein standards and detection antibodies. Figure 5.17, summarises the experiment:

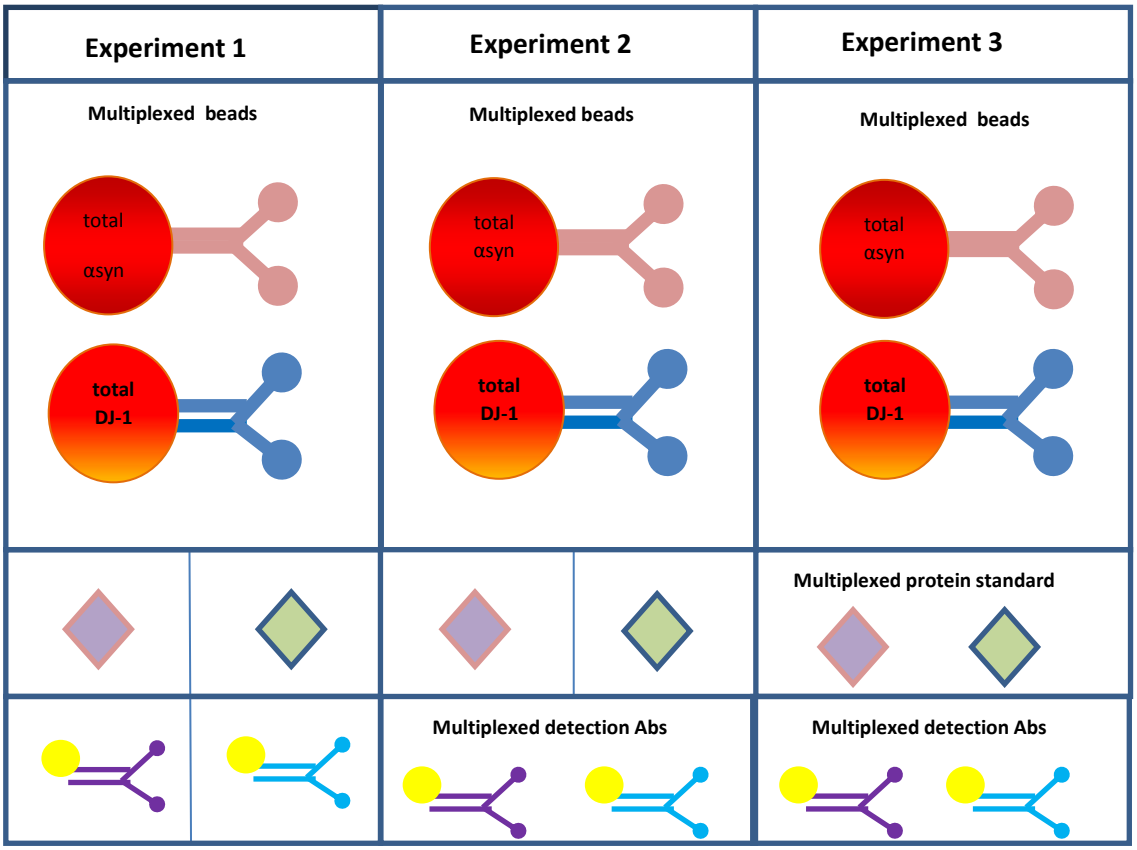

Figure 5.17: Luminex cross reactivity test: *experimental steps taken to determine the presence of cross reactivity when multiplexing total α-synuclein and total DJ-1 Luminex assays. Experiment 1; assay with multiplexed beads only. Experiment 2; assay with multiplexed beads and multiplexed detection antibodies. Experiment 3; assay with multiplexed beads, multiplexed detection antibodies and multiplexed protein standards.*

The results from these three cross reactivity tests showed that the two assays do not cross react. The data obtained are depicted in Figure 5.18.

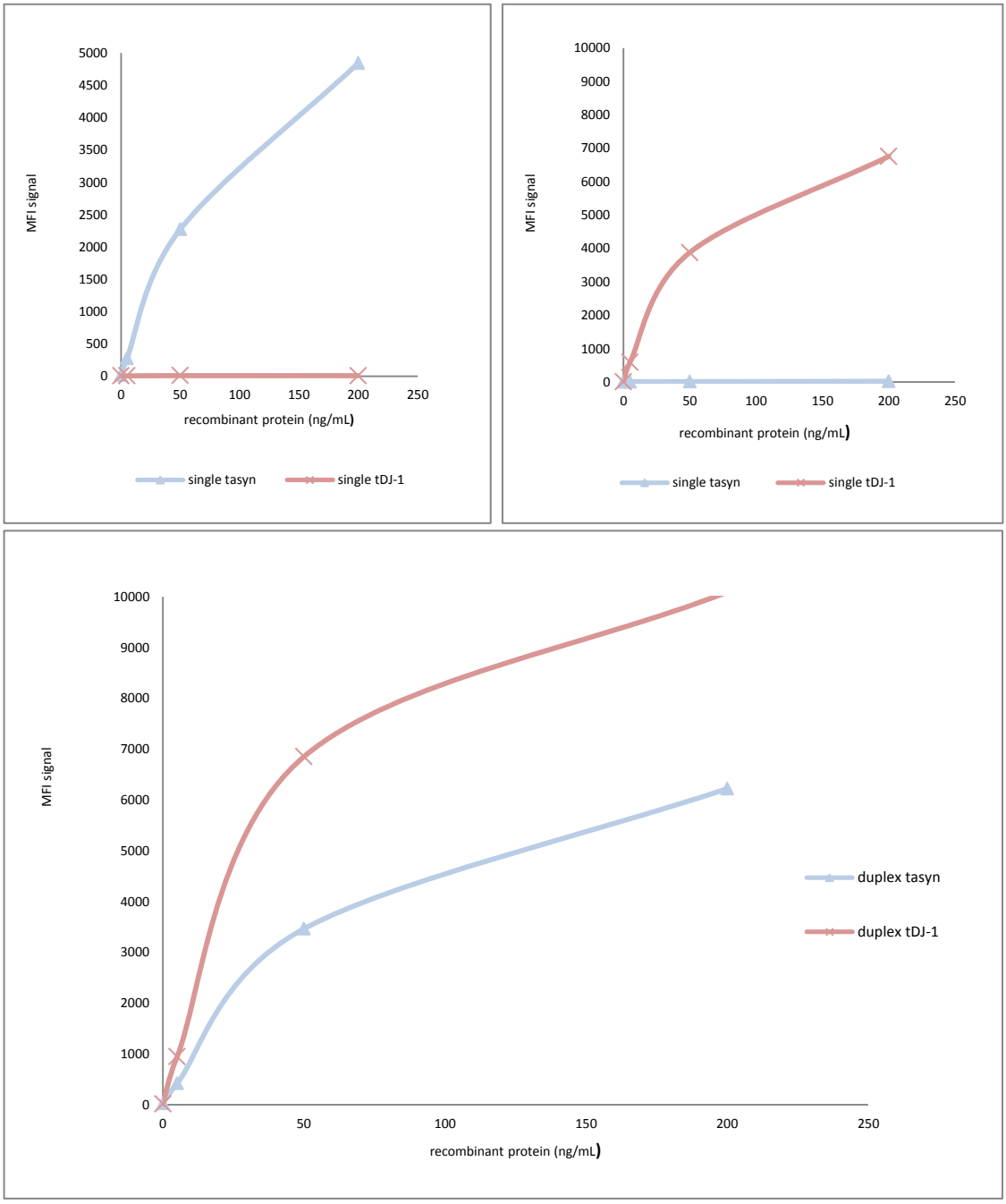

Figure 5.18: Luminex cross reactivity test results: *MFI signals (n=2) obtained from experimental steps taken to determine the presence of cross reactivity when multiplexing total α-synuclein and total DJ-1 Luminex assays***.** *A) assay with multiplexed beads and multiplexed protein with only tαsyn detection antibody. B) assay with multiplexed beads and multiplexed protein with only DJ-1 detection antibody. C) assay with multiplexed beads, multiplexed protein and multiplexed detection antibodies.*

In order to test whether diluting plasma samples x50 against a calibration curve in 1% (v/v) plasma diluent, i.e. as was done with the phosphorylated α-synuclein assay (Chapter 3), a spike recovery test was performed. The data from this test suggested

that the aforementioned conditions would be suitable for this duplex assay. Results from the spike recovery experiment and other validation parameters are shown below.

5.9 Duplex validation: plasma assay for total α-synuclein and total DJ-1

As before, we have used the Lee *et al* (2006b) and Lee, (2009) papers for validating our assays:

This section details the validation experiments performed and the data obtained.

All assays were performed with a calibration curve generated in 1% (v/v) plasma diluent spiked with recombinant α-synuclein and recombinant DJ-1 at the following concentrations: 128, 64, 32, 16, 8, 4, 2, 1, 0.5 and 0 ng/mL.

5.9.1 Spike Recovery

A total of six patient samples were spiked with recombinant α-synuclein and recombinant DJ-1 at high (2000 ng/mL) and low (75 ng/mL) levels. Each spiked sample was analysed alongside the sample without spike. All samples were diluted x 50 with 1% (v/v) plasma diluent prior to analysis and analysed in triplicate. The data obtained are shown in Table 5.1 for total α-synuclein and Table 5.2 for total DJ-1:

Mean blank (ng/mL)	CV%	+ 2000 ng/mL spike (mean)	CV%	Expected (Blank + spike)	% Recovery
0.00	na	1520	6.6	2000	76.0
0.0	na	1739	4.5	2000	86.9
4.2	36.7	1877	11.4	2004	93.7
13.7	na	2271	1.3	2014	112.8
0.00	na	2018	7.1	2000	100.9
0.00	0.0	2047	1.9	2000	102.3
Mean blank (ng/mL)	**CV%**	**+75 ng/mL spike (mean)**	**CV%**	**Expected (Blank + spike)**	**% Recovery**
0.00	na	68	12.2	75	90.4
0.0	na	83	2.8	75	110.7
4.2	36.7	75	6.6	79	94.5
13.7	na	71	4.3	89	80.5
0.00	na	87	8.8	75	115.3
0.00	0.0	69	5.6	75	91.8

Table 5.1: Total α-synuclein Plasma Spike Recovery: *% recovery and precision (%CV) for six plasma samples spiked with 2000 and 75 ng/mL recombinant α-synuclein. Mean n=3.*

The % recovery of total α-synuclein for the spiked samples ranged between 76.0% and 112.8% at the high level spikes with a precision between 1.3% and 11.4%. The low spike recoveries ranged between 80.5% and 115.3% with a precision of 2.8% to 12.2%.

Mean blank (ng/mL)	CV%	+ 2000 ng/mL spike (mean)	CV%	Expected (Blank + spike)	% Recovery
Plasma 1					
0.00	na	2117	3.9	2000	105.8
Plasma 2					
0.50	na	1672	12.2	2001	83.6
Plasma 3					
0.00	na	1982	5.8	2000	99.1
Plasma 4					
18.00	13.6	1481	5.7	2018	73.4
Plasma 5					
0.00	na	2089	7.1	2000	104.5
Plasma 6					
0.00	na	2127	3.8	2000	106.3
Mean blank (ng/mL)	**CV%**	**+75 ng/mL spike (mean)**	**CV%**	**Expected (Blank + spike)**	**% Recovery**
Plasma 1					
0.00	na	86	16.7	75	114.0
Plasma 2					
0.00	na	90	14.2	75	120.0
Plasma 3					
0.00	na	85	7.6	75	113.1
Plasma 4					
17.50	20.2	89	3.4	93	96.0
Plasma 5					
0.00	na	81	8.0	75	107.6
Plasma 6					
0.00	na	78	2.7	75	103.6

Table 5.2: Total DJ-1 Plasma Spike Recovery: *% recovery and precision (%CV) for six plasma samples spiked with 2000 and 75 ng/mL recombinant DJ-1.*

The % recovery of total DJ-1 for the spiked samples ranged between 73.4% and 106.3% at the high level spikes with a precision between 3.8% and 12.2%. The low spike recoveries ranged between 96.0% and 120.0% with a precision of 2.7% to 16.7%.

5.9.2 Parallelism

Upon screening patient samples, levels of total α-synuclein and total DJ-1 levels were very low and not high enough to perform parallelism assessments. One suitable sample was found. The assessment involved analysing the sample at a series of dilutions; 1/5, 1/10, 1/20, 1/40, 1/80 and 1/160.

Dilution Factor	1/Dilution	Mean conc. (ng/mL)	SD	CV%	Dil. Corr. conc. (ng/mL)	Overall Mean Dil. Corr. Conc. (ng/mL)	% Difference
Plasma from Individual 1							
5	0.200	>128	na	na	>128	480	na
10	0.100	117.17	2.93	2.50	1172		144.03
20	0.050	44.37	2.15	4.85	887		84.8
40	0.025	13.9	1.48	10.62	556		15.77
80	0.013	6.08	0.20	3.25	486		1.25
160	0.006	2.49	0.09	3.61	398		-17.02
blank	0	0	0.00	na	0		na

Table 5.3: Total α-synuclein Plasma Parallelism: *Precision (%CV) and % Difference for one plasma sample Analysed at various dilutions with 1% (v/v) plasma assay diluent. % difference calculated from the overall mean result of all dilutions from 1/40 onwards. Each sample analysed in triplicate.*

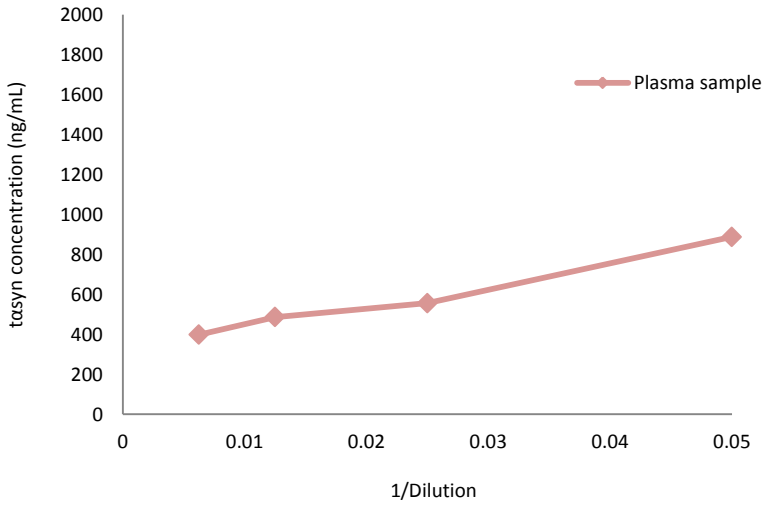

Figure 5.19: Total α-synuclein Plasma Parallelism: *a plasma sample analysed at various dilutions; 1/5, 1/10, 1/20, 1/40 and 1/80, 1/60*

Dilution Factor	1/Dilution	Mean conc. (ng/mL)	SD	CV%	Dil. Corr. conc. (ng/mL)	Overall Mean Dil. Corr. Conc. (ng/mL)	% Difference
Plasma from Individual 1							
5	0.200	10.9	0.24	2.20	55	112	-51.50
10	0.100	8.56	0.08	0.94	86		-23.87
20	0.050	5.15	0.43	8.41	103		-8.4
40	0.025	2.5	0.11	4.27	101		-10.15
80	0.013	1.67	0.06	3.46	133		18.54
160	0.006	0.70	0.11	15.34	113		0.04
blank	0.000	0	0.00	na	0		na

Table 5.4: Total DJ-1 Plasma Parallelism: *Precision (%CV) and % Difference for one plasma sample Analysed at various dilutions with 1% (v/v) plasma assay diluent. % difference calculated from the overall mean result of all dilutions from 1/40 onwards. Each sample analysed in triplicate.*

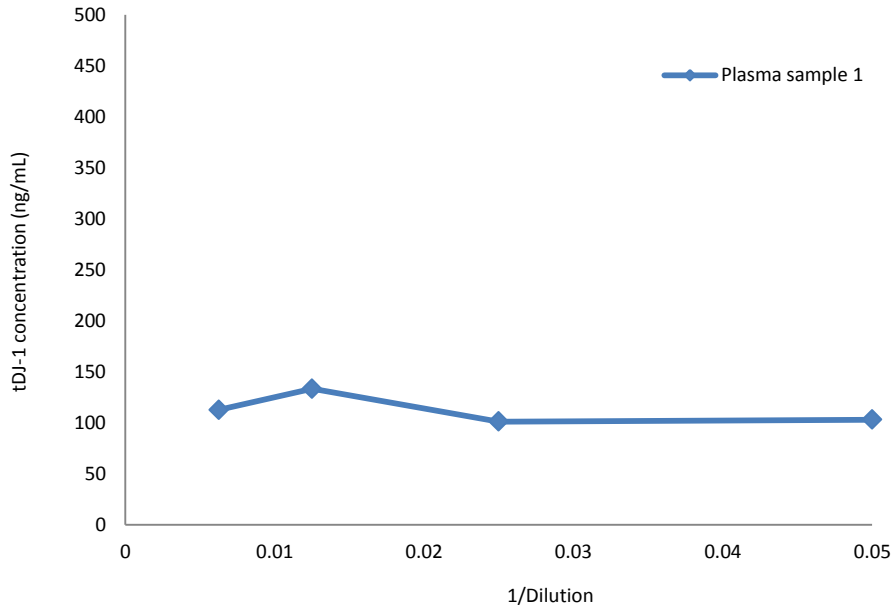

Figure 5.20: Total DJ-1 Plasma Parallelism: *a plasma sample analysed at various dilutions; 1/5, 1/10, 1/20, 1/40 and 1/80, 1/60*

Parallelism for the sample was shown post x40 dilution of the plasma sample. This result and the spike recovery assessment indicated that a dilution of x50 for the plasma samples was sufficient to yield relatively accurate data when using this assay for quantifying total α-synuclein and total DJ-1 levels in plasma.

5.9.3 Dilutional Linearity

A pooled plasma sample was spiked with 1500 ng/mL of recombinant α-synuclein and DJ-1 proteins. This spiked sample was diluted 1/20, 1/40, 1/80, 1/160 and 1/320 - each diluted sample was analysed on the Luminex in triplicate.

Dilution	1/Dilution	Dil. Corr. Result (ng/mL)			Dil. Corr. Mean Result (ng/mL)	Expected Result (ng/mL)	% Difference
1/20	0.05	>ULOQ	>ULOQ	>ULOQ	>ULOQ	na	na
1/40	0.025	1073	1129	1171	1124	1500	-23.3
1/80	0.0125	1230	1277	1252	1253	1500	-16.5
1/160	0.00625	1315	1296	1309	1307	1500	-12.9
1/320	0.003125	1347	1386	1347	1360	1500	-9.3

Table 5.5: Total α-synuclein Plasma Dilutional Linearity: *% Difference for a pooled plasma sample diluted at 1/20, 1/40, 1/80, 1/160 and 1/320, with 1% (v/v) plasma assay buffer.*

Dilution	1/Dilution	Dil. Corr. Result (ng/mL)			Dil. Corr. Mean Result (ng/mL)	Expected Result (ng/mL)	% Difference
1/20	0.05	>ULOQ	>ULOQ	>ULOQ	>ULOQ	na	na
1/40	0.025	1626	1591	1691	1636	1500	9.1
1/80	0.0125	1626	1536	1598	1587	1500	5.8
1/160	0.00625	1581	1502	1469	1517	1500	1.2
1/320	0.003125	1600	1600	1677	1626	1500	8.4

Table 5.6: Total DJ-1 Plasma Dilutional Linearity: *% Difference for a pooled plasma sample diluted at 1/20, 1/40, 1/80, 1/160 and 1/320, with 1% (v/v) plasma assay buffer.*

To further show the linearity of the dilutions, a regression plot for each analyte was performed using Microsoft Excel and is displayed in Figures 5.21 and 5.22.

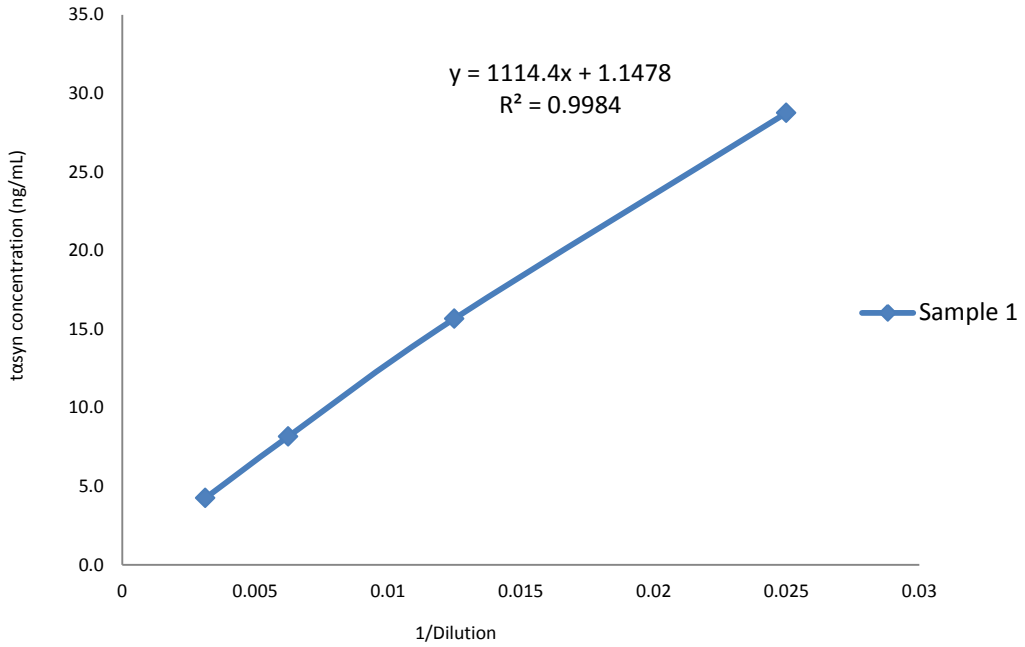

Figure 5.21: Total α-synuclein Plasma Dilutional Linearity: *pooled plasma sample underwent a series of dilutions. Each diluted sample was assayed in the duplex Luminex assay. Mean concentration yielded for each diluted sample was plotted in Microsoft Excel.*

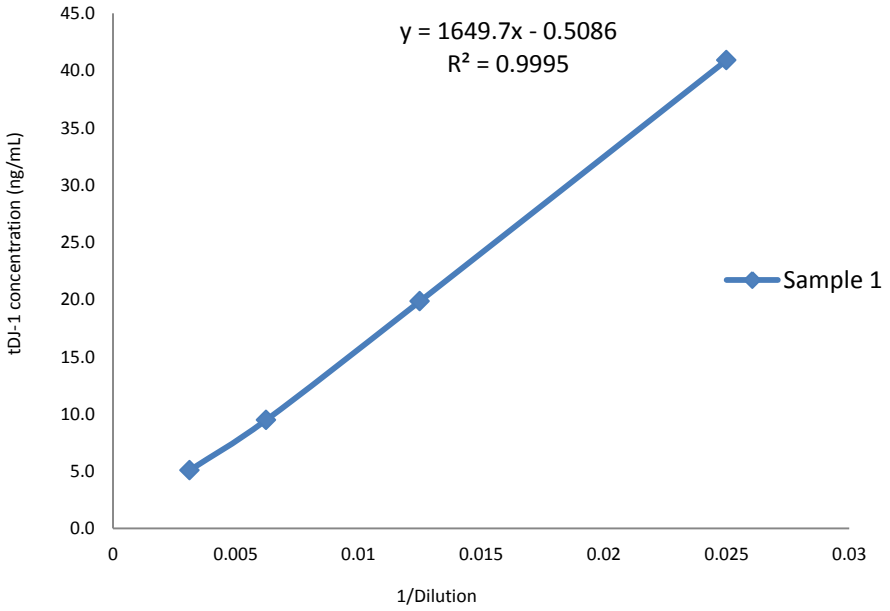

Figure 5.22: Total DJ-1 Plasma Dilutional Linearity: *pooled plasma sample underwent a series of dilutions. Each diluted sample was assayed in the duplex Luminex assay. Mean concentration yielded for each diluted sample was plotted in Microsoft Excel.*

The R^2 value was 0.9984 and 0.9995 for total α-synuclein and total DJ-1, respectively, showing that the samples diluted in a linear fashion.

This experiment was also used to assess hook effect for the assay. The MFI signal for 1500 ng/mL of recombinant total α-synuclein and total DJ-1 did not reduce. A reduction in the signal would have indicated a hook effect.

5.9.4 Accuracy and Precision

A total of six assays were performed on different dates to assess the accuracy and precision of the assay. Five samples; ULOQ, HVS, MVS, LVS and LLOQ, were generated and used for this assessment.

All samples were generated by spiking recombinant α-synuclein and recombinant DJ-1 into neat blank plasma to yield a MFI assay reading in the region of 60, 40, 10, 1.5, 0.5 ng/mL for both proteins, after the x50 assay dilution.

Each sample was assayed in three wells on each assay plate. Both Inter-assay and Intra-assay precision and accuracy has been determined.

Tables 5.7 and 5.9 display the inter-assay data for total α-synuclein and total DJ-1.

Tables 5.8 and 5.10 display the intra-assay data for total α-synuclein and total DJ-1.

Assay Date	ULOQ	HQ	MQ	LQ	LLOQ
07-Dec-14	52.2	39.2	9.9	1.4	0.43
	54.4	39.0	9.4	1.9	0.52
	61.7	39.2	9.0	1.57	0.41
30-Jan-15	62.3	43.5	10.0	1.56	0.52
	64.2	43.4	9.2	1.34	0.49
	73.5	33.4	9.8	1.46	0.57
02-Feb-15	62.1	41.0	10.3	1.59	0.51
	55.0	40.4	9.3	1.66	0.49
	54.3	41.8	10.4	1.68	0.54
04-Feb-15	59.6	36.4	9.6	1.38	0.52
	67.5	38.5	10.0	1.54	0.64
	59.4	40.2	9.9	1.56	0.57
07-Feb-15	59.1	38.5	10.2	1.51	0.60
	60.7	40.5	11.7	1.62	0.80
	62.0	36.6	10.3	1.25	0.78
10-Feb-15	60.8	42.5	10.3	1.78	0.56
	62.3	33.5	10.8	1.57	0.53
	62.5	40.6	10.6	1.57	0.61
Inter-assay data					
Mean	60.7	39.4	10.0	1.55	0.56
SD	5.007	2.923	0.636	0.155	0.101
CV%	8.2	7.4	6.3	10.0	18.1
% Difference/Bias	1.2	-1.6	0.4	3.5	12.1

Table 5.7: Total α-synuclein Plasma Inter-assay Accuracy and Precision: *ULOQ, HVS, MVS, LVS and LLOQ samples were analysed on the Luminex for the quantification of total α-synuclein. The precision was calculated using %CV (SD/mean %) and the bias was calculated using %difference ((observed-expected)/expected * 100)*

Assay Date	Intra-assay data	ULOQ	HQ	MQ	LQ	LLOQ
07-Dec-14	Mean	56.1	39.2	9.4	1.62	0.45
	SD	4.97	0.16	0.42	0.25	0.06
	CV%	8.9	0.4	4.4	15.7	12.9
	%Difference/Bias	-6.5	-2.1	-5.5	8.2	-9.3
30-Jan-15	Mean	66.7	40.1	9.7	1.45	0.53
	SD	6.02	5.83	0.44	0.11	0.04
	CV%	9.03	14.53	4.58	7.58	7.7
	%Difference/Bias	11.1	0.3	-3.4	-3.1	5.3
02-Feb-15	Mean	57.1	41.1	10.0	1.64	0.51
	SD	4.31	0.73	0.63	0.05	0.03
	CV%	7.5	1.8	6.3	2.9	4.9
	%Difference/Bias	-4.8	2.7	0.1	9.6	2.7
04-Feb-15	Mean	62.1	38.4	9.8	1.49	0.58
	SD	4.61	1.90	0.23	0.10	0.06
	CV%	7.4	5.0	2.4	6.6	10.5
	%Difference/Bias	3.6	-4.1	-1.7	-0.4	15.3
07-Feb-15	Mean	60.6	38.5	10.7	1.5	0.7
	SD	1.46	1.98	0.82	0.19	0.11
	CV%	2.4	5.1	7.6	13.0	15.2
	%Difference/Bias	1.0	-3.7	7.1	-2.7	45.3
10-Feb-15	Mean	61.9	38.9	10.6	1.6	0.6
	SD	0.90	4.74	0.22	0.12	0.04
	CV%	1.5	12.2	2.1	7.4	7.1
	%Difference/Bias	3.1	-2.8	5.6	9.3	13.3

Intra-assay data	Intra-CV%	6.1	6.5	4.6	8.9	9.7

Table 5.8: Total α-synuclein Plasma Intra-assay Accuracy and Precision: *ULOQ, HVS, MVS, LVS and LLOQ samples were analysed on the Luminex for the quantification of total α-synuclein. The precision was calculated using CV% (SD/mean %) and the bias was calculated using %difference ((observed-expected)/expected * 100). Intra assay precision was calculated from the average CV% from each individual assay. Intra assay bias was calculated from the average %bias from each individual assay.*

Assay Date	ULOQ	HQ	MQ	LQ	LLOQ
07-Dec-14	51.9	41.4	10.5	1.59	0.55
	54.5	44.0	10.9	1.45	0.47
	55.3	39.4	10.8	1.3	0.44
30-Jan-15	60.9	41.1	9.6	1.31	0.57
	68.3	43.8	9.2	1.49	0.53
	59.7	41.8	9.5	1.47	0.65
02-Feb-15	65.1	46.1	8.6	1.55	0.47
	58.4	38.5	9.5	1.79	0.47
	59.5	43.9	10.7	1.46	0.53
04-Feb-15	58.3	37.1	9.4	1.63	0.51
	64.8	42.3	9.4	1.45	0.54
	60.1	39.4	9.8	1.63	0.57
07-Feb-15	59.6	38.5	10.5	1.69	0.69
	67.5	45.8	10.8	1.71	0.93
	63.7	41.5	9.7	1.48	0.83
10-Feb-15	64.9	44.3	10.6	1.13	0.66
	62.1	41.8	11.5	1.29	0.43
	68.8	42.4	10.3	1.53	0.50
Inter-assay data					
Mean	61.3	41.8	10.1	1.50	0.57
SD	4.766	2.560	0.743	0.167	0.134
CV%	7.8	6.1	7.4	11.2	23.3
% Difference/Bias	2.2	4.6	0.6	-0.2	14.9

Table 5.9: Total DJ-1 Plasma Inter-assay Accuracy and Precision: *ULOQ, HVS, MVS, LVS and LLOQ samples were analysed on the Luminex for the quantification of total DJ-1. The precision was calculated using %CV (SD/mean %) and the bias was calculated using %difference ((observed-expected)/expected * 100.*

Assay Date	Intra-assay data	ULOQ	HQ	MQ	LQ	LLOQ
07-Dec-14	Mean	53.9	41.6	10.7	1.45	0.49
	SD	1.77	2.35	0.20	0.15	0.06
	CV%	3.3	5.7	1.8	10.0	11.7
	%Difference/Bias	-10.2	4.0	7.3	-3.6	-2.7
30-Jan-15	Mean	62.9	42.2	9.4	1.42	0.58
	SD	4.64	1.38	0.18	0.10	0.06
	CV%	7.4	3.3	1.9	6.9	10.5
	%Difference/Bias	4.9	5.6	-5.7	-5.1	16.7
02-Feb-15	Mean	61.0	42.8	9.6	1.60	0.49
	SD	3.59	3.91	1.03	0.17	0.03
	CV%	5.9	9.1	10.7	10.7	7.1
	%Difference/Bias	1.7	7.1	-4.0	6.7	-2.0
04-Feb-15	Mean	61.1	39.6	9.5	1.57	0.54
	SD	3.36	2.64	0.21	0.10	0.03
	CV%	5.5	6.7	2.2	6.6	5.6
	%Difference/Bias	1.8	-1.0	-4.7	4.7	8.0
07-Feb-15	Mean	63.6	41.9	10.3	1.6	0.8
	SD	3.93	3.66	0.55	0.13	0.12
	CV%	6.2	8.7	5.3	7.8	14.8
	%Difference/Bias	5.9	4.8	3.1	8.4	63.3
10-Feb-15	Mean	65.2	42.9	10.8	1.3	0.5
	SD	3.36	1.30	0.61	0.20	0.12
	CV%	5.1	3.0	5.6	15.3	22.2
	%Difference/Bias	8.7	7.1	7.7	-12.2	6.0

Intra-assay data	Intra-CV%	5.6	6.1	4.6	9.6	12.0

Table 5.10: Total DJ-1 Plasma Intra-assay Accuracy and Precision: *ULOQ, HVS, MVS, LVS and LLOQ samples were analysed on the Luminex for the quantification of total DJ-1. The precision was calculated using CV% (SD/mean %) and the bias was calculated using %difference ((observed-expected)/expected * 100). Intra assay precision was calculated from the average CV% from each individual assay. Intra assay bias was calculated from the average %bias from each individual assay.*

The average inter assay precision for total α-synuclein was shown to be ≤ 18.1% with the bias ≤ 12.1%. The inter assay precision for total DJ-1 was ≤ 23.3% and the bias ≤ 14.9.

The assay intra assay precision for total α-synuclein averaged at ≤ 9.7%, and the bias of the spiked known concentrations ranged from -9.3% to 15.3% (one assay yielded a bias of 45.3% at LLOQ, this could be due to sample preparation error). The intra assay precision for total DJ-1 was ≤ 12.0% and the bias ranged between -12.2% and 16.7% (bias of 63.3 was obtained during one assay at the LLOQ, again this could be assigned to error in sample preparation).

5.9.5 Limit of Detection

As before, the method used to ascertain this limit entailed analysing a blank sample 20 times, determining the mean value, and then using the mean + 3*SD as the LOD (Armbruster *et al*, 2008).

The mean MFI reading from 20 replicates of the blank sample (1% (v/v) plasma) for the total α-synuclein assay was measured at 6.3 with a standard deviation of 0.6. Therefore, the mean MFI + 3*SD was calculated to be 8.08.

The mean MFI reading from 20 replicates of the blank sample for the total DJ-1 was measured at 5.8 with a standard deviation of 0.7. Therefore, the mean MFI + 3*SD was calculated to be 7.91.

According to the “Elisa analysis” program (available at http://elisaanalysis.com/app), of 8.08 MFI signal equates to 0.05 ng/mL of total α-synuclein. Correcting this value

for the proposed minimum dilution of x 50 for the assay the LOD was calculated to be 2.5 ng/mL (0.05 * 50).

An MFI signal of 7.91 correlates to a concentration of 0.11 ng/mL of total DJ-1. This equals to 5.4 ng/mL LOD for the total DJ-1 assay after the x 50 MRD correction.

5.10 Duplex validation: CSF assay for total α-synuclein and total DJ-1

The duplex assay for use with CSF samples was validated using the same biomarker validation guidelines as used for the plasma assay (Lee *et al*, 2006b and Lee 2009). This section details the validation experiments performed and the data obtained.

The assays developed so far into project involved using matrix-based diluents for the calibration curve preparation and sample dilution. Unfortunately this was not possible for this duplex assay for use with CSF, due to the lack of sufficient volumes of blank CSF matrix. As a result the accuracy of this assay was expected to be poor.

All assays were performed with a calibration curve generated in PBS/SM01 assay buffer spiked with recombinant α-synuclein and recombinant DJ-1 at the following concentrations: 128, 64, 32, 16, 8, 4, 2, 1, 0.5 and 0 ng/mL. All samples were diluted x5 with PBS/SM01 – this dilution was chosen based on acceptable spike recovery results (see section 5.10.1).

5.10.1 Spike Recovery

Six patient samples were analysed with 40 and 10 ng/mL of recombinant protein spiked into it. Each sample was also analysed alone without any spike material (blank).

Mean blank (ng/mL)	CV%	+ 40 ng/mL spike (mean)	CV%	Expected (Blank + spike)	% Recovery
CSF sample 1					
0.00	na	39.4	4.9	40	98.5
CSF sample 2					
0.00	na	32.3	5.3	40	80.7
CSF sample 3					
0.37	38.3	28.4	6.5	40	70.4
CSF sample 4					
0.55	0.0	42.9	2.1	41	105.7
CSF sample 5					
8.61	21.1	44.9	11.6	49	92.3
CSF sample 6					
6.45	0.0	46.0	6.8	46	99.1
Mean blank (ng/mL)	**CV%**	**+ 10 ng/mL spike (mean)**	**CV%**	**Expected (Blank + spike)**	**% Recovery**
CSF sample 1					
0.00	na	10.8	11.8	10	108.5
CSF sample 2					
0.00	na	7.7	2.7	10	77.4
CSF sample 3					
0.37	38.3	7.4	14.7	10	71.4
CSF sample 4					
0.55	18.9	9.9	0.4	11	94.2
CSF sample 5					
8.61	21.1	19.5	0.4	19	104.6
CSF sample 6					
6.45	0.0	17.3	6.4	16	105.5

Table 5.11: Total α-synuclein CSF Spike Recovery: *% recovery and precision (%CV) for six CSF samples spiked with 40 and 10 ng/mL recombinant α-synuclein. Mean calculated from n=3.*

The % recovery of total α-synuclein for the spiked samples ranged between 70.4% and 105.7% at the high level spikes with a precision between 2.1% and 11.6%.

The low spike recoveries ranged between 71.4% and 108.5% with a precision of 0.4% to 14.7%.

Mean blank (ng/mL)	CV%	+ 40 ng/mL spike (mean)	CV%	Expected (Blank + spike)	% Recovery
CSF sample 1					
0.00	0.00	38.0	12.7	40	95.0
CSF sample 2					
0.00	0.00	40.2	1.3	40	100.5
CSF sample 3					
0.52	5.1	37.0	2.8	41	91.2
CSF sample 4					
1.15	0.0	42.0	16.2	41	102.1
CSF sample 5					
0.00	0.0	28.9	4.6	40	72.3
CSF sample 6					
0.00	0.0	33.8	3.7	40	84.5
Mean blank (ng/mL)	**CV%**	**+ 10 ng/mL spike (mean)**	**CV%**	**Expected (Blank + spike)**	**% Recovery**
CSF sample 1					
0.00	0.00	7.7	3.1	10	77.3
CSF sample 2					
0.00	0.00	10.0	5.4	10	100.0
CSF sample 3					
0.52	5.1	9.4	10.3	11	89.3
CSF sample 4					
1.15	10.4	10.6	10.2	11	94.6
CSF sample 5					
0.00	0.0	7.4	3.0	10	73.7
CSF sample 6					
0.00	0.0	11.2	21.5	15	74.6

Table 5.12: Total DJ-1 CSF Spike Recovery: *% recovery and precision (%CV) for six CSF samples spiked with 40 and 10 ng/mL recombinant DJ-1. Mean calculated from n=3.*

The % recovery of total DJ-1 for the spiked samples ranged between 72.3% and 102.1% at the high level spikes with a precision between 2.8% and 16.2%.

The low spike recoveries ranged between 73.7% and 100% with a precision of 3.0% to 21.5%.

5.10.2 Dilutional Linearity

Three individual CSF samples were spiked with up to 5000 ng/mL of recombinant α-synuclein and DJ-1 recombinant proteins. The spiked samples were diluted 1/10, 1/20, 1/40, 1/80, 1/160 and 1/320 - each diluted sample was analysed on the Luminex in triplicate. Tables 5.13, 5.14 and Figures 5.23 and 5.24 represent data obtained for one of assessed samples.

Dilution	1/Dilution	Result (ng/mL)			Mean Result (ng/mL)	Expected Result (ng/mL)	% Difference
1/40	0.025	> ULOQ	> ULOQ	> ULOQ	> ULOQ	na	Na
1/80	0.0125	> ULOQ	> ULOQ	> ULOQ	> ULOQ	na	Na
1/160	0.00625	na	5314	6075	5694	5000	13.9
1/320	0.003125	4086	4925	5171	4727	5000	-5.5
1/640	0.001562	5818	5600	6131	5850	5000	17.0
1/1280	0.000781	5261	4377.6	5504	5047	5000	0.9

Table 5.13: Total α-synuclein CSF Dilutional Linearity: *% difference for a CSF sample diluted at 1/20, 1/40, 1/80, 1/400, 1/160 and 1/320 with assay buffer.*

The % difference between the expected result and observed result was ≤17.0% - thus samples can be diluted up to 1280 times without compromising the final result.

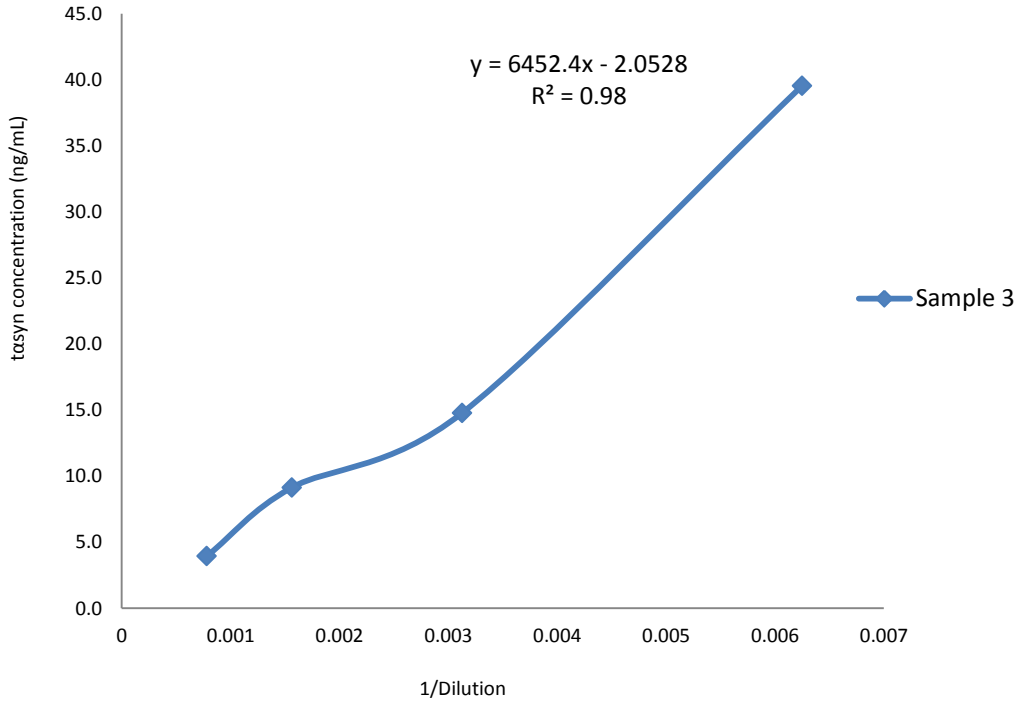

Figure 5.23: Total α-synuclein CSF Dilutional Linearity*: A CSF sample underwent a series of dilutions. Each diluted sample was analysed on the Luminex and results plotted using Microsoft Excel.*

The R^2 value from the regression plot was 0.98 for this particular sample, further showing dilutional linearity.

Dilution	1/Dilution	Result (ng/mL)			Mean Result (ng/mL)	Expected Result (ng/mL)	% Difference
1/40	0.025	> ULOQ	> ULOQ	> ULOQ	> ULOQ	na	Na
1/80	0.0125	>ULOQ	>ULOQ	>ULOQ	> ULOQ	na	Na
1/160	0.00625	5059	4981	4501	4847	5000	-3.1
1/320	0.003125	5043	5290	5158	5164	5000	3.3
1/640	0.0015625	5888	5408	4832	5376	5000	7.5
1/1280	0.00078125	4518	4915	5005	4813	5000	-3.7

Table 5.14: Total DJ-1 CSF Dilutional Linearity: *% difference for a CSF sample diluted at 1/20, 1/40, 1/80, 1/400, 1/160 and 1/320 with assay buffer.*

The % difference between the expected result and observed result was ≤ 7.5% - thus samples can be diluted up to 1280 times without compromising the final result.

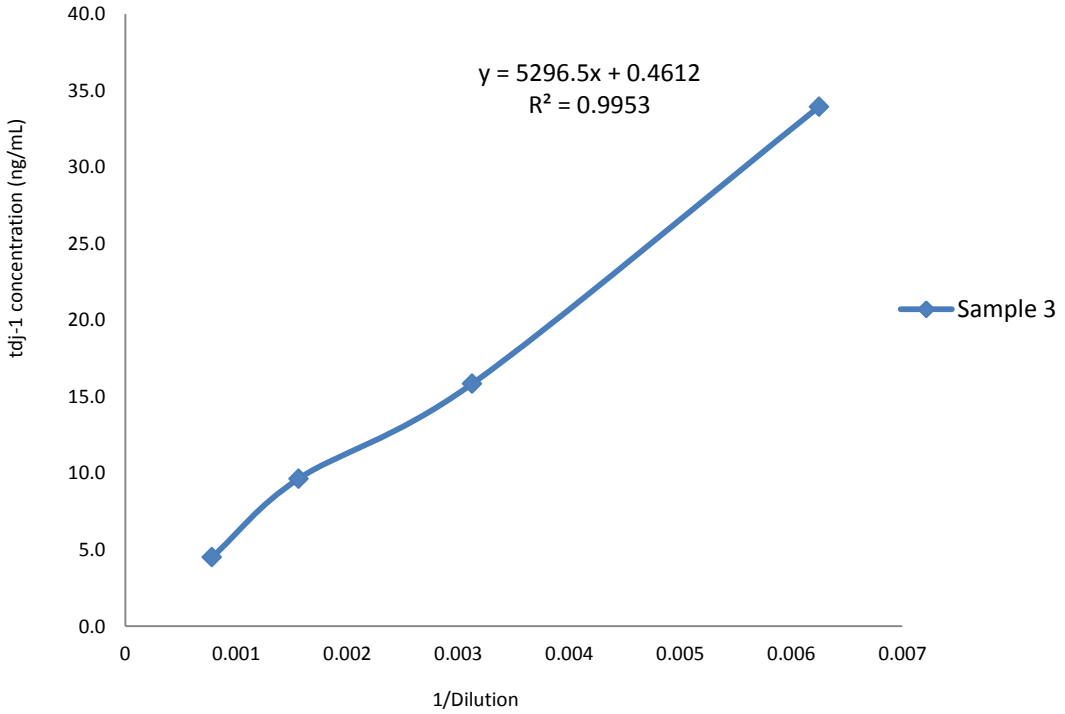

Figure 5.24: Total DJ-1 CSF Dilutional Linearity*: A CSF sample underwent a series of dilutions. Each diluted sample was analysed on the Luminex and results plotted using Microsoft Excel.*

The R^2 value from the total DJ-1 regression plot was 0.995, further showing dilutional linearity.

The additional two samples utilised for this assessment also yielded similar results for both proteins. The % difference was ≤ 20% and R^2 values were ≥ 0.995.

5.10.3 Accuracy and Precision

As with previous assays, a total of six assays were performed on different dates to assess the accuracy and precision of the assay. Five samples; ULOQ, HVS, MVS, LVS and LLOQ, were generated and used for this assessment.

All samples were generated by spiking recombinant α-synuclein and recombinant DJ-1 into neat blank CSF to yield a MFI assay reading in the region of 40, 20, 10, 5 and 2 ng/mL for both proteins, after the x5 assay dilution (the actual spiked concentration was therefore, 200, 100, 50, 25 and 10 ng/mL)

Each sample was assayed in three wells on each assay plate. Both Inter-assay and Intra-assay precision and accuracy has been determined. Subsequent tables display the data obtained for each protein:

Tables 5.15 and 5.16 display the inter-assay data for total α-synuclein and total DJ-1 respectively.

Tables 5.17 and 5.18 display the intra-assay data for total α-synuclein and total DJ-1.

Assay Date	ULOQ	HQ	MQ	LQ	LLOQ
07-Aug-15	42.3	18.7	7.4	4.38	2.30
	36.7	14.2	10.7	4.8	1.12
	45.9	21.9	7.1	4.8	1.71
12-Aug-15	35.5	18.4	8.5	4.99	2.35
	35.6	20.5	9.3	4.69	1.58
	34.6	17.1	8.3	4.51	1.90
14-Aug-15	36.9	19.1	10.1	4.96	1.96
	36.6	19.5	11.2	4.4	1.83
	43.4	20.1	9.4	5.89	1.45
21-Aug-15	42.7	22.6	11.3	6.05	2.54
	45.3	18.8	9.1	5.02	2.11
	38.8	20.2	10.1	5.19	1.86
28-Aug-15	48.4	22.0	8.6	5.84	1.50
	43.1	17.1	12.3	5.78	2.17
	40.9	19.7	10.4	4.92	2.35
Inter-assay data					
Mean	40.5	19.3	9.6	5.08	1.92
SD	4.373	2.168	1.481	0.555	0.397
CV%	10.8	11.2	15.5	10.9	20.7
% Difference/Bias	1.1	-3.4	-4.3	1.6	-4.2

Table 5.15: Total α-synuclein: CSF Inter-assay Accuracy and Precision: *ULOQ, HVS, MVS, LVS and LLOQ samples were analysed on the Luminex for the quantification of total α-synuclein in CSF. The precision was calculated using %CV (SD/mean %) and the bias was calculated using %difference ((observed-expected)/expected * 100)*

Assay Date	ULOQ	HQ	MQ	LQ	LLOQ
07-Aug-15	na	20.4	11.2	6.23	2.23
	44.2	17.9	12.2	5.54	1.76
	47.0	21.4	9.3	5.5	2.24
12-Aug-15	38.7	14.8	8.8	4.05	2.17
	36.4	18.0	8.6	4.63	1.84
	39.9	16.2	7.8	5.39	2.47
14-Aug-15	31.2	22.3	9.1	5.18	2.00
	na	19.1	13.5	4.57	2.13
	39.1	21.0	10.2	6.09	1.90
21-Aug-15	39.7	19.8	11.4	7.69	2.50
	37.5	19.9	11.0	7.7	2.85
	33.5	22.6	10.9	6.97	2.98
28-Aug-15	45.9	26.9	11.7	4.13	1.96
	45.8	20.5	11.4	5.55	2.78
	40.3	20.6	11.4	6.09	2.50
Inter-assay data					
Mean	39.9	20.1	10.6	5.69	2.29
SD	4.813	2.860	1.555	1.141	0.380
CV%	12.1	14.2	14.7	20.1	16.6
% Difference/Bias	-0.2	0.5	5.6	13.7	14.4

Table 5.16: Total DJ-1: CSF Inter-assay Accuracy and Precision: *ULOQ, HVS, MVS, LVS and LLOQ samples were analysed on the Luminex for the quantification of total α-synuclein in CSF. The precision was calculated using %CV (SD/mean %) and the bias was calculated using %difference ((observed-expected)/expected * 100).*

Assay Date	Intra-assay data	ULOQ	HQ	MQ	LQ	LLOQ
07-Aug-15	Mean	41.6	18.2	8.4	4.66	1.71
	SD	4.62	3.90	2.01	0.24	0.59
	CV%	11.1	21.4	24.0	5.2	34.5
	%Difference/Bias	4.1	-8.8	-16.2	-6.8	-14.5
12-Aug-15	Mean	35.2	18.7	8.7	4.73	1.94
	SD	0.56	1.75	0.55	0.24	0.39
	CV%	1.6	9.4	6.3	5.1	19.9
	%Difference/Bias	-12.0	-6.7	-13.2	-5.4	-2.8
14-Aug-15	Mean	39.0	19.6	10.2	5.08	1.75
	SD	3.83	0.47	0.91	0.75	0.27
	CV%	9.8	2.4	8.9	14.8	15.2
	%Difference/Bias	-2.6	-2.2	2.4	1.7	-12.7
21-Aug-15	Mean	42.3	20.5	10.2	5.42	2.17
	SD	3.27	1.91	1.09	0.55	0.34
	CV%	7.7	9.3	10.7	10.2	15.9
	%Difference/Bias	5.7	2.5	1.7	8.4	8.5
28-Aug-15	Mean	44.2	19.6	10.4	5.51	2.01
	SD	3.86	2.47	1.85	0.51	0.45
	CV%	8.7	12.6	17.7	9.3	22.3
	%Difference/Bias	10.4	-2.0	4.1	10.3	0.3

Intra-assay data	Intra-CV%	7.8	11.0	13.5	8.9	21.6

Table 5.17: Total α-synuclein CSF Intra-assay Accuracy and Precision: *ULOQ, HVS, MVS, LVS and LLOQ samples were analysed on the Luminex for the quantification of total DJ-1. The precision was calculated using %CV (SD/mean %) and the bias was calculated using %difference ((observed-expected)/expected * 100).*

Assay Date	Intra-assay data	ULOQ	HQ	MQ	LQ	LLOQ
07-Aug-15	Mean	45.6	19.9	10.9	5.76	2.08
	SD	2.02	1.79	1.52	0.41	0.27
	CV%	4.4	9.0	13.9	7.1	13.2
	%Difference/Bias	14.0	-0.5	8.9	15.1	3.8
12-Aug-15	Mean	38.3	16.3	8.4	4.69	2.16
	SD	1.74	1.58	0.50	0.67	0.32
	CV%	4.5	9.7	5.9	14.3	14.6
	%Difference/Bias	-4.2	-18.4	-16.2	-6.2	8.0
14-Aug-15	Mean	35.1	20.8	10.9	5.28	2.01
	SD	5.64	1.63	2.25	0.76	0.12
	CV%	16.0	7.8	20.6	14.5	5.7
	%Difference/Bias	-12.2	4.0	9.5	5.6	0.5
21-Aug-15	Mean	36.9	20.7	11.1	7.45	2.78
	SD	3.17	1.59	0.25	0.42	0.25
	CV%	8.6	7.7	2.2	5.6	8.9
	%Difference/Bias	-7.8	3.7	10.8	49.1	38.8
28-Aug-15	Mean	44.0	22.7	11.5	5.3	2.4
	SD	3.24	3.68	0.18	1.01	0.42
	CV%	7.4	16.2	1.6	19.3	17.3
	%Difference/Bias	10.0	13.4	14.9	5.1	20.7

Intra-assay data	Intra-CV%	8.2	10.1	8.9	12.2	11.9

Table 5.18: Total DJ-1 CSF Intra-assay Accuracy and Precision: *ULOQ, HVS, MVS, LVS and LLOQ samples were analysed on the Luminex for the quantification of total DJ-1. The precision was calculated using %CV (SD/mean %) and the bias was calculated using %difference ((observed-expected)/expected * 100).*

The average inter assay precision for total α-synuclein and total DJ-1 was shown to be ≤ 20.7% and ≤ 20.1%, respectively. The bias based on the spiked known concentrations was ≤ -4.3% for total α-synuclein and ≤ 14.4 for total DJ-1. .

The intra assay precision for total α-synuclein and total DJ-1 averaged at ≤ 21.6% and ≤ 12.2%. The bias of the spiked known concentrations ranged from -16.2% to 10.4% for total α-synuclein and -18.4% to 20.7% for total DJ-1 (one assay yielded 49.1% and 38.8% bias at the LQ and LLOQ respectively).

5.10.4 Limit of Detection

The mean MFI reading from 20 replicates of the blank sample for this assay was 83.0 with a standard deviation of 5.15 for total α-synuclein and was 42.0 with a standard deviation of 5.15 for total DJ-1. The mean MFI + 3*SD for total α-synuclein and total DJ-1 was 98.6 and 64.5, respectively.

The “Elisa analysis” program (available at http://elisaanalysis.com/app), showed that a MFI signal of 98.6 correlates to a concentration of 0.35 ng/mL of total α-synuclein and 64.5 corresponds to 0.2 ng/mL of total DJ-1 protein. Correcting these values for the proposed minimum dilution of x 5 for the assay, the LOD was calculated to be 1.75 ng/mL for total α-synuclein and 1 ng/mL for total DJ-1.

5.11 Discussion

This chapter describes the development and validation of a duplex Luminex assay for quantifying total α-synuclein and total DJ-1 levels in human plasma and CSF.

An ELISA for measuring total α-synuclein in human plasma and CSF was already developed in house. The purpose of this project was to transfer this assay on to the Luminex platform. Unfortunately, the antibodies used in the ELISA; C211 (capture antibody) and FL140 (detection antibody), did not perform well on the Luminex system. This chapter detailed the troubleshooting experiments performed in order to determine why these antibodies may not have worked on the Luminex. The troubleshooting tests indicated the biotinylated FL140 pAb as the problematic component. The biotinylation confirmation test showed that biotin was present on the antibody, but the functionality test revealed that the biotinylated FL140 pAb was not binding to the α-synuclein protein sufficiently. The biotinylation procedure involved attaching biotin molecules to lysine amino acid residues present on the antibody. Therefore, a plausible explanation for the biotinylation rendering the FL140 pAb inactive, may lie with the possibility that the antigen binding site of FL140 pAb contained lysine residues; modification of these residues may have reconfigured the antigen binding site, leading to its inactivity. However, it was not possible to obtain the actual amino acid sequence of the Fab region of FL140 pAb, therefore it cannot be concluded definitively that it contains lysine residues. Another possible explanation for the inactivity of FL140 pAb may be due to the buffer composition in which the antibody solution is provided – 1.0 ml PBS with 0.1% sodium azide and 0.1% gelatin. The antibody underwent manual Protein A/G purification followed by an ultra-filtration and desalting step, in order to make it suitable for biotinylation. These purification steps may not have been adequate enough to remove agents

such as gelatine and sodium azide which may have hindered the binding between FL140 pAb and biotin.

The total DJ-1 assay was based on the assay described by Hong *et al* (2010). The antibodies used by Hong *et al* (2010), transferred well on to the Luminex but this did not perform as well as the published method, i.e. our assay signal:noise ratio was much lower. Changing the capture antibody improved the performance of this assay and generated a signal:noise ratio that matched the published method. The reason why the capture antibody used by Hong *et al* (2010) did not perform as well in our laboratory may be due to the different types of beads used by Hong *et al* (2010). Their method utilised Liquichip activated beads (LiquiChip-Applications-Handbook.pdf), whereas we used Bio-Rad carboxylated beads that required activating manually with EDC and NHS. The activated beads are no longer available, thus it was not possible to test this possibility.

Singleplex assays for total α-synuclein and total DJ-1 were initially established before combining the two assays to form the duplex assay. Initially, the aim of the project was to develop a multiplex assay comprised of measuring total α-synuclein, total DJ-1 and LRRK2. The LRRK2 assay components cross reacted with the other two assays (results of this cross-reactivity are displayed in Chapter 7) and thus LRRK2 was removed from the multiplex assay.

The duplex assay was validated as previously described in Chapter 3 using the acceptance criteria outlined in Table 3.14. The validation data obtained for the quantification of total α-synuclein and total DJ-1 in human plasma meet all the criteria presented in this table.

The duplex assay for measuring total α-synuclein and total DJ-1 in human CSF also meet the acceptance criteria outlined in the summary table, except for the spike recovery experiments. This was expected as we were unable to use blank CSF as the assay buffer for preparing calibrators and diluting samples. The spike recovery experiments not meeting the acceptance criteria did not pose an issue with being able to use the assay and the data obtained from it. The principle aim for developing this assay was to investigate differences in particular protein levels between samples taken from various neurodegenerative disease groups and healthy controls. The high bias values for the protein levels in the samples anlaysed would be consistent for all samples, thus the data obtained from the various disease groups can still be compared to each other.

The Luminex technology in theory should offer a more sensitive assay for quantifying analytes of interest when compared to the traditional ELISA. An ELISA for measuring total α-synuclein in human plasma had already been developed in house. This in house assay yielded a LOD of 85 ng/mL (sample dilution factor corrected, 1.7 * 50). Thus, the Luminex assay has been found to be far more sensitive, displaying a LOD of 2.5 ng/mL (sample dilution factor corrected, 0.05 * 50).

An assay for total DJ-1 has not been developed in house. Waragai *et al* (2007), have measured total DJ-1 in human plasma using a commercial CircuLexTM Human DJ-1 ELISA Kit (Cat. No. CY-9050, CyLex Co. Ltd. Nagano, Japan). The kit claims to have a sensitivity of 0.92 ng/mL but there is no indication of the dilution factor used during sample analysis. Thus, it cannot be definitively concluded that our Luminex assay for quantifying total DJ-1 in human plasma is more sensitive than this commercial kit.

Chapter 6:

Total α-synuclein and total DJ-1: sample analysis results

6.1 Introduction

Chapter 5 described the development and validation of a duplex Luminex assay for quantifying total α-synuclein and total DJ-1, in human plasma and CSF.

Here, this duplex assay has been used to analyse the same plasma and CSF samples that were tested for phosphorylated α-synuclein levels (see Chapter 4 section 4.1). It was not possible to analyse every single sample due to low sample volume. Analysis of these samples allowed us to assess whether the levels of total α-synuclein and total DJ-1 show significant differences between the different disease groups. Furthermore, it was also possible to investigate correlation relationships between:

- Plasma total α-synuclein vs plasma total DJ-1
- Plasma total α-synuclein vs plasma phosphorylated α-synuclein
- Plasma total DJ-1 vs plasma phosphorylated α-synuclein
- CSF total α-synuclein vs CSF total DJ-1
- CSF total α-synuclein vs CSF phosphorylated α-synuclein
- CSF total DJ-1 vs CSF phosphorylated α-synuclein
- Plasma total α-synuclein vs CSF total α-synuclein
- Plasma total DJ-1 vs CSF total DJ-1

This chapter displays the sample analysis data and the outcomes from this investigation.

6.2 Total α-synuclein levels in plasma samples

The IBM SPSS Statistics 21 package was used to analyse the total α-synuclein levels in plasma samples from GMNC and UCL. The data were not normally distributed as per the Kolgomorov-Smirnov test; therefore the non-parametric Kruskal-Wallis (K-W) test (with post-hoc Mann-Whitney test when K-W was significant) was used in order to determine whether total α-synuclein levels were significantly different between the different disease groups. The data from GMNC and UCL samples were initially analysed independently and a summary of that data is displayed in Tables 6.1 and 6.2. Data from GMNC and UCL were then combined and the same statistical analysis was performed. A summary of the combined data is displayed in Table 6.3.

Disease group	n	tαsyn mean (ng/mL)	tαsyn median (ng/mL)	SD
AD	42	198	12	553
DLB	45	161	23	476
PD	40	31	19	38
MSA	14	27	11	32
PSP	18	24	10	45
CBD	12	96	20	240
Healthy Controls	53	96	25	196

Table 6.1: Total α-synuclein levels in plasma samples from GMNC data summary: *mean, median and SD calculated using Microsoft Excel 2010. Each sample was analysed in triplicate.*

The K-W test revealed that the levels of total α-synuclein were not significantly different (p=0.372) between AD, PD, DLB, MSA, PSP, CBD and healthy controls.

Disease group	n	tαsyn mean (ng/mL)	tαsyn median (ng/mL)	SD
Healthy Controls	19	100	26	163
MSA	20	177	45	262
PD+DLB	18	122	4	273
PSP+CBS	35	72	30	137

Table 6.2: Total α-synuclein levels in plasma samples from UCL data summary: *mean, median and SD calculated using Microsoft Excel 2010. Each sample was analysed in triplicate.*

Total α-synuclein levels between MSA, PD+DLB, PSP+CBS and healthy controls were also not significantly different (p=0.136 by K-W test).

Disease group	n	tαsyn mean (ng/mL)	tαsyn median (ng/mL)	SD
AD	42	198	12	553
DLB	45	161	23	476
PD	57	60	17	159
MSA	34	115	21	213
PSP+CBS	64	64	14	146
Healthy Controls	72	97	26	166

Table 6.3: Total α-synuclein levels in plasma samples from GMNC and UCL combined, data summary: *mean, median and SD calculated using Microsoft Excel 2010. Each sample was analysed in triplicate.*

The p-value by K-W test for the combined data was 0.273, leading to the conclusion that total α-synuclein levels between the various neurodegenerative disorders tested and healthy controls do not significantly differ.

6.3 Total DJ-1 levels in plasma samples

The samples analysed for total α-synuclein were also analysed for total DJ-1. The data was not normally distributed as per the Kolgomorov-Smirnov test. Kruskal-Wallis and Mann-Whitney tests using the IBM SPSS Statistics 21 package were therefore performed. Table 6.4 summarises the data obtained with the samples analysed from GMNC.

Disease group	n	tdj-1 mean (ng/mL)	tdj-1 median (ng/mL)	SD
AD	42	28	11	37
DLB	45	22	5	43
PD	40	32	6	132
MSA	14	27	16	32
PSP	18	20	10	24
CBD	12	25	5	64
Healthy Controls	53	28	12	47

Table 6.4: Total DJ-1 levels in plasma samples from GMNC data summary: *mean, median and SD calculated using Microsoft Excel 2010. Each sample was analysed in triplicate.*

By K-W test it was revealed that there is a significant difference in plasma total DJ-1 levels between AD, DLB, PD, MSA, PSP, CBD and healthy controls (p=0.017).

Prior to performing Mann-Whitney tests on this (GMNC) data set, the data from UCL samples were tested via K-W. Both datasets were then combined and tested via K-W. The data are summarised in Table 6.5 and 6.6.

Disease group	n	tdj-1 mean (ng/mL)	tdj-1 median (ng/mL)	SD
Healthy Controls	19	8	3	11
MSA	20	22	6	35
PD+DLB	18	19	0	52
PSP+CBS	35	7	2	11

Table 6.5: Total DJ-1 levels in plasma samples from UCL data summary: *mean, median and SD calculated using Microsoft Excel 2010. Each sample was analysed in triplicate.*

The K-W test with the UCL samples also showed a significant difference in plasma total DJ-1 levels between MSA, PD, DLB, PSP+CBS and healthy controls (p=0.021).

Disease group	n	tdj-1 mean (ng/mL)	tdj-1 median (ng/mL)	SD
AD	42	28	12	37
DLB	45	23	5	43
PD	58	28	3	113
MSA	34	24	10	33
PSP+CBS	65	14	4	31
Healthy Controls	72	23	10	42

Table 6.6: Total DJ-1 levels in plasma samples from GMNC and UCL combined, data summary: *mean, median and SD calculated using Microsoft Excel 2010. Each sample was analysed in triplicate.*

K-W test on the combined data (GMNC and UCL) showed that total DJ-1 levels in plasma between AD, DLB, PD, MSA, PSP+CBS and healthy controls was significantly different (p=0.01).

Mann Whitney tests were performed on the combined (GMNC and UCL) data set, in order to find the specific groups that showed significant differences in levels of total DJ-1 in plasma. Table 6.7 summarises the p-value data obtained from this test.

	HC	AD	DLB	MSA	PD	PSP+CBS
HC	-	0.274	0.265	0.558	0.004	0.024
AD	0.274	-	0.058	0.738	0.001	0.004
DLB	0.265	0.058	-	0.116	0.165	0.405
MSA	0.558	0.738	0.116	-	0.005	0.013
PD	0.004	0.001	0.165	0.005	-	0.412
PSP+CBS	0.024	0.004	0.405	0.013	0.412	-

Table 6.7: Mann Whitney p-values for total DJ-1 levels in plasma samples from GMNC and UCL combined data: *p-values <0.05 are shaded in grey.*

Significant differences were found between PD vs HC, PD vs AD and PD vs MSA. Furthermore, significant differences were also found between PSP+CBS versus HC, AD and MSA. Receiver Operating Characteristic (ROC) curves were performed in order to assess whether the significant differences in plasma total DJ-1 levels between these disease groups indicate a diagnostic potential for plasma total DJ-1 levels.

The area under the curve (AUC) of ROC curves is a measure of how accurate a diagnostic test is. Figure 6.1 displays the ROC curves for assessing the diagnostic values for PD against HC, AD and MSA. Figure 6.2 presents the ROC curves showing the potential of plasma total DJ-1 to discriminate between PSP+CBS versus HC, AD and MSA

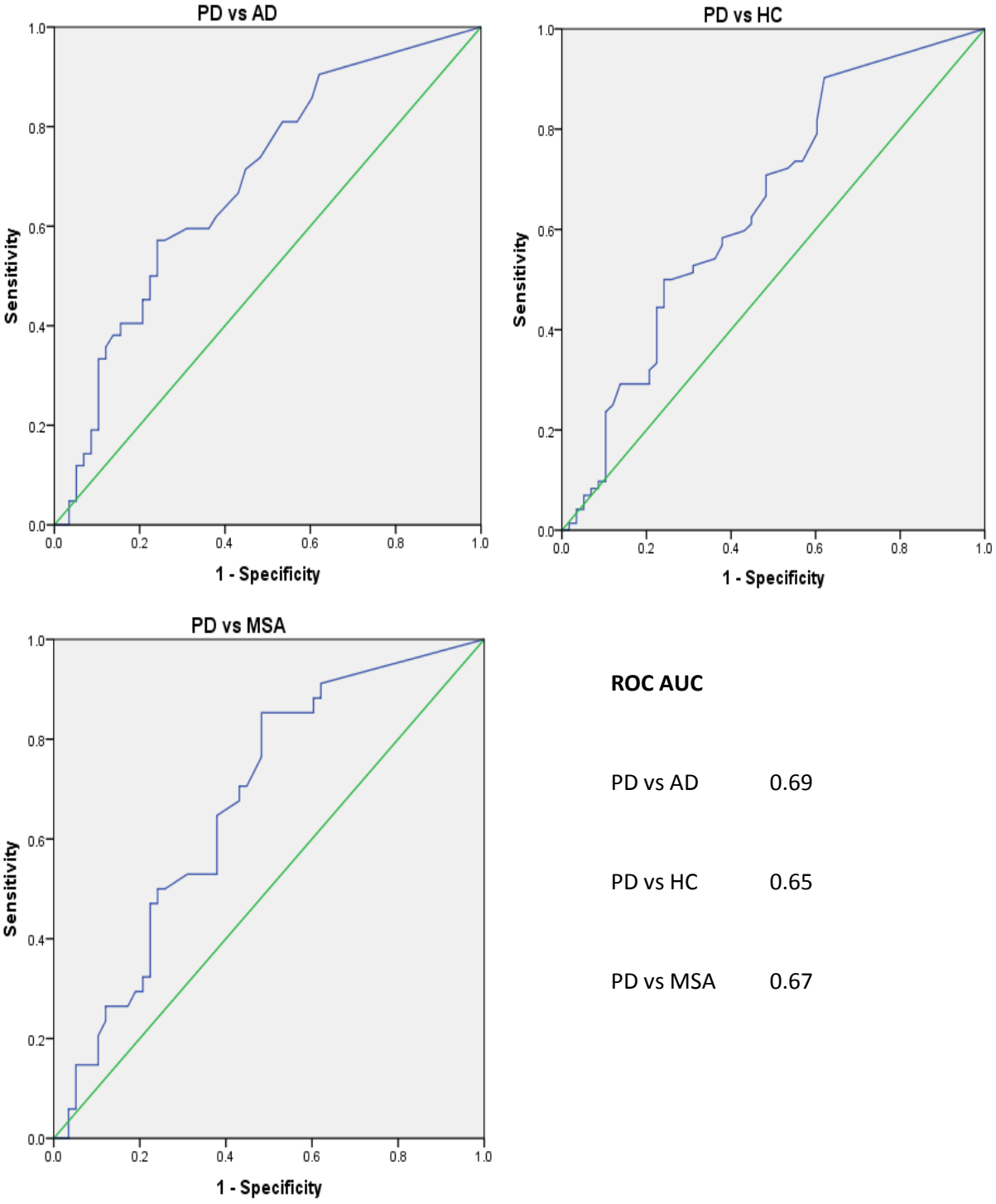

ROC AUC	
PD vs AD	0.69
PD vs HC	0.65
PD vs MSA	0.67

Figure 6.1: ROC curves for assessing the diagnostic potential of plasma total DJ-1: *curves for PD vs AD, PD vs HC and PD vs MSA with AUC of 0.69, 0.65 and 0.67, respectively*

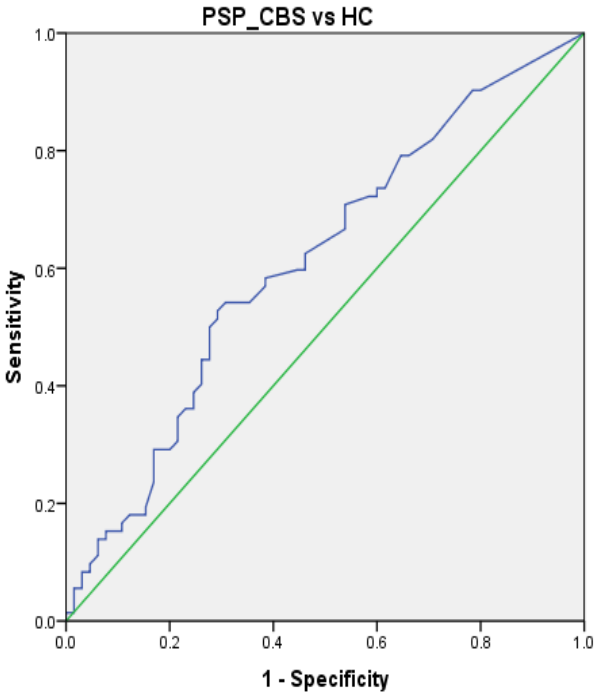

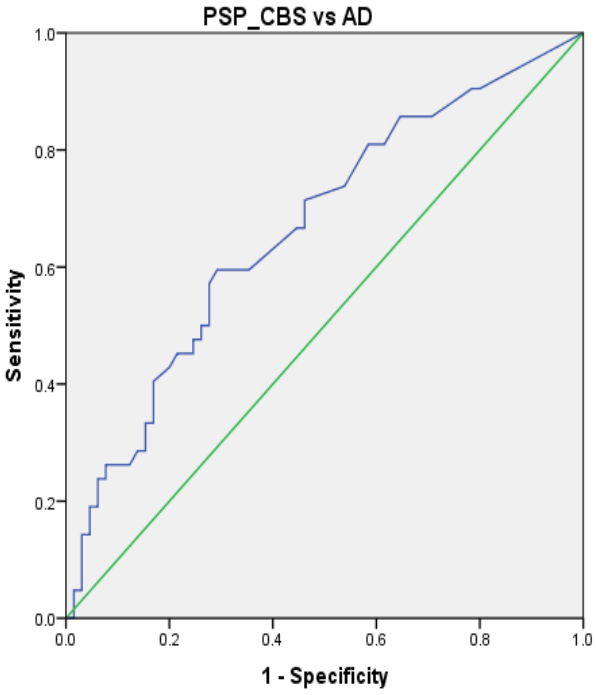

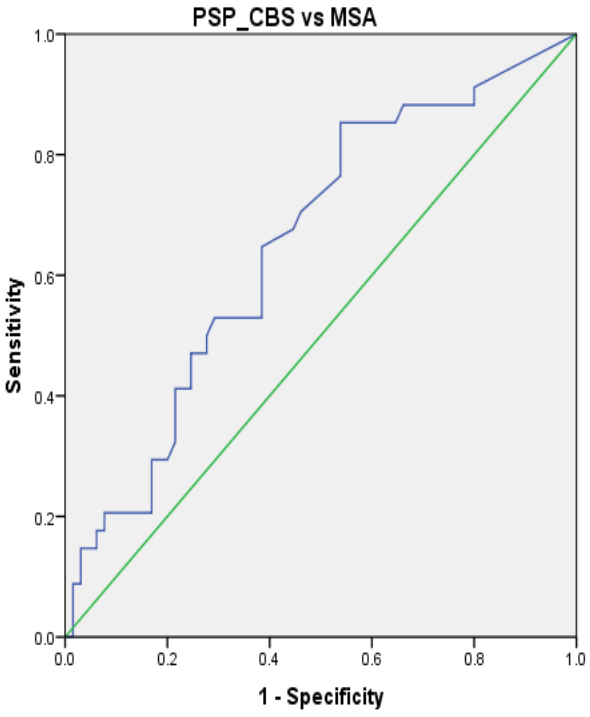

ROC AUC	
PSP+CBS vs HC	0.61
PSP+CBS vs AD	0.67
PSP+CBS vs MSA	0.65

Figure 6.2: ROC curves for assessing the diagnostic potential of plasma total DJ-1: *curves for PSP+CBS vs HC, PSP+CBS vs AD and PSP+CBS vs MSA with AUC of 0.61, 0.67 and 0.65, respectively*

An AUC of ≤ 0.5 is classified as being a “worthless” test and an AUC of 1.0 is classed as a perfect test. The AUC for discriminating between PD, AD, HC and MSA are between 0.65 - 0.69. The AUC for diagnosing between PSP+CBS against HC, AD and MSA are between 0.61 – 0.67. Thus, we can conclude that plasma total DJ-1 carries a fair potential as being a discriminatory diagnostic marker, but with need for considerable improvement.

6.4 Correlation between total α-synuclein, total DJ-1 and phosphorylated α-synuclein in plasma samples

Plasma samples from GMNC and UCL were also analysed for levels of phosphorylated α-synuclein (results discussed in Chapter 3). The data from Chapter 3 and the data displayed in this Chapter were combined to investigate the relationship between plasma levels of phosphorylated α-synuclein, total α-synuclein and total DJ-1.

Combined data were checked for normality using the Kolgomorov-Smirnov test and found to be non-normally distributed. Therefore, the Spearman rank correlation test was adopted to test for any correlation between the three different protein levels.

The Spearman rank correlation test was first performed for the whole dataset, i.e. for all disease groups combined. Table 6.8 and Figure 6.3 display this data.

The correlation data for all disease groups was significant between all three protein levels ($p = <0.005$). The data were therefore separated based on the various disease groups and then tested for correlation via the Spearman rank correlation test. Tables 6.9 to 6.15 and Figures 6.4 to 6.10 present the correlation test data for each disease group.

		Plasma tαsyn	Plasma tDJ-1	Plasma pαsyn
Plasma tαsyn	Correlation coefficient	na	0.562	0.490
	Sig (2 tailed)	na	0.000	0.000
	N	310	310	310
Plasma tDJ-1	Correlation coefficient	0.562	na	0.286
	Sig (2 tailed)	0.000	na	0.000
	N	310	310	310
Plasma pαsyn	Correlation coefficient	0.490	0.286	na
	Sig (2 tailed)	0.000	0.000	na
	N	310	310	310

Table 6.8: GMNC and UCL plasma sample correlation; all disease groups: *spearman rank statistical data obtained from IBM SPSS Statistics 21 package.*

.

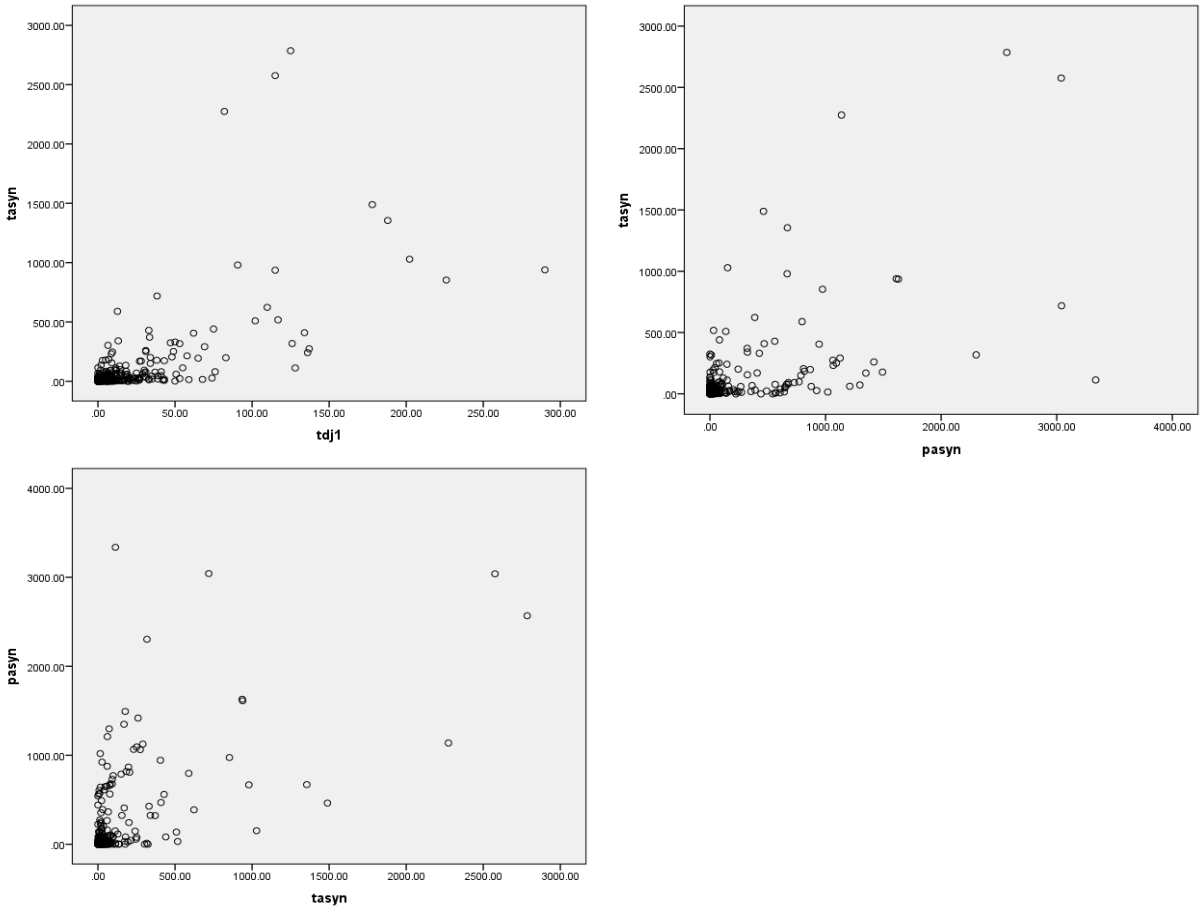

Figure 6.3: GMNC and UCL plasma sample correlation; all disease groups: *scatter plot depicting the spearman rank correlation.*

		Plasma tαsyn	Plasma tDJ-1	Plasma pαsyn
Plasma tαsyn	Correlation coefficient	Na	0.594	0.535
	Sig (2 tailed)	Na	0.000	0.000
	N	42	42	42
Plasma tDJ-1	Correlation coefficient	0.594	na	0.299
	Sig (2 tailed)	0.000	na	0.055
	N	42	42	42
Plasma pαsyn	Correlation coefficient	0.535	0.299	na
	Sig (2 tailed)	0.000	0.055	na
	N	42	42	42

Table 6.9: GMNC and UCL plasma sample correlation; AD only: *spearman rank statistical data obtained from IBM SPSS Statistics 21 package*

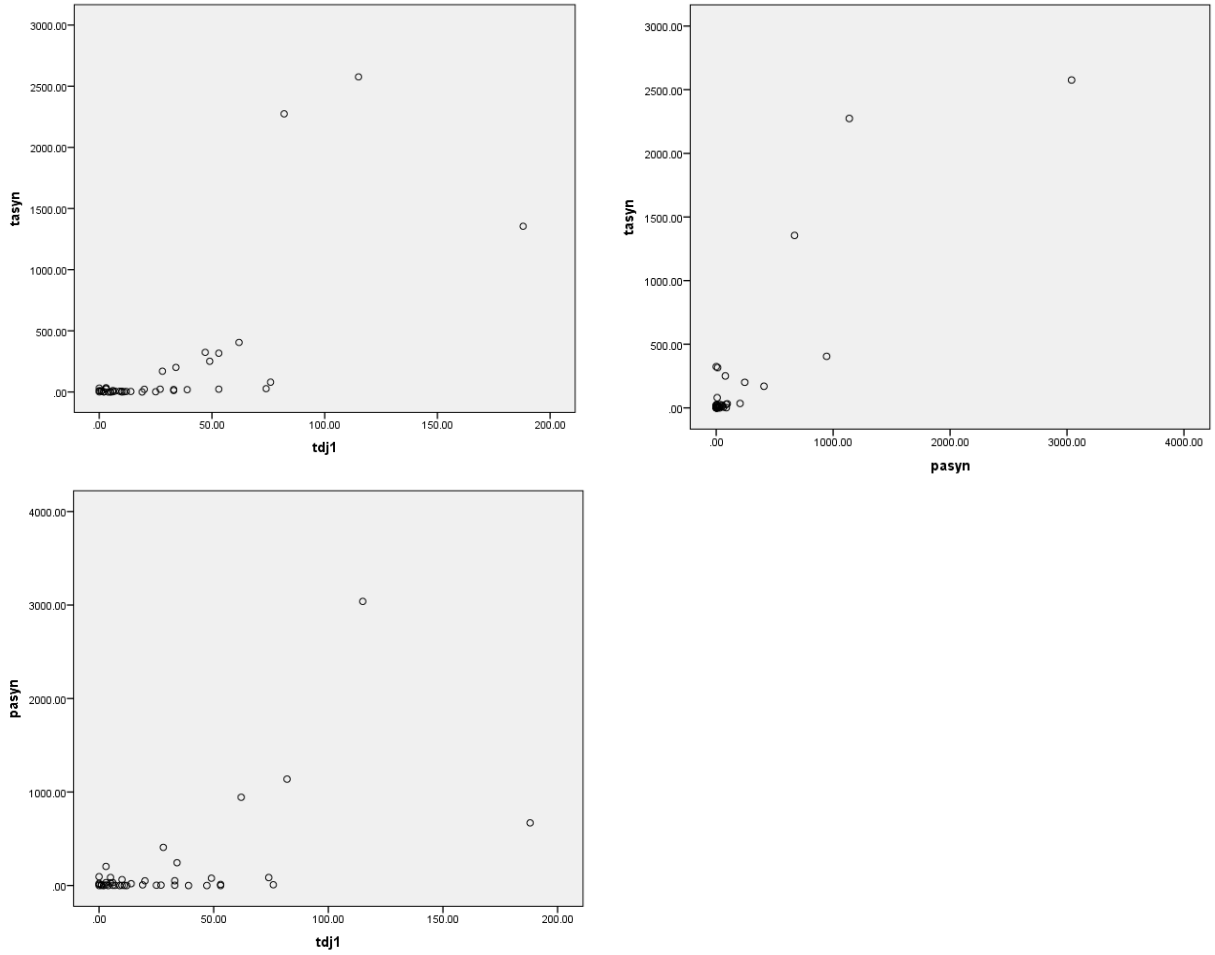

Figure 6.4: GMNC and UCL plasma sample correlation; AD only: *scatter plot depicting the spearman rank correlation.*

		Plasma tαsyn	Plasma tDJ-1	Plasma pαsyn
Plasma tαsyn	Correlation coefficient	na	0.550	0.355
	Sig (2 tailed)	na	0.000	0.008
	N	55	55	55
Plasma tDJ-1	Correlation coefficient	0.550	na	0.234
	Sig (2 tailed)	0.000	na	0.083
	N	55	55	55
Plasma pαsyn	Correlation coefficient	0.355	0.234	na
	Sig (2 tailed)	0.008	0.083	na
	N	55	55	55

Table 6.10: GMNC and UCL plasma sample correlation; PD only: *spearman rank statistical data obtained from IBM SPSS Statistics 21 package*

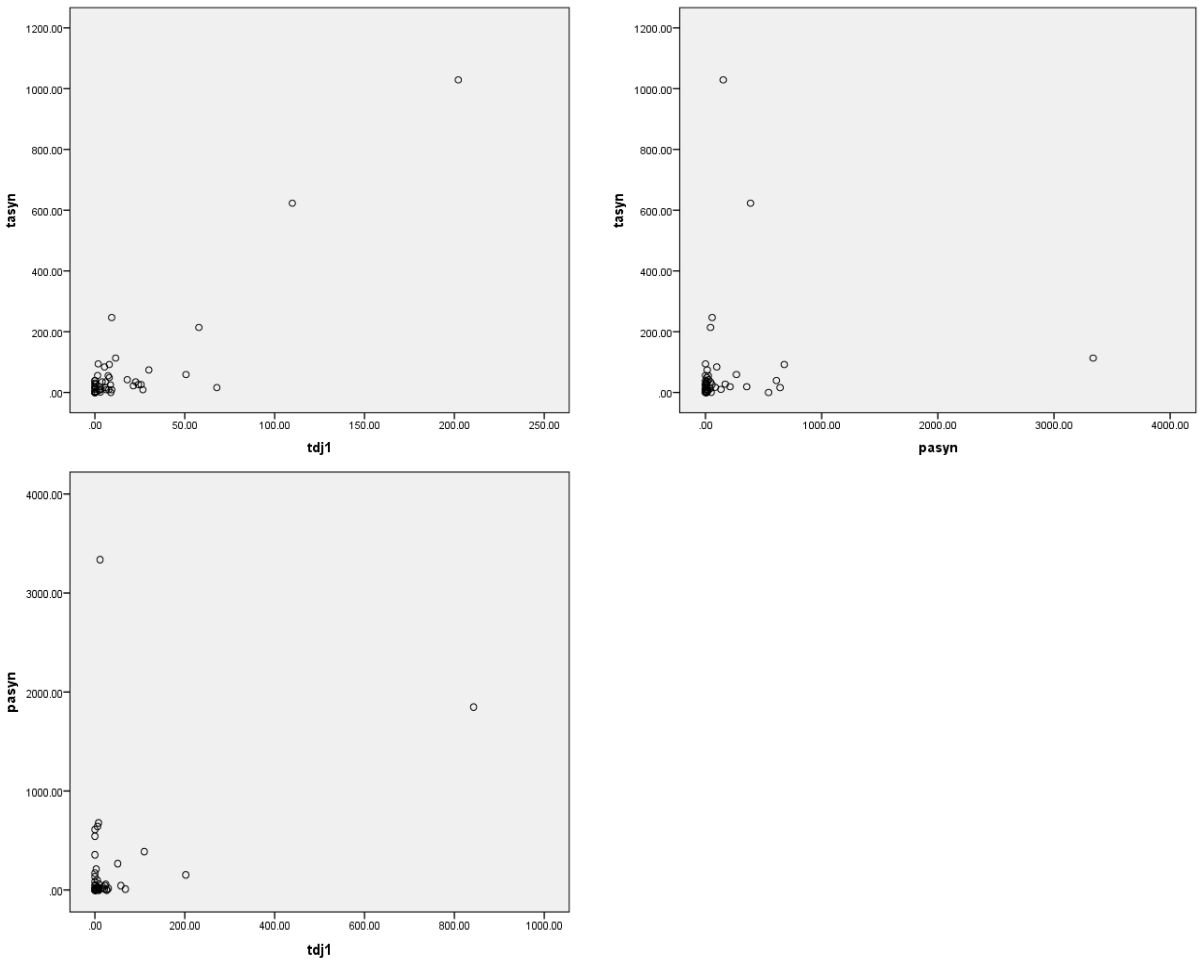

Figure 6.5: GMNC and UCL plasma sample correlation; PD only: *scatter plot depicting the spearman rank correlation.*

		Plasma tαsyn	Plasma tDJ-1	Plasma pαsyn
Plasma tαsyn	Correlation coefficient	na	0.725	0.332
	Sig (2 tailed)	na	0.000	0.026
	N	45	45	45
Plasma tDJ-1	Correlation coefficient	0.725	na	0.294
	Sig (2 tailed)	0.000	na	0.050
	N	45	45	45
Plasma pαsyn	Correlation coefficient	0.332	0.294	na
	Sig (2 tailed)	0.026	0.050	na
	N	45	45	45

Table 6.11: GMNC and UCL plasma sample correlation; DLB only: *spearman rank statistical data obtained from IBM SPSS Statistics 21 package*

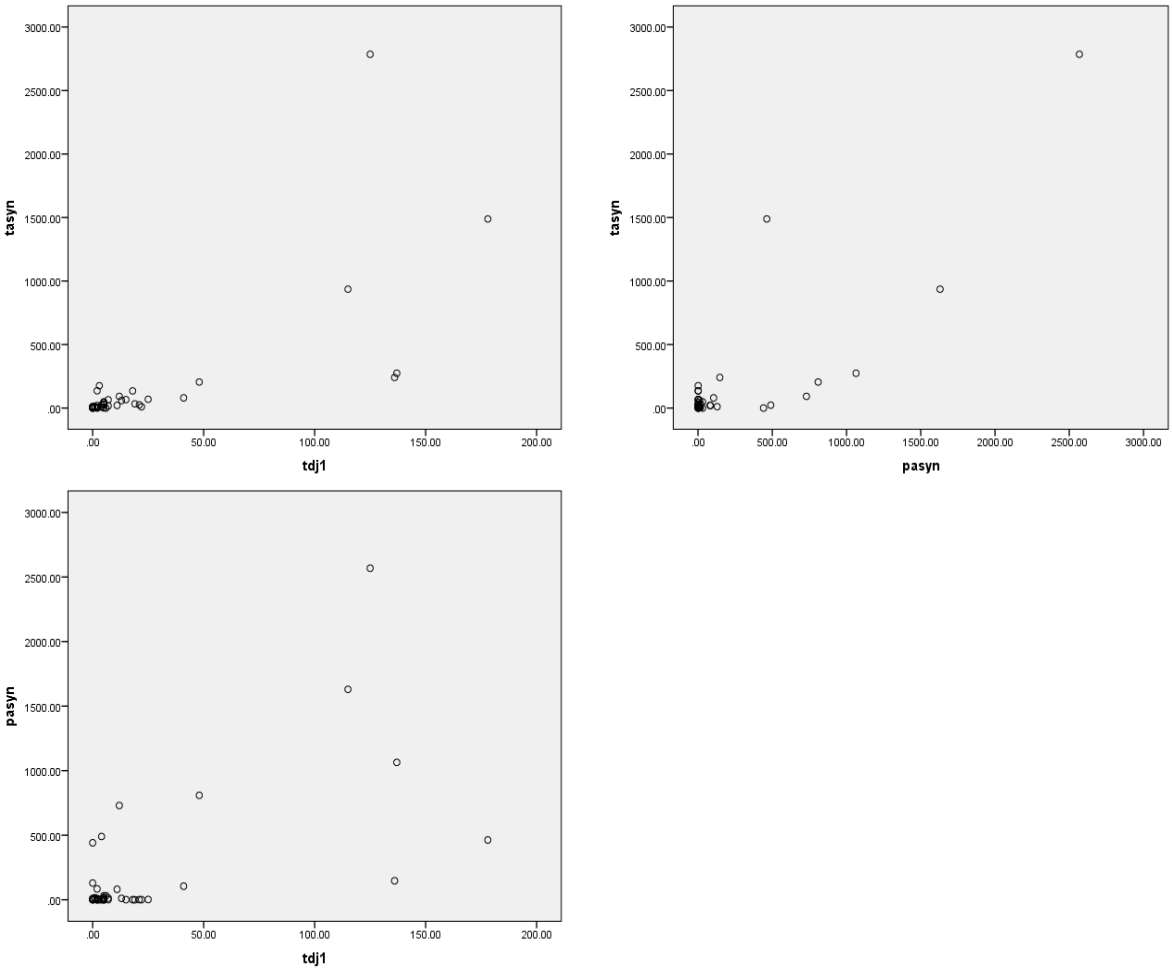

Figure 6.6: GMNC and UCL plasma sample correlation; DLB only: *scatter plot depicting the spearman rank correlation.*

		Plasma tαsyn	Plasma tDJ-1	Plasma pαsyn
Plasma tαsyn	Correlation coefficient	na	0.510	0.468
	Sig (2 tailed)	na	0.002	0.006
	N	33	33	33
Plasma tDJ-1	Correlation coefficient	0.510	na	0.107
	Sig (2 tailed)	0.002	na	0.554
	N	33	33	33
Plasma pαsyn	Correlation coefficient	0.468	0.107	na
	Sig (2 tailed)	0.006	0.554	na
	N	33	33	33

Table 6.12: GMNC and UCL plasma sample correlation; MSA only: *spearman rank statistical data obtained from IBM SPSS Statistics 21 package*

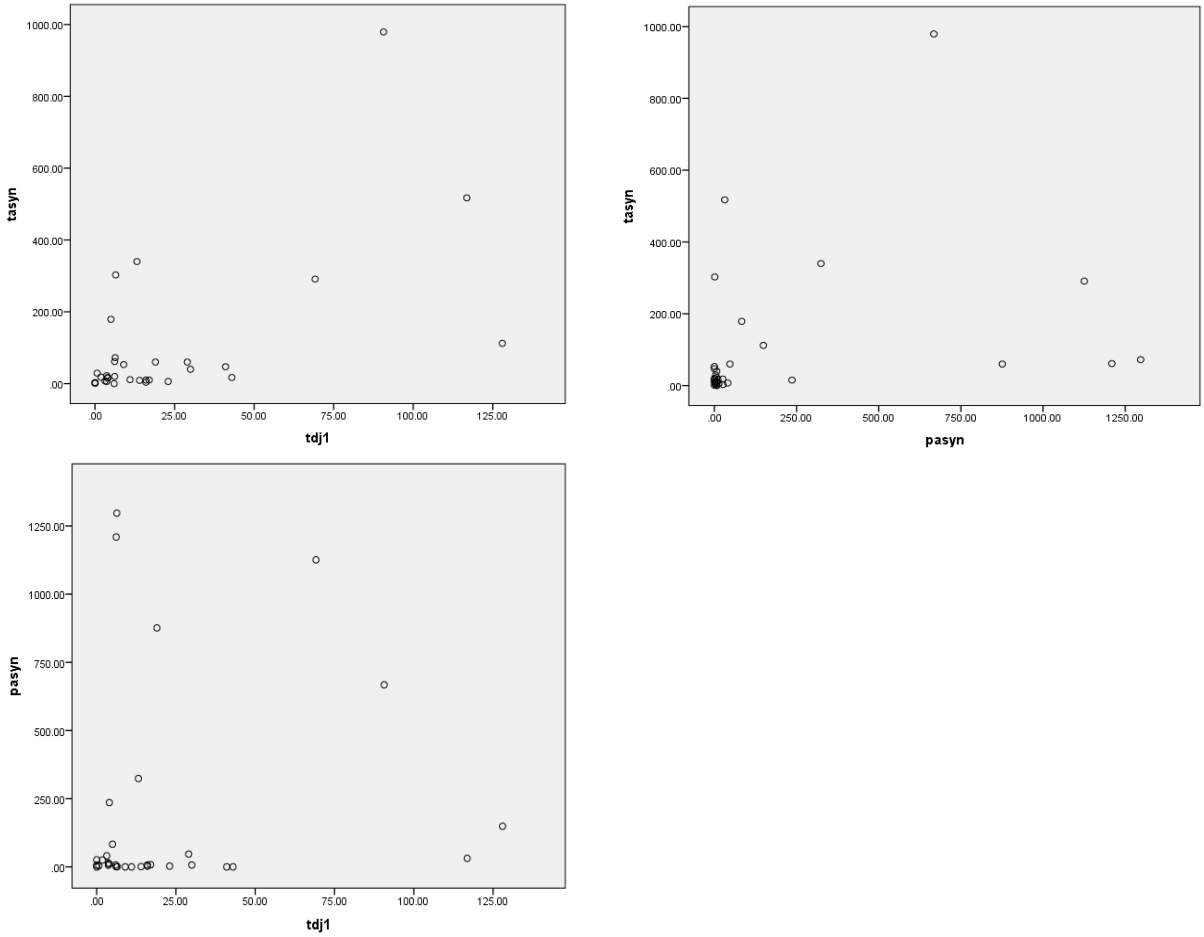

Figure 6.7: GMNC and UCL plasma sample correlation; MSA only: *scatter plot depicting the spearman rank correlation.*

		Plasma tαsyn	Plasma tDJ-1	Plasma pαsyn
Plasma tαsyn	Correlation coefficient	na	0.443	0.618
	Sig (2 tailed)	na	0.002	0.000
	N	45	45	45
Plasma tDJ-1	Correlation coefficient	0.443	na	0.418
	Sig (2 tailed)	0.002	na	0.004
	N	45	45	45
Plasma pαsyn	Correlation coefficient	0.618	0.418	na
	Sig (2 tailed)	0.000	0.004	na
	N	45	45	45

Table 6.13: GMNC and UCL plasma sample correlation; PSP only: *spearman rank statistical data obtained from IBM SPSS Statistics 21 package*

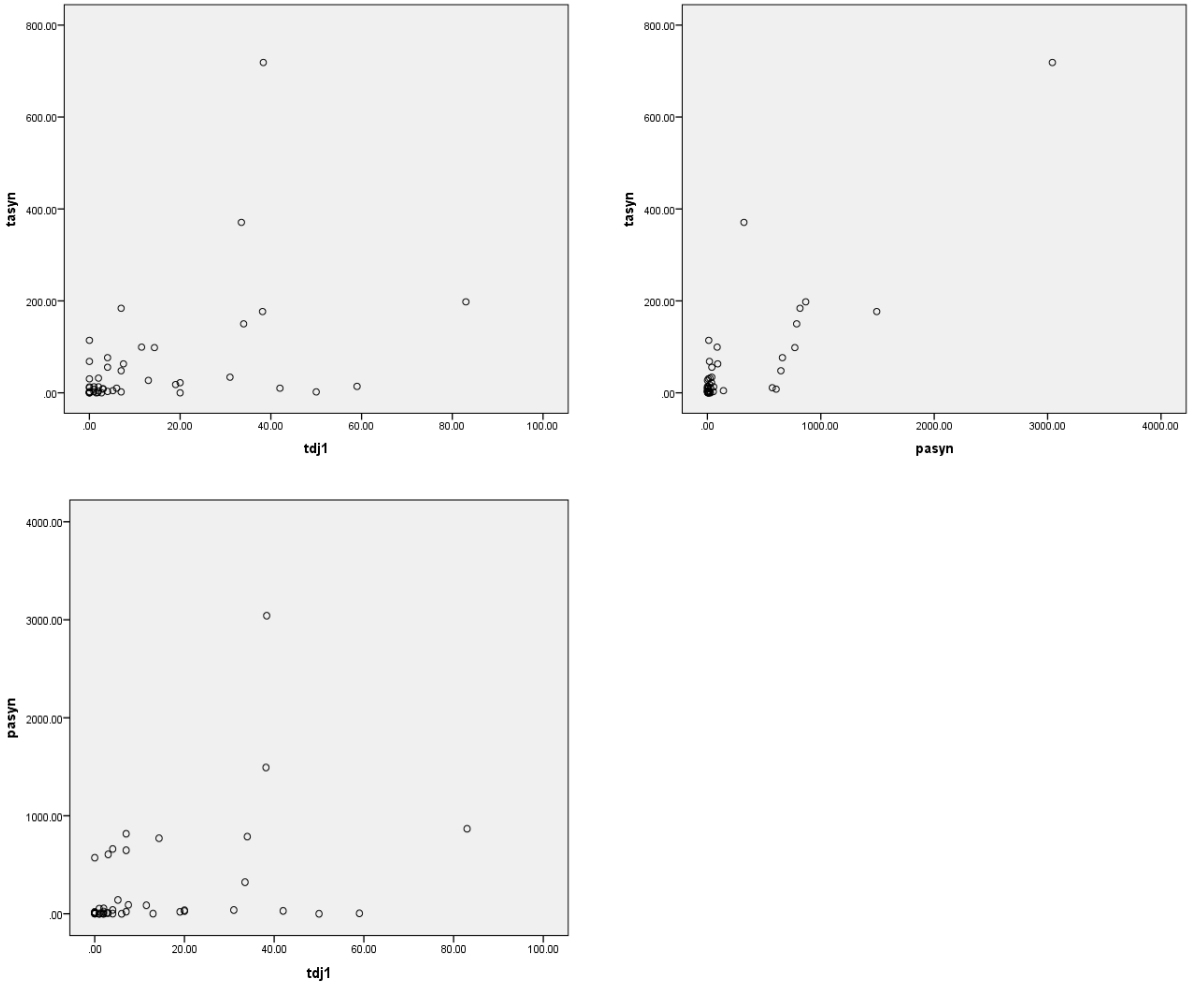

Figure 6.8: GMNC and UCL plasma sample correlation; PSP only: *scatter plot depicting the spearman rank correlation.*

		Plasma tαsyn	Plasma tDJ-1	Plasma pαsyn
Plasma tαsyn	Correlation coefficient	na	0.413	0.614
	Sig (2 tailed)	na	0.088	0.007
	N	18	18	18
Plasma tDJ-1	Correlation coefficient	0.413	na	0.645
	Sig (2 tailed)	0.088	na	0.004
	N	18	18	18
Plasma pαsyn	Correlation coefficient	0.614	0.645	na
	Sig (2 tailed)	0.007	0.004	na
	N	18	18	18

Table 6.14: GMNC and UCL plasma sample correlation; CBS only: *spearman rank statistical data obtained from IBM SPSS Statistics 21 package*

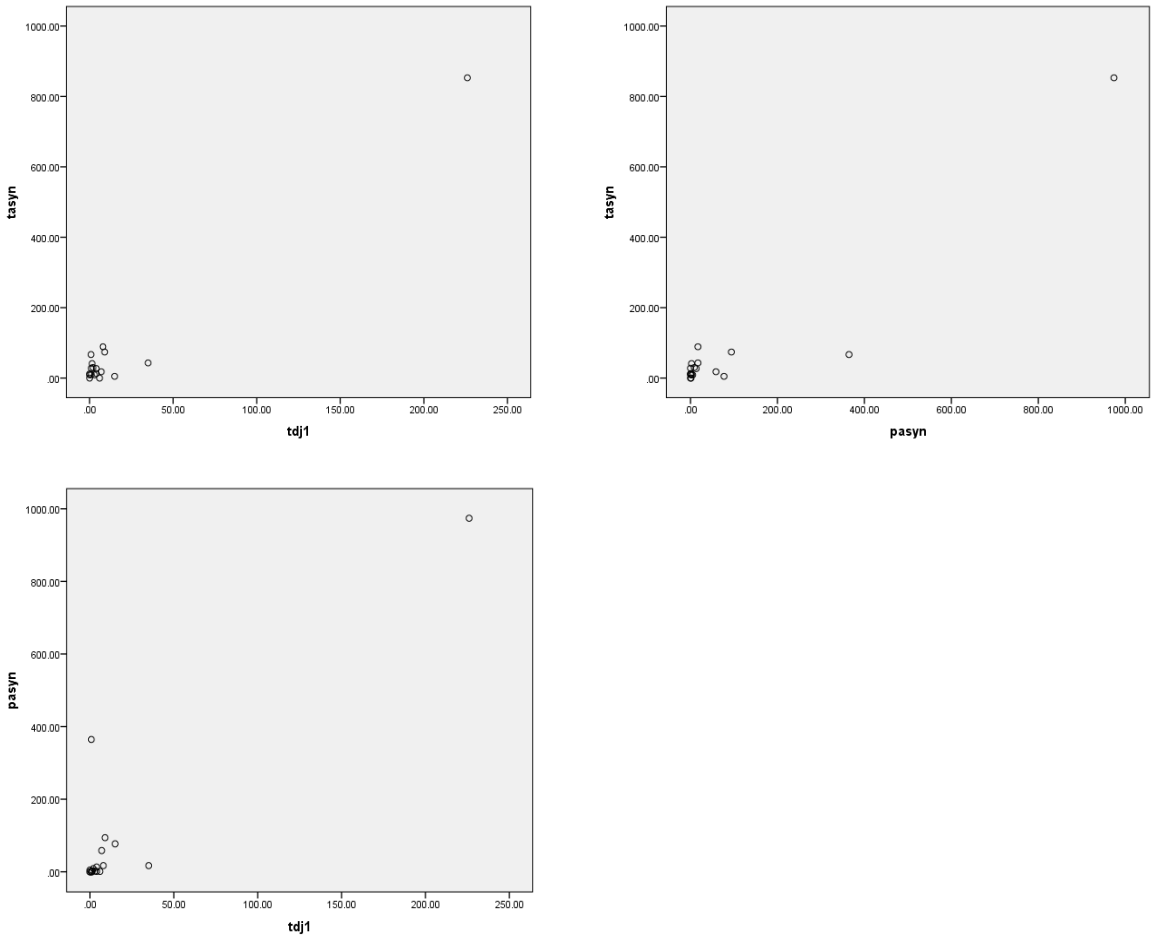

Figure 6.9: GMNC and UCL plasma sample correlation; CBS only: *scatter plot depicting the spearman rank correlation.*

		Plasma tαsyn	Plasma tDJ-1	Plasma pαsyn
Plasma tαsyn	Correlation coefficient	na	0.629	0.587
	Sig (2 tailed)	na	0.000	0.000
	N	72	72	72
Plasma tDJ-1	Correlation coefficient	0.629	na	0.275
	Sig (2 tailed)	0.000	na	0.019
	N	72	72	72
Plasma pαsyn	Correlation coefficient	0.587	0.275	na
	Sig (2 tailed)	0.000	0.019	na
	N	72	72	72

Table 6.15: GMNC and UCL plasma sample correlation; HC only: *spearman rank statistical data obtained from IBM SPSS Statistics 21 package*

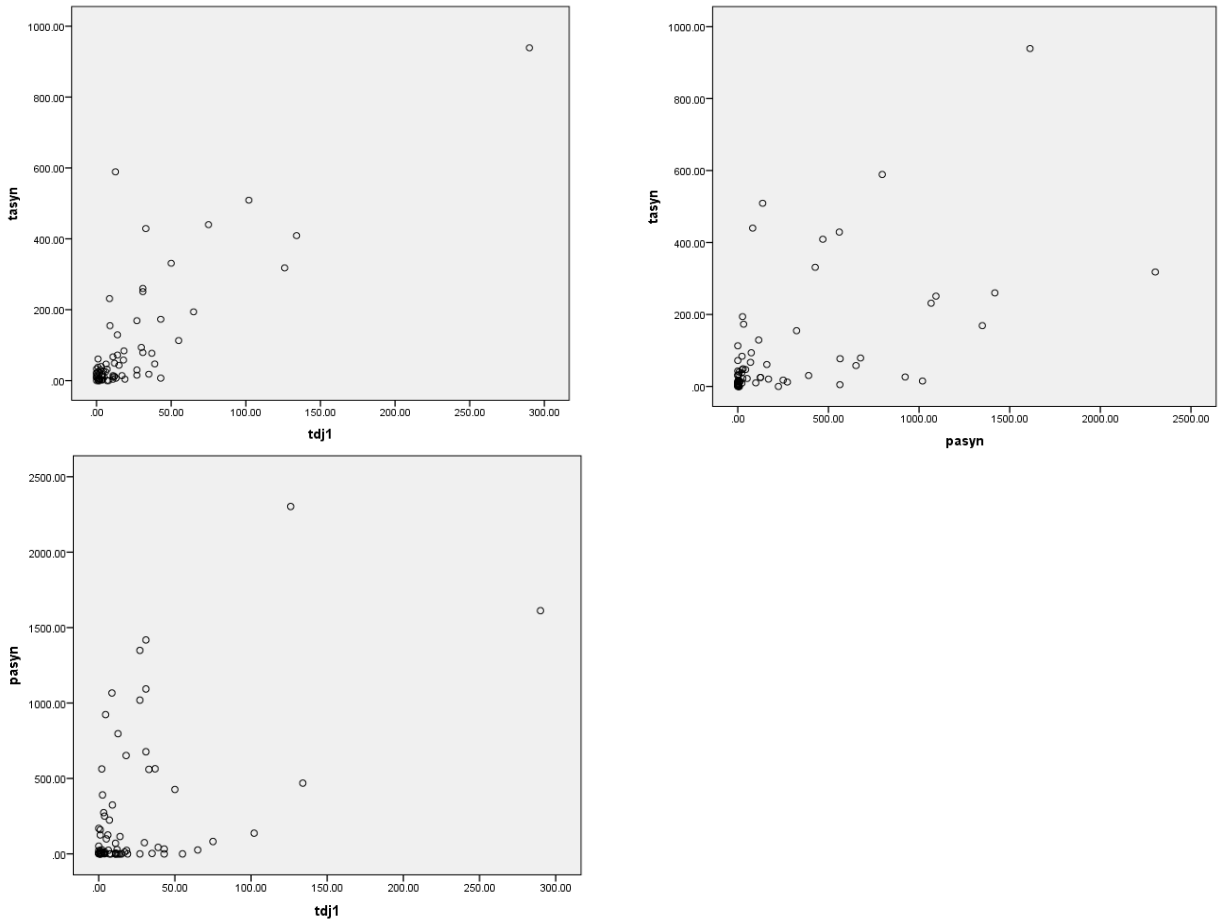

Figure 6.10: GMNC and UCL plasma sample correlation; HC only: *scatter plot depicting the spearman rank correlation.*

A significant correlation (p=<0.05) was found between plasma total α-synuclein and plasma total DJ-1 levels in all disease groups except CBS. All disease groups also showed a significant positive correlation between plasma levels of total α-synuclein and phosphorylated α-synuclein. Correlation between total DJ-1 and phosphorylated α-synuclein was statistically insignificant for AD, PD, DLB and MSA but significant in PSP, CBS and HC groups.

6.5 Total α-synuclein levels in CSF samples

CSF samples obtained from UCL were analysed for levels of total α-synuclein using the Luminex duplex assay. Total α-synuclein levels for all samples analysed were below the assays limit of detection and were thus non detectable.

6.6 Total DJ-1 levels in CSF samples

Total DJ-1 levels were detectable in the CSF samples from UCL and underwent statistical analysis as per the plasma samples, i.e. K-W post Kolgomorov-Smirnov test.

Tables 6.16 summarises the data.

Disease group	n	tDJ-1 mean (ng/mL)	tDJ-1 median (ng/mL)	SD
PD+DLB	17	2.4	2.0	1.4
MSA	17	2.3	2.0	1.7
PSP+CBS	28	1.3	1.3	0.8
Healthy controls	19	2.5	1.6	1.9

Table 6.16: CSF samples from UCL data summary: *mean, median and SD calculated using Microsoft Excel 2010. Each sample was analysed in triplicate.*

Total DJ-1 levels in CSF were significant (p=0.021), as per K-W test. In order to assess whether this significance was confined to a particular disease group or all disease groups, Mann-Whitney tests were performed. The data from this test is summarised in Table 6.17.

	HC	PD+DLB	MSA	PSP+CBS
HC	na	0.59	0.86	0.011
PD+DLB	0.59	Na	0.88	0.010
MSA	0.86	0.88	na	0.024
PSP+CBS	0.011	0.010	0.024	na

Table 6.17: Mann Whitney p-values for total DJ-1 levels in CSF samples from UCL data: *p-values <0.05 are shaded in grey.*

Total DJ-1 levels in CSF were significantly lower in PSP+CBS individuals compared to those categorised in the MSA, PD+DLB and HC groups (p = 0.024, 0,010 and 0,011, respectively).

6.7 Correlation between total α-synuclein, total DJ-1 and phosphorylated α-synuclein in CSF samples

The data obtained from analysing the CSF samples from UCL for total DJ-1 and total α-synuclein using the duplex assay, and phosphorylated α-synuclein using the singleplex assay described in Chapters 3 and 4, were combined and tested for correlation using the non-parametric Spearman rank test.

Table 6.18 and Figure 6.11 present the statistical data.

		CSF tDJ-1	CSF pαsyn
CSF tDJ-1	Correlation coefficient	na	-0.29
	Sig (2 tailed)	na	0.787
	N	89	89
CSF pαsyn	Correlation coefficient	-0.29	na
	Sig (2 tailed)	0.787	na
	N	89	89

Table 6.18: UCL CSF sample correlation; all disease groups: *spearman rank statistical data obtained from IBM SPSS Statistics 21 package correlating CSF tDJ-1 vs pαsyn.*

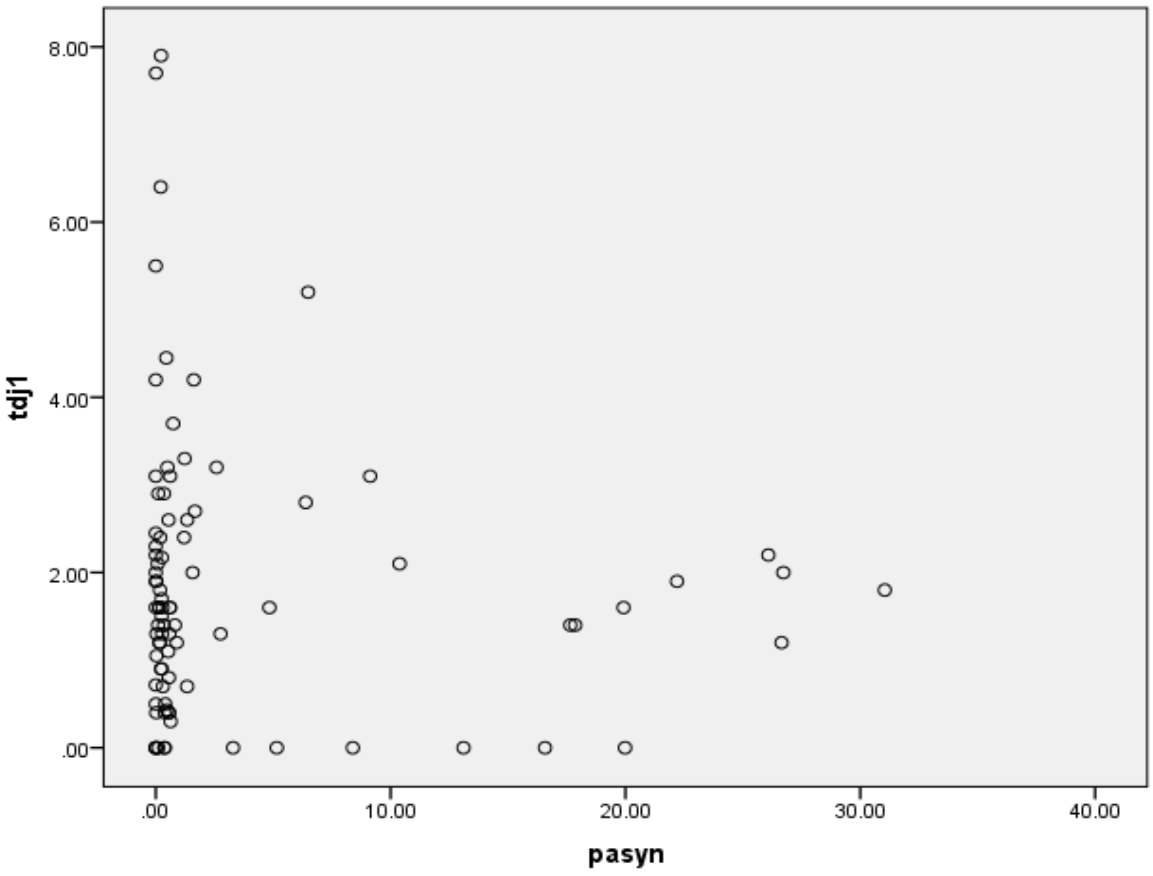

Figure 6.11: UCL CSF sample correlation; all disease groups: *scatter plot depicting the spearman rank correlation for tDJ-1 vs pαsyn.*

There was no significant correlation between levels of total DJ-1, total α-synuclein and phosphorylated α-synuclein in CSF.

6.8 Correlation between total DJ-1 in plasma versus matched CSF samples

The availability of matched plasma and CSF samples from UCL, allowed us to investigate whether levels of plasma total DJ-1 and CSF total DJ-1 within a particular individual correlated. This was initially determined by combining the data obtained for all individuals regardless of their disease group. The data set was checked for normality using the Kolgomorov-Smirnov test and was found to be non-normally distributed. Therefore, the Spearman rank correlation test was adopted to test for any correlation between the plasma and CSF data (Table 6.19; Figure 6.12).

The correlation was insignificant between plasma total DJ-1 and CSF total DJ-1 (p=0.514).

		CSF tDJ-1	Plasma tDJ-1
CSF tDJ-1	Correlation coefficient	na	0.074
	Sig (2 tailed)	na	0.514
	N	81	81
Plasma tDJ-1	Correlation coefficient	0.074	NA
	Sig (2 tailed)	0.514	na
	N	81	81

Table 6.19: Matched plasma vs CSF samples from UCL tDJ-1 correlation: *spearman rank statistical data obtained from IBM SPSS Statistics 21 package.*

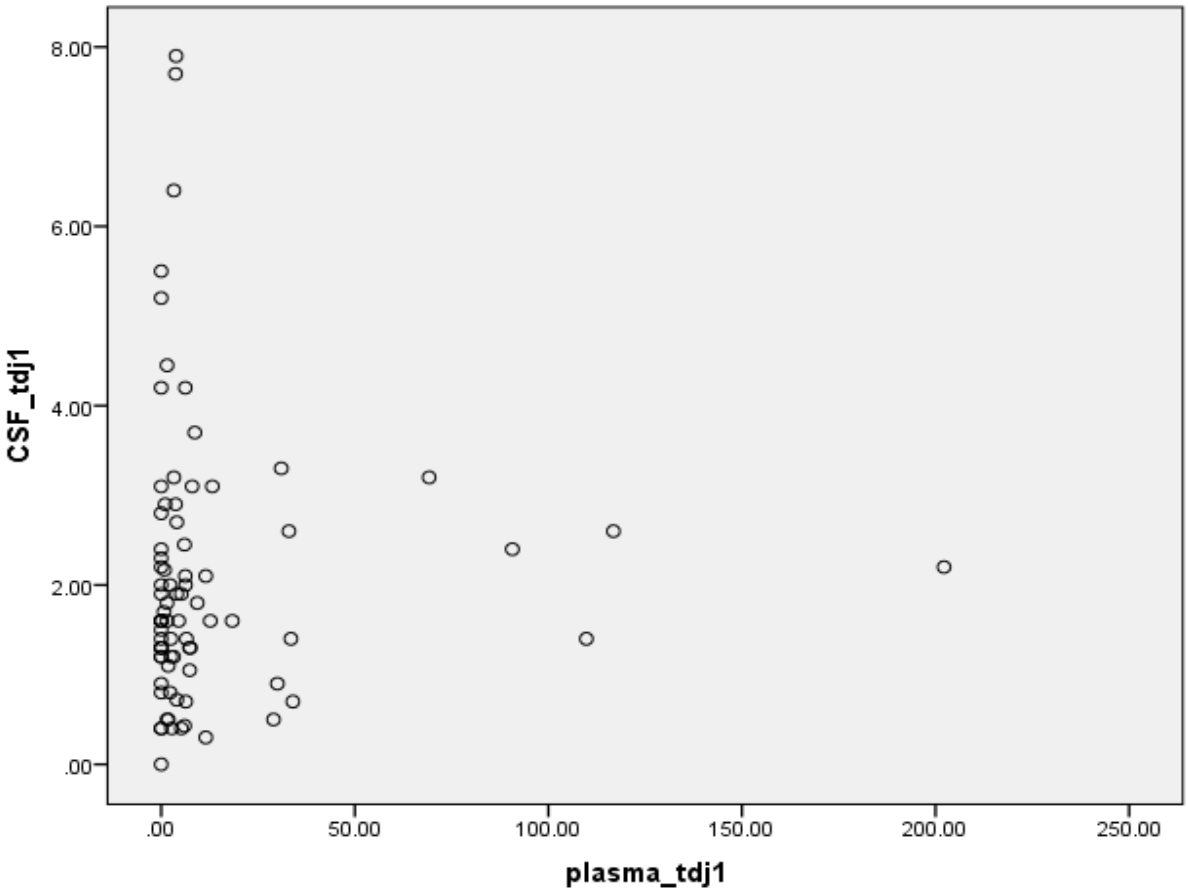

Figure 6.12: Scatter plot for matched plasma vs CSF samples: *total DJ-1 levels in plasma vs CSF*

A correlation test for total α-synuclein was not possible due to levels being undetectable in CSF.

6.9 Total α-synuclein: total DJ-1: phosphorylated α-synuclein ratio assessment

Studies by Wang *et al* (2012) suggested that a ratio between total α-synuclein:phosphorylated α-synuclein in CSF may serve as a better biomarker than the two proteins on their own. In this study, we investigated whether this idea can be adopted for plasma and whether calculating a ratio with plasma total DJ-1 levels carry diagnostic potential.

A ratio for each sample analysed was calculated for total α-synuclein:phosphorylated α-synuclein, total α-synuclein:total DJ-1 and phosphorylated α-synuclein:total DJ-1 levels. The non-parametric K-W test was performed for each ratio assessment to deduce if these values were significantly different between the disease groups and healthy controls. Table 6.20 summarises the data found.

Parameter assessed	p-value by K-W test
phosphorylated α-synuclein : total α-synuclein	0.345
phosphorylated α-synuclein : total DJ-1	0.231
total α-synuclein : total DJ-1	0.098

Table 6.20: Plasma Ratio assessment: *ratio calculated for each plasma sample anlaysed and p-value obtained from K-W test (n=311)*

The ratio assessment was carried out for the CSF samples that were analysed too. Only the ratio between phosphorylated α-synuclein:total DJ-1 was performed, due to total α-synuclein levels being non detectable with our assay. The K-W test showed that there was a significant difference between the different disease groups. Thus, Mann-Whitney tests were performed (see Table 6.21).

	HC	MSA	PD+DLB	PSP+CBS
HC	na	0.224	0.000	0.025
MSA	0.224	Na	0.000	0.225
PD+DLB	0.000	0.000	na	0.033
PSP+CBS	0.025	0.225	0.033	na

Table 6.21: CSF Ratio assessment: *phosphorylated α-synuclein:total DJ-1 ratio Mann-Whitney test. Grey shaded boxes indicate significant p-values <0.05*

Calculating the ratio between phosphorylated α-synuclein and total DJ-1 levels showed a significant difference between PD+DLB, PSP+CBS vs the control group, MSA vs PD+DLB and PSP+CBS vs PD+DLB.

6.10 Longitudinal study: total α-synuclein and total DJ-1

Plasma samples collected longitudinally (every 4 – 6 months for up to 4 years) for PD patients have been analysed using the duplex assay. A total of six individuals were analysed. Figures 6.13 and 6.14 display the data obtained for plasma total α-synuclein and plasma total DJ-1, respectively.

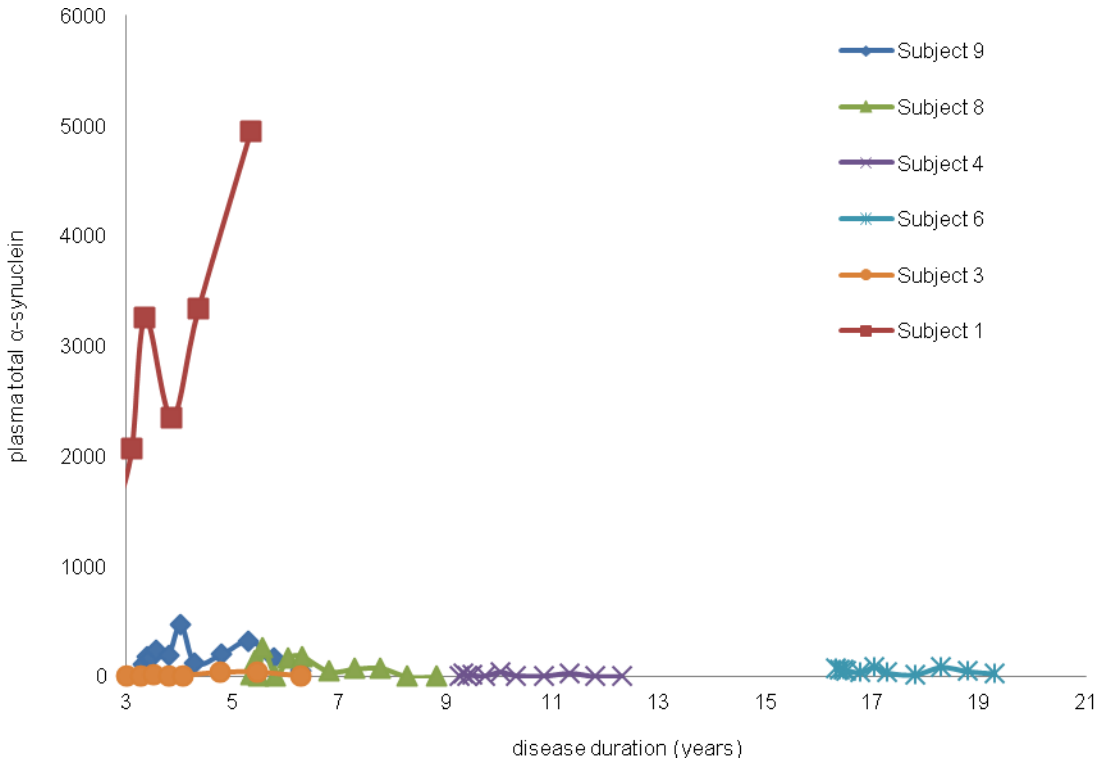

Figure 6.13: Longitudinal plasma total α-synuclein: *longitudinal samples from six PD individuals analysed using the duplex assay. Levels of total α-synuclein analysed at each time point and plotted against the duration of disease for each individual.*

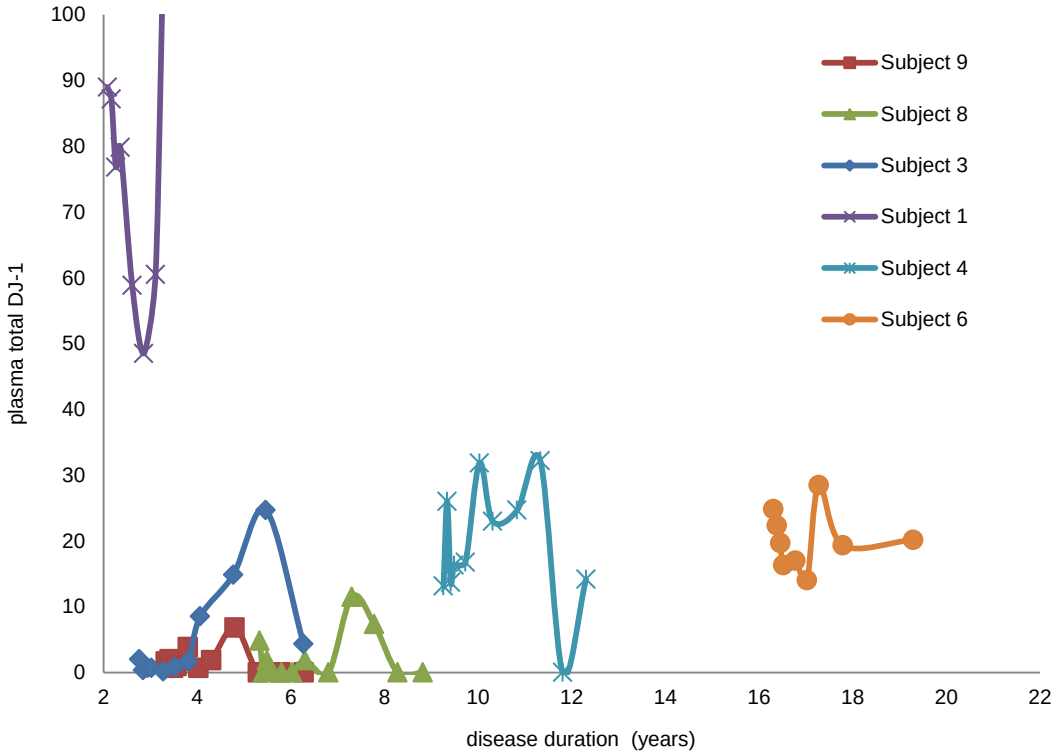

Figure 6.14: Longitudinal plasma total DJ-1: *longitudinal samples from six PD individuals analysed using the duplex assay. Levels of total DJ-1 analysed at each time point and plotted against the duration of disease for each individual.*

There was not enough data in order to generate meaningful statistical data, but a spearman correlation test was performed on the data collected to see if the protein levels correlated with disease duration. There was no significant difference for the total DJ-1 levels but there was a significant difference for total α-synuclein ($p = 0.02$). A correlation between total α-synuclein and total DJ-1 levels in the longitudinal samples was also tested and this generated a p value of < 0.05.

6.11 Discussion

This chapter summarised the data from the analysis of total α-synuclein and total DJ-1 in plasma and CSF collected from individuals with different neurodegenerative disorders as well as healthy controls.

The role and scientific relevance of α-synuclein, with regards to neurodegenerative disorders, has already been discussed (see chapter 4). Table 4.12 of chapter 4, summarises the studies performed so far on plasma total α-synuclein and its potential use as a diagnostic biomarker for neurodegenerative disorders. Present data displayed in this chapter show that there was no significant difference in the levels of plasma total α-synuclein between AD, PD, DLB, MSA, PSP and the control group. These findings disagree with those published by Lee *et al* (2006c), Duran *et al* (2010), who reported increased levels in PD and MSA vs HC and Li *et al* (2007) who found decreased plasma total α-synuclein levels between PD and HC. The disagreement may be attributed to the different analytical methodologies utilised by these various research groups i.e. ELISA and Western blot vs Luminex. This argument is reinforced by the fact that the data presented here does agree with that presented by Shi *et al* (2012), and that both of these sets of results are dependent on the use of a Luminex bead based assay for sample analysis.

Unfortunately, in the present study, total α-synuclein levels were not detectable in CSF. This may be due to the assay format utilised, since other research groups have reported successful detection of the molecule in CSF (see Chapter 4, Table 4.11). It is best practise to use a calibrator diluent that closely matches the samples to be analysed. Unfortunately, for the CSF duplex assay, a matrix-based diluent was not available and this compromised the assay's accuracy and may have resulted in matrix effects that affected the detection of total α-synuclein in the CSF samples. Furthermore, in an attempt to decrease such matrix effects, the assay utilised here involved diluting the samples x5 prior to analysis. Close examination of other research groups' methods of analysis reveals that the CSF samples were either analysed neat (no dilution), or at the most diluted x2. Thus, another plausible reason

for the present assay not detecting any total α-synuclein in CSF is that the analyte/protein may have been diluted out to below the detection limit.

The interest in DJ-1 has intensified as the role of oxidative stress in neurodegenerative disorders has become more apparent (Zondler *et al*, 2014; Ariga *et al*, 2013; Dias *et al*, 2013). A few studies have already investigated the potential use of total DJ-1 in plasma and CSF as a biomarker. Tables 6.22 and 6.23 summarize the findings from other research groups, which show that no clear picture has yet emerged.

Research group	**No. of samples studied**	**Methodology for quantification**	**Summary of findings**
Waragai *et al* (2007)	PD = 104 DLB = 30 HC = 80	ELISA Immunohistochemistry	Increased levels in PD vs controls Increased levels in DLB vs controls
Shi *et al* (2010)	PD = 126 AD = 33 HC = 122	Luminex	No significant difference
Maita *et al* (2008)*	PD = 95 HC = 70 Others = 30	ELISA	No significant difference

Table 6.22: Summary of studies investigating the use of total DJ-1 levels in plasma as a biomarker for neurodegenerative disorders: **Maita et al (2008) used serum for their analysis.*

Research group	No. of samples studied	Methodology for quantification	Summary of findings
Waragai *et al* (2006)	PD = 40 HC = 38	Immunoblot	Increased levels in PD vs controls
Hong *et al* (2010)	PD = 117 AD = 50 HC = 122	Luminex	Decreased levels in PD compared to AD and controls
Herbert *et al* (2014)	PD = 43 MSA = 23 HC = 30	ELISA	Increased levels in PD vs controls and even higher in patients with MSA

Table 6.23: Summary of studies investigating the use of total DJ-1 levels in CSF as a biomarker for neurodegenerative disorders

The data presented in this chapter show that the median total DJ-1 levels in plasma are lower in PD patients in comparison to MSA, AD and the control groups. This is also the case for the PSP versus MSA, AD and control groups. This data does not agree with the other research groups. However, Shi *et al* (2010), who used the Luminex methodology have noted in their publication that although there was no significant difference between the PD, AD and controls, there was a trend of total DJ-1 levels being lower in the PD and AD groups compared to the controls.

The observed decrease in plasma total DJ-1 levels in PD and PSP groups may be given two possible explanations. Oxidative stress is a reputable reason for the degeneration of neurones observed in neurodegenerative disorders. Organisms have developed adaptive responses to counteract the damage caused by oxidative stress (Dias *et al*, 2013). The main role of DJ- 1 is to protect against oxidative stress. Thus, the low DJ-1 levels in individuals with PD and PSP, suggest that such individuals may have failed to develop a DJ-1 mediated adaptive response against

oxidative stress. There have been reports that α-synuclein aggregates contain large complexes of DJ-1 (Meulener *et al*, 2005), which is further supported by the findings that DJ-1 interacts with α-synuclein directly (Zondler *et al*, 2014). Therefore the low levels may be due to the fact that the DJ-1 is sequestered within the aggregates in PD and PSP individuals.

This is the first report in which the potential use of plasma total DJ-1 as a differentiation marker between MSA and other neurodegenerative disorders as well as healthy controls has been investigated. This is therefore the first study to find that plasma total DJ-1 levels carry the potential to differentiate between patients with PD and MSA. This is an important finding, since MSA and PD are both very clinically similar and a diagnostic tool to differentiate between the two would be highly advantageous. However, based on the ROC analysis, there is still scope to improve the use of total DJ-1 as a diagnostic tool; one possible way of increasing the diagnostic value of total DJ-1 is to use it in conjunction with other markers or other methods of diagnosis.

CSF total DJ-1 did not show a significant difference between the PD+DLB, MSA and control groups. Studies by other research groups have reported contradictory results, with Herbert *et al* (2014) reporting high levels in PD as well as MSA patients compared to healthy controls and Hong *et al* (2010) publishing decreased levels in PD patients compared to AD and normal controls. The disparity between current findings and Herbert *et al* (2014) may again be attributed to the different method of analysis utilised; it appears that research groups that have used an ELISA kit as their testing system have reported increased levels of DJ-1 in their test samples. The difference between the data presented in this chapter and by Hong *et al* (2010), may be due to the difference in the number of samples analysed.

Hong *et al* (2010) analysed 117 PD samples, 122 healthy controls and 50 AD samples, which is a much bigger sample pool compared to the number of CSF samples that were available for the study presented in this chapter. CSF total DJ-1 levels were found to be significantly lower in the PSP+CBS group versus the other diseased groups and healthy controls. However, this significant data needs to be approached with caution due to the following reasons:

- Low sample number representing each disease group.
- The lack of a matrix based calibration diluent and sample diluent which compromised the assay accuracy (refer to chapter 5). Using a matrix based diluent would have resulted in a less sensitive assay as evident from the other Luminex based assays developed and described in this thesis. The concentrations of total DJ-1 measured in the CSF samples in this study are very close to the assay LOD (to recall LOD = 1 ng/mL). If a matrix based calibration diluent was utilised for the assay, it is likely that a lot of the samples with currently quantifiable levels of total DJ-1 would be below detection limits, thus affecting the overall significance of the data.

Wang *et al* (2012) mentioned the possibility of using the ratio between CSF total α-synuclein and CSF phosphorylated α-synuclein as a diagnostic tool for differentiating between PD, MSA, PSP patients and healthy controls. Present data unfortunately showed that this is not reproducible when using plasma as the sample matrix. The data has shown that using the ratio between phosphorylated α-synuclein and total DJ-1 levels in CSF carry the potential of differentiating between healthy controls and those classified in the PD+DLB group and PSP+CBS group. The ratio may also differentiate between MSA and PD+DLB as well as PSP+CBS vs the PD+DLB group. However, again this data regarding CSF total DJ-1 levels needs to be approached with caution due to the aforementioned reasons.

Correlation assessments with plasma levels of total α-synuclein, total DJ-1 and phosphorylated α-synuclein have shown positive correlations for all disease groups between phosphorylated α-synuclein vs total α-synuclein and total α-synuclein vs total DJ-1 (latter did not correlate in the CBS group). Interestingly, phosphorylated α-synuclein levels positively correlated with total DJ-1 levels within the PSP, CBS and HC groups but not in the AD, PD, DLB and MSA groups. From these findings we can speculate that DJ-1 works in synergy with non-phosphorylated α-synuclein and not phosphorylated α-synuclein. This is supported by findings from Zondler *et al*, (2014), whose research has found that DJ-1 interacts directly with α-synuclein monomers and oligomers. CSF total DJ-1 and phosphorylated α-synuclein correlations were non-significant as was the correlation between plasma total DJ-1 and CSF total DJ-1, but this data may change as more CSF samples are analysed.

The mini longitudinal study presented in this chapter was not large enough to make valid statistical statements. However, it is worthy to note that the significant difference between the total α-synuclein levels and disease duration was consistent with a previous study performed by Foulds *et al*, 2013, where log transformed total α-synuclein levels have been shown to potentially serve as a disease progression marker. The significant correlation between the two protein levels in the longitudinal samples reinforces the significantly positive correlation found with the one off patient samples already discussed in this chapter.

Chapter 7:

LRRK2 investigation

7.1 Introduction

Mutations in *LRRK2* are the leading cause of both inherited and sporadic PD. Since its discovery in 2004, research has been directed at investigating the role of LRRK2 in neurodegenerative disorders (ND), particularly in PD pathogenesis. Fraser *et al* (2013) showed that LRRK2 is secreted into CSF and has been detected in urine. No research has yet been reported with regards to the possible detection of LRRK2 in plasma. One of the aims of this project was to determine whether LRRK2 could be detected in plasma and CSF and thus deduce if LRRK2 levels carry the potential of being a diagnostic marker.

The first method developed for LRRK2 detection was the Luminex bead based assay system. Western blotting with immunoprecipitation and HPLC was also investigated. This chapter presents the development of the Luminex assay, the data obtained from western blotting and results from the HPLC investigation.

7.2 Luminex assay

Development of the Luminex assays for phosphorylated α-synuclein, total α-synuclein and total DJ-1 showed that carrier free antibodies, i.e. containing no sodium azide or BSA, work best with this assay system. With this in mind two antibodies were selected for the development of the LRRK2 assay:

1. SIG39840; mouse monoclonal antibody; Covance (1 mg/mL)
2. ab133474; rabbit monoclonal antibody; Abcam (0.01 mg/mL)

Both antibodies were tested as a capture reagent and as a detection component, in order to deduce which combination worked the best. Figure 7.1 displays the MFI signals achieved for each combination.

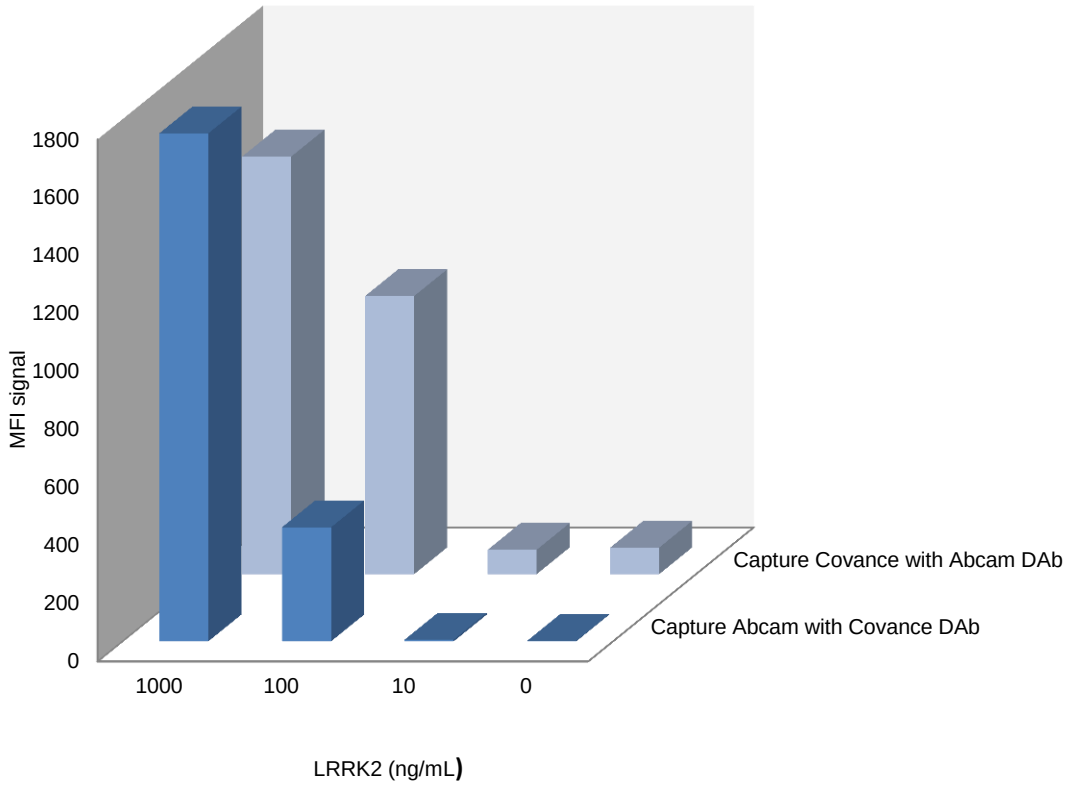

Figure 7.1: Testing different antibody combinations: *Luminex beads coupled with 0.01 µg of each capture Ab were used to capture 1000, 100, 10, and 0 ng/mL of recombinant LRRK2. 2 µg/mL of biotinylated detection Ab and 4 µg/mL of streptavidin-RPE were used as the detection system for the assay. The figure shows the raw MFI signals achieved with the different antibody combinations.*

The Abcam antibody as the capture component and the Covance antibody as the biotinylated detection antibody generated data with the highest signal to noise ratio, due to the low background. Thus, this combination was taken forward in order to optimise the assay.

Optimisation experiments involved bead titration and DAb titration tests.

The bead titration experiment involved using beads captured with 0.005, 0.01, 0.015 and 0.02 µg of the Abcam LRRK2 antibody. Each bead set was then assayed with recombinant LRRK2 protein and 2 µg/mL of the Covance anti-LRRK2 detection antibody. Figure 7.2 display data obtained from the bead titration tests.

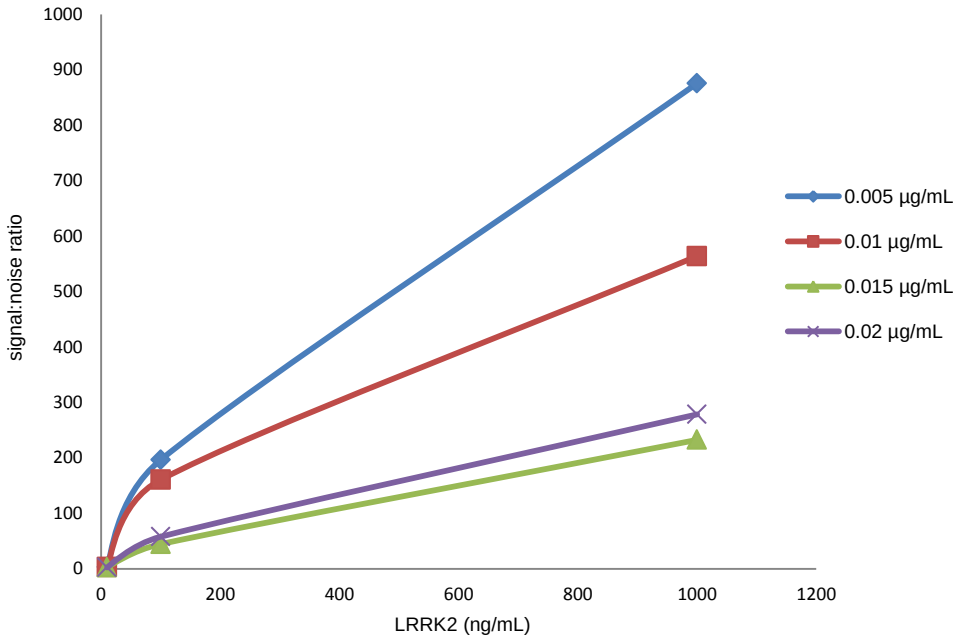

Figure 7.2: Abcam LRRK2 antibody bead titration: *Luminex beads coupled with 0.005, 0.01, 0.015 and 0.02 µg were assayed with 0, 10, 100 and 1000 ng/mL of recombinant LRRK2 protein 2 µg/mL biotinylated detection pAb (Covance) with 4 µg/ml streptavidin-RPE. The figure shows the MFI signals obtained with each bead set at the varying recombinant LRRK2 protein concentrations (n=2)*.

Beads coupled with 0.005 µg of the capture component generated the best signal:noise data. The DAb titration experiment was carried out using these beads. Beads coupled with 0.0025 µg of capture Ab were also tested in order to deduce whether using less capture antibody would further improve assay performance. The DAb titration test was performed with 2 µg/mL and 1 µg/mL of DAb. Figure 7.3 presents the data from this investigation.

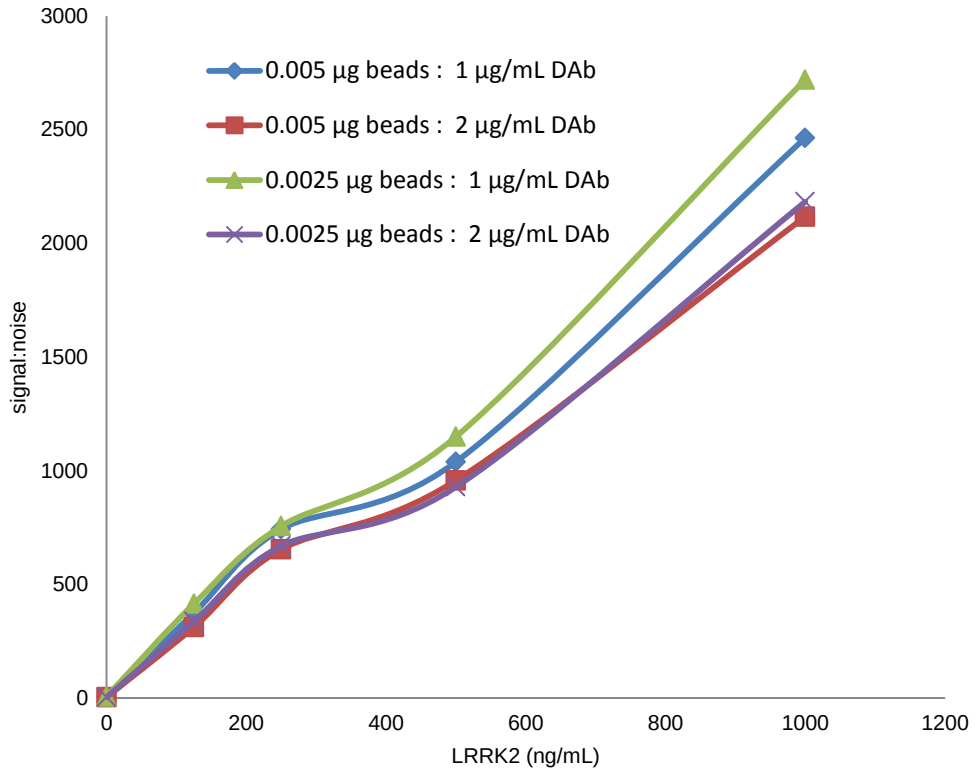

Figure 7.3: Covance LRRK2 antibody DAb titration: *Luminex beads coupled with 0.0025, and 0.005 µg of Abcam LRRK2 antibody were assayed with 1 and 2 µg/mL biotinylated Covance detection antibody with 4 µg/ml streptavidin-RPE, to detect 0, 10, 100 and 1000 ng/mL of recombinant LRRK2 protein. The figure shows the signal:noise ratio obtained with each bead set with varying DAb concentrations (n=2)*.

The best data with regards to signal:noise ratio were obtained with using beads coupled to 0.0025 µg capture Ab, with 1 µg/mL biotinylated DAb. Subsequent experiments were performed using these components.

The original idea was to multiplex this LRRK2 assay with the duplex assay described in chapter 5. The cross reactivity test was performed as described in section 5.8.1, where three tests were performed sequentially. Unfortunately, this LRRK2 assay cross reacted with the duplex assay. Table 7.1 displays the data obtained from this cross reactivity test.

Protein (ng/mL)	multiplexed beads with tDJ-1 DAb			multiplexed beads with tαsyn DAb			multiplexed beads with LRRK2 DAb		
	tαsyn (MFI)	tDJ-1 (MFI)	LRRK2 (MFI)	tαsyn (MFI)	tDJ-1 (MFI)	LRRK2 (MFI)	tαsyn (MFI)	tDJ-1 (MFI)	LRRK2 (MFI)
1000	8	5446	8	9461	8	32	1547	138	7096
	8	5412	7	8581	6	29	1562	132	6836
500	5	2160	5	5692	7	28	104	13	2260
	5	2101	4	6288	7.5	31	116	17	2026
250	4	575	6	1812	6	29	14	5	275
	5	587	5	1766	4	28	14	5	273
0	4	4	6	6	4	26	5	3	5
	4	4	5	6	6	26	4	4	5

Table 7.1: Multiplex cross reactivity test: *multiplex beads comprised of tαsyn, tDJ-1 and LRRK2 beads assayed with individual DAbs specific to each analyte for the detection of recombinant LRRK2. The columns shaded blue indicate the cross reactivity data obtained when using the multiplexed beads with the LRRK2 biotinylated DAb.*

Due to cross reactivity between LRRK2 and the tαsyn/tDJ-1 assays, the LRRK2 assay was used as a singleplex.

Plasma and CSF samples were screened for the presence of LRRK2, using this newly developed Luminex assay The samples screened were taken from healthy individuals as well as individuals with various neurodegenerative diseases.

Figure 7.4 summarises the predicted concentrations of LRRK2 for the plasma samples screened and Figure 7.5 the data obtained from the CSF samples.

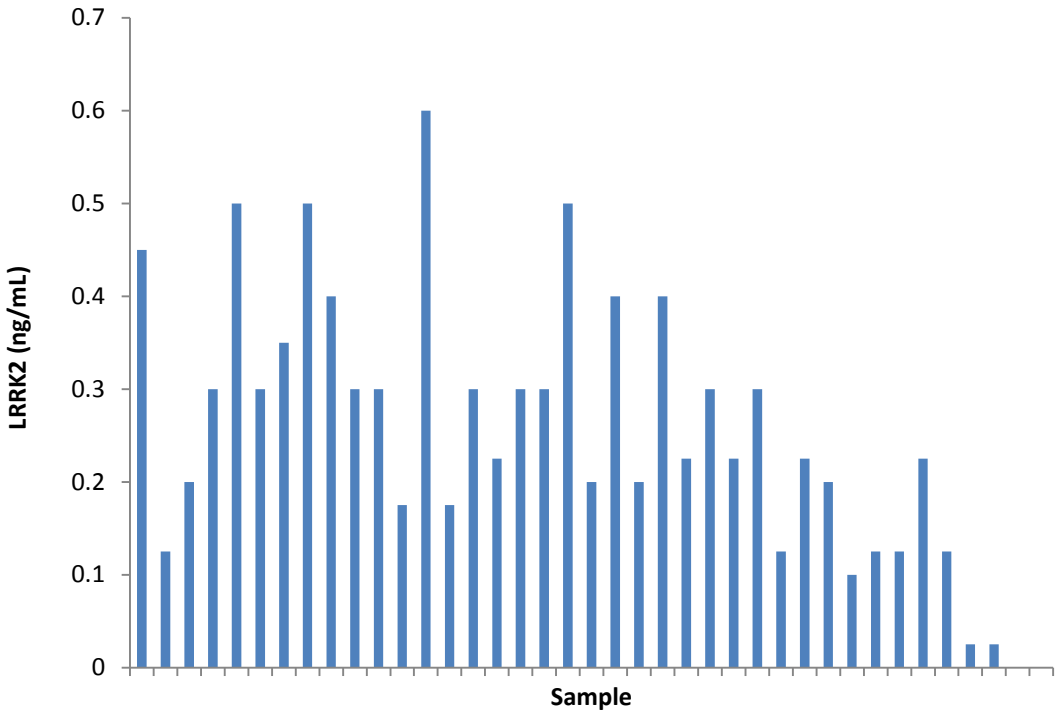

Figure 7.4: CSF LRRK2: *The newly developed Luminex assay was used to screen CSF samples. Each sample was diluted x 5 and analysed in duplicate. The bar chart shows the mean concentration of LRRK2 obtained for each sample.*

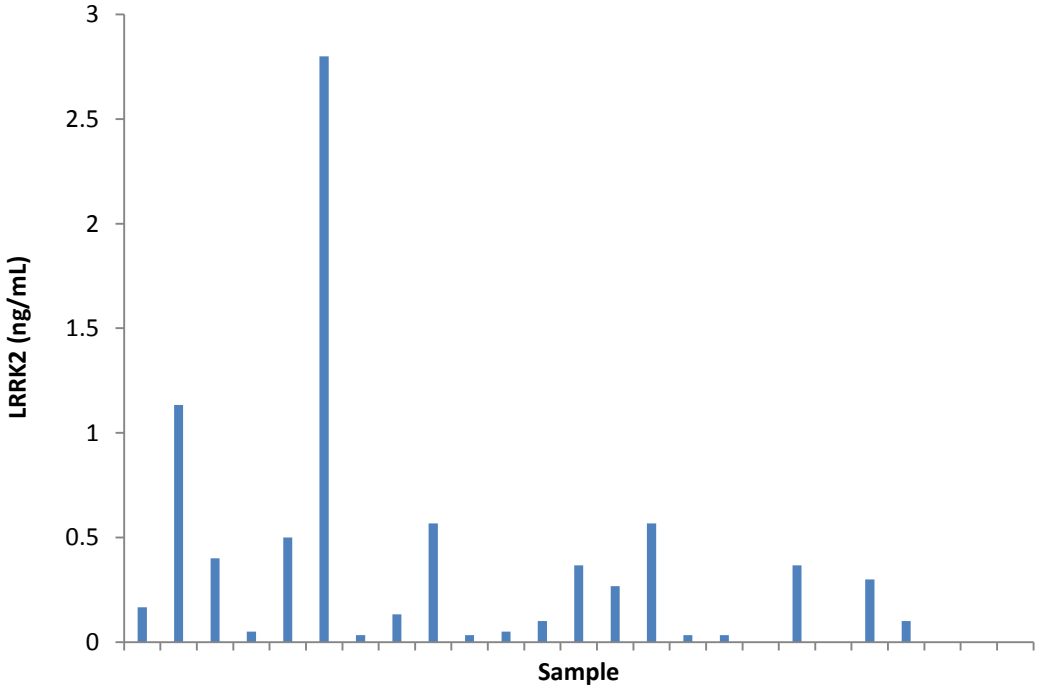

Figure 7.5: Plasma LRRK2: *The Luminex assay was used to analyse plasma samples. Each sample was diluted x 10 and analysed in triplicate. Mean concentrations are displayed.*

The mean CSF LRRK2 was 0.25 ng/mL with std 0.15 and the median 0.225 ng/mL. For plasma LRRK2, the mean was 0.32 ng/mL with std 0.6 and median of 0.1 ng/mL. The LOD of this assay was deduced to be 0.1 ng/mL for CSF and plasma. The values detected for most of the samples screened were lower than the LOD, however, one plasma sample showed a signal that was approximately 30 times above the LOD. In order to deduce whether the Luminex signal for this sample was specific for LRRK2, a spike recovery test was performed.

Blank sample	Sample + 5 ng/mL	Expected (ng/mL)	Sample + 25 ng/mL	Expected (ng/mL)
3.1	7.5	8.1	31.6	28.1

Table 7.2: Spike recovery: *The plasma sample with detectable levels of LRRK2 was spiked with 5 and 25 ng/mL of recombinant LRRK2 protein. The sample with and without spike was analysed in triplicate.*

Spike recovery was 93% and 112% for 5 ng/mL and 25 ng/mL of LRRK2, respectively. The additional increase in LRRK2 concentration upon spiking recombinant LRRK2 into the sample suggests that the value obtained without the spike is specific for the presence of LRRK2, and that the signal was not due to non-specific binding. If the original signal for the sample was due to non-specific binding, the % spike recoveries would have deviated severely (http://www.woongbee.com/0NewHome/RnD/ELISA_HA/Duoset_link/spike_recovery.pdf).

7.3 Western Blot

The Luminex assay system has been reported to be more sensitive than the traditional ELISA technique (Baker *et al*, 2012). However, there are no reports indicating how its performance compares with other techniques such as western blotting. This section displays the data obtained from western blotting 15 plasma and CSF samples that were previously analysed with the Luminex technique. Unfortunately the western blot failed to reveal the presence of any LRRK2 in CSF or plasma.

Additionally, the single sample that yielded a high signal for LRRK2 with the Luminex method was immunoprecipitated (IP) prior to western blotting. Figure 7.6 displays the image obtained from the IP sample.

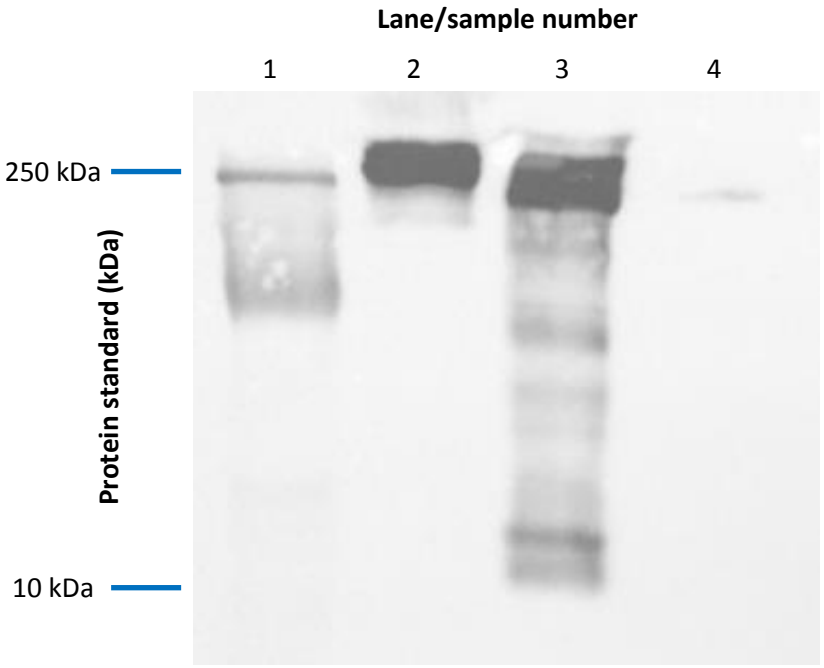

Figure 7.6: LRRK2 IP plasma Western blot image: *Lane 1 represents the protein marker standard. Lane 2 is recombinant LRRK2 spiked (0.5 µg/mL) in buffer, Lane 3 equates to recombinant LRRK2 spiked (0.5 µg/mL) into human plasma and Lane 4 represents the IP plasma sample.*

The western blot data showed that recombinant LRRK2 can be detected via this technique. There is a slight visible band at 250 kDa for the IP sample, that may represent a cleaved form of LRRK2. Unfortunately, upon repeat this band was no longer present. Thus, this band may have been a "spillover" from the neighbouring wells.

7.4 High Performance Liquid Chromatography (HPLC)

As with the western blot, there are no reports regarding the performance of HPLC versus the Luminex. Therefore, the samples previously analysed with the Luminex and western blot methods were also analysed with the HPLC technique.

Prior to analysing the samples, 1 µg recombinant LRRK2 protein was spiked into PBS and analysed, in order to determine whether the column utilised was suitable for the separation and identification of LRRK2, and, if so, at what time the spike corresponding to LRRK2 would show on the chromatogram (retention time). The original column used for this purpose was C18 – this yielded no spike on the chromatogram. Therefore a C4 column was tried, Figure 7.6, chromatograms A) and B) display the resulting chromatogram.

The retention time for 1 µg recombinant LRRK2 was 28 mins. The next step was to deduce whether this retention time for recombinant LRRK2 remained at 28 mins in plasma. Thus, a blank plasma sample was spiked with 1 µg LRRK2 recombinant protein and analysed. Figure 7.7, C) and D) show the chromatograms for the blank plasma and blank plasma + recombinant LRRK2.

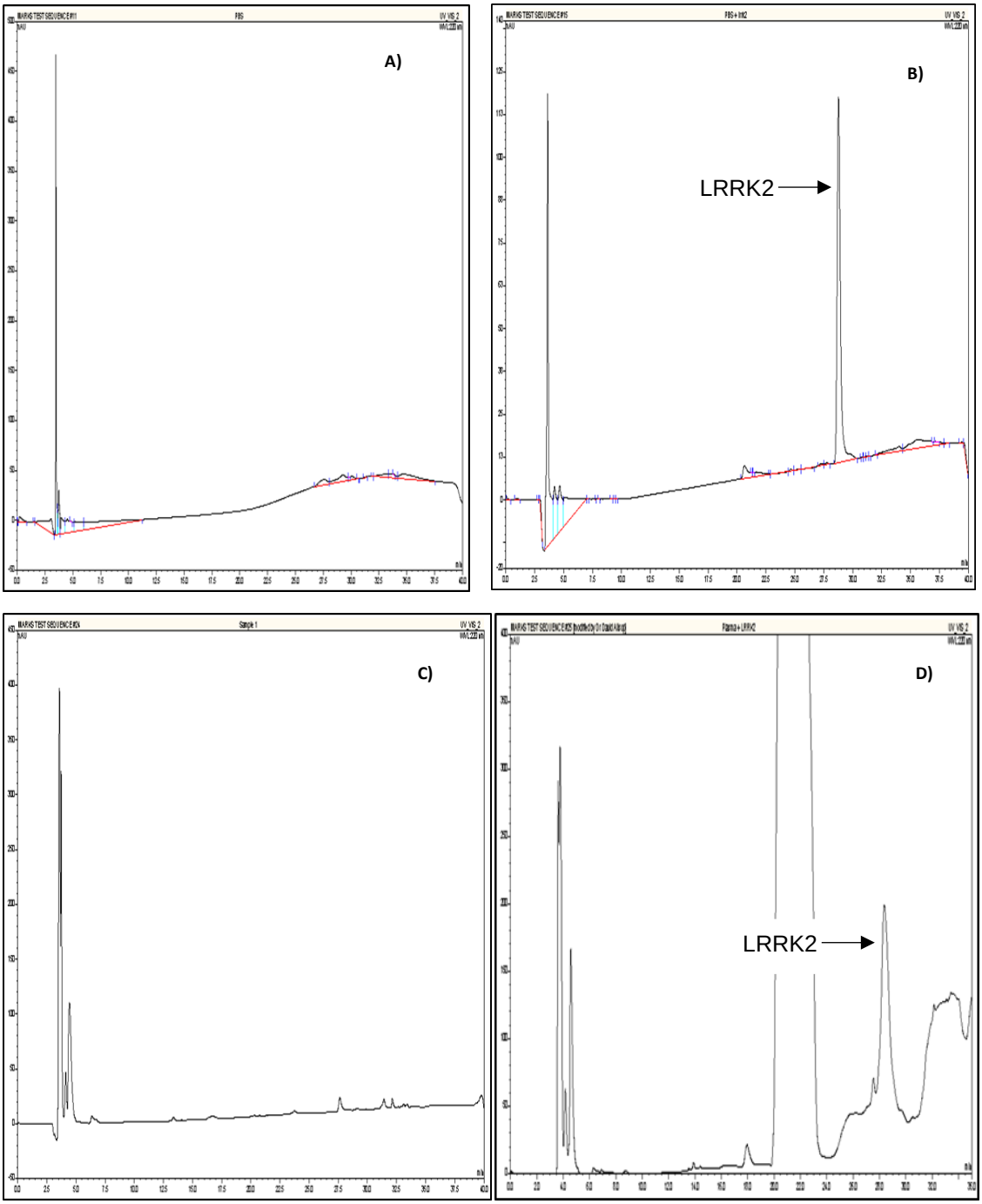

Figure 7.7: HPLC: Plasma LRRK2: *chromatograms obtained with A) PBS only, B) PBS spiked with 1 µg recombinant LRKK2, C) plasma only and D) plasma spiked with 1 µg recombinant LRRK2. The x-axis represents the retention time (RT).*

The retention time remained at 28 mins for recombinant LRRK2 in plasma. Plasma samples analysed yielded chromatograms similar to that presented in Figure 7.7 chromatogram C). Thus, LRRK2 was not detectable in unspiked plasma via the HPLC method.

CSF samples were tested for the presence of LRRK2 via HPLC. Figure 7.8 display the data obtained with CSF spiked with LRRK2 and an example chromatogram obtained for the CSF samples tested.

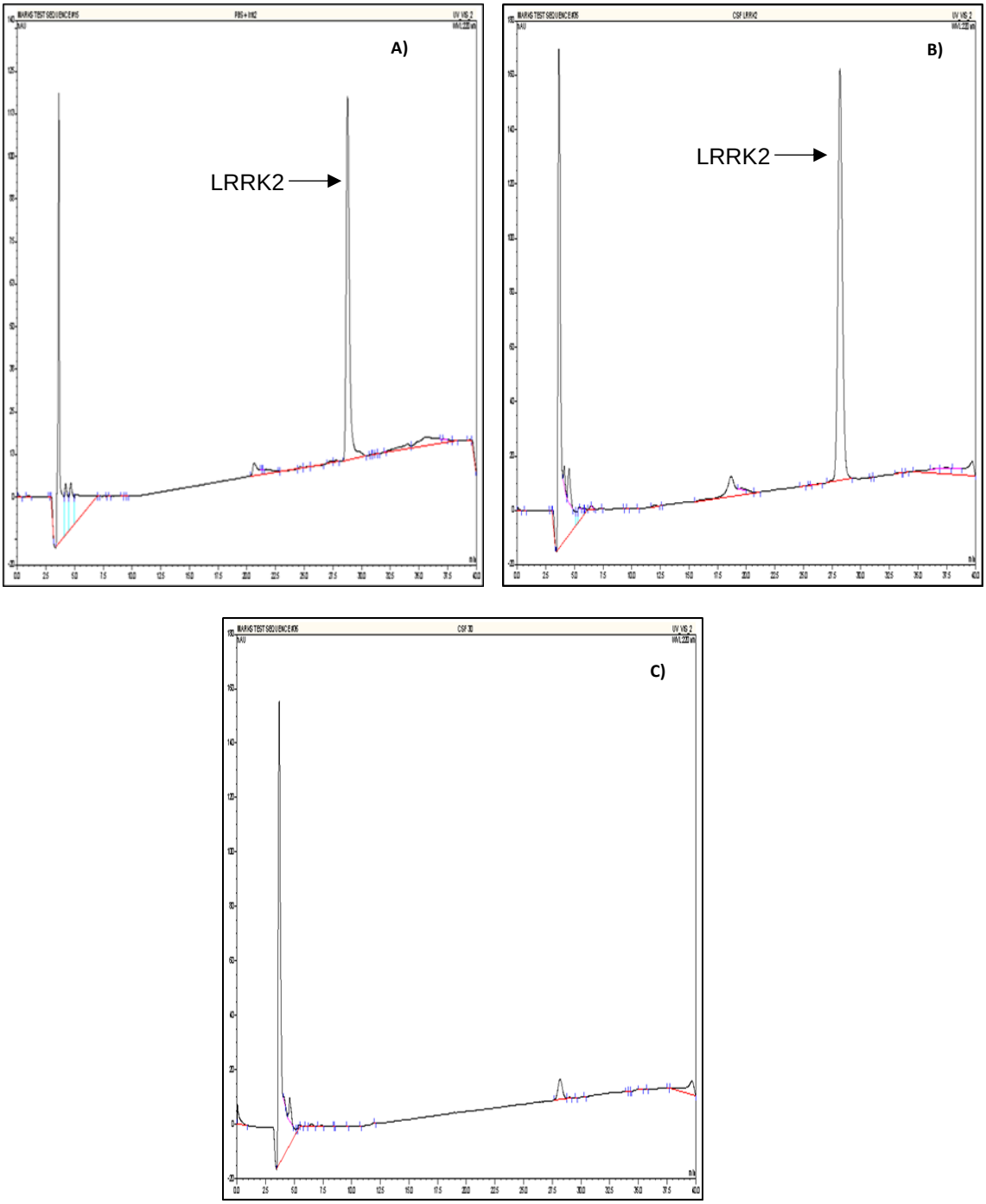

Figure 7.8: HPLC: CSF LRRK2: *chromatograms obtained with A) PBS spiked with 1 µg recombinant LRKK2, B) CSF spiked with 1 µg recombinant LRKK2 and C) CSF only. The x-axis represents the retention time (RT). The small peak in C) may represent LRRK2 but need confirmation via more sensitive methods e.g. mass spectrometry.*

7.5 Discussion

This chapter described the initial experimental steps taken to investigate the potential role for LRRK2 as a biomarker for ND diseases. In order to deduce whether LRRK2 carries biomarker potential, it was important to find out if LRRK2 is actually present in biological fluids. Research into the presence of LRRK2 in biological fluids has been minimal; Fraser *et al* (2013) have provided some evidence for the detection of LRRK2 in CSF and urine exosomes whilst researching the role of LRRK2 in relation to protein 14-3-3. This chapter describes a method for detecting LRRK2 in plasma and CSF using the Luminex bead based system. The detection methods used by Fraser et al (2013) are predominantly western blotting, which would be laborious and slow, and also less quantitative, when compared to the Luminex system.

The samples screened in this investigation revealed that no CSF samples contained detectable LRRK2 and only one plasma sample gave a relatively high signal for LRRK2 - this particular sample was taken from an AD patient. Presence of LRRK2 in plasma may follow the same pattern as α-synuclein in plasma – where levels vary greatly between individuals, i.e. some individuals are high expressors and others have low to non-detectable levels (Foulds *et al*, 2013). However, more samples will need to be tested in order to infer this.

LRRK2 was not detectable via the HPLC and western blot techniques, which suggests that the Luminex may be a more sensitive platform compared to these systems. Future work can incorporate mass spectrometry to confirm and validate the detection of LRRK2 using the Luminex method.

Despite this investigation not revealing substantial evidence for the presence of LRRK2 in biological fluids, it does present an assay system that can be utilised to

advance the research into detecting LRRK2 in plasma and CSF. In addition to a biomarker being valuable as a diagnostic tool, it can also serve as an important tool for use in pharmaceutical research. For instance, the Luminex detection method described in this chapter may prove to be useful in clinical trials where the detection of LRRK2 may act as a pharmacodynamic marker post therapeutic intervention.

Chapter 8:
Final Discussion and Future Work

The incidence rate of neurodegenerative disorders is increasing, thus, the need for accurate and early diagnosis is becoming more vital. Many techniques are being investigated in order to improve early diagnosis of such diseases and allow the monitoring of disease progression to aid therapeutic strategies. Techniques being investigated include, but are not limited to – neuroimaging, genetic variation studies and molecular markers. The latter is the topic presented in this thesis.

Aβ1-42 and tau protein levels in CSF have been identified as biomarkers for AD and many studies have been conducted in order to promote their use in clinical settings (see e.g. Blenow *et al*, 2014; Menendez-Gonzalez, 2014). Currently, no reliable markers have been found for other neurodegenerative disorders such as PD, DLB, MSA, FTLD and MND. For the purpose of this project, some of the key proteins implicated in the pathogenesis of these neurodegenerative disorders were investigated as potential biomarkers, as shown in the table below:

Neurodegenerative disease	Protein(s) implicated
AD	β-amyloid (Aβ), tau
PD	α-synuclein, DJ-1, LRRK2
FTLD	TDP-43
MND	TDP-43
DLB	α-synuclein

The original goal for this study was to investigate the potential of the above proteins as biomarkers, ultimately in a multiplex system. Although studies on Aβ1-42 and tau proteins in CSF have been intense in AD, their use as a plasma-based marker for

this and other neurodegenerative disorders has been minimal. Taking samples of CSF is a relatively invasive procedure, and there has been some debate regarding the safety and wellbeing of patients undergoing repeated lumbar punctures (Menendez-Gonzalez, 2014). Thus, our main aim was to investigate the biomarker effectiveness of these proteins in plasma as opposed to CSF.

Unfortunately, Luminex assays for Aβ1-42 and TDP-43 were not successful (data not included). The antibodies against TDP-43 available for testing with the Luminex assay were very few. In total only three antibodies were commercially available, and were tested as capture and detection components. These antibodies did not generate an acceptable signal:noise ratio and were thus not investigated further. A range of antibodies against Aβ1-42 were commercially available for testing on the Luminex, with antibody combinations generating acceptable Luminex MFI signals. However, the assay performance was not consistent, and, therefore, these assays did not pass the validation stage.

Luminex assays for quantifying phosphorylated α-synuclein, total α-synuclein, and total DJ-1 in human plasma and CSF were successful. ELISA assays have been deemed as the gold standard method for protein detection (Wilson, 2013). However, based on the data obtained in this project, the Luminex assays have proved to be more sensitive than ELISA based assays. The improvement in assay performance may be attributed to the use of microsphere beads in the Luminex technology. During ELISA, capture antibody is passively immobilised on to the walls of a microtitre well, leading to the possibility of unspecific hydrophobic binding. The Luminex utilises beads onto which the capture antibody is chemically attached via covalent bonds – reducing the risk of such unspecific binding. Additionally, the surface area of a microtitre plate compared to a well containing many beads is drastically reduced – further reducing the occurrence of non-specific binding in the

Luminex system (Baker *et al*, 2012). High sensitivity and specificity as well as good accuracy and precision are desired features for assays used in biomarker research. The present project showed that the developed Luminex assays described in this thesis meet these requirements.

A lot of biomarker research has been dedicated to α-synuclein; not surprising since α-synuclein is the major protein component involved in some important neurodegenerative disorders, namely PD, MSA and DLB. Currently, results regarding the use of α-synuclein as a biomarker have been variable between different research groups (chapters 4 and 6 discuss these in detail). This project assessed both total α-synuclein and its phosphorylated form. Studies with phosphorylated α-synuclein have been minimal, especially in plasma. Unfortunately, in this present study, neither total α-synuclein nor phosphorylated α-synuclein in CSF or plasma showed significant value as a differentiation marker. Apart from differences in the methodology used for detection, and variation in sample number, a recent study published by Stewart *et al* (2015) suggests another plausible reason for the variation in results amongst research groups, especially regarding phosphorylated α-synuclein. Stewart *et al* (2015) conducted a large scale longitudinal and cross-sectional study with phosphorylated α-synuclein in CSF samples collected from PD patients, and correlated the values with the disease stage for each individual. Their research suggested that levels of phosphorylated α-synuclein follow a trend in which high levels of phosphorylated α-synuclein are detectable in patients at the very early stage of PD and low levels in those at the late stage. This type of trend may be extended to other disease groups such as MSA and DLB and, furthermore, may also be applicable to studies with plasma. Indeed, Foulds *et al* (2013) have recently reported that plasma total α-synuclein levels increase with time for up to 20 years after the appearance of initial symptoms of PD,

suggesting that consideration of stage of disease is also important for analysis of α-synuclein in plasma. These two publications highlight a possible limitation in our study and stress the importance of obtaining disease stage and severity information from the samples analysed. The possibility of the trend proposed by Stewart *et al* (2015) being replicated in plasma is strengthened by our finding that phosphorylated α-synuclein in CSF correlates with plasma phosphorylated α-synuclein. This further supports the suggestion that plasma can reflect the environment of the brain and reinforces the use of plasma for biomarker studies as opposed to CSF, which would be preferred for practical reasons.

Multiple factors have been associated with the onset of neurodegenerative disorders. Amongst these multiple factors, oxidative stress has been suggested as a possible cause. In light of this and the fact that mutations in *DJ-1* lead to early onset PD, its role as a biomarker was investigated. The overall position of DJ-1 as a biomarker is similar to α-synuclein, where results so far are variable between research groups – though it is worthy to note that studies relating to DJ-1 have been less intense than those with α-synuclein. The study conducted for this project revealed that DJ-1 does carry potential as a biomarker that can differentiate between PD and HC as well as between PD and MSA, with DJ-1 levels in plasma being significantly lower in PD. This is the first study in which the capability of DJ-1 in plasma to differentiate between these two clinically similar diseases (i.e. PD and MSA) has been assessed. However, the ROC curve analysis revealed that DJ-1 may not serve very well as a single diagnostic marker for PD vs HC, or PD vs MSA, but does hold promise as a biomarker, possibly if used in conjunction with other diagnostic techniques, and this is worth pursuing.

Correlation studies with DJ-1 and α-synuclein also revealed some interesting insights into the possible interactions or synergy between the two proteins. It appears that

DJ-1 levels and total α-synuclein levels in plasma show a positive correlation with one another, but DJ-1 levels do not correlate with phosphorylated α-synuclein. Thus, individuals expressing low levels of DJ-1 also have low levels of total α-synuclein, and, conversely, high DJ-1 expressors also tend to show high total α-synuclein levels. Since low DJ-1 levels are implicated in some diseased states, DJ-1 interaction with α-synuclein may be neuroprotective, and the absence of DJ-1 may hinder this neuroprotection. This leads to a possible therapeutic strategy, where levels of DJ-1 can be increased in those with low levels, to boost neuroprotection.

Mutations in *LRRK2* are the leading contributor to the genetic cause of late onset PD. Research into the role of LRRK2 in PD pathogenesis is ongoing and the potential of using LRRK2 therapeutics is being investigated (Lee *et al*, 2012). In this project, several techniques have been explored in order to determine if LRRK2 is detectable in biological fluids such as CSF and plasma. The data obtained from this project with recombinant LRRK2 indicate that techniques such as the Luminex, western blotting and HPLC can be adopted to detect LRRK2 in human plasma and CSF. However, from the samples analysed within this study, it cannot be definitively concluded that LRRK2 is present and measurable in human CSF and plasma. Analysis of more samples may provide a greater insight into the biomarker potential for LRRK2. Additionally, if LRRK2 based therapeutics are pursued, assays such as the Luminex LRRK2 assay described herein could prove to be a useful tool.

Progress towards understanding and developing potential treatment strategies for neurodegenerative disorders has been rapid, but more research is still needed in order to understand the disease mechanisms. The work presented in this thesis shows that research into biomarkers for diagnostic purposes for such diseases can also lead to interesting insights into the pathophysiology of these debilitating disorders.

Future work

1. Expand on the multiplex assay

Neurodegenerative disorders are multicausal with the possibility that factors leading to disease differ amongst those affected. Thus, it would seem fitting to have multiple markers for diagnostic purposes. The Luminex technology offers the possibility of developing a multiplex assay whereby multiple molecular markers can be measured simultaneously from a single sample. These molecular markers can range from inflammatory markers to molecules similar to those discussed in this thesis. As a follow on to the present study, other PD related molecules can be added to the existing multiplex assay, such as:

- Parkin: mutations in *Parkin* have been associated with the onset of autosomal recessive PD as well as sporadic PD. Parkin is a component of the UPS and has a role as an ubiquitin E3 ligase, with its loss of function leading to PD pathogenesis. Substrates for Parkin are still relatively unknown, but previous studies have revealed that α-synuclein may be a substrate, either directly or indirectly (Dawson *et al*, 2010). Previous studies at Lancaster (Foulds. P, 2008 PhD thesis) have suggested that Parkin is present in human blood plasma.

- Oxidized DJ-1: the role of DJ-1 has been covered in detail in this thesis. The mechanism of action for DJ-1 involves its cysteine residue at position 106 being oxidised. Thus, levels of oxidised DJ-1 in CSF and plasma can be measured in order to investigate its potential as a biomarker (Saito, 2014).

- Glucocerebrosidase: mutations in the glucocerebrosidase gene have revealed them to be an important risk factor for PD. The protein is involved in the lysosomal degradation pathway and its loss of function leads to PD pathogenesis. Knowledge concerning its presence in human biological fluids has not yet been

investigated; therefore including this protein in the multiplex panel may provide interesting information regarding its value as a biomarker as well as its mechanism of action and interaction with other proteins.

- An attempt to modify the LRRK2 assay once more antibodies are commercially available can be attempted, in order to multiplex it in with the other molecules.

Additionally, the assay panel can be expanded to include markers relevant to various neurodegenerative disorders other than PD, for example:

- TDP-43: a RNA/DNA binding protein that is the major component found in the protein inclusions associated with FTLD-U and MND. As mentioned previously, a Luminex assay for TDP-43 has been attempted but the major drawback was the poor availability of antibodies. Therefore, if more antibodies become available the development of this assay can be revisited.

- FUS: another RNA/DNA binding protein that has been linked to the MND-FUS. Like TDP-43, mutations in FUS lead to the formation of FUS aggregates, thus may be worth pursuing as a potential biomarker candidate.

- Neurofilament: neurofilament proteins are a predominant feature of neuronal axons and have a key role in the growth and maintenance of nerve cells. Recent studies by Lu *et al* (2015) have shown that levels of neurofilament light chain protein (NF-L) can differentiate between MND and healthy controls. Furthermore, serum NF-L levels are higher in FTD patients than in healthy controls. Therefore, adding this to the Luminex multiplex panel may serve to discriminate FTD or MND from other brain diseases.

- Neurogranin: this is a postsynaptic protein that is a member of the calpactin family and is involved in calcium signalling (Represa *et al*, 1990). It is expressed exclusively in the brain and specific to the dendritic spines (Chang *et al*, 1997). Neurogranin levels in CSF from AD pateints have been shown to be higher in comparison to cognitively normal individuals (Thorsell *et al*, 2010; Kvartsberg *et al*, 2015; Kester *et al*, 2015). Cortical neurones expressing neurogranin have also been shown to degenerate in the late stages of PD (McKeith *et al*, 2005b) and Koob *et al*, 2014 have shown that neurogranin binds to α-synuclein, thus making it a potential biomarker for further investigation.

- Synaptotagmin: a synaptic vesicle protein that has been found to be raised in AD patients versus controls (Davidsson *et al*, 1996). More recently, Sesar *et al*, 2016 has shown a siginificant association between SNPs in *SYT11*, which codes for the protein synaptotagmin XI.

- Synaptosomal associated protein-25 (SNAP-25): this protein is an important component of the membrane-fusion SNARE complex which is essential for mediating synaptic communication (Jahn *et al*, 1999). Increased levels of CSF SNAP-25 in AD patients have been found in comparison to control groups (Brinkmalm *et al*, 2014).

2. Longitudinal sample analysis

Longitudinal plasma samples from 198 PD patients, with samples collected at 10-11 visit points over a period of 4 years, have already been collected as part of a previous study (Foulds *et al*, 2013) and are available for testing. These valuable samples can be analysed with the expanded multiplex assay to assess if any of the

molecules carry potential as early diagnostic markers for PD, or markers of disease progression.

Moreover, some PD patients develop dementia as the disease progresses. Thus, a study with these longitudinal samples and the multiplex assay may reveal a marker that can help to identify those people who will ultimately progress on to develop dementia.

Demographic data, such as disease stage, disease severity as per the UPDRS and Hoehn and Yahr scores, and information regarding medication, is also available for this longitudinal cohort of patients with PD. Information such as this will allow interesting correlation studies to reveal possible relationships between molecular markers and disease severity – similar to those investigated by Stewart *et al* (2015).

Furthermore, a whole blood sample was also taken from the enrolled PD patients. This whole blood sample can be used for genomic studies that can show if any of the patients have abnormal mutations or particular gene polymorphisms. The genomic data can be compared against the molecular marker data and assessed for any corresponding relationships.

3. Mass spectrometry

This technique can be developed and used alongside the Luminex multiplex assay in order to validate/confirm the data obtained from the latter. Samples would need to undergo special treatment in order to deplete them of high abundance proteins, such as albumin. Post treatment, these samples can be fractionated by HPLC and then analysed using mass spectrometry. Alternatively, if the protein of interest generates an acceptable band via the western blot technique, the mass spectrometry method can confirm that this particular band corresponds to the protein of interest.

References

Aarsland, D., Andersen, K., Larsen, J. P., Lolk, A., and Kragh-Sørensen, P. (2003) Prevalence and characteristics of dementia in Parkinson disease: an 8-year prospective study, *Arch Neurol*, *60*, 387-392.

Aerts, M. B., Esselink, R. A., Abdo, W. F., Bloem, B. R., and Verbeek, M. M. (2012) CSF α-synuclein does not differentiate between parkinsonian disorders, *Neurobiol Aging*, *33*, 430.e431-433.

Agarraberes, F. A., Terlecky, S. R., and Dice, J. F. (1997) An intralysosomal hsp70 is required for a selective pathway of lysosomal protein degradation, *J Cell Biol*, *137*, 825-834.

Agorogiannis, E., Agorogiannis, G., Papadimitriou, A., and Hadjigeorgiou, G. (2004) Protein misfolding in neurodegenerative diseases, *Neuropathology and Applied Neurobiology*, *30*, 215-224.

Aguzzi, A., and O'Connor, T. (2010) Protein aggregation diseases: pathogenicity and therapeutic perspectives, *Nature Reviews Drug Discovery*, *9*, 237-248.

Akazawa, Y. O., Saito, Y., Hamakubo, T., Masuo, Y., Yoshida, Y., Nishio, K., Shichiri, M., Miyasaka, T., Iwanari, H., Mochizuki, Y., Kodama, T., Noguchi, N., and Niki, E. (2010) Elevation of oxidized DJ-1 in the brain and erythrocytes of Parkinson disease model animals, *Neurosci Lett*, *483*, 201-205.

Al-Sarraj, S., King, A., Troakes, C., Smith, B., Maekawa, S., Bodi, I., Rogelj, B., Al-Chalabi, A., Hortobagyi, T., and Shaw, C. (2011) p62 positive, TDP-43 negative, neuronal cytoplasmic and intranuclear inclusions in the cerebellum and hippocampus define the pathology of C9orf72-linked FTLD and MND/ALS, *Acta Neuropathologica*, *122*, 691-702.

Anderson, J. P., Walker, D. E., Goldstein, J. M., de Laat, R., Banducci, K., Caccavello, R. J., Barbour, R., Huang, J., Kling, K., Lee, M., Diep, L., Keim, P. S., Shen, X., Chataway, T., Schlossmacher, M. G., Seubert, P., Schenk, D., Sinha, S., Gai, W. P., and Chilcote, T. J. (2006) Phosphorylation of Ser-129 is the dominant pathological modification of α-synuclein in familial and sporadic Lewy body disease, *J Biol Chem*, *281*, 29739-29752.

Ariga, H., Takahashi-Niki, K., Kato, I., Maita, H., Niki, T., and Iguchi-Ariga, S. (2013) Neuroprotective Function of DJ-1 in Parkinson's Disease, *Oxidative Medicine and Cellular Longevity*.

Armbruster, D. A., and Pry, T. (2008) Limit of blank, limit of detection and limit of quantitation, *Clin Biochem Rev*, *29 Suppl 1*, S49-52.

Armstrong, R. A., Kotzbauer, P. T., Perlmutter, J. S., Campbell, M. C., Hurth, K. M., Schmidt, R. E., and Cairns, N. J. (2014) A quantitative study of α-synuclein pathology in fifteen cases of dementia associated with Parkinson disease, *J Neural Transm (Vienna)*, *121*, 171-181.

Bak, T. H., and Hodges, J. R. (2008) Corticobasal degeneration: clinical aspects, *Handb Clin Neurol*, *89*, 509-521.

Baker, H. N., Murphy, R., Lopez, E., and Garcia, C. (2012) Conversion of a capture ELISA to a Luminex xMAP assay using a multiplex antibody screening method, *J Vis Exp*.

Bandopadhyay, R., Kingsbury, A. E., Cookson, M. R., Reid, A. R., Evans, I. M., Hope, A. D., Pittman, A. M., Lashley, T., Canet-Aviles, R., Miller, D. W., McLendon, C., Strand, C., Leonard, A. J., Abou-Sleiman, P. M., Healy, D. G., Ariga, H., Wood, N. W., de Silva, R., Revesz, T., Hardy, J. A., and Lees, A. J. (2004) The expression of DJ-1 (PARK7) in normal human CNS and idiopathic Parkinson's disease, *Brain*, *127*, 420-430.

Barbour, R., Kling, K., Anderson, J., Banducci, K., Cole, T., Diep, L., Fox, M., Goldstein, J., Soriano, F., Seubert, P., and Chilcote, T. (2008) Red blood cells are the major source of α-synuclein in blood, *Neurodegenerative Diseases*, *5*, 55-59.

Barral, J., Broadley, S., Schaffar, G., and Hartl, F. (2004) Roles of molecular chaperones in protein misfolding diseases,*Seminars in Cell & Developmental Biology*, *15*, 17-29.

Bartels, T., Choi, J., and Selkoe, D. (2011) α-Synuclein occurs physiologically as a helically folded tetramer that resists aggregation, *Nature*, *477*, 107-U123.

Baulac, S., LaVoie, M., Strahle, J., Schlossmacher, M., and Xia, W. (2004) Dimerization of Parkinson's disease - causing DJ-1 and formation of high molecular weight complexes in human brain, *Molecular and Cellular Neuroscience*, *27*, 236-246.

Bellani, S., Sousa, V. L., Ronzitti, G., Valtorta, F., Meldolesi, J., and Chieregatti, E. (2010) The regulation of synaptic function by α-synuclein, *Commun Integr Biol*, *3*, 106-109.

Bennett, M. C. (2005) The role of α-synuclein in neurodegenerative diseases, *Pharmacol Ther*, *105*, 311-331.

Beyer, K. (2006) α-Synuclein structure, posttranslational modification and alternative splicing as aggregation enhancers, *Acta Neuropathologica*, *112*, 237-251.

Bisaglia, M., Mammi, S., and Bubacco, L. (2009) Structural insights on physiological functions and pathological effects of α-synuclein, *Faseb Journal*, *23*, 329-340.

Bonifati, V., Rizzu, P., van Baren, M., Schaap, O., Breedveld, G., Krieger, E., Dekker, M., Squitieri, F., Ibanez, P., Joosse, M., van Dongen, J., Vanacore, N., van Swieten, J., Brice, A., Meco, G., van Duijn, C., Oostra, B., and Heutink, P. (2003) Mutations in the DJ-1 gene associated with autosomal recessive early-onset parkinsonism, *Science*, *299*, 256-259.

Boot, B. P., Orr, C. F., Ahlskog, J. E., Ferman, T. J., Roberts, R., Pankratz, V. S., Dickson, D. W., Parisi, J., Aakre, J. A., Geda, Y. E., Knopman, D. S., Petersen, R. C., and Boeve, B. F. (2013) Risk factors for dementia with Lewy bodies: a case-control study, *Neurology*, *81*, 833-840.

Boxer, A., and Boeve, B. (2007) Frontotemporal dementia treatment: Current symptomatic therapies and implications of recent genetic, biochemical, and neuroimaging studies, *Alzheimer Disease & Associated Disorders*, *21*, S79-S87.

Braak, H., Rüb, U., Gai, W. P., and Del Tredici, K. (2003) Idiopathic Parkinson's disease: possible routes by which vulnerable neuronal types may be subject to neuroinvasion by an unknown pathogen, *J Neural Transm (Vienna)*, *110*, 517-536.

Bradley, R. (1991) Bovine spongiform encephalopathy (BSE): the current situation and research, *Eur J Epidemiol*, *7*, 532-544.

Breitve, M. H., Chwiszczuk, L. J., Hynninen, M. J., Rongve, A., Brønnick, K., Janvin, C., and Aarsland, D. (2014) A systematic review of cognitive decline in dementia with Lewy bodies versus Alzheimer's disease, *Alzheimers Res Ther*, *6*, 53.

Breydo, L., and Uversky, V. (2011) Role of metal ions in aggregation of intrinsically disordered proteins in neurodegenerative diseases, *Metallomics*, *3*, 1163-1180.

Breydo, L., Wu, J. W., and Uversky, V. N. (2012) A-synuclein misfolding and Parkinson's disease, *Biochim Biophys Acta*, *1822*, 261-285.

Brinkmalm, A., Brinkmalm, G., Honer, W. G., Frölich, L., Hausner, L., Minthon, L., Hansson, O., Wallin, A., Zetterberg, H., Blennow, K., and Öhrfelt, A. (2014) SNAP-25 is a promising novel cerebrospinal fluid biomarker for synapse degeneration in Alzheimer's disease, *Mol Neurodegener*, *9*, 53.

Brundin P, et al. (2010) Prion-like transmission of protein aggregates in neurodegenerative diseases. *Nat Rev Mol Cell Biol*. *11*, 301–307

Burre, J., Sharma, M., Tsetsenis, T., Buchman, V., Etherton, M., and Sudhof, T. (2010) α-Synuclein Promotes SNARE-Complex Assembly in Vivo and in Vitro, *Science*, *329*, 1663-1667.

Chandler, R. L. (1961) Encephalopathy in mice produced by inoculation with scrapie brain material, *Lancet*, *1*, 1378-1379.

Chang, J. W., Schumacher, E., Coulter, P. M., Vinters, H. V., and Watson, J. B. (1997) Dendritic translocation of RC3/neurogranin mRNA in normal aging, Alzheimer disease and fronto-temporal dementia, *J Neuropathol Exp Neurol*, *56*, 1105-1118.

Chaudhuri, T., and Paul, S. (2006) Protein-misfolding diseases and chaperone-based therapeutic approaches, *Febs Journal*,*273*, 1331-1349.

Che, M., Jiang, Y., Xie, Y., Jiang, L., and Hu, H. (2011) Aggregation of the 35-kDa fragment of TDP-43 causes formation of cytoplasmic inclusions and alteration of RNA processing, *Faseb Journal*, *25*, 2344-2353.

Chen, A. K., Lin, R. Y., Hsieh, E. Z., Tu, P. H., Chen, R. P., Liao, T. Y., Chen, W., Wang, C. H., and Huang, J. J. (2010) Induction of amyloid fibrils by the C-terminal fragments of TDP-43 in amyotrophic lateral sclerosis, *J Am Chem Soc*, *132*, 1186-1187.

Chhangani, D., Joshi, A., and Mishra, A. (2012) E3 Ubiquitin Ligases in Protein Quality Control Mechanism, *Molecular Neurobiology*, *45*, 571-585.

Chiang, H. L., Terlecky, S. R., Plant, C. P., and Dice, J. F. (1989) A role for a 70-kilodalton heat shock protein in lysosomal degradation of intracellular proteins, *Science*, *246*, 382-385.

Clements, C. M., McNally, R. S., Conti, B. J., Mak, T. W., and Ting, J. P. (2006) DJ-1, a cancer- and Parkinson's disease-associated protein, stabilizes the antioxidant transcriptional master regulator Nrf2, *Proc Natl Acad Sci U S A*, *103*, 15091-15096.

Cookson, M. (2003) Pathways to parkinsonism, *Neuron*, *37*, 7-10.

Cookson, M. R. (2010) The role of leucine-rich repeat kinase 2 (LRRK2) in Parkinson's disease, *Nat Rev Neurosci*, *11*, 791-797.

Cuervo, A. M., and Dice, J. F. (1996) A receptor for the selective uptake and degradation of proteins by lysosomes, *Science*, *273*, 501-503.

Cuervo, A. M., and Dice, J. F. (2000) Age-related decline in chaperone-mediated autophagy, *J Biol Chem*, *275*, 31505-31513.

Cuervo, A. M., Stefanis, L., Fredenburg, R., Lansbury, P. T., and Sulzer, D. (2004) Impaired degradation of mutant alpha-synuclein by chaperone-mediated autophagy, *Science*, *305*, 1292-1295.

Cullie J, Chelle PL. (1939) Experimental transmission of trembling to the goat. *Comptes Rendus des Seances de l'Academie des Sciences 208*, 1058–1160.

Cummings, J., Raynaud, F., Jones, L., Sugar, R., and Dive, C. (2010) Fit-for-purpose biomarker method validation for application in clinical trials of anticancer drugs, *Br J Cancer*, *103*, 1313-1317.

Davidsson, P., Jahn, R., Bergquist, J., Ekman, R., and Blennow, K. (1996) Synaptotagmin, a synaptic vesicle protein, is present in human cerebrospinal fluid: a new biochemical marker for synaptic pathology in Alzheimer disease?, *Mol Chem Neuropathol*, *27*, 195-210.

Dawson, T. M., and Dawson, V. L. (2010) The role of parkin in familial and sporadic Parkinson's disease, *Mov Disord*, *25 Suppl 1*, S32-39.

De Duve, C., and Wattiaux, R. (1966) Functions of lysosomes, *Annu Rev Physiol*, *28*, 435-492.

Deane, R., Bell, R. D., Sagare, A., and Zlokovic, B. V. (2009) Clearance of amyloid-beta peptide across the blood-brain barrier: implication for therapies in Alzheimer's disease, *CNS Neurol Disord Drug Targets*, *8*, 16-30.

Dias, V., Junn, E., and Mouradian, M. M. (2013) The role of oxidative stress in Parkinson's disease, *J Parkinsons Dis*, *3*, 461-491.

Dice, J. F., Terlecky, S. R., Chiang, H. L., Olson, T. S., Isenman, L. D., Short-Russell, S. R., Freundlieb, S., and Terlecky, L. J. (1990) A selective pathway for degradation of cytosolic proteins by lysosomes, *Semin Cell Biol*, *1*, 449-455.

Dickson, D. W. (2001) A-synuclein and the Lewy body disorders, *Curr Opin Neurol*, *14*, 423-432.

Dobson, C. (2004) Experimental investigation of protein folding and misfolding, *Methods*, *34*, 4-14.

Dobson, C. (2005) Protein misfolding and its links with human disease., *Abstracts of Papers of the American Chemical Society*, *229*, U719-U719.

Dunning, C., Reyes, J., Steiner, J., and Brundin, P. (2012) Can Parkinson's disease pathology be propagated from one neuron to another?, *Progress in Neurobiology*, *97*, 205-219.

Duran, R., Barrero, F. J., Morales, B., Luna, J. D., Ramirez, M., and Vives, F. (2010) Plasma α-synuclein in patients with Parkinson's disease with and without treatment, *Mov Disord*, *25*, 489-493.

El-Agnaf, O., Salem, S., Paleologou, K., Cooper, L., Fullwood, N., Gibson, M., Curran, M., Court, J., Mann, D., Ikeda, S., Cookson, M., Hardy, J., and Allsop, D. (2003) α-synuclein implicated in Parkinson's disease is present in extracellular biological fluids, including human plasma, *Faseb Journal*, *17*, 1945.

El-Agnaf, O., Salem, S., Paleologou, K., Curran, M., Gibson, M., Court, J., Schlossmacher, M., and Allsop, D. (2006) Detection of oligomeric forms of α-synuclein protein in human plasma as a potential biomarker for Parkinson's disease,*Faseb Journal*, *20*, 419-425.

Eliezer, D., Kutluay, E., Bussell, R., and Browne, G. (2001) Conformational properties of alpha-synuclein in its free and lipid-associated states, *J Mol Biol*, *307*, 1061-1073.

Emmanouilidou, E., Melachroinou, K., Roumeliotis, T., Garbis, S. D., Ntzouni, M., Margaritis, L. H., Stefanis, L., and Vekrellis, K. (2010) Cell-produced alpha-synuclein is secreted in a calcium-dependent manner by exosomes and impacts neuronal survival, *J Neurosci*, *30*, 6838-6851.

Englander, S., Mayne, L., and Krishna, M. (2007) Protein folding and misfolding: mechanism and principles, *Quarterly Reviews of Biophysics*, *40*, 287-326.

Eskelinen, E. L., Cuervo, A. M., Taylor, M. R., Nishino, I., Blum, J. S., Dice, J. F., Sandoval, I. V., Lippincott-Schwartz, J., August, J. T., and Saftig, P. (2005) Unifying nomenclature for the isoforms of the lysosomal membrane protein LAMP-2, *Traffic*, *6*, 1058-1061.

Esler, W. P., Stimson, E. R., Jennings, J. M., Vinters, H. V., Ghilardi, J. R., Lee, J. P., Mantyh, P. W., and Maggio, J. E. (2000) Alzheimer's disease amyloid propagation by a template-dependent dock-lock mechanism, *Biochemistry*, *39*, 6288-6295.

Ferman, T. J., Boeve, B. F., Smith, G. E., Lin, S. C., Silber, M. H., Pedraza, O., Wszolek, Z., Graff-Radford, N. R., Uitti, R., Van Gerpen, J., Pao, W., Knopman, D., Pankratz, V. S., Kantarci, K., Boot, B., Parisi, J. E., Dugger, B. N., Fujishiro, H., Petersen, R. C., and Dickson, D. W. (2011) Inclusion of RBD improves the diagnostic classification of dementia with Lewy bodies, *Neurology*, *77*, 875-882.

Fjorback, A., Varming, K., and Jensen, P. (2007) Determination of α-synuclein concentration in human plasma using ELISA, *Scandinavian Journal of Clinical & Laboratory Investigation*, *67*, 431-435.

Forno, L. S. (1996) Neuropathology of Parkinson's disease, *J Neuropathol Exp Neurol*, *55*, 259-272.

Foulds, P. G., and Lancaster University. Theses. (2008) A study of **-synuclein, parkin and TDP-43 : proteins implicated in neurodegenerative disease.

Foulds, P. G., Diggle, P., Mitchell, J. D., Parker, A., Hasegawa, M., Masuda-Suzukake, M., Mann, D. M., and Allsop, D. (2013) A longitudinal study on α-synuclein in blood plasma as a biomarker for Parkinson's disease, *Sci Rep*, *3*, 2540.

Foulds, P., Davidson, Y., Mishra, M., Hobson, D., Humphreys, K., Taylor, M., Johnson, N., Weintraub, S., Akiyama, H., Arai, T., Hasegawa, M., Bigio, E., Benson, F., Allsop, D., and Mann, D. (2009) Plasma phosphorylated-TDP-43 protein levels correlate with brain pathology in frontotemporal lobar degeneration, *Acta Neuropathologica*, *118*, 647-658.

Foulds, P., Mann, D., and Allsop, D. (2012) Phosphorylated α-synuclein as a potential biomarker for Parkinson's disease and related disorders, *Expert Review of Molecular Diagnostics*, *12*, 115-117.

Foulds, P., McAuley, E., Gibbons, L., Davidson, Y., Pickering-Brown, S., Neary, D., Snowden, J., Allsop, D., and Mann, D. (2008) TDP-43 protein in plasma may index TDP-43 brain pathology in Alzheimer's disease and frontotemporal lobar degeneration, *Acta Neuropathologica*, *116*, 141-146.

Foulds, P., Mitchell, J., Parker, A., Turner, R., Green, G., Diggle, P., Hasegawa, M., Taylor, M., Mann, D., and Allsop, D. (2011) Phosphorylated α-synuclein can be detected in blood plasma and is potentially a useful biomarker for Parkinson's disease, *Faseb Journal*, *25*, 4127-4137.

Fraser, K. B., Moehle, M. S., Daher, J. P., Webber, P. J., Williams, J. Y., Stewart, C. A., Yacoubian, T. A., Cowell, R. M., Dokland, T., Ye, T., Chen, D., Siegal, G. P., Galemmo, R. A., Tsika, E., Moore, D. J., Standaert, D. G., Kojima, K., Mobley, J. A., and West, A. B. (2013) LRRK2 secretion in exosomes is regulated by 14-3-3, *Hum Mol Genet*, *22*, 4988-5000.

Frydman, J. (2001) Folding of newly translated proteins in vivo: the role of molecular chaperones, *Annu Rev Biochem*, *70*, 603-647.

Fujiwara, H., Hasegawa, M., Dohmae, N., Kawashima, A., Masliah, E., Goldberg, M. S., Shen, J., Takio, K., and Iwatsubo, T. (2002) α-Synuclein is phosphorylated in synucleinopathy lesions, *Nat Cell Biol*, *4*, 160-164.

Gendron, T., Josephs, K., and Petrucelli, L. (2010) Review: Transactive response DNA-binding protein 43 (TDP-43): mechanisms of neurodegeneration, *Neuropathology and Applied Neurobiology*, *36*, 97-112.

George, J. (2002) The synucleins, *Genome Biology*, *3*.

Geser, F., Martinez-Lage, M., Kwong, L., Lee, V., and Trojanowski, J. (2009) Amyotrophic lateral sclerosis, frontotemporal dementia and beyond: the TDP-43 diseases, *Journal of Neurology*, *256*, 1205-1214.

Geser, F., Pryulovic, D., O'Dwyer, L., Hardiman, O., Bede, P., Bokde, A., Trojanowski, J., and Hampel, H. (2011) On the development of markers for pathological TDP-43 in amyotrophic lateral sclerosis with and without dementia, *Progress in Neurobiology*, *95*, 649-662.

Gibbs, C. J., Gajdusek, D. C., Asher, D. M., Alpers, M. P., Beck, E., Daniel, P. M., and Matthews, W. B. (1968) Creutzfeldt-Jakob disease (spongiform encephalopathy): transmission to the chimpanzee, *Science*, *161*, 388-389.

Gilman, S., Wenning, G. K., Low, P. A., Brooks, D. J., Mathias, C. J., Trojanowski, J. Q., Wood, N. W., Colosimo, C., Dürr, A., Fowler, C. J., Kaufmann, H., Klockgether, T., Lees, A., Poewe, W., Quinn, N., Revesz, T., Robertson, D., Sandroni, P., Seppi, K., and Vidailhet, M. (2008) Second consensus statement on the diagnosis of multiple system atrophy, *Neurology*,*71*, 670-676.

Goedert, M. (2001) Alpha-synuclein and neurodegenerative diseases, *Nat Rev Neurosci*, *2*, 492-501.

Gregersen, N., Bolund, L., and Bross, P. (2005) Protein misfolding, aggregation, and degradation in disease, *Molecular Biotechnology*, *31*, 141-150.

Gregersen, N., Bross, P., Vang, S., and Christensen, J. (2006) Protein misfolding and human disease, *Annual Review of Genomics and Human Genetics*, *7*, 103-124.

Griffith, J. S. (1967) Self-replication and scrapie, *Nature*, *215*, 1043-1044.

Guerreiro, P. S., Huang, Y., Gysbers, A., Cheng, D., Gai, W. P., Outeiro, T. F., and Halliday, G. M. (2013) LRRK2 interactions with α-synuclein in Parkinson's disease brains and in cell models, *J Mol Med (Berl)*, *91*, 513-522.

Guo, W., Chen, Y., Zhou, X., Kar, A., Ray, P., Chen, X., Rao, E. J., Yang, M., Ye, H., Zhu, L., Liu, J., Xu, M., Yang, Y., Wang, C., Zhang, D., Bigio, E. H., Mesulam, M., Shen, Y., Xu, Q., Fushimi, K., and Wu, J. Y. (2011) An ALS-associated mutation affecting TDP-43 enhances protein aggregation, fibril formation and neurotoxicity, *Nat Struct Mol Biol*, *18*, 822-830.

Hansen, C., Angot, E., Bergström, A. L., Steiner, J. A., Pieri, L., Paul, G., Outeiro, T. F., Melki, R., Kallunki, P., Fog, K., Li, J. Y., and Brundin, P. (2011) α-Synuclein propagates from mouse brain to grafted dopaminergic neurons and seeds aggregation in cultured human cells, *J Clin Invest*, *121*, 715-725.

Hartl, F., Bracher, A., and Hayer-Hartl, M. (2011) Molecular chaperones in protein folding and proteostasis, *Nature*, *475*, 324-332.

Hasegawa, M.; Fujiwara, H.; Nonaka, T.; Wakabayashi, K.; Takahashi, H.; Lee, V.M.; Trojanowski, J.Q.; Mann, D.; Iwatsubo, T. (2002) Phosphorylated alpha-synuclein is ubiquitinated in alpha-synucleinopathy lesions. *J. Biol. Chem. 277*, 49071–49076.

Hely, M. A., Reid, W. G., Adena, M. A., Halliday, G. M., and Morris, J. G. (2008) The Sydney multicenter study of Parkinson's disease: the inevitability of dementia at 20 years, *Mov Disord*, *23*, 837-844.

Herbert, M. K., Eeftens, J. M., Aerts, M. B., Esselink, R. A., Bloem, B. R., Kuiperij, H. B., and Verbeek, M. M. (2014) CSF levels of DJ-1 and tau distinguish MSA patients from PD patients and controls, *Parkinsonism Relat Disord*, *20*, 112-115.

Hong, D., Han, S., Fink, A., and Uversky, V. (2011) Characterization of the Non-Fibrillar α-Synuclein Oligomers,*Protein and Peptide Letters*, *18*, 230-240.

Hong, Z., Shi, M., Chung, K., Quinn, J., Peskind, E., Galasko, D., Jankovic, J., Zabetian, C., Leverenz, J., Baird, G., Montine, T., Hancock, A., Hwang, H., Pan, C., Bradner, J., Kang, U., Jensen, P., and Zhang, J. (2010) DJ-1 and α-synuclein in human cerebrospinal fluid as biomarkers of Parkinson's disease, *Brain*, *133*, 713-726.

Horwich, A. (2002) Protein aggregation in disease: a role for folding intermediates forming specific multimeric interactions,*Journal of Clinical Investigation*, *110*, 1221-1232.

Houlton, S. (2011) Neurodegenerative diseases A quick look at protein folding, *Chemistry & Industry*, 11-11.

Huang, Q., and Figueiredo-Pereira, M. (2010) Ubiquitin/proteasome pathway impairment in neurodegeneration: therapeutic implications, *Apoptosis*, *15*, 1292-1311.

Hughes, A. J., Daniel, S. E., and Lees, A. J. (2001) Improved accuracy of clinical diagnosis of Lewy body Parkinson's disease, *Neurology*, *57*, 1497-1499.

Hughes, A. J., Daniel, S. E., Kilford, L., and Lees, A. J. (1992) Accuracy of clinical diagnosis of idiopathic Parkinson's disease: a clinico-pathological study of 100 cases, *J Neurol Neurosurg Psychiatry*, *55*, 181-184.

Irwin, D. J., Lee, V. M., and Trojanowski, J. Q. (2013) Parkinson's disease dementia: convergence of α-synuclein, tau and amyloid-β pathologies, *Nat Rev Neurosci*, *14*, 626-636.

Jahn, R., and Südhof, T. C. (1999) Membrane fusion and exocytosis, *Annu Rev Biochem*, *68*, 863-911.

Johnson, B. S., McCaffery, J. M., Lindquist, S., and Gitler, A. D. (2008) A yeast TDP-43 proteinopathy model: Exploring the molecular determinants of TDP-43 aggregation and cellular toxicity, *Proc Natl Acad Sci U S A*, *105*, 6439-6444.

Johnson, B. S., Snead, D., Lee, J. J., McCaffery, J. M., Shorter, J., and Gitler, A. D. (2009) TDP-43 is intrinsically aggregation-prone, and amyotrophic lateral sclerosis-linked mutations accelerate aggregation and increase toxicity, *J Biol Chem*, *284*, 20329-20339.

Kang, J. H., Irwin, D. J., Chen-Plotkin, A. S., Siderowf, A., Caspell, C., Coffey, C. S., Waligórska, T., Taylor, P., Pan, S., Frasier, M., Marek, K., Kieburtz, K., Jennings, D., Simuni, T., Tanner, C. M., Singleton, A., Toga, A. W., Chowdhury, S., Mollenhauer, B., Trojanowski, J. Q., Shaw, L. M., and Initiative, P. s. P. M. (2013) Association of cerebrospinal fluid β-amyloid 1-42, T-tau, P-tau181, and α-synuclein levels with clinical features of drug-naive patients with early Parkinson disease, *JAMA Neurol*, *70*, 1277-1287.

Kasai, T., Tokuda, T., Ishigami, N., Sasayama, H., Foulds, P., Mitchell, D., Mann, D., Allsop, D., and Nakagawa, M. (2009) Increased TDP-43 protein in cerebrospinal fluid of patients with amyotrophic lateral sclerosis, *Acta Neuropathologica*, *117*, 55-62.

Kasuga, K., and Ikeuchi, T. (2012) [Cerebrospinal fluid and plasma biomarkers for dementia with lewy bodies], *Brain Nerve*, *64*, 505-513.

Kasuga, K., Nishizawa, M., and Ikeuchi, T. (2012) α-Synuclein as CSF and Blood Biomarker of Dementia with Lewy Bodies,*Int J Alzheimers Dis*, *2012*, 437025.

Kato, I., Maita, H., Takahashi-Niki, K., Saito, Y., Noguchi, N., Iguchi-Ariga, S. M., and Ariga, H. (2013) Oxidized DJ-1 inhibits p53 by sequestering p53 from promoters in a DNA-binding affinity-dependent manner, *Mol Cell Biol*, *33*, 340-359.

Kawakami, F., and Ichikawa, T. (2015) The Role of α-Synuclein and LRRK2 in Tau Phosphorylation, *Parkinsons Dis*, *2015*, 734746.

Kester, M. I., Teunissen, C. E., Crimmins, D. L., Herries, E. M., Ladenson, J. H., Scheltens, P., van der Flier, W. M., Morris, J. C., Holtzman, D. M., and Fagan, A. M. (2015) Neurogranin as a Cerebrospinal Fluid Biomarker for Synaptic Loss in Symptomatic Alzheimer Disease, *JAMA Neurol*, *72*, 1275-1280.

Kitada, T., Asakawa, S., Hattori, N., Matsumine, H., Yamamura, Y., Minoshima, S., Yokochi, M., Mizuno, Y., and Shimizu, N. (1998) Mutations in the parkin gene cause autosomal recessive juvenile parkinsonism, *Nature*, *392*, 605-608.

Kokalj, S., Stoka, V., Kenig, M., Guncar, G., Turk, D., and Zerovnik, E. (2005) A central role for protein aggregation in neurodegenerative disease; Mechanistic and structural studies of human stefins, *Acta Chimica Slovenica*, *52*, 27-33.

Koob, A. O., Shaked, G. M., Bender, A., Bisquertt, A., Rockenstein, E., and Masliah, E. (2014) Neurogranin binds α-synuclein in the human superior temporal cortex and interaction is decreased in Parkinson's disease, *Brain Res*, *1591*, 102-110.

Kordower, J. H., Chu, Y., Hauser, R. A., Freeman, T. B., and Olanow, C. W. (2008) Lewy body-like pathology in long-term embryonic nigral transplants in Parkinson's disease, *Nat Med*, *14*, 504-506.

Kovacs, G. G., Breydo, L., Green, R., Kis, V., Puska, G., Lőrincz, P., Perju-Dumbrava, L., Giera, R., Pirker, W., Lutz, M., Lachmann, I., Budka, H., Uversky, V. N., Molnár, K., and László, L. (2014) Intracellular processing of disease-associated α-synuclein in the human brain suggests prion-like cell-to-cell spread, *Neurobiol Dis*, *69*, 76-92.

Kraft, C., Kijanska, M., Kalie, E., Siergiejuk, E., Lee, S. S., Semplicio, G., Stoffel, I., Brezovich, A., Verma, M., Hansmann, I., Ammerer, G., Hofmann, K., Tooze, S., and Peter, M. (2012) Binding of the Atg1/ULK1 kinase to the ubiquitin-like protein Atg8 regulates autophagy, *EMBO J*, *31*, 3691-3703.

Krüger, R., Kuhn, W., Müller, T., Woitalla, D., Graeber, M., Kösel, S., Przuntek, H., Epplen, J. T., Schöls, L., and Riess, O. (1998) Ala30Pro mutation in the gene encoding alpha-synuclein in Parkinson's disease, *Nat Genet*, *18*, 106-108.

Kvartsberg, H., Portelius, E., Andreasson, U., Brinkmalm, G., Hellwig, K., Lelental, N., Kornhuber, J., Hansson, O., Minthon, L., Spitzer, P., Maler, J. M., Zetterberg, H., Blennow, K., and Lewczuk, P. (2015) Characterization of the postsynaptic protein neurogranin in paired cerebrospinal fluid and plasma samples from Alzheimer's disease patients and healthy controls, *Alzheimers Res Ther*, *7*, 40.

Lashuel, H., Overk, C., Oueslati, A., and Masliah, E. (2013) The many faces of α-synuclein: from structure and toxicity to therapeutic target, *Nature Reviews Neuroscience*, *14*, 38-48.

Laskowska, E., Matuszewska, E., and Kuczynska-Wisnik, D. (2010) Small Heat Shock Proteins and Protein-Misfolding Diseases, *Current Pharmaceutical Biotechnology*, *11*, 146-157.

Lecker, S., Goldberg, A., and Mitch, W. (2006) Protein degradation by the ubiquitin-proteasome pathway in normal and disease states, *Journal of the American Society of Nephrology*, *17*, 1807-1819.

Lee, B. D., Dawson, V. L., and Dawson, T. M. (2012) Leucine-rich repeat kinase 2 (LRRK2) as a potential therapeutic target in Parkinson's disease, *Trends Pharmacol Sci*, *33*, 365-373.

Lee, H. J., Khoshaghideh, F., Lee, S., and Lee, S. J. (2006a) Impairment of microtubule-dependent trafficking by overexpression of α-synuclein, *Eur J Neurosci*, *24*, 3153-3162.

Lee, H. J., Khoshaghideh, F., Patel, S., and Lee, S. J. (2004) Clearance of alpha-synuclein oligomeric intermediates via the lysosomal degradation pathway, *J Neurosci*, *24*, 1888-1896.

Lee, H., Bae, E., Jang, A., Ho, D., Cho, E., Suk, J., Yun, Y., and Lee, S. (2011) Enzyme-linked immunosorbent assays for α-synuclein with species and multimeric state specificities, *Journal of Neuroscience Methods*, *199*, 249-257.

Lee, H., Suk, J., Bae, E., Lee, J., Paik, S., and Lee, S. (2008) Assembly-dependent endocytosis and clearance of extracellular α-synuclein, *International Journal of Biochemistry & Cell Biology*, *40*, 1835-1849.

Lee, J. (2009) Method validation and application of protein biomarkers: basic similarities and differences from biotherapeutics, *Bioanalysis*, *1*, 1461-1474.

Lee, J., Devanarayan, V., Barrett, Y., Weiner, R., Allinson, J., Fountain, S., Keller, S., Weinryb, I., Green, M., Duan, L., Rogers, J., Millham, R., O'Brien, P., Sailstad, J., Khan, M., Ray, C., and Wagner, J. (2006b) Fit-for-purpose method development and validation for successful biomarker measurement, *Pharmaceutical Research*, *23*, 312-328.

Lee, P. H., Lee, G., Park, H. J., Bang, O. Y., Joo, I. S., and Huh, K. (2006c) The plasma α-synuclein levels in patients with Parkinson's disease and multiple system atrophy, *J Neural Transm (Vienna)*, *113*, 1435-1439.

Lee, V. M., and Trojanowski, J. Q. (2006) Mechanisms of Parkinson's disease linked to pathological α-synuclein: new targets for drug discovery, *Neuron*, *52*, 33-38.

Lewy FH., (1912) Paralysis agitans. I Pathologische Anatomie. *In Handbuch der Neurologie III. Springer, Berlin*, 920-933.

Li, J. Q., Tan, L., and Yu, J. T. (2014) The role of the LRRK2 gene in Parkinsonism, *Mol Neurodegener*, *9*, 47.

Li, Q., Mok, S., Laughton, K., McLean, C., Cappai, R., Masters, C., Culvenor, J., and Horne, M. (2007) Plasma α-synuclein is decreased in subjects with Parkinson's disease, *Experimental Neurology*, *204*, 583-588.

Lin, X., Cook, T., Zabetian, C., Leverenz, J., Peskind, E., Hu, S., Cain, K., Pan, C., Edgar, J., Goodlett, D., Racette, B., Checkoway, H., Montine, T., Shi, M., and Zhang, J. (2012) DJ-1 isoforms in whole blood as potential biomarkers of Parkinson disease, *Scientific Reports*, *2*.

Liscic, R., Grinberg, L., Zidar, J., Gitcho, M., and Cairns, N. (2008) ALS and FTLD: two faces of TDP-43 proteinopathy,*European Journal of Neurology*, *15*, 772-780.

Litvan, I., Mega, M. S., Cummings, J. L., and Fairbanks, L. (1996) Neuropsychiatric aspects of progressive supranuclear palsy, *Neurology*, *47*, 1184-1189.

Liu, C. W., Corboy, M. J., DeMartino, G. N., and Thomas, P. J. (2003) Endoproteolytic activity of the proteasome, *Science*, *299*, 408-411.

Lu, C. H., Macdonald-Wallis, C., Gray, E., Pearce, N., Petzold, A., Norgren, N., Giovannoni, G., Fratta, P., Sidle, K., Fish, M., Orrell, R., Howard, R., Talbot, K., Greensmith, L., Kuhle, J., Turner, M. R., and Malaspina, A. (2015) Neurofilament light chain: A prognostic biomarker in amyotrophic lateral sclerosis, *Neurology*, *84*, 2247-2257.

Lu, C. H., Macdonald-Wallis, C., Gray, E., Pearce, N., Petzold, A., Norgren, N., Giovannoni, G., Fratta, P., Sidle, K., Fish, M., Orrell, R., Howard, R., Talbot, K., Greensmith, L., Kuhle, J., Turner, M. R., and Malaspina, A. (2015) Neurofilament light chain: A prognostic biomarker in amyotrophic lateral sclerosis, *Neurology*, *84*, 2247-2257.

Luk, K. C., Kehm, V., Carroll, J., Zhang, B., O'Brien, P., Trojanowski, J. Q., and Lee, V. M. (2012) Pathological α-synuclein transmission initiates Parkinson-like neurodegeneration in nontransgenic mice, *Science*, *338*, 949-953.

Lykkebo, S., and Jensen, P. (2002) A-synuclein and presynaptic function - Implications for Parkinson's disease,*Neuromolecular Medicine*, *2*, 115-129.

Mackenzie, I., Foti, D., Woulfe, J., and Hurwitz, T. (2008) Atypical frontotemporal lobar degeneration with ubiquitin-positive, TDP-43-negative neuronal inclusions, *Brain*, *131*, 1282-1293.

Maita, C., Tsuji, S., Yabe, I., Hamada, S., Ogata, A., Maita, H., Iguchi-Ariga, S. M., Sasaki, H., and Ariga, H. (2008) Secretion of DJ-1 into the serum of patients with Parkinson's disease, *Neurosci Lett*, *431*, 86-89.

Malek, N., Swallow, D., Grosset, K. A., Anichtchik, O., Spillantini, M., and Grosset, D. G. (2014) A-synuclein in peripheral tissues and body fluids as a biomarker for Parkinson's disease - a systematic review, *Acta Neurol Scand*, *130*, 59-72.

Maroteaux, L., Campanelli, J. T., and Scheller, R. H. (1988) Synuclein: a neuron-specific protein localized to the nucleus and presynaptic nerve terminal, *J Neurosci*, *8*, 2804-2815.

Martins-Branco, D., Esteves, A., Santos, D., Arduino, D., Swerdlow, R., Oliveira, C., Januario, C., and Cardoso, S. (2012) Ubiquitin proteasome system in Parkinson's disease: A keeper or a witness?, *Experimental Neurology*, *238*, 89-99.

Mata, I. F., Ross, O. A., Kachergus, J., Huerta, C., Ribacoba, R., Moris, G., Blazquez, M., Guisasola, L. M., Salvador, C., Martinez, C., Farrer, M., and Alvarez, V. (2006a) LRRK2 mutations are a common cause of Parkinson's disease in Spain,*Eur J Neurol*, *13*, 391-394.

Mata, I. F., Wedemeyer, W. J., Farrer, M. J., Taylor, J. P., and Gallo, K. A. (2006b) LRRK2 in Parkinson's disease: protein domains and functional insights, *Trends Neurosci*, *29*, 286-293.

Mata, I., Shi, M., Agarwal, P., Chung, K., Edwards, K., Factor, S., Galasko, D., Ginghina, C., Griffith, A., Higgins, D., Kay, D., Kim, H., Leverenz, J., Quinn, J., Roberts, J., Samii, A., Snapinn, K., Tsuang, D., Yearout, D., Zhang, J., Payami, H., and Zabetian, C. (2010) SNCA Variant Associated With Parkinson Disease and Plasma α-Synuclein Level, *Archives of Neurology*, *67*, 1350-1356.

McKeith, I. G. (2006) Consensus guidelines for the clinical and pathologic diagnosis of dementia with Lewy bodies (DLB): report of the Consortium on DLB International Workshop, *J Alzheimers Dis*, *9*, 417-423.

McKeith, I. G., Burn, D. J., Ballard, C. G., Collerton, D., Jaros, E., Morris, C. M., McLaren, A., Perry, E. K., Perry, R., Piggott, M. A., and O'Brien, J. T. (2003) Dementia with Lewy bodies, *Semin Clin Neuropsychiatry*, *8*, 46-57.

McKeith, I. G., Dickson, D. W., Lowe, J., Emre, M., O'Brien, J. T., Feldman, H., Cummings, J., Duda, J. E., Lippa, C., Perry, E. K., Aarsland, D., Arai, H., Ballard, C. G., Boeve, B., Burn, D. J., Costa, D., Del Ser, T., Dubois, B., Galasko, D., Gauthier, S., Goetz, C. G., Gomez-Tortosa, E., Halliday, G., Hansen, L. A., Hardy, J., Iwatsubo, T., Kalaria, R. N., Kaufer, D., Kenny, R. A., Korczyn, A., Kosaka, K., Lee, V. M., Lees, A., Litvan, I., Londos, E., Lopez, O. L., Minoshima, S., Mizuno, Y., Molina, J. A., Mukaetova-Ladinska, E. B., Pasquier, F., Perry, R. H., Schulz, J. B., Trojanowski, J. Q., Yamada, M., and DLB, C. o. (2005a) Diagnosis and management of dementia with Lewy bodies: third report of the DLB Consortium,*Neurology*, *65*, 1863-1872.

McKeith, I., and Cummings, J. (2005b) Behavioural changes and psychological symptoms in dementia disorders, *Lancet Neurol*, *4*, 735-742.

McKhann, G., Albert, M., Grossman, M., Miller, B., Dickson, D., and Trojanowski, J. (2001) Clinical and pathological diagnosis of Frontotemporal Dementia - Report of the work group on Frontotemporal Dementia and Pick's disease,*Archives of Neurology*, *58*, 1803-1809.

McKhann, G., Drachman, D., Folstein, M., Katzman, R., Price, D., and Stadlan, E. M. (1984) Clinical diagnosis of Alzheimer's disease: report of the NINCDS-ADRDA Work Group under the auspices of Department of Health and Human Services Task Force on Alzheimer's Disease, *Neurology*, *34*, 939-944.

McLean, J., Hallett, P., Cooper, O., Stanley, M., and Isacson, O. (2012) Transcript expression levels of full-length α-synuclein and its three alternatively spliced variants in Parkinson's disease brain regions and in a transgenic mouse model of α-synuclein overexpression, *Molecular and Cellular Neuroscience*, *49*, 230-239.

Menéndez-González, M. (2014) Biomarkers in neurodegenerative disorders: translating research into clinical practice, *Front Aging Neurosci*, *6*, 281.

Meulener, M. C., Graves, C. L., Sampathu, D. M., Armstrong-Gold, C. E., Bonini, N. M., and Giasson, B. I. (2005) DJ-1 is present in a large molecular complex in human brain tissue and interacts with α-synuclein, *J Neurochem*, *93*, 1524-1532.

Michell, A., Lewis, S., Foltynie, T., and Barker, R. (2004) Biomarkers and Parkinson's disease, *Brain*, *127*, 1693-1705.

Muchowski, P., and Wacker, J. (2005) Modulation of neurodegeneration by molecular chaperones, *Nature Reviews Neuroscience*, *6*, 11-22.

Murphy, R., and Kendrick, B. (2007) Protein misfolding and aggregation, *Biotechnology Progress*, *23*, 548-552.

Naeem, A., and Fazili, N. (2011) Defective Protein Folding and Aggregation as the Basis of Neurodegenerative Diseases: The Darker Aspect of Proteins, *Cell Biochemistry and Biophysics*, *61*, 237-250.

Nagakubo, D., Taira, T., Kitaura, H., Ikeda, M., Tamai, K., Iguchi-Ariga, S. M., and Ariga, H. (1997) DJ-1, a novel oncogene which transforms mouse NIH3T3 cells in cooperation with ras, *Biochem Biophys Res Commun*, *231*, 509-513.

Nakamura, T., and Lipton, S. (2009) Cell death: protein misfolding and neurodegenerative diseases, *Apoptosis*, *14*, 455-468.

Neumann, M., Kwong, L., Sampathu, D., Trojanowski, J., and Lee, V. (2007) TDP-43 proteinopathy in frontotemporal lobar degeneration and amyotrophic lateral sclerosis - Protein misfolding diseases without amyloidosis, *Archives of Neurology*,*64*, 1388-1394.

Noda, T., Suzuki, K., and Ohsumi, Y. (2002) Yeast autophagosomes: de novo formation of a membrane structure, *Trends Cell Biol*, *12*, 231-235.

Orenstein, S. J., Kuo, S. H., Tasset, I., Arias, E., Koga, H., Fernandez-Carasa, I., Cortes, E., Honig, L. S., Dauer, W., Consiglio, A., Raya, A., Sulzer, D., and Cuervo, A. M. (2013) Interplay of LRRK2 with chaperone-mediated autophagy, *Nat Neurosci*, *16*, 394-406.

Ostrerova, N., Petrucelli, L., Farrer, M., Mehta, N., Choi, P., Hardy, J., and Wolozin, B. (1999) alpha-Synuclein shares physical and functional homology with 14-3-3 proteins, *J Neurosci*, *19*, 5782-5791.

Park, M. J., Cheon, S. M., Bae, H. R., Kim, S. H., and Kim, J. W. (2011a) Elevated levels of α-synuclein oligomer in the cerebrospinal fluid of drug-naïve patients with Parkinson's disease, *J Clin Neurol*, *7*, 215-222.

Park, M. J., Cheon, S. M., Bae, H. R., Kim, S. H., and Kim, J. W. (2011b) Elevated levels of α-synuclein oligomer in the cerebrospinal fluid of drug-naïve patients with Parkinson's disease, *J Clin Neurol*, *7*, 215-222.

Parnetti, L., Farotti, L., Eusebi, P., Chiasserini, D., De Carlo, C., Giannandrea, D., Salvadori, N., Lisetti, V., Tambasco, N., Rossi, A., Majbour, N. K., El-Agnaf, O., and Calabresi, P. (2014b) Differential role of CSF α-synuclein species, tau, and Aβ42 in Parkinson's Disease, *Front Aging Neurosci*, *6*, 53.

Polymeropoulos, M. H., Higgins, J. J., Golbe, L. I., Johnson, W. G., Ide, S. E., Di Iorio, G., Sanges, G., Stenroos, E. S., Pho, L. T., Schaffer, A. A., Lazzarini, A. M., Nussbaum, R. L., and Duvoisin, R. C. (1996) Mapping of a gene for Parkinson's disease to chromosome 4q21-q23, *Science, 274,* 1197-1199.

Polymeropoulos, M. H., Lavedan, C., Leroy, E., Ide, S. E., Dehejia, A., Dutra, A., Pike, B., Root, H., Rubenstein, J., Boyer, R., Stenroos, E. S., Chandrasekharappa, S., Athanassiadou, A., Papapetropoulos, T., Johnson, W. G., Lazzarini, A. M., Duvoisin, R. C., Di Iorio, G., Golbe, L. I., and Nussbaum, R. L. (1997) Mutation in the alpha-synuclein gene identified in families with Parkinson's disease, *Science*, *276*, 2045-2047.

Prusiner, S. B. (1982) Novel proteinaceous infectious particles cause scrapie, *Science*, *216*, 136-144.

Prusiner, S. B., Woerman, A. L., Mordes, D. A., Watts, J. C., Rampersaud, R., Berry, D. B., Patel, S., Oehler, A., Lowe, J. K., Kravitz, S. N., Geschwind, D. H., Glidden, D. V., Halliday, G. M., Middleton, L. T., Gentleman, S. M., Grinberg, L. T., and Giles, K. (2015) Evidence for α-synuclein prions causing multiple system atrophy in humans with parkinsonism, *Proc Natl Acad Sci U S A*, *112*, E5308-5317.

Rachakonda, V., Pan, T., and Le, W. (2004) Biomarkers of neurodegenerative disorders: How good are they?, *Cell Research*, *14*, 347-358.

Ramirez-Alvarado, M., and Conn, P. (2008) Principles of Protein Misfolding, *Molecular Biology of Protein Folding, Pt B*, *84*, 115-160.

Rao, S., Hofmann, L., and Shakil, A. (2006) Parkinson's disease: Diagnosis and treatment, *American Family Physician*, *74*, 2046-2054.

Recchia, A., Debetto, P., Negro, A., Guidolin, D., Skaper, S., and Giusti, P. (2004) α-synuclein and Parkinson's Disease, *Faseb Journal*, *18*, 617-626.

Reesink, F. E., Lemstra, A. W., van Dijk, K. D., Berendse, H. W., van de Berg, W. D., Klein, M., Blankenstein, M. A., Scheltens, P., Verbeek, M. M., and van der Flier, W. M. (2010) CSF α-synuclein does not discriminate dementia with Lewy bodies from Alzheimer's disease, *J Alzheimers Dis*, *22*, 87-95.

Rehman, H. U. (2001) Multiple system atrophy, *Postgrad Med J*, *77*, 379-382.

Represa, A., Deloulme, J. C., Sensenbrenner, M., Ben-Ari, Y., and Baudier, J. (1990) Neurogranin: immunocytochemical localization of a brain-specific protein kinase C substrate, *J Neurosci*, *10*, 3782-3792.

Rudenko, I. N., and Cookson, M. R. (2010) 14-3-3 proteins are promising LRRK2 interactors, *Biochem J*, *430*, e5-6.

Sacino, A., and Giasson, B. (2012) Does a prion-like mechanism play a major role in the apparent spread of α-synuclein pathology?, *Alzheimers Research & Therapy*, *4*.

Saito, Y. (2014) Oxidized DJ-1 as a possible biomarker of Parkinson's disease, *J Clin Biochem Nutr*, *54*, 138-144.

Salem, S. A., and Lancaster University. Theses. Biological Sciences. (2005) Study of a-synuclein, implicated in Parkinson's disease, in human brain, cerebrospinal fluid and blood plasma.

Santucci, R., Sinibaldi, F., and Fiorucci, L. (2008) Protein folding, unfolding and misfolding: Role played by intermediate states, *Mini-Reviews in Medicinal Chemistry*, *8*, 57-62.

Savitt, J., Dawson, V., and Dawson, T. (2006) Diagnosis and treatment of Parkinson disease: molecules to medicine,*Journal of Clinical Investigation*, *116*, 1744-1754.

Schmidt, K. S., Mattis, P. J., Adams, J., and Nestor, P. (2005) Test-retest reliability of the dementia rating scale-2: alternate form, *Dement Geriatr Cogn Disord*, *20*, 42-44.

Schumacher, A., Friedrich, P., Diehl-Schmid, J., Ibach, B., Perneczky, R., Eisele, T., Vukovich, R., Foerstl, H., and Riemenschneider, M. (2009) No association of TDP-43 with sporadic frontotemporal dementia, *Neurobiology of Aging*, *30*, 157-159.

Serpell, L. C., Berriman, J., Jakes, R., Goedert, M., and Crowther, R. A. (2000) Fiber diffraction of synthetic alpha-synuclein filaments shows amyloid-like cross-beta conformation, *Proc Natl Acad Sci U S A*, *97*, 4897-4902.

Sesar, A., Cacheiro, P., López-López, M., Camiña-Tato, M., Quintáns, B., Monroy-Jaramillo, N., Alonso-Vilatela, M. E., Cebrián, E., Yescas-Gómez, P., Ares, B., Rivas, M. T., Castro, A., Carracedo, A., and Sobrido, M. J. (2016) Synaptotagmin XI in Parkinson's disease: New evidence from an association study in Spain and Mexico, *J Neurol Sci*, *362*, 321-325.

Shendelman, S., Jonason, A., Martinat, C., Leete, T., and Abeliovich, A. (2004) DJ-1 is a redox-dependent molecular chaperone that inhibits alpha-synuclein aggregate formation, *PLoS Biol*, *2*, e362.

Shi, M., and Zhang, J. (2011) CSF α-synuclein, tau, and amyloid β in Parkinson's disease, *Lancet Neurol*, *10*, 681; author's reply 681-683.

Shi, M., Bradner, J., Hancock, A., Chung, K., Quinn, J., Peskind, E., Galasko, D., Jankovic, J., Zabetian, C., Kim, H., Leverenz, J., Montine, T., Ginghina, C., Kang, U., Cain, K., Wang, Y., Aasly, J., Goldstein, D., and Zhang, J. (2011) Cerebrospinal Fluid Biomarkers for Parkinson Disease Diagnosis and Progression, *Annals of Neurology*, *69*, 570-580.

Shi, M., Furay, A. R., Sossi, V., Aasly, J. O., Armaly, J., Wang, Y., Wszolek, Z. K., Uitti, R. J., Hasegawa, K., Yokoyama, T., Zabetian, C. P., Leverenz, J. B., Stoessl, A. J., and Zhang, J. (2012) DJ-1 and αSYN in LRRK2 CSF do not correlate with striatal dopaminergic function, *Neurobiol Aging*, *33*, 836.e835-837.

Shi, M., Liu, C., Cook, T. J., Bullock, K. M., Zhao, Y., Ginghina, C., Li, Y., Aro, P., Dator, R., He, C., Hipp, M. J., Zabetian, C. P., Peskind, E. R., Hu, S. C., Quinn, J. F., Galasko, D. R., Banks, W. A., and Zhang, J. (2014) Plasma exosomal α-synuclein is likely CNS-derived and increased in Parkinson's disease, *Acta Neuropathol*, *128*, 639-650.

Shi, M., Zabetian, C., Hancock, A., Ginghina, C., Hong, Z., Yearout, D., Chung, K., Quinn, J., Peskind, E., Galasko, D., Jankovic, J., Leverenz, J., and Zhang, J. (2010) Significance and confounders of peripheral DJ-1 and α-synuclein in Parkinson's disease, *Neuroscience Letters*, *480*, 78-82.

Shimura, H.; Schlossmacher, M.G.; Hattori, N.; Frosch, M.P.; Trockenbacher, A.; Schneider, R.; Mizuno, Y.; Kosik, K.S.; Selkoe, D.J. (2001) Ubiquitination of a new form of alpha-synuclein by parkin from human brain: Implications for Parkinson’s disease. *Science, 293*, 263–269.

Soti, C., and Csermely, P. (2002) Chaperones and aging: role in neurodegeneration and in other civilizational diseases,*Neurochemistry International*, *41*, 383-389.

Soto, C. (2003) Unfolding the role of protein misfolding in neurodegenerative diseases, *Nature Reviews Neuroscience*, *4*, 49-60.

Soto, C., and Estrada, L. (2008) Protein misfolding and neurodegeneration, *Archives of Neurology*, *65*, 184-189.

Soto, C., and Martin, Z. (2009) Therapeutic strategies against protein misfolding in neurodegenerative diseases, *Expert Opinion on Drug Discovery*, *4*, 71-84.

Spillantini, M. G., Crowther, R. A., Jakes, R., Cairns, N. J., Lantos, P. L., and Goedert, M. (1998) Filamentous α-synuclein inclusions link multiple system atrophy with Parkinson's disease and dementia with Lewy bodies, *Neurosci Lett*,*251*, 205-208.

Spillantini, M. G., Schmidt, M. L., Lee, V. M., Trojanowski, J. Q., Jakes, R., and Goedert, M. (1997) Alpha-synuclein in Lewy bodies, *Nature*, *388*, 839-840.

Stefani, M. (2004) Protein misfolding and aggregation: new examples in medicine and biology of the dark side of the protein world, *Biochimica Et Biophysica Acta-Molecular Basis of Disease*, *1739*, 5-25.

Stewart, T., Sossi, V., Aasly, J. O., Wszolek, Z. K., Uitti, R. J., Hasegawa, K., Yokoyama, T., Zabetian, C. P., Leverenz, J. B., Stoessl, A. J., Wang, Y., Ginghina, C., Liu, C., Cain, K. C., Auinger, P., Kang, U. J., Jensen, P. H., Shi, M., and Zhang, J. (2015) Phosphorylated α-synuclein in Parkinson's disease: correlation depends on disease severity, *Acta Neuropathol Commun*, *3*, 7.

Suchowersky, O., Gronseth, G., Perlmutter, J., Reich, S., Zesiewicz, T., Weiner, W. J., and Neurology, Q. S. S. o. t. A. A. o. (2006) Practice Parameter: neuroprotective strategies and alternative therapies for Parkinson disease (an evidence-based review): report of the Quality Standards Subcommittee of the American Academy of Neurology, *Neurology*, *66*, 976-982.

Sui, Y. T., Bullock, K. M., Erickson, M. A., Zhang, J., and Banks, W. A. (2014) A synuclein is transported into and out of the brain by the blood-brain barrier, *Peptides*, *62*, 197-202.

Tan, J., Wong, E., and Lim, K. (2009) Protein Misfolding and Aggregation in Parkinson's Disease, *Antioxidants & Redox Signaling*, *11*, 2119-2134.

Tanik, S. A., Schultheiss, C. E., Volpicelli-Daley, L. A., Brunden, K. R., and Lee, V. M. (2013) Lewy body-like α-synuclein aggregates resist degradation and impair macroautophagy, *J Biol Chem*, *288*, 15194-15210.

Tateno, F., Sakakibara, R., Kawai, T., Kishi, M., and Murano, T. (2012) α-Synuclein in the cerebrospinal fluid differentiates synucleinopathies (Parkinson Disease, dementia with Lewy bodies, multiple system atrophy) from Alzheimer disease, *Alzheimer Dis Assoc Disord*, *26*, 213-216.

Thomas, K. J., McCoy, M. K., Blackinton, J., Beilina, A., van der Brug, M., Sandebring, A., Miller, D., Maric, D., Cedazo-Minguez, A., and Cookson, M. R. (2011) DJ-1 acts in parallel to the PINK1/parkin pathway to control mitochondrial function and autophagy, *Hum Mol Genet*, *20*, 40-50.

Thorsell, A., Bjerke, M., Gobom, J., Brunhage, E., Vanmechelen, E., Andreasen, N., Hansson, O., Minthon, L., Zetterberg, H., and Blennow, K. (2010) Neurogranin in cerebrospinal fluid as a marker of synaptic degeneration in Alzheimer's disease, *Brain Res*, *1362*, 13-22.

Tokuda, T., Qureshi, M., Ardah, M., Varghese, S., Shehab, S., Kasai, T., Ishigami, N., Tamaoka, A., Nakagawa, M., and El-Agnaf, O. (2010) Detection of elevated levels of α-synuclein oligomers in CSF from patients with Parkinson disease,*Neurology*, *75*, 1766-1772.

van Dijk, K. D., Bidinosti, M., Weiss, A., Raijmakers, P., Berendse, H. W., and van de Berg, W. D. (2014) Reduced α-synuclein levels in cerebrospinal fluid in Parkinson's disease are unrelated to clinical and imaging measures of disease severity, *Eur J Neurol*, *21*, 388-394.

van Dijk, K. D., Persichetti, E., Chiasserini, D., Eusebi, P., Beccari, T., Calabresi, P., Berendse, H. W., Parnetti, L., and van de Berg, W. D. (2013) Changes in endolysosomal enzyme activities in cerebrospinal fluid of patients with Parkinson's disease, *Mov Disord*, *28*, 747-754.

Vekrellis, K., Xilouri, M., Emmanouilidou, E., Rideout, H., and Stefanis, L. (2011) Pathological roles of α-synuclein in neurological disorders, *Lancet Neurology*, *10*, 1015-1025.

Venda, L., Cragg, S., Buchman, V., and Wade-Martins, R. (2010) α-Synuclein and dopamine at the crossroads of Parkinson's disease, *Trends in Neurosciences*, *33*, 559-568.

Verstraete, E., Kuiperij, H., van Blitterswijk, M., Veldink, J., Schelhaas, H., van den Berg, L., and Verbeek, M. (2012) TDP-43 plasma levels are higher in amyotrophic lateral sclerosis, *Amyotrophic Lateral Sclerosis*, *13*, 446-451.

Wakabayashi, K., Hayashi, S., Kakita, A., Yamada, M., Toyoshima, Y., Yoshimoto, M., and Takahashi, H. (1998a) Accumulation of α-synuclein/NACP is a cytopathological feature common to Lewy body disease and multiple system atrophy, *Acta Neuropathol*, *96*, 445-452.

Wakabayashi, K., Yoshimoto, M., Tsuji, S., and Takahashi, H. (1998b) α-Synuclein immunoreactivity in glial cytoplasmic inclusions in multiple system atrophy, *Neurosci Lett*, *249*, 180-182.

Wang, Y., Shi, M., Chung, K. A., Zabetian, C. P., Leverenz, J. B., Berg, D., Srulijes, K., Trojanowski, J. Q., Lee, V. M., Siderowf, A. D., Hurtig, H., Litvan, I., Schiess, M. C., Peskind, E. R., Masuda, M., Hasegawa, M., Lin, X., Pan, C., Galasko, D., Goldstein, D. S., Jensen, P. H., Yang, H., Cain, K. C., and Zhang, J. (2012) Phosphorylated α-synuclein in Parkinson's disease, *Sci Transl Med*, *4*, 121ra120.

Waragai, M., Nakai, M., Wei, J., Fujita, M., Mizuno, H., Ho, G., Masliah, E., Akatsu, H., Yokochi, F., and Hashimoto, M. (2007) Plasma levels of DJ-1 as a possible marker for progression of sporadic Parkinson's disease, *Neurosci Lett*, *425*, 18-22.

Waragai, M., Wei, J., Fujita, M., Nakai, M., Ho, G. J., Masliah, E., Akatsu, H., Yamada, T., and Hashimoto, M. (2006) Increased level of DJ-1 in the cerebrospinal fluids of sporadic Parkinson's disease, *Biochem Biophys Res Commun*, *345*, 967-972.

Warraich, S., Yang, S., Nicholson, G., and Blair, I. (2010) TDP-43: A DNA and RNA binding protein with roles in neurodegenerative diseases, *International Journal of Biochemistry & Cell Biology*, *42*, 1606-1609.

Wennström, M., Surova, Y., Hall, S., Nilsson, C., Minthon, L., Boström, F., Hansson, O., and Nielsen, H. M. (2013) Low CSF levels of both α-synuclein and the α-synuclein cleaving enzyme neurosin in patients with synucleinopathy, *PLoS One*, *8*, e53250.

Wilson, R. (2013) Sensitivity and specificity: twin goals of proteomics assays. Can they be combined?, *Expert Rev Proteomics*, *10*, 135-149.

Winslow, A. R., Chen, C. W., Corrochano, S., Acevedo-Arozena, A., Gordon, D. E., Peden, A. A., Lichtenberg, M., Menzies, F. M., Ravikumar, B., Imarisio, S., Brown, S., O'Kane, C. J., and Rubinsztein, D. C. (2010) α-Synuclein impairs macroautophagy: implications for Parkinson's disease, *J Cell Biol*, *190*, 1023-1037.

Wolozin, B. (2012) Regulated protein aggregation: stress granules and neurodegeneration, *Molecular Neurodegeneration*,*7*.

Wood, S. J., Wypych, J., Steavenson, S., Louis, J. C., Citron, M., and Biere, A. L. (1999) alpha-synuclein fibrillogenesis is nucleation-dependent. Implications for the pathogenesis of Parkinson's disease, *J Biol Chem*, *274*, 19509-19512.

Wood-Kaczmar, A., Gandhi, S., and Wood, N. (2006) Understanding the molecular causes of Parkinson's disease, *Trends in Molecular Medicine*, *12*, 521-528.

Xilouri, M., Kyratzi, E., Pitychoutis, P., Papadopoulou-Daifoti, Z., Perier, C., Vila, M., Maniati, M., Ulusoy, A., Kirik, D., Park, D., Wada, K., and Stefanis, L. (2012) Selective neuroprotective effects of the S18Y polymorphic variant of UCH-L1 in the dopaminergic system, *Human Molecular Genetics*, *21*, 874-889.

Xilouri, M., Vogiatzi, T., Vekrellis, K., Park, D., and Stefanis, L. (2009) Abberant alpha-synuclein confers toxicity to neurons in part through inhibition of chaperone-mediated autophagy, *PLoS One*, *4*, e5515.

Xu, J., Kao, S. Y., Lee, F. J., Song, W., Jin, L. W., and Yankner, B. A. (2002) Dopamine-dependent neurotoxicity of alpha-synuclein: a mechanism for selective neurodegeneration in Parkinson disease, *Nat Med*, *8*, 600-606.

Xu, S. (2007) Aggregation drives "misfolding" in protein amyloid fiber formation, *Amyloid-Journal of Protein Folding Disorders*, *14*, 119-131.

Xu, Y., Zhang, Y., Lin, W., Cao, X., Stetler, C., Dickson, D., Lewis, J., and Petrucelli, L. (2011) Expression of mutant TDP-43 induces neuronal dysfunction in transgenic mice, *Molecular Neurodegeneration*, *6*.

Xu, Z. (2012) Does a loss of TDP-43 function cause neurodegeneration?, *Molecular Neurodegeneration*, *7*.

Yates, D. (2011) Neurodegenerative disease: α-synuclein gets a new look, *Nature Reviews Neuroscience*, *12*.

Yu, J., and Lyubchenko, Y. (2009) Early Stages for Parkinson's Development: α-Synuclein Misfolding and Aggregation,*Journal of Neuroimmune Pharmacology*, *4*, 10-16.

Yue, Z., and Yang, X. W. (2013) Dangerous duet: LRRK2 and α-synuclein jam at CMA, *Nat Neurosci*, *16*, 375-377.

Zarranz, J. J., Alegre, J., Gómez-Esteban, J. C., Lezcano, E., Ros, R., Ampuero, I., Vidal, L., Hoenicka, J., Rodriguez, O., Atarés, B., Llorens, V., Gomez Tortosa, E., del Ser, T., Muñoz, D. G., and de Yebenes, J. G. (2004) The new mutation, E46K, of alpha-synuclein causes Parkinson and Lewy body dementia, *Ann Neurol*, *55*, 164-173.

Zhong, N., Kim, C. Y., Rizzu, P., Geula, C., Porter, D. R., Pothos, E. N., Squitieri, F., Heutink, P., and Xu, J. (2006) DJ-1 transcriptionally up-regulates the human tyrosine hydroxylase by inhibiting the sumoylation of pyrimidine tract-binding protein-associated splicing factor, *J Biol Chem*, *281*, 20940-20948.

Zhou, J. (2000) Protein misfolding and disease., *Progress in Biochemistry and Biophysics*, *27*, 579-584.

Zondler, L., Miller-Fleming, L., Repici, M., Gonçalves, S., Tenreiro, S., Rosado-Ramos, R., Betzer, C., Straatman, K. R., Jensen, P. H., Giorgini, F., and Outeiro, T. F. (2014) DJ-1 interactions with α-synuclein attenuate aggregation and cellular toxicity in models of Parkinson's disease, *Cell Death Dis*, *5*, e1350.

Websites used:

http://www.asha.org/uploadedFiles/ASHA/Events/hcare-conf/2012-HCBI-Presentation-Neurodegenerative-Diseases-Classification.pdf - accessed Nov 2013

http://www.luminexcorp.com/prod/groups/public/documents/lmnxcorp/reagents-beads.jpg - accessed Dec 2013 and May 2013

http://elisaanalysis.com/app replacing http://readerfit.com – accessed May 2013 to July 2015.

www.parkinsons.org – accessed Jan 2013

www.epda.eu.com – accessed Feb 2013

www.emory.edu/ADRC/dementias/frontotemporal_dementia/index.html - accessed March 2013

http://www.med.emory.edu/ADRC/dementias/frontotemporal_dementia/index.html - accessed March 2013

www.oxfordmnd.net/information/nomenclature - accessed March 2013

http://www.alznc.org/index.php/alzheimers-similar-diseases/21-frontal-temporal-lobe-dementias - accessed April 2013

www.nhs.uk/conditions/motor-neurone-disease/Pages/Diagnosis.aspx - accessed April 2013

www.patient.co.uk – accessed April 2013

www.nhs.uk/conditions/motor-neurone-disease/Pages/Diagnosis.aspx - accessed April 2013

http://www.nhs.uk/Conditions/Motor-neurone-disease/Pages/Treatment.aspx - accessed April 2013

http://www.ema.europa.eu/docs/en_GB/document_library/Scientific_guideline/2011/08/WC500109686.pdf - accessed May 2013

www.patient.co.uk/doctor/multiple-system-atrophy - accessed April 2014

www.multiplesystematrophy.org/about-msa/types-symptoms - accessed April 2014

www.parkinsons.ie/Atypical-MSA) - accessed April 2014

www.msatrust.org.uk/wp-content/uploads/2011/07/MSA-Trust-Research-Strategy.pdf - accessed April 2014

www.mayoclinic.org/diseases-conditions/multiple-system-atrophy/basics/tests-diagnosis/con-20027096 - - accessed April 2014

msatrust.org.uk/living-with-msa/newly-diagnosed/treatment-management-of-msa - accessed April 2014

http://www.mayoclinic.org/diseases-conditions/rem-sleep-behavior-disorder/basics/symptoms/con-20036654 - accessed April 2014

www.alz.org/dementia/dementia-with-lewy-bodies-symptoms.asp - accessed April 2014

emedicine.medscape.com/article.com/article/1135041-overview - accessed April 2014

emedicine.medscape.com/article/1135041-treatment - accessed April 2014

Appendices

Appendix 1: Luminex assay protocol

1. Microspheres diluted 1 in 20 in PBS+ 0.05% (v/v) tween 20 (PBST), vortex to remove doublets

2. Prepare the standards in serial dilution in assay buffer (SM01:PBS)

3. Pre wet 96-well filter microplate with 200µl PBST and use vacuum manifold to aspirate wash solution. Blot filter plate dry with paper towel.

4. Add 20 µl diluted microspheres to each well (Total 5,260 Beads/well)

2. Add 200 µl PBST to each well. Aspirate plates via the vacuum manifold and blot dry on paper towel

3. Pipette 50 µl of diluted standard or sample per well. Agitate on a microplate shaker for 2 hrs at room temperature and covered with aluminium foil

4. Agitate on a microplate shaker overnight at 4^{o}C, covered with aluminium foil

5. Following incubation aspirate and blot filter plate dry with paper towel

6. Wash plate with 200µl PBST and use vacuum manifold to aspirate wash solution. Blot filter plate dry with paper towel. (Repeat 2 times)

7. Add 50 µl/well diluted biotinylated secondary antibody in assay buffer (SM01:PBS) and agitate on a shaker covered with aluminium foil for 1 hr at room temperature in the dark.

8. Add 50 µl/ well Streptavidin diluted at 4ug/ml in PBST, agitate on a shaker covered with aluminium foil for 30 mins at room temperature in the dark

9. Following incubation, aspirate and blot filter plate dry with paper towel

10. Wash plate 3 times with 200µl PBST using vacuum manifold

11. Resuspend beads in 125 µl of Luminex sheath fluid and agitate on a shaker for 1 min, at high speed

12. Read plate in Luminex 200 machine